

# Vanderbilt University

## 2015-2016 NASA Student Launch

### Preliminary Design Review



November 6, 2015

Andrew Voss, *President, Design Engineer*  
Mitchell Masia, *Vice President, Website Manager*  
Robinson Rutherford, *Treasurer, Design Engineer*  
Justin Broughton, *CFD, Design Engineer*  
David Hirsch, *CAD, Design Engineer*  
Matthew Kelley, *CAD, Design Engineer*  
Andrew Martin, *Design Engineer*  
Quinlan Monk, *Design Engineer*  
Rebecca Riley, *DAQ, Electrical Engineer*  
Dylan Shane, *Design Engineer*  
Derek Phillips, Chris Romanoski, Henry Bristol, *Field Engineers*  
Ben Gasser, *Student Safety Officer*  
Chris Lyne, *CFD Engineer*  
Peter Orme, *Dynamics Engineer*  
Dexter Watkins, *Instrumentation Engineer*  
Dr. Brian Lawson, *Dynamics Mentor*  
Robin Midgett, *Safety and Rocketry Mentor*  
Dr. Heather Johnson, *Faculty Advisor for Outreach*  
Dr. Amrutar Anilkumar, *Project Advisor*

## ***Table of Contents***

---

1	General Information .....	10
1.1	Faculty Advisors .....	10
1.1.1	Project Advisor .....	10
1.1.2	Outreach Advisor .....	10
1.2	Mentors.....	10
1.2.1	Safety and Rocketry Mentor .....	10
1.2.2	Student Safety Officer.....	10
1.2.3	Dynamics Mentor.....	10
1.3	Team Members.....	10
1.3.1	Senior Design Team.....	10
1.3.2	Graduate Students .....	12
1.3.3	Field Engineers .....	12
1.4	NAR Association.....	12
1.5	Vanderbilt Aerospace Design Lab Constitution.....	13
2	Summary of Project .....	14
2.1	Team Summary .....	14
2.2	Launch Vehicle Summary.....	14
2.3	Payload Summary .....	15
3	Changes Made Since Proposal .....	17
3.1	Changes Made to Vehicle Criteria .....	17
3.2	Changes Made to Payload Criteria.....	17
3.3	Changes Made to Project Plan .....	17
4	Vehicle Criteria.....	19
4.1	Selection, Design, and Verification of Launch Vehicle.....	19
4.1.1	Mission Statement and Mission Success Criteria .....	19
4.1.2	Launch Vehicle Design.....	21
4.1.3	Performance Characteristics and Verification of Systems.....	36
4.1.4	Vehicle Verification Plan and Status .....	39
4.1.5	Vehicle Development Risk and Risk Mitigation .....	44
4.1.6	Planning of Manufacturing, Verification, Integration, and Operations .....	56
4.1.7	Confidence and Maturity of Design.....	56
4.1.8	Dimensional Drawings.....	57
4.1.9	Electrical Schematics for Recovery System .....	60

4.1.10	Mass Statement .....	60
4.2	Comparison of Subscale to Full-Scale Launch Vehicle.....	61
4.2.1	Comparison Overview .....	61
4.2.2	Vehicle Design Comparison .....	62
4.2.3	Dimensional Drawings of Subscale .....	64
4.2.4	Flight Vehicle Test Sequence .....	67
4.3	Recovery Subsystem .....	67
4.3.1	Recovery System Overview.....	67
4.3.2	Rocket Separation .....	68
4.3.3	Drogue Parachute Recovery .....	70
4.3.4	Main Parachute Recovery .....	70
4.3.5	Avionics and Avionics Bays.....	71
4.3.6	Deployment Charge and Altimeter Layout.....	74
4.3.7	Recovery System Testing .....	75
4.3.8	Rocket Avionics Bay – Structural.....	77
4.4	Mission Performance Predictions .....	78
4.4.1	Mission Performance Criteria.....	78
4.4.2	Simulations and Predictions.....	79
4.4.3	Kinetic Energy .....	84
4.4.4	Drift Calculations.....	84
4.5	Interfaces and Integration.....	85
4.5.1	Payload Integration Plan .....	85
4.5.2	Interfaces within Launch Vehicle .....	88
4.5.3	Interfaces between Launch Vehicle and Ground .....	88
4.5.4	Interfaces between Launch Vehicle and Ground Launch System .....	88
4.6	Launch Operations Procedures.....	89
4.6.1	Launch System and Platform .....	89
4.6.2	Launch Checklist .....	89
4.7	Vehicle Safety and Environment.....	95
4.7.1	Safety Officer.....	95
4.7.2	Preliminary Failure Modes Analysis .....	95
4.7.3	Personnel Hazards and Concerns.....	95
4.7.4	Standard Operating Procedures.....	101
4.7.5	Environmental Hazards and Concerns.....	101

5	Payload Criteria .....	102
5.1	Selection, Design, and Verification of Payload Experiment.....	102
5.1.1	Fuel Delivery and Liquid Fuel Tank Slosh Abatement Systems .....	102
5.1.2	Hydrogen Peroxide Monopropellant Thruster .....	131
5.1.3	Structural Analysis.....	133
5.1.4	Payload Instrumentation Systems .....	138
5.1.5	Performance Characteristics and Evaluation and Verification Metrics .....	143
5.1.6	Verification Plan and Status.....	146
5.1.7	Preliminary Integration Plan .....	149
5.1.8	Precision, Repeatability, and Recovery .....	149
5.1.9	Drawings and Electrical Schematics, Payload.....	149
5.1.10	Key Components and Desired Results.....	151
5.1.11	Mass Statement .....	151
5.2	Payload Concept Features and Definition .....	152
5.2.1	Creativity and Originality .....	152
5.2.2	Uniqueness and Significance .....	153
5.2.3	Challenge Level .....	154
5.3	Payload Science.....	155
5.3.1	Fuel Delivery System Science .....	155
5.3.2	Monopropellant Thruster Science .....	163
5.3.3	Structural Analysis Science .....	171
5.4	Payload Safety and Environment .....	175
5.4.1	Safety Officer.....	175
5.4.2	Preliminary Analysis of Failure Modes and Mitigations .....	175
5.4.3	Personal Hazards and Concerns.....	181
5.4.4	Environmental Concerns.....	182
6	Activity Plan .....	183
6.1	Budget Plan .....	183
6.2	Preliminary Timeline.....	191
6.3	Educational Engagement Plan & Status.....	192
6.3.1	Educational Plan .....	192
6.3.2	Educational Lesson Plan Summary .....	193
6.3.3	Educational Lesson Plan Details.....	194
7	Conclusion .....	198

8 Appendix .....	199
------------------	-----

## List of Figures

Figure 1: CAD model of the launch vehicle .....	14
Figure 2: Layout of the subscale vehicle .....	15
Figure 3: Concept of flight operations .....	21
Figure 4: Tail Section Schematic Demonstrating Motor Retention.....	22
Figure 5: Block diagram of force transmission.....	23
Figure 6: Fins and motor tube are inserted into lower half of jig .....	25
Figure 7: Top two plates of jig are assembled .....	25
Figure 8: Initial epoxy fillet once cured.....	26
Figure 9: Populating the carbon fiber fillets with epoxy .....	26
Figure 10: Preparing vacuum bag over one section of fillets .....	27
Figure 11: Fin and motor tube assembly curing inside of jig .....	27
Figure 12: Complete fin and motor tube assembly slid into body tube .....	28
Figure 13: Nose cone with parachute packing.....	30
Figure 14: Tail cone mold making.....	31
Figure 15: The tail cone mold in the trimming stage.....	32
Figure 16: The two halves of the mold split .....	32
Figure 17: Template for carbon fiber to make the tail cone .....	33
Figure 18: Tail cone layup with peel ply and some breather added .....	34
Figure 19: Tail cone in the vacuum bag.....	34
Figure 20: The tail cone layup (right) after being split from the mold .....	35
Figure 21: The complete carbon fiber composite tail cone.....	35
Figure 22: General payload requirements.....	39
Figure 23: Risk assessment matrix .....	45
Figure 24: Launch vehicle .....	57
Figure 25: Full-scale payload bay.....	58
Figure 26: Full-scale tail section.....	58
Figure 27: Full-scale nose cone .....	59
Figure 28: Fin design .....	59
Figure 29: Schematic of avionics hardware .....	60
Figure 30: Comparison of Key Criteria between Full-Scale and Subscale Flight Vehicles.....	62
Figure 31: Subscale vehicle .....	65
Figure 32: Subscale payload bay .....	65
Figure 33: Subscale tail section .....	66
Figure 34: Subscale nosecone .....	66
Figure 35: Recovery System Flowchart.....	68
Figure 36: Top view of magnetic arming switch .....	73

Figure 37: Bottom view of magnetic arming switch showing soldered connections .....	73
Figure 38: Preliminary CAD of the Avionics Bay and Connectivity Components .....	74
Figure 39: Main altimeter test results, Apogee Deployment Delay = 0s, Main Deployment Altitude = 700' .....	76
Figure 40: Backup altimeter test results, Apogee Deployment Delay = 1s, Main Deployment Altitude = 500' .....	77
Figure 41: Location of centers of gravity and pressure of rocket .....	79
Figure 42: Acceleration vs. Time (maximum acceleration of +12g) .....	81
Figure 43: Velocity vs. Time (maximum velocity at motor burnout is 650 fps) .....	81
Figure 44: Static Stability Margin vs. Time (stability margin starts at 1.9 and quickly increases to 2.5) .....	82
Figure 45: Cesaroni L1720 Thrust Curve .....	82
Figure 46: Rocket Apogee vs. Launch Mass changes (baseline: 30.5 lb) .....	83
Figure 47: Rocket Apogee vs. Ground Wind Speed (11 mph ground winds are typical in April) .....	83
Figure 48: Drift vs. Wind Speed for Full-Scale Launch .....	84
Figure 49: CAD of Vanderbilt's 2013-2014 USLI rocket with externally mounted ramjets .....	86
Figure 50: Modified tail cone with internally mounted monopropellant thrusters .....	87
Figure 51: Diagram of thruster-pylon configuration attached to a bulkhead .....	87
Figure 52: Diagram of sensor placement for subscale launch .....	88
Figure 53: Safety structure flowchart .....	96
Figure 54: Schematic of thruster and fuel system payload .....	102
Figure 55: (a) USLI 13-14 Fuel Tank insert schematic with the trajectory that a bubble has to take to reach the pickup, (b) USLI 15-16 Fuel Tank insert design .....	104
Figure 56: Functional Architecture of Fuel Delivery System Modules .....	106
Figure 57: CAD Model of subscale fuel delivery payload .....	106
Figure 58: Acrylic Fuel Tank CAD and Actual .....	107
Figure 59: Cyclical Stress .....	109
Figure 60: Operation Window .....	110
Figure 61: USLI '14 SAS Design .....	111
Figure 62: VADL Drop Test Stand Schematic .....	112
Figure 63: USLI 14 Drop Test Stand -1g Results .....	113
Figure 64: Fluid Level is Below Bobbin Level .....	114
Figure 65: Fluid Leaking Out of the Top Bobbin .....	114
Figure 66: Filling Error Bubble .....	115
Figure 67: A Typical Sponge .....	115
Figure 68: Sponge Width Change .....	116
Figure 69: Theoretical Gap Design .....	117
Figure 70: USLI 16 Sponge Design Version 1 CAD View 1 .....	117
Figure 71: USLI 16 Sponge Design Version 1 CAD View 2 (dimensions in mm) .....	118
Figure 72: USLI 16 Sponge Design Version 1 CAD View 3 (dimensions in mm) .....	118

Figure 73: USLI 16 Sponge Design Version 1 Actual .....	119
Figure 74: No Baffle Fuel Tank Slosh.....	120
Figure 75: USLI '16 Sponge Design Version 1 Drop Test .....	121
Figure 76: USLI '16 Sponge Design Version 1 Drop Test with Fluid Level Lines (Red = Current Level, Green = Level from Previous Frame) and Bottom of Baffle Line (Blue).....	122
Figure 77: Sponge Design Comparisons.....	124
Figure 78: USLI Version 2 Sponge Design Theoretical Design.....	126
Figure 79: USLI 16 Sponge Design Version 2 CAD View 1 .....	127
Figure 80: USLI 16 Sponge Design Version 2 CAD View 2 (dimensions in mm).....	127
Figure 81: USLI 16 Sponge Design Version 2 CAD View 3 (dimensions in mm).....	128
Figure 82: Schematic of a general debouncing circuit.....	129
Figure 83: GoPro Hero 3 White Edition.....	130
Figure 84: GoPro Camera Mount CAD .....	130
Figure 85: GoPro attached to the Drop Test Stand .....	131
Figure 86: Internal thruster geometry .....	132
Figure 87: Overview of structural analysis initiative.....	134
Figure 88: Woven Fiber microstructure and computer discretizations.....	135
Figure 89: Accelerometer Board and Battery Pack .....	137
Figure 90: Abaqus Finite Element Model.....	138
Figure 91: The Ansys Finite Element Model.....	138
Figure 92: Old RDAS used in previous years.....	139
Figure 93: Top view of proposed electronics layout .....	140
Figure 94: Side view of proposed electronics bay .....	140
Figure 95: Proposed bay design if multiple vertical layers are required .....	140
Figure 96: Flowchart of fuel delivery instrumentation .....	141
Figure 97: Schematic of data flow from the instrumentation subsystems .....	149
Figure 98: Data flow in Accelerometer Dataloggers .....	150
Figure 99: Schematic of the fuel delivery system.....	150
Figure 100: Air Bubble Separation mechanism from USLI '13 .....	156
Figure 101: USLI '13 Fuel Container Design.....	156
Figure 102: Schematic of the Drop Test Stand.....	158
Figure 103: Drop Test Stand lifted to its maximum height .....	159
Figure 104: Drop Test Stand Dynamics Model .....	160
Figure 105: Drop Test Stand Accelerometer .....	161
Figure 106: expected trends plotting new coefficient of drag to reference coefficient of drag ratio for multiple values of $D_2/D_1$ .....	165
Figure 107: expected trends plotting new static stability margin to reference static stability margin for multiple values of $D_2/D_1$ .....	165
Figure 108: Geometry for subscale rocket's initial drag simulations .....	166

Figure 109: Magnified view of the nosecone mesh with a) a mesh of medium fineness and b) a mesh of medium fineness with added inflation's effect on the original mesh .....	167
Figure 110: Axial flow of 100m/s a) velocity volume plot with velocity vectors b) pressure volume plot with pressure surface on the rocket.....	167
Figure 111: Geometry for initial simulation to establish center of pressure for subscale rocket	168
Figure 112: Flow visualization for the center of pressure a) velocity volume plot with velocity vectors b) pressure volume plot.....	168
Figure 113: Center of pressure relative to the tip of the nosecone .....	169
Figure 114: Thruster response surface plot.....	170
Figure 115: Thrust contours plot.....	170
Figure 116: Abaqus 257.42 Hz Bending Mode .....	174
Figure 117: Ansys 153.35 Hz Bending Mode .....	174
Figure 118: Risk assessment matrix .....	176
Figure 119: Overall budget distribution.....	191
Figure 121: Simplified schematic of the fan cart demo .....	195
Figure 122: Bottle Rocket launch stand.....	196
Figure 123: Gantt Chart for project plan.....	200
Figure 124: Gantt Chart for project plan.....	201

## **List of Tables**

Table 1: Summary Table for the Vehicle Systems .....	37
Table 2: Review of requirements and verification plan.....	39
Table 3: Vehicle Development Risk Table .....	46
Table 4: Vehicle Failure Modes and Risk Assessment.....	49
Table 5: Propulsion Failure Modes and Risk Assessment.....	51
Table 6: Recovery System Failure Modes and Risk Assessment.....	53
Table 7. Mass Statement .....	60
Table 8: Comparison of Key Parameters for Full-Scale Launch vs. Subscale Launch .....	63
Table 9: Summary of differences between Full-Scale and Subscale .....	63
Table 10: Summary of parameters used in simulations .....	79
Table 11: Risk and Risk Mitigation table for hazardous materials.....	97
Table 12: Average Percent Deviation from Ideal .....	123
Table 13: Updated Average Percent Deviation from Ideal.....	125
Table 14: SAS Volumes.....	128
Table 15: 3D elasticity tensor for 2x2 twill woven carbon fiber .....	135
Table 16: Summary of R-DAS operating characteristics .....	142
Table 17: System Analysis Summary Table for Fuel Delivery System .....	143
Table 18: System Analysis Summary Table for Thruster System .....	144
Table 19: Summary of Verification Plan for Fuel Delivery System .....	146

Table 20: Summary of Verification Plan for Monopropellant Thruster .....	147
Table 21: Summary of Structural Analysis payload Verification Plan.....	148
Table 22: Mass Statement for subsection payload.....	152
Table 23: Monopropellant Thruster Risk and Mitigation Table.....	177
Table 24: Fuel Delivery System Risk and Mitigation Table .....	178
Table 25: Structural Analysis Risk and Mitigation Table .....	180
Table 26: Itemized list of expenditures.....	183
Table 27: Relevant previous year purchases.....	190
Table 28: Timeline .....	191

# *1 General Information*

---

## 1.1 Faculty Advisors

---

### **1.1.1 Project Advisor**

---

Dr. Amrutar Anilkumar  
Professor of the Practice  
Department of Mechanical Engineering  
[Amrutar.V.Anilkumar@Vanderbilt.edu](mailto:Amrutar.V.Anilkumar@Vanderbilt.edu)

### **1.1.2 Outreach Advisor**

---

Dr. Heather Johnson  
Assistant Professor of the Practice of Science Education  
Department of Teaching and Learning  
[Heather.J.Johnson@Vanderbilt.edu](mailto:Heather.J.Johnson@Vanderbilt.edu)

## 1.2 Mentors

---

### **1.2.1 Safety and Rocketry Mentor**

---

Robin Midgett  
Safety and Rocketry Mentor  
Senior Electronics Technician  
NAR Level II Certified  
Department of Mechanical Engineering  
[Robin.Midgett@Vanderbilt.edu](mailto:Robin.Midgett@Vanderbilt.edu)

### **1.2.2 Student Safety Officer**

---

Ben Gasser  
Graduate Student, Mechanical Engineering  
[Benjamin.W.Gasser@Vanderbilt.edu](mailto:Benjamin.W.Gasser@Vanderbilt.edu)

### **1.2.3 Dynamics Mentor**

---

Brian Lawson, PhD  
Post-Doctoral Researcher, Mechanical Engineering  
[Brian.E.Lawson@Vanderbilt.edu](mailto:Brian.E.Lawson@Vanderbilt.edu)

## 1.3 Team Members

---

### **1.3.1 Senior Design Team**

---

Andrew Voss  
*President, Design Engineer*  
Senior, Mechanical Engineering  
[andrew.d.voss@Vanderbilt.Edu](mailto:andrew.d.voss@Vanderbilt.Edu)

Mitch Masia  
*Vice President, Website Manager*  
Senior, Computer Engineering  
[mitchell.j.masia@Vanderbilt.Edu](mailto:mitchell.j.masia@Vanderbilt.Edu)

Rob Rutherford  
*Treasurer, Design Engineer*  
Senior, Mechanical Engineering  
[robinson.p.rutherford@Vanderbilt.Edu](mailto:robinson.p.rutherford@Vanderbilt.Edu)

Justin Broughton  
*CFD Engineer*  
Senior, Mechanical Engineering  
[Justin.d.broughton@vanderbilt.edu](mailto:Justin.d.broughton@vanderbilt.edu)

David Hirsch  
*CAD, Design Engineer*  
Senior, Mechanical Engineering  
[David.a.hirsch@vanderbilt.edu](mailto:David.a.hirsch@vanderbilt.edu)

Matt Kelley  
*CAD, Design Engineer*  
Senior, Mechanical Engineering  
[Matthew.j.kelley@vanderbilt.edu](mailto:Matthew.j.kelley@vanderbilt.edu)

Drew Martin  
*Design Engineer*  
Senior, Mechanical Engineering  
[Andrew.m.martin@vanderbilt.edu](mailto:Andrew.m.martin@vanderbilt.edu)

Quin Monk  
*Design Engineer*  
Senior, Mechanical Engineering  
[Quinlan.l.monk@vanderbilt.edu](mailto:Quinlan.l.monk@vanderbilt.edu)

Rebecca Riley  
*DAQ, Electrical Engineer*  
Junior, Computer Engineering  
[Rebecca.a.riley@vanderbilt.edu](mailto:Rebecca.a.riley@vanderbilt.edu)

Dylan Shane

*Design Engineer*  
Senior, Mechanical Engineering  
[Dylan.o.shane@vanderbilt.edu](mailto:Dylan.o.shane@vanderbilt.edu)

### **1.3.2 Graduate Students**

---

Chris Lyne  
*CFD Engineer*  
Graduate Student, Mechanical Engineering  
[Christopher.t.lyne@vanderbilt.edu](mailto:Christopher.t.lyne@vanderbilt.edu)

Peter Orme  
*Dynamics Engineer*  
Graduate Student, Civil Engineering  
[Peter.orme@vanderbilt.edu](mailto:Peter.orme@vanderbilt.edu)

Dexter Watkins  
*Instrumentation Engineer*  
Graduate Student, Mechanical Engineering

### **1.3.3 Field Engineers**

---

Derek Philips  
Junior, Mechanical Engineering  
[Derek.j.philips@vanderbilt.edu](mailto:Derek.j.philips@vanderbilt.edu)

Chris Romanoski  
Freshman, Mechanical Engineering  
[Christopher.romanoski@vanderbilt.edu](mailto:Christopher.romanoski@vanderbilt.edu)

Henry Bristol  
Freshman, Mechanical Engineering  
[Henry.bristol@vanderbilt.edu](mailto:Henry.bristol@vanderbilt.edu)

## **1.4 NAR Association**

---

Music City Missile Club, NAR #589  
Officers:      Brian Godfrey, *President*  
                  Chris Dondanville, *Vice-President*  
                  Robin Midgett, *Treasurer*, treasurer@mc2rocketry.com  
                  Fred Kepner, *Secretary*  
                  Russ Bruner, *Advisor*

## 1.5 Vanderbilt Aerospace Design Lab Constitution

---

### **Preamble:**

The Vanderbilt Aerospace Design Lab is a volunteer student organization that has two primary purposes: it competes in the NASA SL (Student Launch) Rocket Competition and conducts aerospace related educational outreach to middle schools and high schools in Middle Tennessee. The Vanderbilt Aerospace Design Lab activities apply directly to Engineering students and their practice, as well as to students from schools of Arts and Science, educating those who may be interested in school science teaching.

### **Constitutional Articles:**

- a. The Vanderbilt Aerospace Design Lab must have a mechanical engineering professor who serves as the faculty advisor. In addition, the lab must also have a financial advisor pursuant to Vanderbilt policy.
- b. All students are welcome to participate in the aerospace lab with caveat that the largest membership that can compete and be active in the SL competition is 17 members; however, preference is given to upperclassmen (seniors and juniors).
- c. Students who want to join the lab and compete in the SL competition must demonstrate qualities that will contribute to the lab's mission and success at the competition. Such qualities may include prior rocketry experience, interest in aerospace engineering or science teaching as a career, a good academic standing, and a strong work ethic in a field that is of use to the team (particularly educational outreach or engineering).
- d. The lab meets every Thursday from 12:15-1:00 in the Mechanical Engineering Hall in Olin School of Engineering.
- e. The NASA SL Competition serves as the senior design project for the Mechanical Engineering Curriculum.
- f. Members of the Vanderbilt Aerospace Design Lab who participate in the SL Competition must be actively involved in the lab and dedicate several hours per week to working on competition related items.
- g. The members of the Vanderbilt Aerospace Design Lab must actively seek to promote Aerospace and STEM education and outreach in Middle Tennessee.
- h. The President, Vice President, Secretary, and Treasurer of the Aerospace team that participates in the SL Competition must be recommended by the Vanderbilt Aerospace Design Lab faculty advisor.
- i. Any amendments to this Constitution can be made by a vote of the members and approved by the faculty advisor.

### **Member's Rights and Expectations**

- j. Any member of the Vanderbilt Aerospace Design Lab cannot be discriminated based on sexual orientation, gender, race, ethnicity, or socio-economic class.
- k. Members of the Vanderbilt Aerospace Design Lab must show an enthusiastic and professional involvement in the lab.
- l. Any member who is a part of the SL competition must represent Vanderbilt University with all due decorum and professionalism.

# *2 Summary of Project*

---

## 2.1 Team Summary

---

The Vanderbilt Aerospace Design Lab is a student organization located in Nashville, Tennessee. The Project Faculty Advisor is Dr. Amrutur Anilkumar, Professor of Mechanical Engineering, and the Safety and Rocketry Mentor is Robin Midgett (NAR Level II Certified, NAR #589). The team's Outreach Advisor is Dr. Heather Johnson, Assistant Professor of the Practice of Science Education in the Department of Teaching & Learning. The mailing address of the lab is as follows:

Amrutur Anilkumar  
Department of Mechanical Engineering  
VU Station B #351592  
2301 Vanderbilt Place  
Nashville, TN 37235-1592

## 2.2 Launch Vehicle Summary

---



**Figure 1: CAD model of the launch vehicle**

Vanderbilt's full scale rocket will have a body diameter of 5.5", an overall length of 102", and an overall weight of 37.9 lbf. at take-off (30.5 lbf. w/o motor). The selected motor is a Cesaroni L1720, which is an off-the-shelf reloadable 75 mm motor. This specific motor has been chosen for its short burn time of 2.1sec allowing for desired higher impulsive launch loads and high initial vehicle velocity (~85 fps) as the rocket departs the launch rail causing straighter flight while remaining subsonic throughout ascent. The predicted and targeted altitude of the rocket is 5300 ft. AGL for typical ground windspeed of 11 mph. The recovery system for this rocket is a dual deployment system comprised of a drogue parachute deployed at apogee, and a main deployed at 700ft AGL. The recovery system is controlled by a redundant pair of barometric pressure based altimeters. The main parachute (12 ft. elliptical) will be housed in the nose cone of the rocket and the drogue (2.5ft elliptical) will be housed in the aft of the avionics bay.

Vanderbilt's subscale model has a body diameter of 5.5", an overall length of 79" and an overall weight of 24.3 lbf. (20.1 lbf. w/o motor). The selected motor for the subscale launch vehicle is a Cesaroni K1440, which again is chosen for its short burn time of 1.7 sec as well as a similar propulsive profile to ensure similar G-levels at takeoff and similar flight velocities between the subscale and full scale models. This model had a predicted and targeted altitude of 4900 ft. AGL. The recovery system for the subscale rocket is a dual deployment system, comprised of one drogue parachute (2ft elliptical) deployed at apogee and the main (10 ft. elliptical) deployed at 700ft AGL

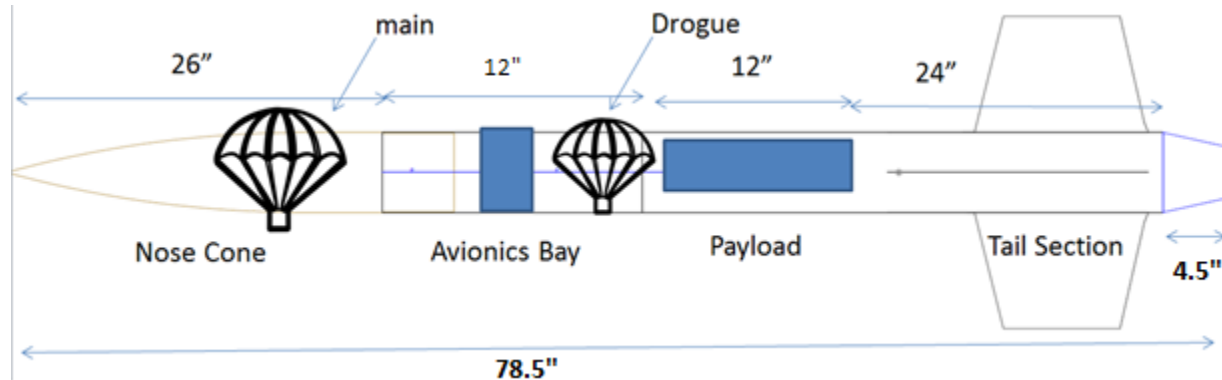


**Figure 2: Layout of the subscale vehicle**

From tail to tip, the rocket begins with a robust tail section, which is bolted to a 12" payload experimentation section. Above the payload are the drogue parachute, the avionics, the main parachute, and the nosecone. All sections are entirely carbon fiber composite with 1/16" thickness, with the exception of the polystyrene nose cone, which is extended with 10 inches of blue tube 2.0 to house the main parachute. Carbon fiber has been selected for its high strength to weight ratio, stiffness to weight ratio, flexibility in design and geometry, and workability.

## 2.3 Payload Summary

---

The Vanderbilt Aerospace Design Lab's rocket will carry a payload to test:

1. Liquid Fuel Tank Slosh Abatement System validated through in flight flow visualization supplemented by preliminary ground based drop testing and fuel injection experimentation
2. Performance analysis of a Green Monopropellant Hydrogen Peroxide Thruster
3. Structural Analysis of the launch vehicle in flight

The Lab's Liquid Fuel Tank Slosh Abatement System is designed to provide consistent, air-free fuel to the thruster under rapid deceleration. It is designed to safely maximize fuel extraction from a passive tank both in pulsed and continuous mode. The system will be evaluated through a linear spring and gravity based drop test stand and simultaneous flow visualization of two tanks during pre-competition flights with an onboard camera system to determine the best design.

The Monopropellant Thruster is designed to provide a constant thrust force after Main Engine Cutoff (MECO). It is designed to decompose a pressurized Hydrogen Peroxide fluid using an

iridium catalyst bed and output thrust through a specially designed nozzle. A ground based test facility, consisting partially of a strain gauge and fuel tank, will be used to evaluate the thrusters' performance before launch.

The structural analysis systems have the goal of developing a vehicle finite element model to represent the vehicle geometry, material properties, mass properties, and stiffness properties. This model will be correlated to in-flight accelerometer data and ground based modal impact test data to increase model certainty. The correlated model is then used to analyze vehicle stresses using flight data to understand loading cases, and low model uncertainty to optimize vehicle mass.

# *3 Changes Made Since Proposal*

---

## 3.1 Changes Made to Vehicle Criteria

---

The competition rocket dimensions have been optimized as follows:

- (i) Rocket length changed to 102" from 116"
- (ii) Pad weight 37.9 lbf. as opposed to 42.5 lbf.
- (iii) Cesaroni L 1720 instead of L 2375 motor
- (iv) Main parachute of 12 ft. elliptical instead of 12 ft. toroidal.
- (v) Monopropellant thrusters drag-camouflaged in tail section as opposed to flying outside to reduce vehicle drag and lower required motor impulse

## 3.2 Changes Made to Payload Criteria

---

The initial proposal had two potential designs for the fuel tank—one based on dynamics and one based on statics. The dynamic design has not changed. The static design has been altered to incorporate angled channels instead of vertical for surface tension effects. The validity of both of these designs for abating slosh will be tested during the subscale launch.

Another change since the proposal was the design and construction of the VADL Drop Test Stand. The design and results of this stand are detailed later in the design review (Section 5.3.1.3.4 VADL Drop Test Stand and Section 5.3.1.5 Relevancy of Data and Analysis). It consists of a spring and gravity accelerated platform with an accompanying frame that allows the simulation of negative gravity conditions similar to those experienced during flight. This will allow improved ground based testing speed and quality.

## 3.3 Changes Made to Project Plan

---

The team had previously planned on completing one subscale launch before the end of October. As the project developed, we have made the decision to push the launch date back to the middle of November. This will allow the team to verify all aspects of the rocket and payload before putting it through launch conditions. A comprehensive timeline reflecting this change is shown in section 6.2 of this document.

The team originally created a very comprehensive presentation for students at our educational outreach events. After the first event presenting to the Percy Priest Elementary School Encore Scholars, we quickly realized that such a comprehensive presentation was unnecessary and that a greater emphasis should be placed on interactivity. Subsequently, we substantially cut down the length and time required for the presentation portion of future events, leaving more time for the interactive fan-cart and bottle-rocket demonstration. These events are far more engaging for the students, and are also pertinent to their understanding of forces in relation to rocket flight.

The budgetary plan has been adjusted from the budget presented in the proposal. Travel expenses and experiments and bench scale testing have been decreased significantly to increase the amount allocated to payload components (fuel delivery system, monopropellant thruster, and structural health monitoring). A full breakdown of the budget and the budget distribution can be viewed in section 6.1.

# *4 Vehicle Criteria*

---

## 4.1 Selection, Design, and Verification of Launch Vehicle

---

### **4.1.1 Mission Statement and Mission Success Criteria**

---

#### **4.1.1.1 Mission Statement**

---

Our mission is to successfully build, test, and fly a rocket carrying multiple scientific payloads that will enable us to collect valuable data in flight. The first payload is a liquid fuel tank with an integrated slosh mitigation component that will ensure complete fuel extraction even when subject to microgravity by preventing the formation of air bubbles in the fuel lines. This specialized fuel tank will be vetted using a green monopropellant thruster that will generate a consistent, small amount of thrust if continuously fed its liquid fuel. Continuous decomposition in this case will signify to us that no air entered the fuel lines during flight. The second payload is a series of onboard sensors to gather structural health data and perform structural analysis.

#### **4.1.1.2 Requirements**

---

First and foremost, for the mission to be a success, it must be conducted in accordance with all NASA imposed requirements and regulations, from planning to construction to final execution. Beyond this however, the Vanderbilt Aerospace Design Lab has identified a list of additional requirements and mission success criteria.

##### **4.1.1.2.1 Launch Vehicle Requirements**

1. The rocket must be designed and built with all safety considerations, risk mitigation procedures, and environmental concerns in mind.
2. The launch vehicle shall be capable of being transported in sections and assembled on the launch site.
3. All pressure vessels must have a minimum factor of safety of at least 4 against all load cases and maximum expected operating pressure.
4. All payload components must be supported by internal structures anchored at bulkheads rather than directly to the rocket body.
5. No internal cavities in the launch vehicle shall be isolated from the atmospheric pressure (and thus create an inadvertent pressure vessel).
6. Cavities containing black powder charges must be isolated from all other components (excluding corresponding chute when applicable).
7. The launch vehicle must minimize unnecessary mass.
8. The aft section must be capable of withstanding high temperatures (200+°F) in order to withstand the recirculation of hot air during initial launch phase.

##### **4.1.1.2.2 Recovery System Requirements**

1. The launch vehicle shall incorporate redundant deployment charges and corresponding altimeter settings to increase vehicle reliability.
2. The launch vehicle shall cover all parachutes with a fire retardant blanket so as to mitigate fire exposure during deployment events.
3. The launch vehicle shall incorporate an anti-zipper design so as to avert a potential "zipper" effect that can result in damage to the rocket body. The main parachute and drogue parachute shroud lines can deploy with sufficient force to tear through the launch vehicle body tube. Such an event could cause severe damage to the launch vehicle, and thus, the launch vehicle could become non-reusable.
4. The altimeter arming switches must reside within the avionics bay and not within the chute compartments to prevent the switches or wires from being sheared off during chute deployments.

#### 4.1.1.3 Mission Success Criteria

---

##### 4.1.1.3.1 Launch Vehicle Mission Success Criteria

1. The launch vehicle must attain an altitude of 5280 ft. AGL  $\pm 150\text{ft}$ .
2. The fuel delivery system is activated at launch using 'g' detection.
3. The monopropellant thrusters are ignited during flight and thrust measured.
4. The drogue/main chute must deploy within 2.0sec after apogee is reached.
5. The landing speed of the rocket from the drogue parachute shall be around 70 fps to minimize drift.
6. The landing energy of the heaviest section be less than 75 lbf-ft.
7. All parts of the rocket are recovered and are launch ready within three hours.

##### 4.1.1.3.2 Fuel Tank Success Criteria

1. Hydrogen peroxide thruster fires and sustains thrust for no less than 5 seconds.
2. All designs and operations are focused on team safety.
3. Fuel is provided continuously to the thruster aided by the fuel tank slosh abatement system.
4. A majority of the 200cc tank's fuel is extracted during flight.
5. The system must be capable of venting if excessive pressures are reached in the fuel tank.
6. There must be a method to verify the functionality of the Slosh Abatement System.
7. The system must be accessible and secured while in the rocket and fit within the confines of the rocket geometry.
8. The system must be modular in design to enable simple troubleshooting, ease of installation, and performance upgrades.

##### 4.1.1.3.3 Monopropellant Thruster Success Criteria

1. Both thrusters generate 20N of consistent thrust for 5 seconds.
2. Data collection on thruster performance at altitude for the full thrust duration.
3. Full decomposition of hydrogen peroxide within the catalysts bed.
4. Standard operating procedures are followed for all Hydrogen Peroxide handling.

#### 4.1.1.3.4 Structural Analysis Success Criteria

1. No structural vehicle failures across all launches.
2. Accelerometers remain rigidly attached to rocket structure throughout takeoff, apogee, and landing.
3. Accelerometers collect usable data for the entirety of flight time.
4. Modal frequencies are within 15% between test and finite element models.
5. Modal Assurance Criterion is above 80% on diagonal and below 20% on off-diagonal terms in Cross-Orthogonality check between modal test data and Finite Element Model simulations.

## 4.1.2 Launch Vehicle Design

---

The Vanderbilt Aerospace Club's Student Launch vehicle has been designed to provide the testing environment for this year's various payload experiments and be successfully recovered so that it can be reused if desired. Our launch vehicle will have a body diameter of 5.5" and a total length of 102". The assembled weight of the vehicle will be approximately 38 lbs. All vehicle primary structures have been made out of carbon fiber for robust strength, stiffness, and formability properties at lightweight. The concept of flight operations is listed below.

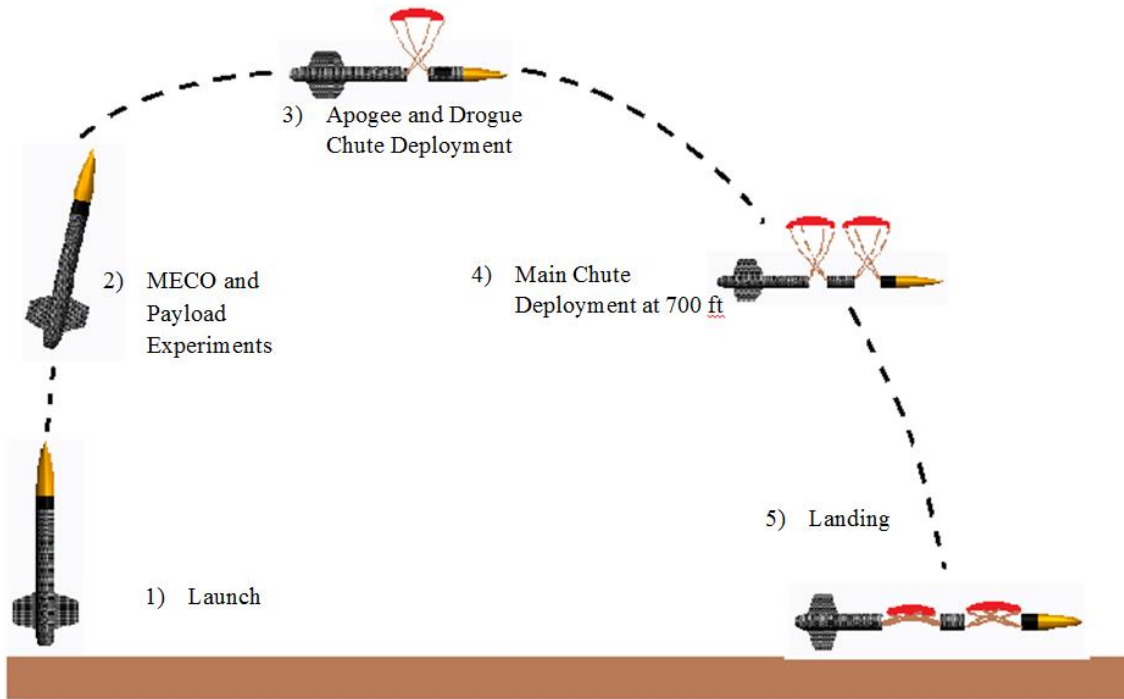


Figure 3: Concept of flight operations

The vehicle systems will be described in detail along with their functional requirements and performance characteristics. The systems are as follows:

1. Propulsion
2. Stability

3. Structures
4. Aerodynamics
5. Recovery

#### 4.1.2.1 Propulsion

---

The function of the Propulsion System is to launch the rocket from the ground into flight with the proper amount of thrust. The Motor, Motor Retention, and Launch-Rail Interface are the subsystems of the Propulsion System. The propulsion subsystems are described below.

##### 4.1.2.1.1 Motor Selection

Motor Selection is a critical first step in rocket design that directly impacts all subsequent design decisions. For this rocket, the chosen motor is a Cesaroni L1720 for its extremely fast burn time and high impulse. This motor's characteristics impose a large load on the rocket's structure, which will be discussed in subsequent sections.

##### 4.1.2.1.2 Motor Retention

The substantial force of the rocket motor on the rocket body (resultant from ~13-14 g's) necessitates a very robust motor retention system. This system not only has to withstand tremendous amounts of force but also must resist off-axis vibration to ensure straight flight.

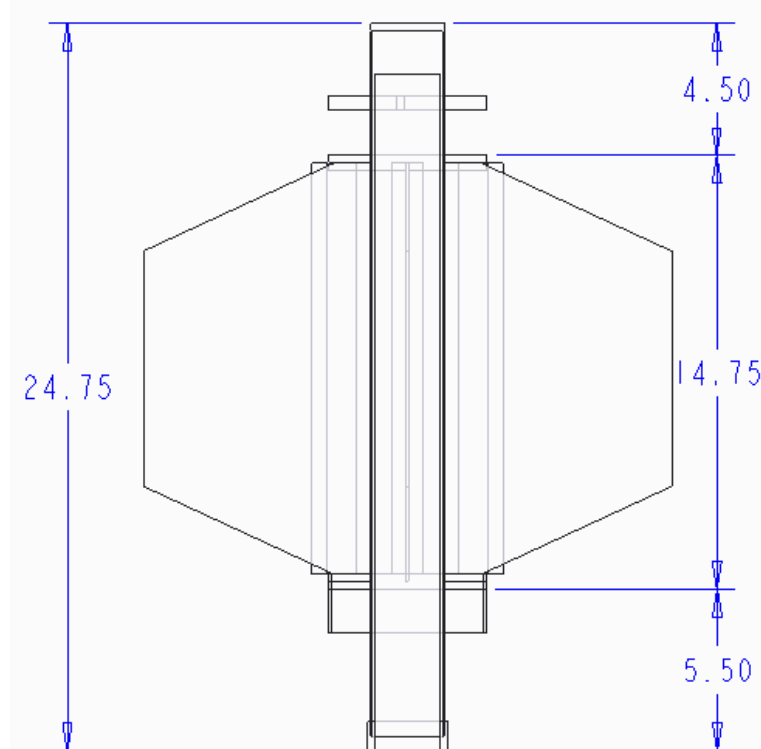


**Figure 4: Tail Section Schematic Demonstrating Motor Retention**

As can be seen in Figure 5, the motor tube transmits the force from the motor to the main body via the centering rings and fins. The centering rings are chemically etched with hydrochloric

acid and epoxied to both the motor tube and the main body. The fins are attached to the motor tube and the main body with two sets of carbon fiber fillets that are epoxied in place and cured in a vacuum.

The following block diagram shows how the force of the motor is transmitted throughout the rocket body:

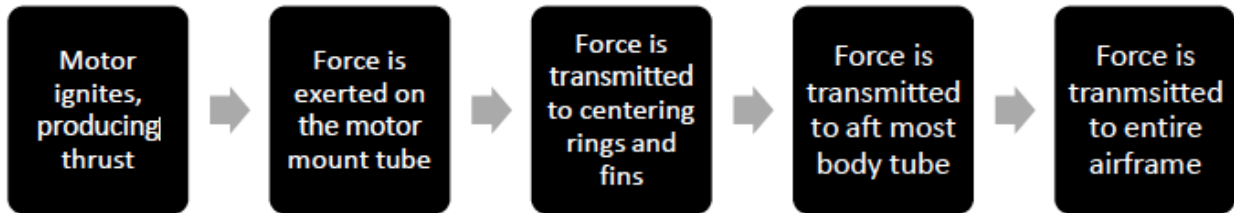


Figure 5: Block diagram of force transmission

The motor itself is held in the motor mount with a standard screw-cap positive retention system, which makes it impossible for the motor to come loose unexpectedly during flight or recovery. This transmits all of the motor force directly up the motor tube. The four rocket fins are mounted directly to the motor tube with carbon fiber fillets and stick through the tail section body tube, also attaching with carbon fiber fillets. The strength of the carbon fiber and large surface area of connection make this an effective mode of force transfer. Centering rings placed just fore and aft of the fins and attached to each with epoxy provide a backup mode of force transfer, and assist in precision fin alignment.

#### 4.1.2.1.3 Launch Rail Interface

We will be utilizing 1.5" I-shaped launch lugs that slide onto the launch rail. These will be purchased from Giant Leap Rocketry, are manufactured by Acme Conformal Rail Guides, and are made out of 6061-T6 aircraft aluminum. The base of the rail guide that interfaces with the rocket body tube will follow a 6.0" curvature (this has been shown to work for the 5.5" diameter rocket body tubes because the difference in arc length is not significant for the relatively small chord length covered by the launch lugs). The launch lugs will be permanently joined to the rocket body tube with JB weld after both the rocket body tube surface & the rail guides have been treated with 220 grit sand paper. This will ensure the JB weld has better penetration and bonding between the body tube and the launch lug. JB weld is chosen for its flexibility relative to epoxy, which will ensure resistance to small torsional loads applied while mounting the rocket to the launch-rail. The launch lugs will be spaced approximately 24" apart. They will be offset approximately 180° from the payload access window. The tail fin section launch lug will be installed with precise measurements that guarantee the launch lugs are located halfway in between the two fins that correspond to the side opposite the payload window. Then, two aluminum L-rods will be held in place that give machined straight lines for insertion of the second launch lug which is located on the payload section. This rig will help verify that a straight line connects both launch lugs, and that there will not be misalignment issues.

#### 4.1.2.2 Stability System

---

The Stability System ensures that our rocket will fly as high as desired and as straight as possible. The two subsystems that affect Stability are Rocket Fins and Mass Adjustments. The stability subsystems are described below.

##### 4.1.2.2.1 Fins

Symmetry is essential in the design of the fins because an asymmetric design would generate a moment about the center of mass of the rocket. This symmetric design is possible with three fins, but much more feasible with four fins. Thus, we decided to build the four fin design using a jig to ensure that the fins are mounted at perfect right angles to each other.

The strength of these fins and this “through-the-wall” design, along with the suitability of the material, has been verified through previous years’ experiences and tests. This year’s team will verify this specific design and our construction techniques through a full-scale test flight before the competition. This year’s team will also test this design during a subscale launch before competition. The fin stability system will be successful if (i) there is no visible damage to the fins upon recovery (cracks, breaks, chips, etc.), and (ii) the trajectory of the rocket is largely straight and vertical.

The fins for the rocket are important to both stabilizing rocket flight and transmitting the motor thrust to the main body of the rocket. To achieve high strength and robustness, the fins will be constructed from Dragon Plate 1/8” quasi-isentropic carbon fiber sheet. The material was selected for its strength, rigidity, precision when forming, and light weight. Carbon fiber in general offers a huge advantage with its unparalleled strength to weight ratio. Fin material will be ordered in premade sheets and water-jet cut to shape as specified by our CAD drawings.

For the assembly of fins the motor tube, a jig has been constructed, as shown below. The panels are all laser cut, and are held together by adjustable nuts on four threaded rods. This allows the location of the fins to be precisely adjusted and then rigidly locked into place, assuring the fins are at the correct height, radial location, and angle.



**Figure 6: Fins and motor tube are inserted into lower half of jig**



**Figure 7: Top two plates of jig are assembled**

The attachment of fins will follow the same procedure as construction of the subscale rocket, detailed here and pictured below. After sanding and cleaning all surfaces, the fins were attached to the motor tube with an epoxy fillet along the edges of the fin pressed against the motor tube. This provided initial stability, as well as a built up corner for our next carbon fiber layup, reducing the eventual stress concentrations along the joint. While still in the jig, the carbon fiber fillets were added. This consisted of two layers of carbon fiber running from the bottom of one fin, across part of the motor tube, and up the adjacent fin. Additional carbon fiber strands were added in the corner of the joint to again build up the fillet before the layers of fabric were added. Once the carbon fiber was populated with epoxy, it cured under vacuum compression. As shown in the figure below, each of the four sections was covered by a breather and a bleeder, with the bagging material sealing to the rocket body with sealant tape. One vacuum pump was used for

the entire setup, so that all fillets could cure at the same time. Slots cut into the body tube allow it to be slid over the fin and motor tube assembly. The process of applying carbon fiber fillets is again repeated between the body tube and the “through-the-wall” portion of the fins.



**Figure 8: Initial epoxy fillet once cured**



**Figure 9: Populating the carbon fiber fillets with epoxy**

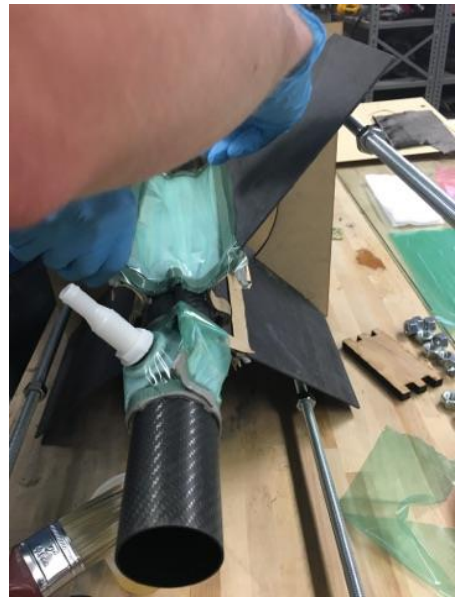


**Figure 10: Preparing vacuum bag over one section of fillets**



**Figure 11: Fin and motor tube assembly curing inside of jig**



**Figure 12: Complete fin and motor tube assembly slid into body tube**

#### **4.1.2.2.2 Mass Adjustments**

The rocket will be constructed pursuant to the designs presented in this document. However, after fabrication of the rocket and payload are complete, the mass of each section and major component will be measured in order to better determine the location of the CG. If the CG is not within a 2" vertical window of the current calculated CG location, ballast mass may be added to compensate. More information on the CG and Stability Margin can be found in section 4.4.2: *Simulations and Predictions* of this report.

#### **4.1.2.3 Structural Systems**

---

The Structural Systems of this rocket allow the rocket to maintain its shape and integrity even through post-launch descent. The structures also provide for payload support and integration. The structural subsystems include the Rocket Body Tube, Tube Coupling, and Payload Integration. The structural subsystems are described below.

##### **4.1.2.3.1 Rocket Body Tube**

In past years, Vanderbilt has used Blue Tube, a durable paper-based material for model rocketry, for its rocket body tubes. However, this year the rocket will use a higher impulse motor, increasing the launch loads significantly. Using carbon fiber, with its high strength to weight ratio, upgrades the overall rocket structure to match these new loads. Carbon Fiber construction parallels the structural analysis payload allowing for addition of fibers and material in areas of high stress and removal of thickness and strength where mass reduction can be achieved. These initiatives complement each other by allowing for the challenging modeling of anisotropic materials to enhance the structural analysis payload, and the certainty of mission success in vehicle design. In addition, carbon fiber is an emerging aerospace industry standard, while blue

tube is a material limited mainly to applications in model rocketry. Verification of the carbon fiber tubing is given in section 4.1.3.3.1 *Rocket Body Tube Verification*.

There are four main sections of the rocket: tail section, payload section, avionics section, and nosecone. The **tail section** is primarily responsible for transmitting thrust loads from the motor to the rest of the rocket. It will contain the fins, motor mount, motor retention, and payload thruster, coming to a total length of 28.5". Forward of that will be the **payload section** itself, rigidly bolted to the tail section. Inside the 12" section of body tube, the payload bay will contain the internal payload equipment and electronics. The **forward section**, or avionics bay, is made of a 12" body tube and holds the avionics and drogue parachute, placed on the payload section side. The upper most section is the **nose cone**, which is discussed in more detail in 4.1.2.4.1, along with the placement of the main parachute inside of it.

Carbon fiber tubes will be purchased from a manufacturer, with the body tubes having an outer diameter of 5.5". The cutting of carbon fiber is currently done with a handheld Dremel and a Perma-Grit tungsten carbide abrasive tool. This can be used to cut section lengths, fin slots, and windows. A standard operating procedure has been developed for carbon fiber cutting and dust producing operations. To achieve perfectly clean surfaces, especially for mating sections of tube, additional sanding can be performed if any edges do not align.

#### 4.1.2.3.2 Tube Coupling

Since the rocket design calls for three body tubes that must separate during the recovery phase, there must be an adequate system for keeping the different sections together during ascent. This is possible through coupling of the separate tube partitions.

Tube coupling will be achieved by using slightly smaller diameter carbon fiber coupler tubes. With an outer diameter of ~5.35", these tubes fit snugly into the main rocket body tubing. A 19.5" section of coupler tube will be cut and slid into the payload section of the rocket to join all three main sections together. It will be bonded to the payload section body tube with West Systems 105 Epoxy, due to its excellent adhesive properties on composite materials, leaving a 3.75" flange on either side of the body tube. Once cured, the body tubes of the forward section and tail section will be slid over the coupling flange and aligned with the payload section. Four  $\frac{1}{4}$ " holes will be drilled 90° apart for the bolts that will join tail section to the payload section. Proper alignment is important for a tight fit to ensure rocket stability, and will be achieved by drilling holes while sections are mated for perfect alignment. Aluminum nuts set into curved wooden fittings will then be epoxied to the inside of the holes of the coupling section using Devcon 2-ton epoxy due to its strong adhesion with both ferrous and non-ferrous metals. Low profile aluminum bolts will be anchored in these nuts during final assembly to secure the payload and tail section. To attach the forward section, 3 7/64" holes will be drilled 120° apart while the forward section and payload section are mated. Three small shear pins will be placed in these holes to temporarily hold the two sections together during flight before charges in the forward section blow, causing the shear pins to break and the two sections to split apart, releasing the drogue parachute. By using bolts and shear pins, sections can be quickly assembled and disassembled while remaining secure in flight.

#### 4.1.2.3.3 Payload Integration

The payload bay also houses structural components of the rocket. Refer to section 4.5.1 *Payload Integration Plan* for a detailed description and analysis of the payload integration.

#### 4.1.2.4 Aerodynamics Systems

---

The aerodynamic subsystems include the rocket's nose cone and tail cone. These subsystems give the rocket an aerodynamic advantage and are described below.

##### 4.1.2.4.1 Nose Cone

The purpose of the nosecone is to add an aerodynamic shape to the forward end of the rocket, reducing drag. The nosecone is attached to the rocket via 4-40 nylon shear pins, as well as to the main parachute shock cord. The nosecone is a tangent ogive-shaped plastic nosecone from LOC precision rocketry. This selection for material and shape have been tested and verified by previous years' experiences, and will be ensured once again during the full-scale test launch. Using a heritage nose cone allowed for reduction of monetary and scheduling costs while ensuring no risk is added to the vehicle.

In addition to lending an aerodynamic profile to the rocket, the nose cone will also house the main parachute and deployment charges. The parachute will be wrapped in a large fire blanket to protect it from the heat of the deployment charges. Additionally, the parachute assembly's shock chord will be tethered via bulkhead mounted U-brackets and locking carabiner to both the nose cone and the avionics bay. The bulkhead mounted inside the nose cone tip consists of two laser cut birch plywood rings, one with an outer diameter of 4" and the other 4 1/2". They are tied together by 1/4"-20 threaded aluminum rods and nuts. Aluminum U-bolts are bolted into the larger bulk head then the bulkhead assembly is epoxied to the inside of the nosecone with 2-ton Devcon epoxy and later filleted with the same epoxy. The reason for the two piece bulk head is to provide more surface contact between the bulkhead and the nosecone for the epoxy to bind. It is crucial that the main parachute does not rip the bulk head out of the nose cone upon deployment.

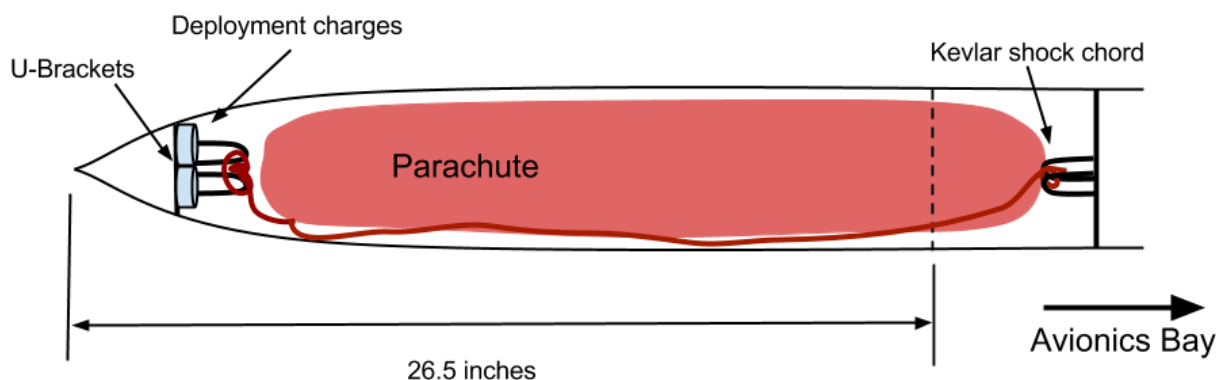


Figure 13: Nose cone with parachute packing

##### 4.1.2.4.2 Tail Cone

Basic fluid dynamics establishes that any drastic cross section change along the rocket will increase the drag profile of the body. In order to reduce this effect on the base of the rocket a tail

cone was added with a diminishing cross sectional area so that the rocket body tube is more streamlined. The end of the tail cone in the subscale design extends 5.5" past the end of the tail-section's carbon fiber and is slightly regressed from the motor exit nozzle. The post fin region is where the tail cone resides. It will be able to withstand the short duration of high temperature air just before takeoff. Following the loading of the motor and its assembly, the tail cone is affixed to the main tail section using four expanding plastic rivets.

The team-designed tail cone for the subscale launch was laid up out of 6 layers of 3k 5.7 oz 2x2 twill carbon fiber cloth and Fiber Glast System 2000 epoxy resin (see epoxy resin standard operating procedure in appendix). The part was cured in a vacuum bag at room temperature in a 2 piece female split mold.



**Figure 14: Tail cone mold making**

After designing the tail cone in Creo Parametric, the team utilized rapid prototyping technology to 3D print the boat tail geometry to produce a master upon which to build the female mold around. To surface finish the part, sanding with 200 grit, 400 grit, and 800 grit sandpaper was done, and the mold was waxed and buffed with 3 coats of Mequiar's Mirror Glaze. As seen in the figure above, a 1/4" piece of acrylic was laser cut to fit the outer geometry of the tail cone. This acrylic is used to make the flanges of the 2 piece mold. 7 locator notches were added circumferentially around the cone to allow for fitting the two pieces of the mold together. Orange tooling gel coat was applied in a thick layer to the master male mold and the acrylic and allowed to form. After this was solidified, 2 layers of fiberglass and polyester resin (see polyester resin standard operating procedure in appendix) were added to complete the first half of the mold. After allowing for the polyester resin to cure, the half was split from the acrylic, and the same process was repeated to create the second half of the female split mold.



**Figure 15: The tail cone mold in the trimming stage**

After this was complete, the edges of the mold were trimmed to create a solid compact mold. In the above figure, the top half of the mold has been trimmed, and the excess tooling gel coat from the other half is visible. Upon full trimming the mold was split from the 3D printed master tail cone geometry.



**Figure 16: The two halves of the mold split**

The mold was completed with adding more layers of wax to the layup surface and adding holes for bolting the two halves together. The next step in tail cone fabrication was to perform the carbon fiber wet layup. 6 plies of fabric were chosen to reach the target wall thickness of 1/16". We chose to use 4 pieces of carbon fiber per layer to optimally conform to the geometry. A template for one of these pieces can be seen below.



**Figure 17: Template for carbon fiber to make the tail cone**

These fibers were laid up sequentially in the tail cone mold using System 2000 resin and 120 minute hardener. The tail cone is comprised of 24 pieces of carbon fiber forming 6 layers of thickness, and all seams were offset to improve strength and uniformity of thickness. All layers were applied in a single layup process to maximize layer bonding and part strength. The next step was the addition of perforated peel ply to allow for excessive resin to escape the part and for easy demolding. After peel ply, breather/bleeder material was added to allow a uniform vacuum to be pulled and to absorb excess resin, and then finally Stretchlon 200 vacuum bag was placed over the whole mold.



**Figure 18:** Tail cone layup with peel ply and some breather added



**Figure 19:** Tail cone in the vacuum bag

The assembly in the above figure was connected to our vacuum pump and cured for 3 days. The piece was split from the mold by removing the vacuum, the bag, the breather and peel ply, and working the mold off of the piece after removing the mold bolts. The part split from the mold is shown below on the right.



**Figure 20:** The tail cone layup (right) after being split from the mold

The final step was to trim the excess material and check the fit with coupler tube.



**Figure 21:** The complete carbon fiber composite tail cone

For the full scale launch, a similar process will be used to create a tail cone with a complex adaptive geometry to accommodate gas thrusters in the aft of the tail section while still providing aerodynamic shrouding.

#### 4.1.2.5 Recovery

---

The function of the Recovery System is to ensure a safe landing of the vehicle after rocket flight. This is accomplished with three subsystems: the Drogue Parachute, the Main Parachute, and the Recovery Electronics. The recovery system will be discussed in detail in section 4.3 *Recovery Subsystem* of this document.

## **4.1.3 Performance Characteristics and Verification of Systems**

---

### **4.1.3.1 Propulsion Verification**

---

#### **4.1.3.1.1 Motor Retention Verification**

The motor retention subsystem is a mission critical component that must support a peak acceleration of  $\sim 13$  g and accompanying amplified load of the weight of the rocket motor. The motor retention system that will be used has successful heritage with several other previous Vanderbilt teams (including the USLI 2014 and 2015 teams). Additionally, the system will be verified with two full scale launches prior to the USLI competition in April. The motor retention system will be judged successful if it fulfills the requirements in section 4.1.2.1.2 *Motor Retention* of this report.

#### **4.1.3.1.2 Launch Rail Interface Verification**

The launch-rail interface will be verified by placing the launch vehicle on the launch rail. If the launch vehicle is perpendicular to the launch pad for the entire length of the rocket, then the launch lugs are aligned properly. This will be confirmed via geometric measurements that form two lines along the launch pad and launch vehicle. Through this process, a reference orientation may be established. If the lines have slopes such that they are the negative reciprocals, mathematically, they must be perpendicular.

### **4.1.3.2 Stability System Verification**

---

#### **4.1.3.2.1 Fin Assembly Verification**

There is successful heritage on previous Vanderbilt USLI teams on this type of fin assembly. Also, there will be one full-scale launch vehicle flight that will visibly validate that there is no noticeable launch vehicle spin during flight.

#### **4.1.3.2.2 Mass Adjustments Verification**

The vertical location of the center of gravity will be determined with the tip of the nose cone as the origin and measuring each individual sections' and large components' mass and distance from this point. From this, the center of gravity with respect to the vertical orientation of the rocket can be calculated.

### **4.1.3.3 Structural Verification**

---

#### **4.1.3.3.1 Rocket Body Tube Verification**

Since the rocket body tube will experience its largest compressive forces during motor burn, with the weight of the rocket pulling it down and the thrust of the motor pushing up, the compressive strength of the carbon fiber tube material must be considered. These specifications for the 5.5" diameter carbon fiber tube cannot be easily found online, so to be completely sure of its load carrying ability, the rocket body tube sections have been placed in a load cell and tested for their ultimate compressive strengths. The load cell used for testing is located in the Material Science Laboratory on campus. A 12" section has been compression tested in the Vanderbilt Materials Science hydraulic press.

The load frame engaged previously unknown failsafe measures, halting the test after reaching only 17810 lbs., and before the tube reached failure. Extrapolation of this preliminary data shows that a 12" section of body tube will not reach yielding (with a criterion of 1.75% strain) until a compressive force of 43590 lbs. is applied. For a 25lbs. rocket undergoing 14g acceleration, this translates to a safety factor of over 120.

#### 4.1.3.3.2 Tube Coupling Verification

The coupling of the three sections will be tested first during deployment tests and then through the one full-scale launch scheduled before the final launch in competition. This will ensure that the sections joined by the  $\frac{1}{4}$ "-20 bolts do not fail, and the tail section and payload section maintain rigid connection throughout the entire flight and recovery stages. Also, the deployment tests will prove the reliability of the shear pins to hold until the drogue charges are blown. These methods have proven successful for past teams, which is why they have been incorporated into this team's design as well.

#### 4.1.3.3.3 Payload Integration Verification

The deployment tests and the two test launches will verify that the retention ring system works properly, and that the H<sub>2</sub>O<sub>2</sub> fuel tank and the air tank do not come loose throughout flight and recovery. This design has a successful heritage proven in past SL competitions.

The two test launches will also verify that the thruster housings and electronics bay are sufficiently secure and strong enough to withstand the drag forces experienced during flight. This design has also been proved successful by past teams who used the same mounting system.

**Table 1: Summary Table for the Vehicle Systems**

System	Brief Description	Functional Requirements and Performance Characteristics	Verification Metrics
<i>Airframe and Fin Assembly</i>	The design of the fins and how they will be mounted to the rocket body, as well as the structure of the airframe.	Must be structurally sound, resist flutter, and produce stable flight.	Computer analysis, sound construction methods, final test with full-scale test launch.
<i>Motor Retention</i>	How the motor is held in the rocket body and able to transmit thrust to the airframe.	Must be structurally sound and not allow the motor to move relative to the airframe for the duration of the flight.	Sound construction methods, can be tested with sub-scale and full-scale test launch.
<i>Tube Coupling</i>	The method of attaching one body	Must be structurally sound and not allow any significant bending of	Sound construction methods, ground testing, sub-scale and full-scale test

	tube to another.	the airframe. Must also house payload, payload electronics, and avionics.	launch.
<i>External Payload Mounting Equipment</i>	The method of attaching the external elements of the payload to the rocket body.	Must be structurally sound and aerodynamically shaped but still allow for scientific instrumentation.	Stress analysis on components for forces experienced during 13g launch, with significant factor of safety built in, also tested during sub-scale and full-scale test launch.
<i>Avionics and Avionics Bay</i>	The electronics and electronics housing associated with the parachute deployment system.	Must be a redundant system that successfully deploys the two parachutes at the appropriate times during rocket flight.	Ground testing to ensure electronics are in working order and will act appropriately to deploy recovery system. Will also be tested during full-scale test launch.
<i>Recovery</i>	The parachute system that ensures safe recovery of the rocket and all of its components.	Must deploy drogue parachute at apogee and main parachute at pre-set altitude. Must produce descent rates within the range allowed by the rules of competition. All sections must remain under parachute for the duration of the descent.	Will be subject to extensive ground testing for black powder charge sizing, as well as shear pin size and count. System will be tested during full-scale test flight.
<i>Internal Payload Mounting Equipment</i>	The equipment and method required to secure all internally mounted payload elements.	Must not allow for motion of any part during rocket flight. Must allow for delivery of pressurized fuel to the ramjet engine at the appropriate time. Must safely vent pressure during inactive phase while waiting for launch.	Extensive ground testing and mathematical analysis. Completely tested during full-scale test launch.
<i>Payload Electronics and Payload Electronics</i>	The electronics and electronics housing required to actuate, instrument, and measure payload	Must be a redundant system capable of accurately starting and measuring the thrust produced by the ramjet	Subject to extensive ground testing to ensure that electronics are functioning properly and will make accurate measurements.

<i>Bay</i>	scientific criteria.	engine. Must be structurally sound so that no components move during rocket flight.	Timely activation of instrumentation and actuation will be tested during full-scale test flight.
<i>Nosecone</i>	The fore-most part of the rocket body.	Must be aerodynamic and structurally sound.	Computer simulation and full-scale test flight.
<i>Launch Rail Interface</i>	The method and equipment required to mount the entire rocket to the launch pad.	Must allow for smooth transition to flight following motor ignition.	Physically tested with the launch pad/rail once the rocket is fully assembled.

#### 4.1.4 Vehicle Verification Plan and Status

This section will address each of the rules of the competition in terms of what the verification plan is and the current status of that plan.

3. Competition and Payload Requirements				
Each team shall choose any 2 payloads from Task 1, or have the choice to participate in the Centennial Challenge competition (Task 2).				
<table border="1"> <thead> <tr> <th>Task 1 (select any 2)</th> <th>Task 2</th> </tr> </thead> <tbody> <tr> <td>           3.1.1 Atmospheric Measurements            3.1.2 Landing Hazards Detection            3.1.3 Liquid Sloshing in Micro-G            3.1.4 Propulsion System Analysis            3.1.5 Payload Fairing Design and Deployment            3.1.6 Aerodynamic Analysis            3.1.7 Design your own (limit of one)         </td><td>           3.1.8 Centennial Challenge – MAV         </td></tr> </tbody> </table>	Task 1 (select any 2)	Task 2	3.1.1 Atmospheric Measurements 3.1.2 Landing Hazards Detection 3.1.3 Liquid Sloshing in Micro-G 3.1.4 Propulsion System Analysis 3.1.5 Payload Fairing Design and Deployment 3.1.6 Aerodynamic Analysis 3.1.7 Design your own (limit of one)	3.1.8 Centennial Challenge – MAV
Task 1 (select any 2)	Task 2			
3.1.1 Atmospheric Measurements 3.1.2 Landing Hazards Detection 3.1.3 Liquid Sloshing in Micro-G 3.1.4 Propulsion System Analysis 3.1.5 Payload Fairing Design and Deployment 3.1.6 Aerodynamic Analysis 3.1.7 Design your own (limit of one)	3.1.8 Centennial Challenge – MAV			
3.1. The payload shall be designed to be recoverable and reusable. Reusable is defined as being able to be launched again on the same day without repairs or modifications.				

Figure 22: General payload requirements

A color coding system has been developed for the verification statuses listed below. Green means that the verification plan is complete. Yellow means that the verification plan is currently in progress. Red indicates that the verification plan is currently incomplete.

Table 2: Review of requirements and verification plan

Requirement	Verification Plan	Status
The launch vehicle shall fly a science or engineering payload.	The VU Aerospace Club has chosen a monopropellant thruster, liquid slosh abatement	The payload is currently in the development and

	in Micro-G, and structural analysis payloads to meet and verify NASA Student Launch Science requirements.	testing phase of design.
The launch vehicle shall fly to the predicted altitude.	Computer simulation along with flight testing will verify that the design meets this altitude requirement.	Computer simulation has given a weight estimate that our rocket must approach for the motor that we have selected.
The vehicle shall carry one PerfectFlite Stratologger or ALT 15 altimeter for recording of the official altitude used in the competition scoring.	Perfect Flight Stratologger altimeters will be purchased and one will be designated as responsible for recording the official competition altitude.	Complete. Altimeters have been purchased, designated, and tested.
<b>The recovery system shall have the following characteristics:</b>		
The recovery system shall be designed to be armed at the pad.	There will be arming, screw-style switches that will be mounted such that they can be engaged while the rocket is standing on the pad.	Complete
The launch vehicle shall stage the deployment of its recovery devices, where the drogue parachute is deployed at apogee and a main parachute is deployed at a much lower altitude.	This will be controlled by the altimeters and black powder charges. These will be ground tested prior to launch, and confirmed through full-scale flight testing.	Electronics have been tested. Parachute needs testing.
At landing, each independent or tethered section of the launch vehicle shall have a maximum kinetic energy of 75 ft-lbf.	This will be demonstrated through computer simulations, and verified with full-scale test flight.	Computer simulations have been completed, and a subscale flight test will occur on November 14, 2015
The recovery system electronics shall be completely independent of the payload electronics.	The recovery system electronics and payload electronics are housed in different coupler sections in the rocket body.	Complete

The recovery system shall contain redundant altimeters.	There will be two sets of redundant altimeters, each pair controlling a separate black powder charge.	Complete
Each altimeter shall be armed with a dedicated arming switch.	The arming switches are mounted on the rocket body and each one will activate its own altimeter.	Complete
Each altimeter shall have a dedicated power supply.	There will be a 9V battery controlling each altimeter (4 of them). These will be wired such that the circuit is completed when the arming switch is engaged.	Complete
Each arming switch shall be accessible from the exterior of the rocket airframe.	The arming switches are mounted externally on the rocket body with epoxy. They can be accessed when the rocket is upright on the launch pad.	Complete
Each arming switch shall be capable of being locked in the ON position for launch.	This requirement of the arming switches has been tested by previous years, and will be tested by this year's team during the full-scale launch	Complete
Removable shear pins shall be used for both the drogue and main parachute compartments.	The number and size of shear pins to be used will be determined through mathematical analysis and then confirmed with ground testing, and eventually full-scale flight testing.	Mathematical analysis has been complete. Ground testing will occur prior to the subscale flight, and full-scale flight testing will occur in February, 2016
An electronic tracking device shall be installed in each independent section of the launch vehicle and shall transmit the position of the independent section to a ground receiver.	There will be a radio transmitter that will be tested on the ground to ensure functionality. It will also be tested with the full-scale test launch.	Incomplete

The recovery system electronics shall be shielded from all onboard transmitting devices.	This will be ground tested to ensure that the electronics experience no interference from transmitting devices and do not prematurely set off black powder charges or have disrupted pressure readings.	Incomplete
The launch vehicle and payload shall be designed to be recoverable and reusable.	The vehicle is design with a recovery system. The effectiveness will be modeled mathematically, and confirmed through full-scale test flight.	Computer simulations are complete. The full recovery system has yet to be tested.
<b>The Payload shall have the following characteristics:</b>		
A payload component investigating liquid sloshing in microgravity to support liquid propulsion system upgrades and development shall be included.	A liquid slosh-abatement monitoring system will be built and incorporated into the rocket.	In Progress
A payload component investigating structural and dynamic analysis of the airframe, propulsion, and electrical systems during boost.	A series of accelerometers will be placed at key points along the rocket to collect data.	Accelerometers have been acquired and are currently being calibrated and ground tested.
The launch vehicle shall be capable of being prepared for flight at the launch site within 2 hours, from the time the waiver opens.	This will be ensured by using a procedural checklist and being prepared to assemble the rocket prior to arriving at the field on competition day. Also, the team will practice set up during the full-scale test launch	Complete
The launch vehicle shall be capable of remaining in launch-ready configuration at the pad for a minimum of one hour without losing the functionality of any on-board equipment.	The life-span of the batteries controlling the equipment will be tested such that no functionality will be lost after at least one hour of pad time.	Incomplete. Will be verified before full-scale flight.

The launch vehicle shall be launched from a standard 12 V firing system (provided at the Range) using a standard 10 s. countdown.	This is a standard design feature, and will be tested during the sub-scale and full-scale test launch.	Complete
The launch vehicle shall require no external circuitry or ground support equipment to initiate the launch.	This will be confirmed by the final design of the rocket. All actuations and measurements will be made on-board without the assistance of ground based equipment.	Incomplete
Data from the payload shall be collected, analyzed, and reported by the team following the scientific method.	The team will have practice collecting, analyzing, and reporting data from the various ground testing throughout the year, as well as from the extensive education we have all received on the subject of the scientific method.	Incomplete.  Will be completed following the subscale launch scheduled for November 14, 2015.
The launch vehicle shall use a commercially available solid motor propulsion system using ammonium perchlorate composite propellant which is approved and certified by NAR, TRA, and/or CAR.	The motor we choose must meet this requirement and be approved by NASA.	Complete.  The selected motor is the Cesaroni Pro-75 L1720, which meets this requirement.
Pressure vessels on the vehicle should be approved by the RSO and meet NASA safety criteria.	The on-board fuel tank that we design must meet these safety requirements and be reviewed by our safety officer and by NASA.	In progress
All teams shall successfully launch and recover their full scale rocket prior to FRR in its final flight configuration.	This will be confirmed by conducting a full-scale test launch prior to launch, and successfully recovering the rocket in its entirety with no significant damage.	Incomplete.  Full-scale test will take place in February, 2016

Each team shall use a launch and safety checklist.	The launch and safety checklist will be completed once the specific integration designs for the payload are completed.	Complete
Students on the team shall do 100% of the work on the project.	The rocket and payload will be completely designed and built by student members.	In progress
The rocketry mentor supporting the team shall have been certified by NAR for the motor impulse of the launch vehicle, and the rocketeer shall have flown and successfully recovered a minimum of 15 flights.	Robin Midgett has flown at least 20 flights that qualify for this requirement and he is certified by NAR Level II for the motor impulse of the launch vehicle.	Complete

## 4.1.5 Vehicle Development Risk and Risk Mitigation

---

### 4.1.5.1 Risk Assessment Matrix

---

In order to fully assess the risks associated with the launch, we have developed a risk assessment matrix that categorizes and ranks all risks according to their likelihood of occurrence and severity of consequence. Likelihood of occurrence is given a rating from 1 – 5 with 1 being the least likely and 5 the most. The corresponding designations for each in order from 1 – 5 are **rare, unlikely, moderate, probable, and very likely**. The consequence is given a rating from A – E with A being the least consequence and E being the greatest. The designations for each in order from A – E are trivial, minor, moderate, high, and critical. When each scale is set up in a matrix, a combination of the two values can be very enlightening as to the relevance of the risk.

Interpreting the risk designation is also quite intuitive since low alphanumeric combinations correspond to the least worrisome risks while high alphanumeric combinations represent larger risks.

Color-coding has also been added to the matrix to designate which risks require mitigation of some sort. Risks highlighted in green are considered low risk and either require no mitigation or have no reasonable means of additional mitigation. These have either a very low risk of occurrence or the consequence of occurrence is so small that serious consideration to mitigate the risk is not necessary. Risks highlighted in yellow and considered moderate risks and should be mitigated in some way however possible, but the overall risk posed to the mission and safety of those involved has been deemed acceptable. Risks highlighted in yellow are more serious than those in green and can have serious consequences on the success of the mission or the safety of those involved, but the combination of their occurrence and consequence ratings places them in the middle of the matrix. This means that the risk to mission success or injury is either fairly low/unlikely or that the risk has been mitigated in some way to bring it down from the most serious category. The most critical category is highlighted in red, signifying that these are the

most hazardous risks to either mission success/personal safety or have the greatest likelihood of occurrence. These risks are deemed unacceptable and must be mitigated in some way for the rocket/payload to be safe to launch. In the tables outlining risks for the various sections/payloads of the rocket, no risk can be classified with a red rating post-mitigation.

	Consequence					
Likelihood		Trivial	Minor	Moderate	High	Critical
	Rare	A1	B1	C1	D1	E1
	Unlikely	A2	B2	C2	D2	E2
	Moderate	A3	B3	C3	D3	E3
	Probable	A4	B4	C4	D4	E4
	Very Likely	A5	B5	C5	D5	E5

Figure 23: Risk assessment matrix

The explicit meanings of each likelihood and consequence rating are outlined as follows:

### Likelihood

- Rare (1) – Chances of occurrence are almost non-existent. Mitigation need only exist for the most critical risks.
- Unlikely (2) – Chances of occurrence are very low but do exist. Mitigation should exist for high-risk consequences.
- Moderate (3) – Chances of occurrence are moderate. Mitigation should exist for all risks resulting in greater than minor consequence.
- Probable (4) – Occurrence is more likely than not. Mitigation should occur for all but the most trivial risks.
- Very Likely (5) – Occurrence is to be expected. Mitigation is required for all but the most trivial risks.

### Consequence

- Trivial (A) – Occurrence of risk results in no effect on rocket/payload performance or safety of all persons involved. No mitigation is needed.
- Minor (B) – Occurrence of risk results in minor damage that is either easily repairable or has no effect on rocket/payload performance. No risk for injury to persons involved. Mitigation should exist for the most likely risks.
- Moderate (C) – Occurrence of risks results in some damage to rocket/payload that could negatively affect performance and/or result in minor injury to persons involved. Mitigation should exist for most risks.
- High (D) – Occurrence of risk results in major damage to rocket/payload that will negatively affect performance and/or result in serious injury to persons involved. Mitigation should exist for all but the rarest risks.

- Critical (E) – Occurrence of risk results in catastrophic damage to rocket/payload that will eliminate performance capability and/or result in serious injury/death to persons involved or bystanders. Mitigation must exist where possible.

### **Combined Rating**

- Low (Green) – Risk falls within an acceptable range of probability and consequence. Mitigation strategies should be implemented if possible but are not mission critical.
- Moderate (Yellow) – Risk should be evaluated for potential mitigation strategies.
- Critical (Red) – Risk has an unacceptable level of likelihood and consequence. Mission should not proceed until viable mitigation strategies are created and implemented.

#### 4.1.5.2 Vehicle Development Risk Table

---

All risks recognized by members of the team have been recorded and evaluated by the safety officer. Each risk has been given a risk assessment rating prior to any mitigation as well as post-mitigation in order to quantify the steps taken by the team in designing and fabricating the rocket/payloads to make it as safe and reliable as possible. In all following risk assessment tables, each risk has been outlined along with possible causes, overall effect to the rocket/payload, mitigation strategy, verification of implemented verification strategies, and two risk assessment values for pre- and post-mitigation that have been color-coded for easy comparison.

**Table 3: Vehicle Development Risk Table**

Project Management Risk and Mitigation				
Risk	Overall Effect	Risk Rating	Mitigation Strategy	Post-Mitigation Risk Rating
Unavailability of parts or delays in parts delivery	Cause delays in construction of the rocket and payload attachment scheme. Could lead to rushing through work or settling with parts that are not compatible with an ideal design.	B3	Start the design process very early, and allow room in the design for the use of parts other than those initially selected: flexibility in design without the compromise of safety or science value.	A3

Vehicle Testing Failure	Vehicle parts are destroyed or damaged during ground testing or flight testing. Could lead to ordering new materials late in the year and running the risk of not completing the project on time.	E3	Design the vehicle components after extensive mathematical and physics analysis in order to ensure that a damaging failure will not occur. Only conduct tests with the potential to cause damage once a robust design has been developed and implemented. Set up an inventory of spare parts and components for building a second rocket within a week	E1
Weather Launch Delays	Inability to meet CDR and FRR timelines and obligations	D2	Have multiple possibilities for launch by working with launch clubs in the Tri-State area of TN, AL, and KY.	D1
Failure of AGSE Electronics	Inability to pick up and place payload into rocket	E3	Test, Test, and Re-test AGSE electronics. Set up minimum deliverables even if some sub systems fail	E1
Failure of flight altimeter	Inability to deploy drogue and/or main parachutes	D2	Test and certify altimeters in simulated altitude chambers Fly two altimeters for redundancy	D1
Failure of NASA marked altimeter	Inability to report flight altitude	C2	Test and certify altimeter Fly USLI competition altimeter in Payload Electronics bay to minimize effect of blasts during drogue and main deployments	C1
Access to Machine Shops	Delays in fabrication of various parts or rushed work. Impact on timely completion of the project.	B2	Ensure that contact with the machine shop operators is constant, and that available times for access are established.	B1

Personnel Shortage	Student or faculty members could be unavailable, which can lead to higher workloads for others, or the lack of technical knowledge of some system aspect.	B2	Make sure that the knowledge of rocket construction and testing techniques is known by the entire team. Make sure that the schedule is known by everyone so that people are not voluntarily absent/unavailable at inopportune times.	B1
School Holidays	Slows down the project and threatens timely completion and available times for testing.	A2	Ensure that the schedule for work and testing is designed with school holidays in mind, such that the team does not expect to have full access to equipment or personnel during those times.	A1
Budget Costs	Could threaten the feasibility of the project, as well as a violation of the rules of the competition.	C2	Keep a detailed budget and projected budget to minimize the chance of overspending. Make sure that every purchase is justified.	C1
Equipment Breakdown	Machine shop or laboratory equipment breakdown could cause a slowdown in production and threaten the timely completion of the project.	C1	Ensure that the team has access to multiple machine shops in case equipment in one place fails. Also, ensure that equipment is used and stored properly to minimize the likelihood that such a failure will occur.	B1
Ambiguous Product Lead Time	If the amount of time it takes for parts to ship is ambiguous or unknown, there could be unexpected delays in project development.	C3	Ensure somebody is responsible for knowing the lead times on all parts, and trying to eliminate all the ambiguity.	C2

Delays in Critical Path	If a portion of the project that is necessary to complete the next portion takes longer to complete than expected, there could be delays in project development.	C3	Make sure that realistic expectations are set for completion of elements along the critical path.	C2
Communication breakdown between team members	Failure to meet deadlines; failure to show results	D2	Frequent meetings to improve team morale and stress the importance of timelines, and chain of command.  Recalibration of deliverables based on progress.	D1

#### 4.1.5.3 Vehicle Failure Modes and Risk Assessment

Table 4: Vehicle Failure Modes and Risk Assessment

Vehicle Failure Modes and Risk Assessment					
Risk	Cause	Overall Effect	Risk Rating	Mitigation Strategy	Post-Mitigation Risk Rating
CG is too far aft	Poor overall rocket and section design  Unnecessary weight	Insufficient stability for reliable flight	C3	Proper simulation of rocket characteristics using <i>RockSim</i> .  Add ballast to nose cone of rocket if needed, which has ample room for dead weight.	B2
CP is too far forward	Poor overall rocket and section design  Fin area too small	Insufficient stability for reliable flight	C3	Proper simulation of rocket characteristics using <i>RockSim</i>  Increase fin size to move CP further back.	B2
Nose cone damage	Damage in landing of previous launches or during travel  Not properly sealed from environmental hazards	Unstable flight  Unusable nose cone	C3	Strong nose cone selection  Protective paint coating  Evaluate structural integrity after and before each launch	B2

Premature section separation	Failure of shear pins	Deploy at incorrect altitude Potential damage to/loss of rocket	D2	Proper shear pin sizing/strength	D1
Carbon fiber joint failure	Weak adhesion Loss of material strength	Unstable flight Damage to/loss of rocket	C3	Follow proper procedure for applying carbon fiber joints, including proper surface preparation, epoxy selection, and vacuum bagging technique	B2
Rocket sections do not assemble	Coupler tube shoulder joints at improper size Poor communication between section designs	Loss of stability Potential damage to/loss of rocket	E2	Clear outline of rocket design Verification of design an assembly at each stage of project	D1
Fin failure or weakness	Damage in landing of previous launches or during travel Not properly sealed from environmental hazards	Unstable flight	D3	Correct construction techniques Protective epoxy coating Evaluate structural integrity after and before each launch	D2
Rocket comes loose from launch pad	Rail Lugs not securely mounted to rocket Extreme wind Team error in aligning rocket while attaching to pad	Rocket breaks free during initial phase of launch Potential damage to rocket, bystanders, and property Potential loss of rocket and payload.	D4	Button type screw on lugs used on rocket for secure attachment Careful precision of alignment while guiding rocket on launch rail	C2
Fuel leakage	Improper seal on connections and fittings	Fuel saturating rocket interior Possible ignition and catastrophic failure of rocket	E3	Teflon tape used for all fuel connections	E2
Buckling or shearing of airframe	Shear pins do not shear Bulkheads unable to withstand force from motor	Unstable flight Potential loss of rocket	E3	Selection of strong airframe materials Use of proper manufacturing techniques	E2

	during launch  Weak bulkheads; poor seal to rocket body and/or motor tube					
Premature rocket separation	Faulty separation charge wiring	Unstable flight  Recovery failure	E3	Proper shear pins selection  Ground-based deployment and altimeter testing	E2	
	Shear pins too small	Unable to reach target altitude				
	Altimeter malfunction	Potential loss of rocket				
Center ring failure	Unable to withstand motor force during launch	Reduced stability	E3	Proper ring size and construction  Sufficiently strong materials used	E2	
	Weak ring; poor seal to body and motor tube	Damage to/loss of rocket				
Bulkhead failure	Unable to withstand motor force during launch	Damage to/loss of avionics, payload, or rocket	E3	Proper construction  Test for stability	E2	
	Weak ring	Unstable flight				
	Poor seal to body and motor tube					

#### 4.1.5.4 Propulsion Failure Modes and Risk Assessment

Table 5: Propulsion Failure Modes and Risk Assessment

Propulsion Failure Modes and Risk Assessment					
Risk	Cause	Overall Effect	Risk Rating	Mitigation Strategy	Post-Mitigation Risk Rating
Motor igniter fails	Faulty/incorrect igniter	Rocket does not launch	C2	Proper igniter selection setup	C1
		Need to replace		Proper power source	
Motor is misaligned	Fins assembled to motor tube at an angle  Centering rings do not center	Unstable flight	D2	Proper assembly of tail section using centering rings and fin alignment jig  Pre-flight inspection of	C1

	motor			motor alignment Careful machining of centering rings	
Propellant fails to ignite	Improper motor packing  Faulty propellant grain  Damage during transportation	Rocket does not launch  Need to replace	D2	Proper ignition setup  Safety advisor oversees motor packing by student safety officer	D1
Premature propellant burnout	Improper motor packing  Faulty propellant grain	Altitude estimate not reached	D2	Proper motor assembly  Static fire testing	D1
Propellant explodes	Improper motor packing  Faulty propellant grain  Damage during transportation	Destruction of motor casing  Catastrophic failure of rocket  Potential injury to team or bystanders	E2	Proper motor assembly  Safety advisor oversees motor packing by student safety officer	E1
Propellant burns through casing	Improper motor packing  Faulty propellant grain or casing  Damage during transportation	Loss of thrust  Loss of stability  Catastrophic failure of rocket	E2	Proper motor assembly  Safety advisor oversees motor packing by student safety officer  Verification testing	E1
Improper assembly of motor	Incorrect spacing between propellant grains  Motor case improperly cleaned  End caps improperly secured	Motor failure including  Unstable flight  Altitude estimate not reached  Potential damage to/loss of rocket	E2	Ensure proper training and supervision by safety advisor for motor assembly by student safety officer	E1
Motor mount fails	Insufficient mount strength  Damage during previous launch/transportation	Motor launches through rocket  Damage to/loss of rocket  Unstable flight	E3	Proper motor mount construction  Load verification testing  Test launches	E2

Transportation/handling damage	Improper protection during transportation/handling	Unusable motor Incapable of safe launch  Potential damage to/loss of rocket if used	E3	Proper storage overseen by safety advisor and student safety officer  Certified member handling	E2
--------------------------------	--	--	----	---	----

#### 4.1.5.5 Recovery System Failure Modes and Risk Assessment

Table 6: Recovery System Failure Modes and Risk Assessment

Recovery System Failure Modes and Risk Assessment					
Risk	Cause	Overall Effect	Risk Rating	Mitigation Strategy	Post-Mitigation Risk Rating
Lack of adequate space for parachutes	Improper budgeting of rocket space  Poor translations of needs to rocket design	Inc capable of safe launch	E2	Clear outline of rocket design  Verification of design needs met	D1
Descent rate too slow	Parachute $C_d$ too high  Cross-sectional area to great	Potential to land outside of authorized zone	C3	Verification testing of recovery system	C2
Payload parachute fails to deploy	Not enough drag in the air to blow the parachute out	Destruction of the payload compartment  Potential harm to spectators or environment	E3	Use shallow parachute chamber and secondary small chutes	D2
Payload Section fails to separate	Payload section charges fail to cause separation	Additional mass added to main falling section  Failure to complete payload jettison objective	E3	Calculations have been made that show failure of payload section separation does not cause excessive landing energy increase (shown after this table).  Backup charges installed.	B2
Onboard fire in parachute compartment	Combustible material near separation charges	Potential damage to or loss of rocket, avionics or payload bay	D2	Isolation of ejection charges from flammable material	D1

				Ground-based deployment testing	
Parachute tear	Parachute snags upon separation Improper transportation/storage	Decreased parachute performance leading to potential damage to/loss of rocket	D3	Inspect material for defects Proper and consistent packing technique Removal of potential snags within parachute compartment	C2
Avionics bay not properly sealed	Holes in rocket body or avionics bay Gaps between sections	Premature detonation of charges Estimated altitude not reached Potential damage to/loss of rocket	D3	Putty used in required areas to seal holes and gaps	D2
Descent rate too fast	Parachute $C_d$ too low Cross-sectional area to small	Potential damage to or loss of rocket or payload	D3	Verification testing of recovery system	D2
Parachute or shroud line tangle	Improper transportation, storage, or packing	Decreased parachute performance leading to potential damage to or loss of rocket	D4	Proper packing of recovery system Proper and consistent method of folding and storing after each use	C2
Parachute melts	Improper separation of/insulation between charges and parachute Improper storage	Decreased parachute performance leading to potential damage to/loss of rocket	D4	Proper shielding from ejection charges Ground-based testing	D2
Rocket ripped apart upon chute deployment	Zippering effect of parachute harness	Catastrophic failure of recovery system Damage to/loss of rocket and payload	E3	Use Fireball anti-zippering device to distribute load to body	E1
Low battery	Not properly replacing before launch	Failure to ignite charges to deploy parachute Deploy at incorrect altitude Potential damage	E3	Pre-launch checklist ensures battery switch if low power	E1

		to/loss of rocket			
Parachute sections come apart	Inadequate parachute design  Poor stitching between sections	Catastrophic failure of recovery system  Damage to/loss of rocket and payload	E3	Use semi-flat felled seam between sections  Verification testing of recovery system	E2
Shroud lines become unattached	Weak stitching or materials	Catastrophic failure of recovery system  Damage to/loss of rocket and payload	E3	Sew reinforcement onto shroud lines	E2
Parachute breakaway	Harness failure; weak mounting of recovery system to rocket body	Loss of parachute  Catastrophic damage to/loss of rocket/payload  Potential damage/injury to property/persons on ground	E3	Design strong retention system with shock absorption  Load testing; multiple body attachment points	E2
Parachute deployment failure	Parachute sticks in nosecone  Charges fail to deploy	Catastrophic damage to/loss of rocket/ payload  Potential damage/injury to property/persons on ground	E3	Ground test deployment  Additional drogue parachute attached to main parachute	E2
Separation failure	Overly strong shear pins  Inadequate charge or failure to detonate  Altimeter failure	Catastrophic damage to/loss of rocket on landing  Potential damage/injury to property/persons on ground	E3	Deployment charge testing  Proper shear pin sizing/strength  Altimeter testing  Redundant charges and altimeters  Slightly oversized ejection charges	E2
Altimeter failure	Wires become unconnected  Loss of power  Arming switches fail	Failure to ignite charges to deploy parachute  Deploy at incorrect altitude  Potential catastrophic damage to/loss of	E3	Employ backup altimeter  Dedicated power supply  Test for altimeter function prior to launch	E2

		rocket			
Arming switch failure	Faulty component Short in circuit	Failure to ignite charges to deploy parachute  Deploy at incorrect altitude  Potential catastrophic damage to/loss of rocket	E3	Test switches prior to rocket assembly  Ground-based deployment test	E2
Shock cord failure	Faulty shock cord Fatigue failure	Parachute disconnect from rocket  Potential catastrophic damage to/loss of rocket	E3	Inspect shock cord before packing parachutes	E2
Shroud lines or shock cords tangle after deployment	Excess rocket rotation Shock cords too long	Potential for parachute to not fully deploy  Potential catastrophic damage to/loss of rocket	E3	Flight testing of recovery system  Minimize shock cord length to nose cone  Maximize cord length to tail section to reduce rotation	E2

#### 4.1.6 Planning of Manufacturing, Verification, Integration, and Operations

---

A copy of the Vanderbilt Student Launch Schedule can be found in the Appendix.

#### 4.1.7 Confidence and Maturity of Design

---

The 2015-2016 Vanderbilt Aerospace Design Lab is confident in its design capabilities as well as in this particular design. Each year, we build upon the successes of the prior year's team, making a continually stronger rocket.

The designs that the team has made are all based on mathematical calculations, computer simulations, or the experience of other rocketeers. These design choices are then all rigorously tested to ensure that all safety parameters are met, that the team will benefit from overcoming engineering challenges, and that a meaningful demonstration of the task at hand can be completed.

The maturity of our vehicle also increases over each of our three pre-competition launches, resulting in a fully-vetted design.

#### 4.1.8 Dimensional Drawings

---

Dimensional drawings for the launch vehicle that are not included elsewhere in this document can be found below.

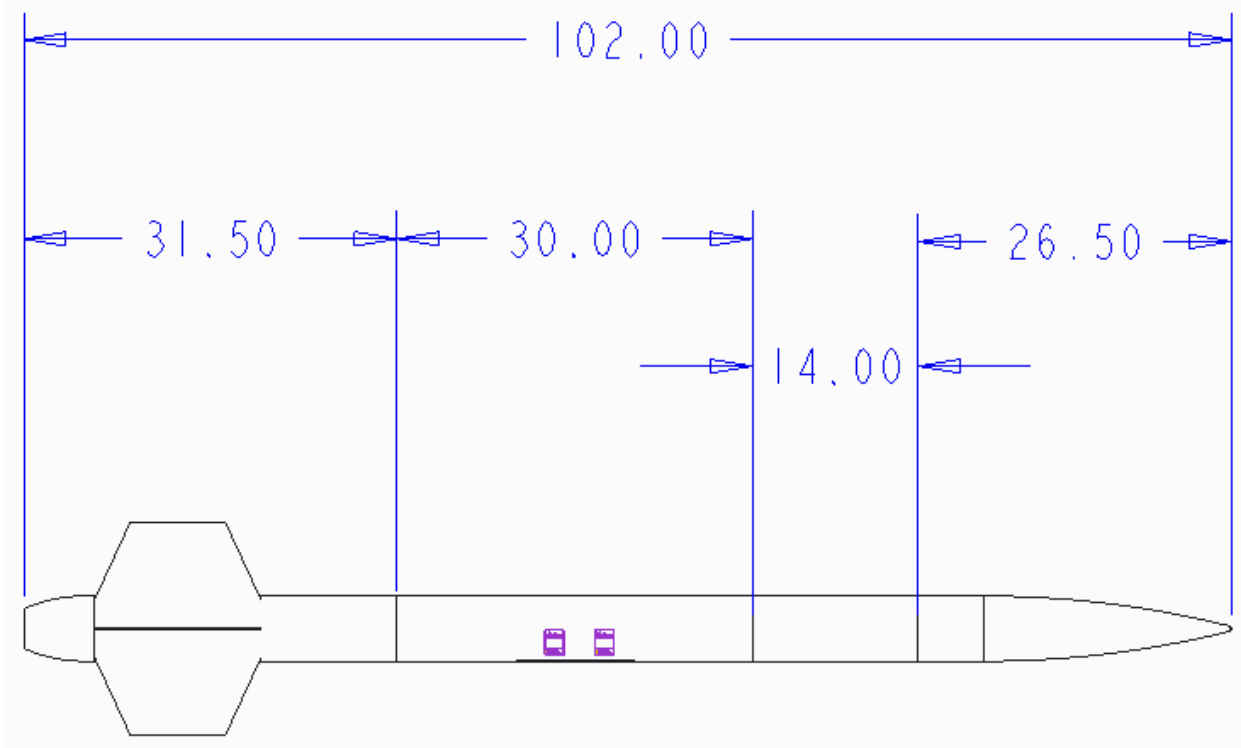
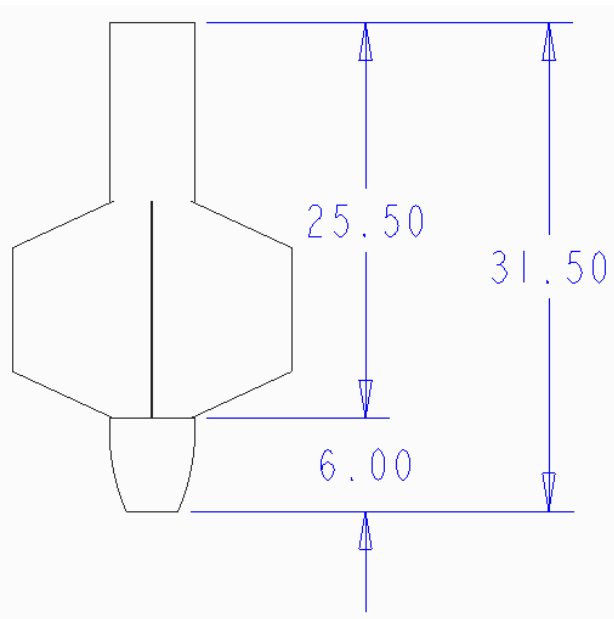


Figure 24: Launch vehicle



**Figure 25: Full-scale payload bay**



**Figure 26: Full-scale tail section**

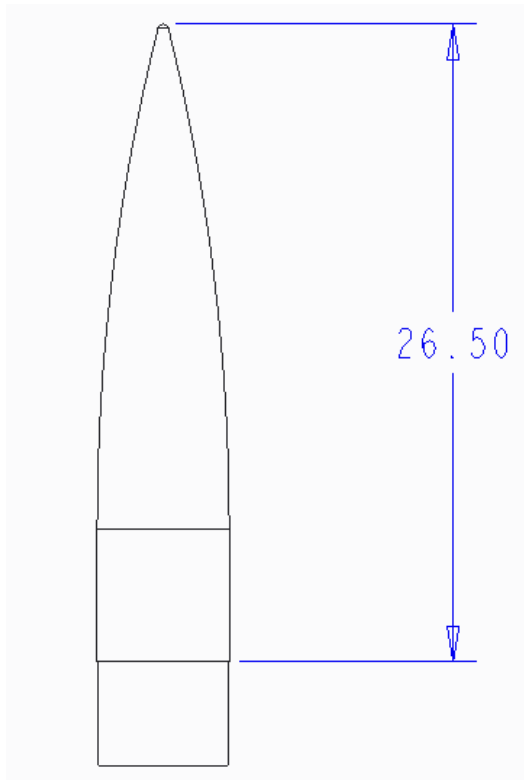


**Figure 27:** Full-scale nose cone

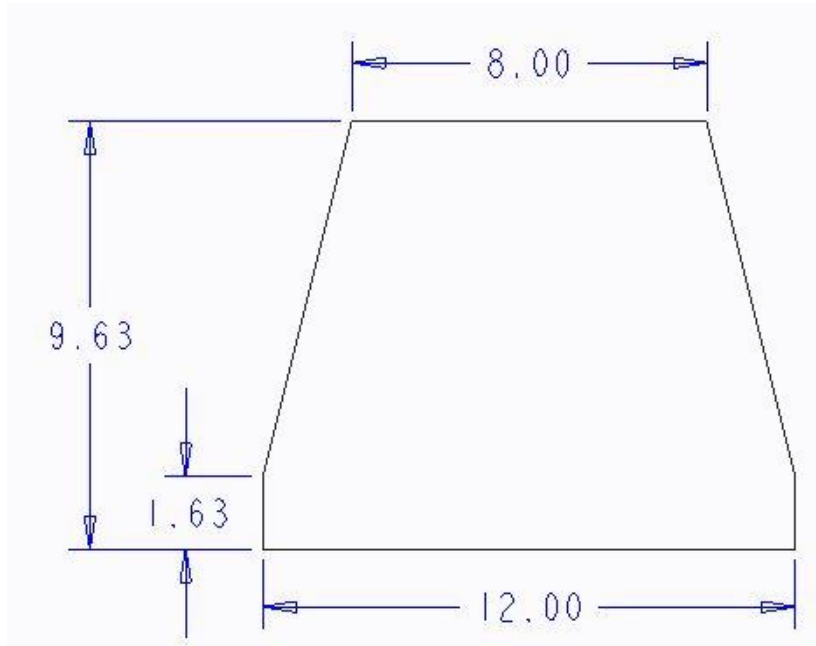


**Figure 28:** Fin design

#### **4.1.9 Electrical Schematics for Recovery System**

---

The recovery system will be a self-contained electronics bay housing two independent power, altimeter, and ejection charge systems. This level of redundancy is to ensure reliability in the mission-critical recovery activities. A high-level schematic of a single recovery system is shown below:

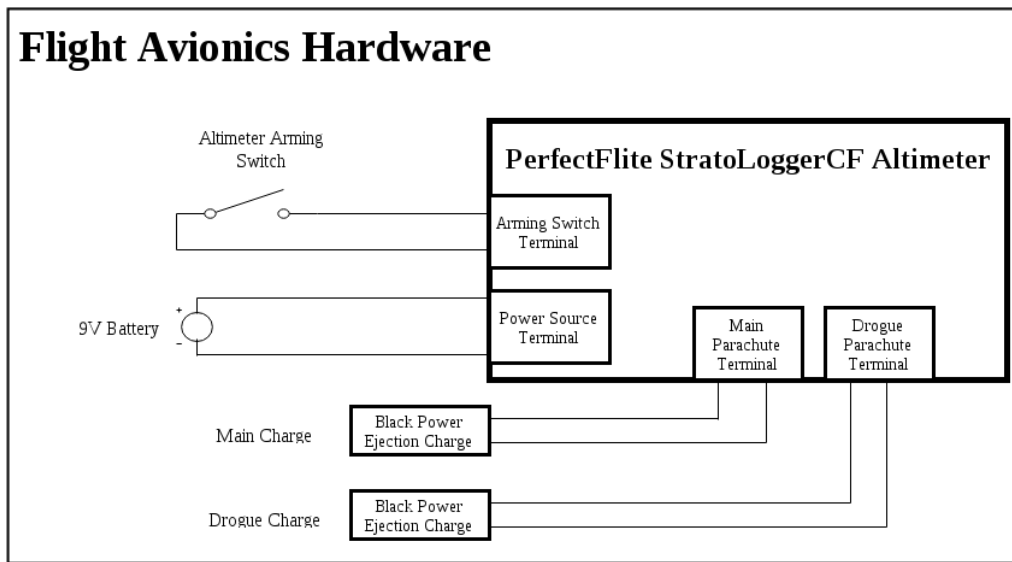


**Figure 29: Schematic of avionics hardware**

#### **4.1.10 Mass Statement**

---

The following table details the mass of the rocket components for both the subscale and full-scale rockets.

**Table 7. Mass Statement**

Section	Subscale Rocket	Full-scale Rocket	
		Actual Mass (lbs)	Lower Mass Limit (lbs)
Tail Section (Body Tube, Fins, Tail Cone, Motor, Payload Thruster Assembly)	11.2	12.5	15.5
Payload Section (Body and Coupling Tube, Fuel System, Payload Electronics, Structural Components)	5	6	10

Avionics Section (Body Tube, Avionics Bay, Drogue Parachute)	3	3	5
Nose Cone & Main Parachute	6	5.5	7.5
Total	25.2	27	38

With this year's rocket seeing several design changes over rockets from past years, these mass estimates drew more from our subscale rocket than from weighing sections from previous rockets. Complete sections and individual components were weighed with an allowance for additional fasteners and other assembly components. A more detailed comparison of the subscale and full-scale rocket can be found in section *4.2 Comparison of Subscale to Full-Scale Launch Vehicle*. Most of the additional vehicle mass comes from addition payload length and payload components which will be included on the full-scale but not on the subscale. A larger motor and larger parachutes will also add somewhat to the full-scale vehicle weight.

Simulations shown in section *4.4.2: Simulations and Predictions* detail how changes in mass affect the maximum altitude.

## 4.2 Comparison of Subscale to Full-Scale Launch Vehicle

---

### 4.2.1 Comparison Overview

In order to accurately represent our fullscale launch with a subscale launch we had to incorporate several factors. Of these factors, we decided that Launch ‘g’, Max vehicle velocity, Rail exit velocity, apogee reached, Landing drift, Static stability margin, rocket length, and motor impulse were to be compared. If the rocket scaling is perfect, then there should be parity in several of the flight-related parameters, and the only variable changed is the motor impulse to accommodate a heavier rocket. We have the subscale and fullscale rockets differing by a 56% mass, and the selected motor impulses differing by about the same margin, establishing excellent parity. The chart below is a visual representation of the comparison of these values for the full-scale and subscale models.

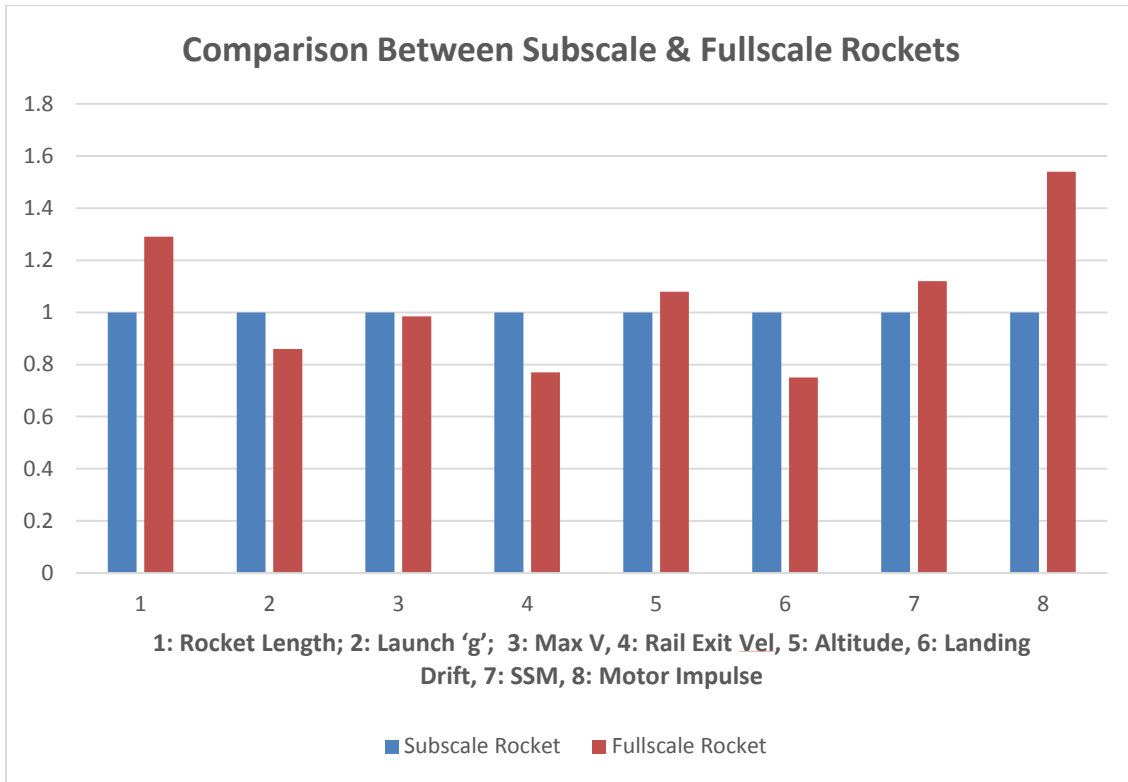


**Figure 30: Comparison of Key Criteria between Full-Scale and Subscale Flight Vehicles**

As can be seen in the chart above, we have achieved parity in Static Stability Margin, take-off acceleration, maximum velocity, apogee altitude, and landing drift. We have a slightly lower takeoff speed, but the speed of 85 fps is much larger than the 45 fps minimum required to clear the launch pad with acceptable stability.

#### 4.2.2 Vehicle Design Comparison

The full scale rocket is a different, larger, and more mature adaptation of the subscale rocket. The subscale rocket contains a flow visualization payload containing 2 fuel tank test beds, but lacks functioning hydrogen peroxide thrusters and the associated electronics and fuel delivery system. The full scale rocket is expected to have an extended custom tail cone for accommodating the monopropellant thrusters. As well the tail section will increase in length to accommodate a larger motor. The full scale rocket will contain a pressure holding peroxide fuel tank with mass increased from the flow visualization test beds. A compressed gas tank for fuel delivery will reside in an extended payload section. This fuel delivery system will also contain a non-negligible payload electronics suite adding significant length and mass to the rocket. Rocket organization and recovery system design will be designed similarly, implementing lessons learned from the subscale launch.

The goal of the subscale launch vehicle will be characterizing the dynamic launch environment for fuel delivery system optimization and structural analysis. The goal of the full scale launch will be flight based testing of the monopropellant thruster, anti-slosh fuel tank, and further advancement of the structural agenda of the VADL drawn out in section 5.3.3.

Table 8: Comparison of Key Parameters for Full-Scale Launch vs. Subscale Launch

Comparison	Subscale	FULLSCALE	% difference
Length	79"	102"	+29%
Launch 'g'	14	12	-14%
Max Velocity	660 fps	650 fps	-1.5%
Rail Exit Velocity	110 fps	85 fps	-23%
Altitude	4900 ft.	5300 ft.	+8%
Landing Drift*	300 ft.	220 ft.	-20%
Static Stability Margin	1.7	1.9	+12%

Table 9: Summary of differences between Full-Scale and Subscale

Dimension/Description	Full-Scale Model	Subscale Model
<b>Payload Section</b>		
Parachute Diameter (in)	48	42
Parachute CD	2.2	1.2
Landing Mass (lb)	8	5.5
Parachute Deployment Altitude (ft AGL)	1000	700
Landing Speed (fps)	16.47	21.14
Max Landing Energy (lbf-ft)	33.6	38.2
<b>Main Section</b>		

<b>Drogue Parachute Diameter (in)</b>	36	N/A
<b>Drogue Parachute CD</b>	1.2	N/A
<b>Drogue Parachute Deployment Altitude (ft AGL)</b>	3300	N/A
<b>Main Parachute Diameter (in)</b>	144	72
<b>Main Parachute CD</b>	1.5	2.2
<b>Main Parachute Deployment Altitude (ft AGL)</b>	700	1000
<b>Landing Mass (lb)</b>	26	17.2
<b>Landing Speed (fps)</b>	12	16.11
<b>Max Landing Energy (lbf-ft)</b>	26.8	26.9
<b>Motor Details</b>		
<b>Motor Description</b>	Cesaroni Pro-75 L1720	Cesaroni Pro-54 K1440
<b>Diameter (mm)</b>	75	54
<b>Length (cm)</b>	48.6	57.2
<b>Total Weight (g)</b>	3341	1892.6
<b>Average Thrust (N)</b>	1771.0	1437.0
<b>Max Thrust (N)</b>	1946.0	1828.9
<b>Total Impulse (Ns)</b>	3660.0	2372.0
<b>Burn Time (s)</b>	2.0	1.7

#### **4.2.3 Dimensional Drawings of Subscale**

---

Dimensional drawings for the subscale vehicle that are not included elsewhere in this document can be found below.

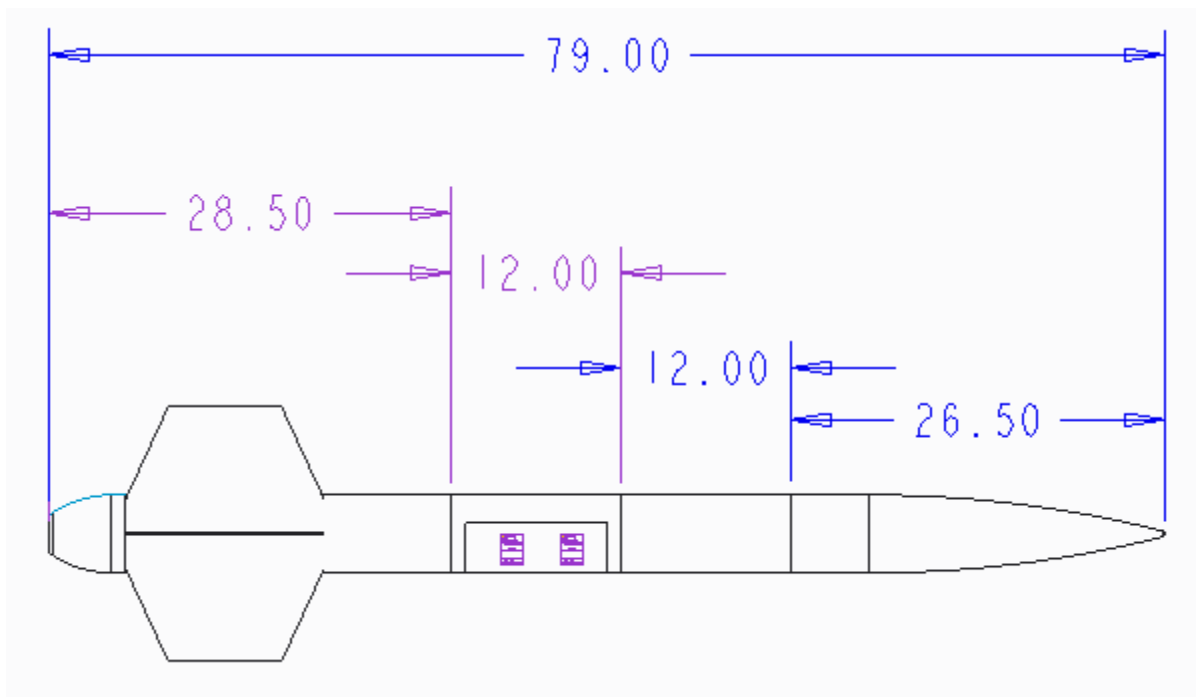


**Figure 31: Subscale vehicle**

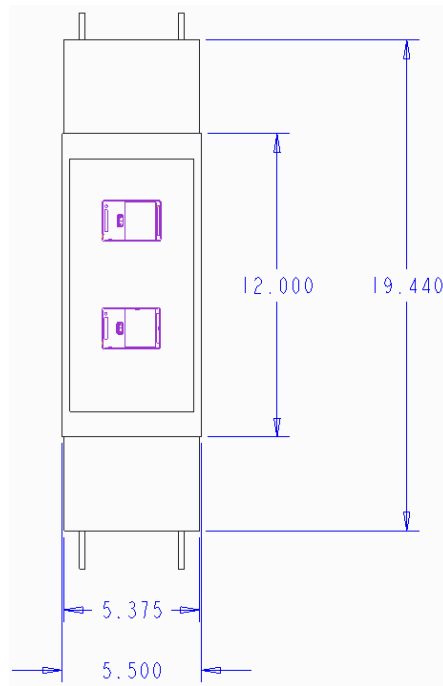


**Figure 32: Subscale payload bay**

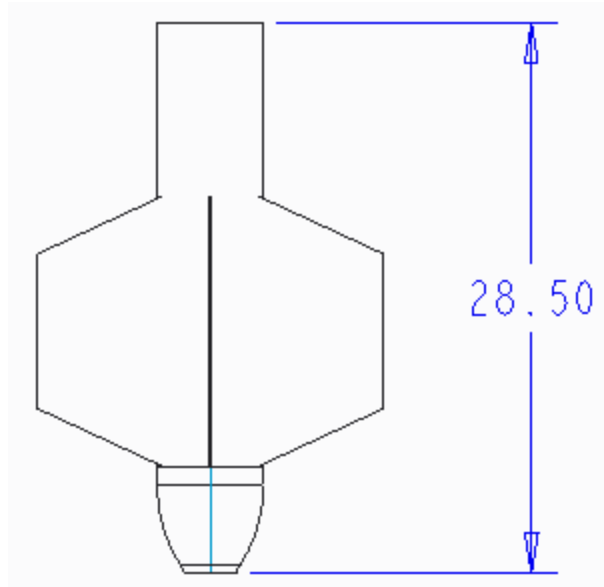


**Figure 33:** Subscale tail section

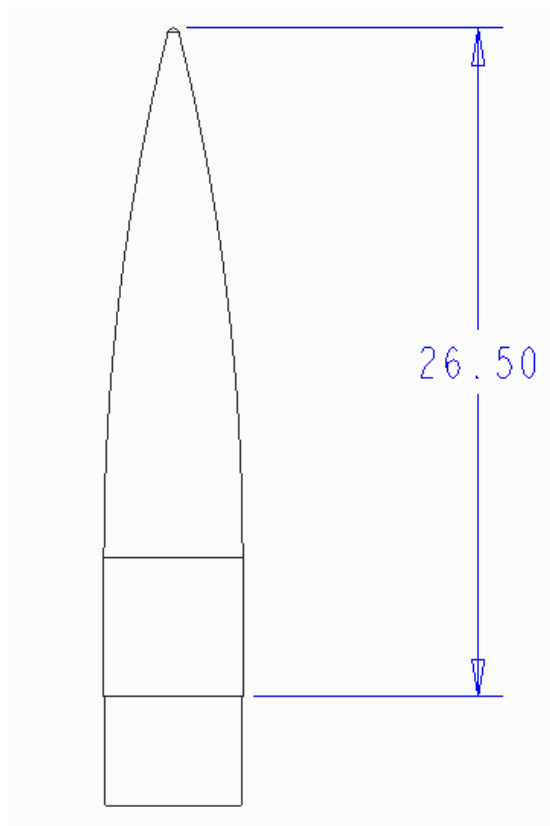


**Figure 34:** Subscale nosecone

#### **4.2.4 Flight Vehicle Test Sequence**

---

A confident launch manifest with well-defined goals has been laid out for the 2015-2016 VADL project.

The team will launch the subscale launch vehicle in the middle of November 2015. This launch is defined by successful arrival at apogee and recovery system deployment, as well as critical data collection for payload experiments. On this launch 2 GoPro Cameras will record flow dynamics in acrylic fuel tanks with prototype baffling designs. This is one of the key opportunities for the team to validate slosh abatement designs in the true launch environment and collection of this data is paramount to mission success. Dynamic accelerometer data will be collected on this launch as well from 3 3 axis accelerometers sampling at 800 Hz. The subscale launch will be a critical step in allowing the team to study and improve design of vehicle and payload systems for the competition vehicle.

Following this subscale launch the team will perform a test launch of the full scale vehicle in February 2016. This launch will contain evolved payload experiments and tests, including a more mature structural data acquisition suite and will be the maiden flight of the monopropellant thruster and fuel delivery system. This launch will give the team understanding of launch vehicle and payload performance behavior that can improve the project for the competition.

### **4.3 Recovery Subsystem**

---

#### **4.3.1 Recovery System Overview**

---

Recovery of the launch vehicle will be accomplished by a drogue parachute deploying at apogee and a main parachute deploying around 700 ft. Two independent PerfectFlite Stratologger altimeters will initiate all parachute deployment and will also collect altitude data. One altimeter will be considered the “main” while the second altimeter will be a redundant “backup” altimeter. Each altimeter will have its own battery, arming switch, and black powder charges. This same basic setup has functioned well in previous rockets, but improvements will be made using past experiences.

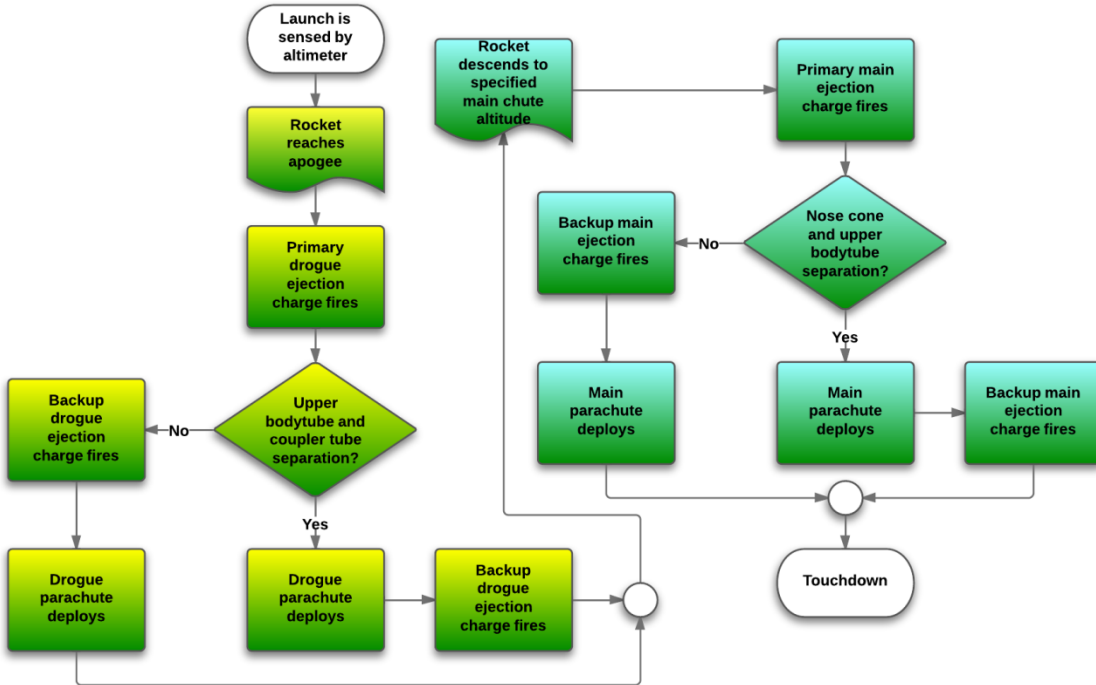


**Figure 35: Recovery System Flowchart**

### 4.3.2 Rocket Separation

Rocket separation will occur in two events: the forward event and the aft event. The two separation events will occur (1) at the joint between the nosecone and upper body tube (2) at the joint between the upper body tube and the payload. The hollow nosecone will house the larger main parachute, while the empty space between the avionics bay and the payload bay will house the drogue parachute.

Physical separation will be achieved via controlled detonation of pyrotechnic charges located on the aft avionics bay bulkhead and within the nosecone to create positive pressure inside the parachute bays. The pyrotechnic charges selected for both deployment events are 4F black powder charges specifically sized to create at least 215 lbs of separation force per charge. For each deployment event both a primary and a backup charge, each capable of independently forcing separation and controlled by their own altimeters, will be detonated to ensure rocket separation.

The maximum shear strength of #4-40 nylon screws is  $\cong 71$  lb per screw.

$$F = \sigma A = 10,000 \frac{lb}{in^2} * \frac{\pi}{4} * (0.095\ in)^2 = 70.88\ lb$$

Black powder exhaust gases behave as ideal gases.

$$PV = nRT$$

$$R = 266 \frac{lb - in}{lbm R^\circ}$$

$$T = 3300 R^\circ$$

The black powder exhaust gases can be simplified to do work only on the rocket's bulkheads

$$Area = \frac{\pi d^2}{4} = \frac{\pi}{4} * (5.45 in)^2 = 23.33 in^2$$

The volume of the parachute, shock cord, u-bolts, and blast caps can be ignored. (This leads to a conservative answer). Therefore volume is a function of area and chamber length only.

$$Volume = V = A * L$$

In order to successfully separate, 213 pounds of force must be generated by the blast charges at each junction.

$$3 \frac{screws}{junction} * 70.88 \frac{lb}{screw} = 212.64 lb$$

Pressure can then be calculated.

$$P = \frac{F}{A} = \frac{212.64 lb}{23.33 in^2} = 9.1 psi$$

The volumes for both the main and drogue chambers can be calculated ( $17.25 - 402.443; 5 - 116.65$ )

$$V_{main} = A * L_{main} = 23.33 in^2 * 17.25 in = 402.443 in^3$$

$$V_{drogue} = A * L_{drogue} = 23.33 in^2 * 5.0 in = 116.65 in^3$$

The mass of 4F black powder needed for each chamber can then be calculated using the ideal gas law

$$PV_{main} = n_{main}RT$$

$$9.1 \frac{lb}{in^2} * 402.443 in^3 = n_{main} * 266 \frac{lb - in}{lbm R^\circ} * 3300 R^\circ$$

$$n_{main} = 0.004 lbm = 1.8 g$$

And

$$PV_{drogue} = n_{drogue}RT$$

$$9.1 \frac{lb}{in^2} * 116.65 in^3 = n_{drogue} * 266 \frac{lb - in}{lbm R^\circ} * 3300 R^\circ$$

$$n_{drogue} = 0.0012 lbm = 0.549 g$$

Applying a factor of safety of 2 and rounding gives the following values for black power masses

$$n_{main} = 3.5 \text{ grams}$$

$$n_{drogue} = 1.1 \text{ grams}$$

### 4.3.3 Drogue Parachute Recovery

---

The first separation event occurs immediately after the rocket reaches apogee and initiates the drogue recovery process. Drogue recovery will use a 30" diameter *fruity-chute* elliptical parachute. This will provide a stabilized descent at approximately 69ft/sec for a rocket of weight 34 lbf. after motor burn off. A Nomex/Kevlar parachute protection pad will surround the parachute to prevent it from being burned by hot ejection gasses. For moderate to high wind conditions a 30" drogue chute is ideally suited to forestall excessive wind drift. The drogue parachute will attach to a 30ft. Kevlar  $\frac{1}{2}$ " shock cord via quick link. The shock cord connects to a short  $\frac{1}{2}$ " wide Kevlar harness near the ejection charges where fireproof material is needed. The shock cord, rated minimally at 3000lb, will tether the drogue parachute to the aft end of the avionics bay and the forward end of the tail section, again using quick links. Furthermore, nine 43" nylon shroud lines (86" continuous) will attach the parachute to the shock cord. A cross stitch seam type using #400 flat line threads will connect the nylon parachute sections. These parachute materials will be lightweight but also strong enough to safely return the rocket to the ground. Using quick links, the shock cord will tether the parachute to the tail section and the forward section (rigidly bolted to the body tube) via two  $\frac{1}{4}$ " aluminum U bolts. These U bolts will be bolted to bulkheads within the rocket. The same attachment method will be used for the payload chute shock cord on the payload section side.

Landing speed with a 30" drogue from 5200 ft. to 700ft is calculated as follows:

$$V_{ld} = \sqrt{\frac{mg}{0.5\rho C_D A}} = \sqrt{\frac{151N}{0.5 * 1\frac{kg}{m^3} * 1.5 * 0.456m^2}} = 21 \frac{m}{s} = 69 \text{ fps}$$

### 4.3.4 Main Parachute Recovery

---

The second separation event occurs at 700ft. and initiates the payload recovery process. Payload recovery will use a 12 ft. diameter *elliptical* type parachute. This will provide a stabilized descent at approximately 13.4 ft. /sec. A Nomex/Kevlar parachute protection pad will surround the parachute to prevent it from being burned by hot ejection gasses. Depending on wind conditions, the drogue chute size may change to forestall excessive wind drift.

Landing speed with a 12ft main from 700ft is calculated as follows:

$$V_{lm} = \sqrt{\frac{mg}{0.5\rho C_D A}} = \sqrt{\frac{151N}{0.5 * 1.1\frac{kg}{m^3} * 1.5 * (0.456m^2 + 10.5)}} = 4 \frac{m}{s} = 13.4 \text{ fps}$$

The heaviest section is the tail+payload section weighing at 24lbf. The landing energy of the heaviest section is:

$$KE_{largest\ part} = \frac{\left(\frac{W}{g}\right) \cdot V^2}{2} = \frac{(24) \cdot 13.4\ f\ ps^2}{2 \times 32.2} = 67\ lbf-ft < 75\ lbf-ft$$

The landing energy assumes absolutely no ground wind; however, our experience has been that the ground windspeed contributes to lofting and the actual landing speeds with the main are substantially lower.

The payload parachute will be connected with a quick link to a 15 ft., 1/2" wide Kevlar shock cord rated minimally at 3000lb. The shock cord connects to a short 1/2" wide Kevlar harness near the ejection charges where fireproof material is needed. The parachute will be made from 1.102 Rip Stop Nylon. Furthermore, nine 200" nylon shroud lines (400" continuous) will attach the parachute to the shock cord. A cross stitch seam type using #400 flat line threads will connect the 18 nylon parachute sections. These parachute materials will be lightweight but also strong enough to safely return the rocket to the ground. In addition, the simple bell parachute type will allow for ease of manufacturing

#### **4.3.5 Avionics and Avionics Bays**

---

The avionics bay is designed to house all of the electronics required for activation of the recovery system. It must protect these electronics from many things including but not limited to: the explosive forces experienced during black powder ejection charge ignition and the vibrations during rocket flight. Because the PerfectFlite StratoLoggerCF altimeters in this rocket use barometric sensing to determine altitude AGL, the avionics bay must provide exposure to the atmosphere. This will allow the altimeters to sense external pressure such that they may accurately record altitude, trigger the drogue parachute deployment at apogee and the main parachute deployment at the desired altitude. Furthermore, the avionics bay must allow for altimeter activation on the launch pad once the rocket is fully assembled.

The location and size of the static pressure ports are important. The ports must be located on the altimeter bay and need to be situated such that there is minimal air turbulence caused by obstructions forward of the ports. To calculate the size of the static pressure ports, we use a formula from "Modern High-Power Rocketry 2", written by Mark Canepa.

The equation for single static pressure port sizing is given below.

$$D_P = \frac{V_b}{400}$$

Where  $D_P$  is the diameter of the port, and  $V_b$  is the volume of the avionics bay. This equation is valid for altimeter bay volumes of up to 100 cubic inches.

For multiple static pressure ports, we have the following formula:

$$\widehat{D_p} = \frac{2D_p}{N}$$

where N is the desired number of static pressure ports.

Applying these formulas to our avionics bay, we have:

$$D_p = \frac{4in * \pi * 2.6in^2}{400} = 0.212 \text{ in}$$

Should we desire four static port holes, the diameter of each port should be:

$$\widehat{D_p} = \frac{2D_p}{N} = \frac{2 * 0.212\text{in}}{4} = 0.106 \text{ in}$$

Verification of the port sizes will come from inspection of the rocket velocity data, which will confirm that parachutes were ejected at the appropriate altitudes. Additionally, proper parachute deployment will also verify the ports are appropriately sized.

In order to prevent premature arming of the ejection charges by the altimeters while the rocket is being assembled or carried to the launch pad, the avionics bay must be designed such that the altimeters can be easily turned on from the exterior of the rocket body while the rocket is on the pad and ready to launch. To accomplish this, two arming screw switches (one for each redundant recovery system) are accessible from outside the rocket will be mounted to the avionics bay. Leads to the altimeters are soldered to these screw switches for security. The altimeters cannot be powered on until the switches close the connection. An electrical schematic of this can be found in section 3.1.9 *Electrical Schematics for the Recovery System* of this report.

Two arming switch alternatives were evaluated for flight this year. Traditionally, the VADL has employed screw switches because once they are armed, they will not accidentally change state to the off position due to vibrations and high-g takeoff conditions, ensuring high reliability performance. The performance of these switches is validated by years of experience and successful recoveries. As a design alternative, the avionics team this year researched, purchased, and tested a magnetic arming switch for the altimeters. This switch uses a field-effect sensor to detect a pass of a rare-earth magnet within 1" of the switch for arming/disarming. State is shown by a blue LED (on = active). With proper placement, this design would have allowed the VADL to arm the altimeters post-assembly from outside the rocket body. This would eliminate confusion and time in arming the switches, which in the past is done carefully by using a screw driver to turn the screw switches, located inside the payload bay. With the magnetic sensor, a simple pass over the exterior body could arm the switch. Unfortunately, in test, the magnetic switch showed high variance and unreliability in the ability to be armed. The advertised 1" arming radius was more accurately about 1/4", and even then, an operator would have to make between 2-3 passes with the magnet for the switch to activate. Because of this lack of reliability, the team made the decision to abort using magnetic arming switches in favor of the time-tested screw switch arming method. An image of the magnetic arming switch and required connections is shown below.

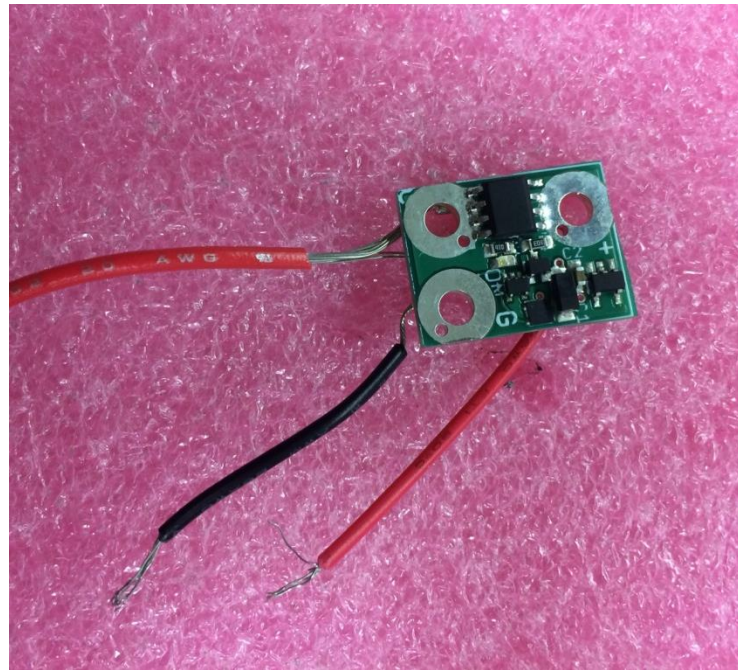


Figure 36: Top view of magnetic arming switch

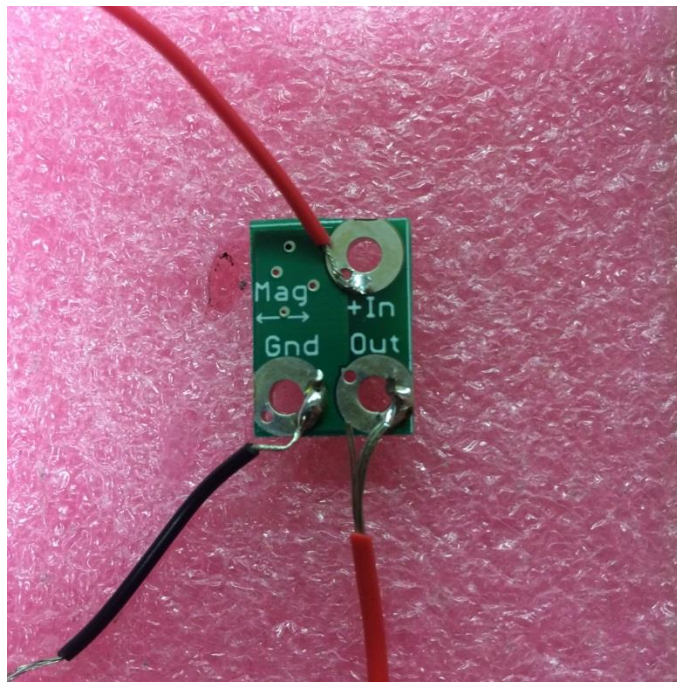


Figure 37: Bottom view of magnetic arming switch showing soldered connections

This year, the arming switches will be mounted inside the avionics bay, but will still be switched on from outside the rocket body. This is opposed to mounting the switch just internal to the body, but exterior of the bay. This will prevent the possibility of the drogue chute shearing the switch during deployment- leading to power loss of the altimeters.

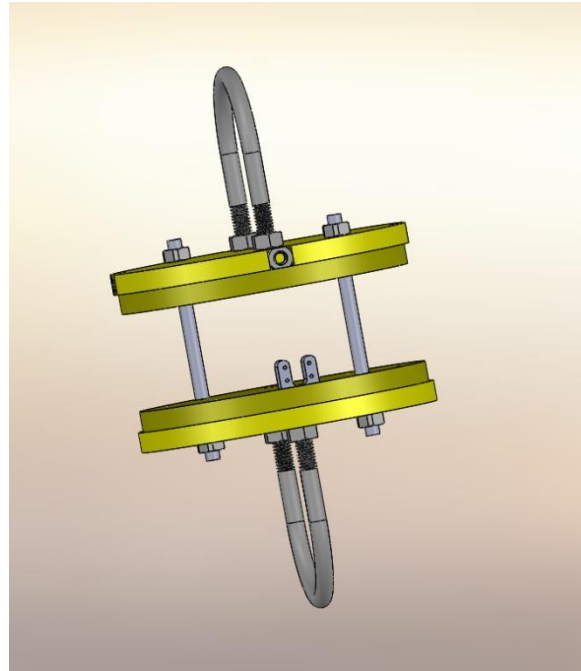


Figure 38: Preliminary CAD of the Avionics Bay and Connectivity Components

#### **4.3.6 Deployment Charge and Altimeter Layout**

---

Each altimeter is connected to its own power source (9V battery) and its own dedicated screw-based arming switch. They both have access to the same port holes for barometric sensing in order to maintain consistency among the devices. Subsequently, each independent altimeter has two outputs- one electric-match for ignition of the drogue chute deployment blast charge, and one electric match for ignition of the main chute deployment blast charge. This makes the systems completely redundant; timing settings for both altimeters ensure this as well.

The two altimeters, mounted perpendicular to the direction of takeoff of the rocket use a main-backup deployment schema. The main altimeter is set to fire the drogue chute ignition charge upon apogee detection. For redundancy, the backup altimeter, which theoretically should sense apogee simultaneously as the main, has a one-second ignition delay on the drogue chute charge. This is planned purposefully such that if the main altimeter malfunctions, the backup can deploy the drogue chute. Additionally, this delay is meant to limit the force exerted on the rocket from the blast charges to prevent excess shearing.

For main parachute deployment, the same scheme is used. At the specified deployment altitude (e.g. 700'), the main altimeter is set to ignite the main parachute deployment charge. For redundancy, the backup altimeter is set to perform this action at a lower altitude (e.g. 500'). Not only does this enforce reliability standards; however, it also limits the shearing force present if both charges fired simultaneously. Both charges for the drogue and the main parachutes will use 1.1 and 3.5 grams of black powder, respectively. Calculations for these blast charge values are shown above in section 4.3.2 *Rocket Separation*.

### **4.3.7 Recovery System Testing**

---

A complete test of the deployment system on the rocket is carried out before each launch. The test consists of two different aspects: testing the deployment charges / rocket separation, and testing the altimeters.

To test the rocket separation, the rocket is fully assembled with the parachutes properly packed and installed and all appropriate amounts of black powder in their respective locations. Igniters are connected to a custom control box allowing them to be manually ignited. The rocket is placed in a safe outdoor location with no objects or people near it. The entire protocol is monitored and managed by Safety mentor Robin Midgett and student safety officer Ben Gasser. The payload charges are then ignited. After verifying proper separation, the payload section is moved to the side to avoid collisions, and the drogue charge is fired. After again verifying proper separation, the drogue section is moved next to the payload section and the main charges are fired and separation is verified. This completes the test of the rocket separation, and verifies the proper amount of black powder, proper shear screw usage, and to a certain extent proper parachute packing.

Aside from testing the magnetic altimeter arming switch (see *Avionics and Avionics Bays*) both PerfectFlite StratoLoggerCF altimeters were tested for accuracy and ignition performance in a pressurization chamber. Mounted on a test bed with arming switches and electric matches (to test ignition), the VADL conducted basic flight simulation in the university's Energetics Laboratory. Using the main-backup altimeter scheme described in *Deployment Charge and Altimeter Layout*, the team programmed the necessary parameters for the altimeters, and tested them simultaneously. Results of the experimentation are shown below.

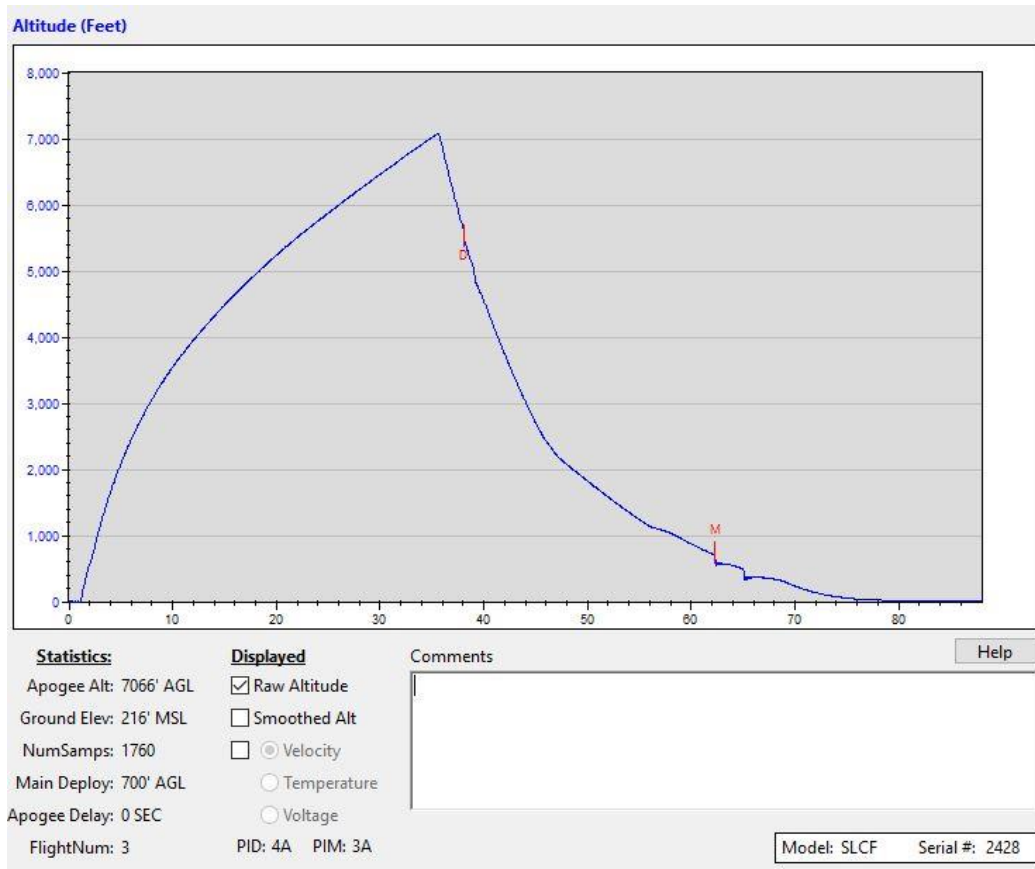
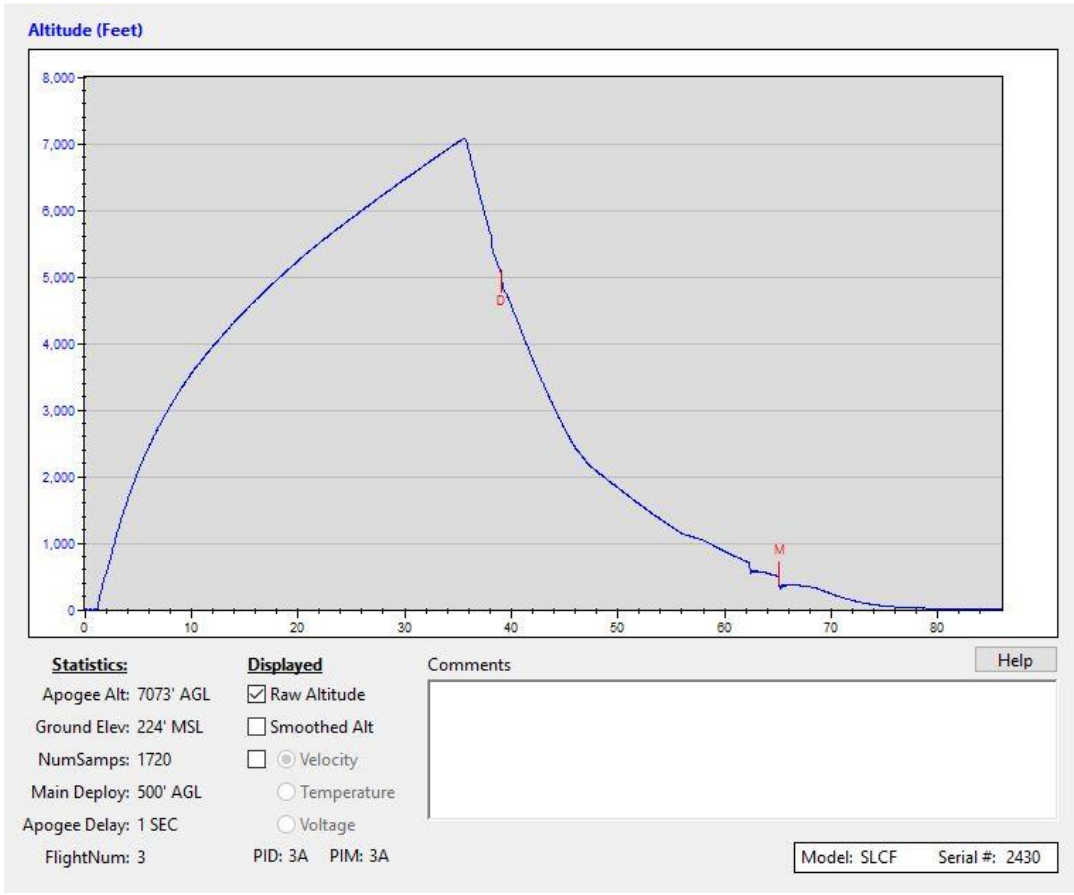


Figure 39: Main altimeter test results, Apogee Deployment Delay = 0s, Main Deployment Altitude = 700'



**Figure 40: Backup altimeter test results, Apogee Deployment Delay = 1s, Main Deployment Altitude = 500'**

The results of the altimeter testing were as expected: near identical altitudes and redundancy in drogue and main ejection charges. The altitudes sensed by the altimeters were off by 7'; however, apogee was detected by both altimeters simultaneously. This is reassuring, because even with the slight altitude discrepancy, the apogee deployment event will still happen a separate times, limiting the potential shearing force on the rocket and drogue chute. Additionally, it is important to note that both altimeters sense the momentary pressure disturbance of the main ejection charge firing at 62s-65s in simulated flight. This means that both altimeters are in good working order, and are consistent. Also note the correctness of the 700' (main) and 500' (backup) main parachute deployments at 62s and 65s, respectively.

#### 4.3.8 Rocket Avionics Bay – Structural

The rocket avionics bay, which is mounted inside the forward section of the rocket (between the main and drogue parachutes) will consist of a small section of coupling carbon fiber, two bulk heads, threaded aluminum rods, and four U-bolts. The 3.5" length coupling tube will be used so that the electronics bay can slide into the larger diameter rocket tube of the forward section and be bolted in place. This tube will also allow the avionics bay to be easily sealed from the blast pressure. Two  $\frac{1}{4}$ "-20, 5 1/2" long 6061-T6 aluminum threaded rods will be cut to hold the electronics bay together. The two bulk heads will be laser cut and consist of two separate 3/8" birch plywood pieces glued together. One will have an outer diameter equal to the outer diameter

of the coupling tube and the other will have an outer diameter equal to the inner diameter of the coupling tube, so it can slide in and be held in place. The bulkheads will have holes for the two threaded rods in addition to one  $\frac{1}{4}$ " U-bolt where the parachute shock cords can be attached. The electronics will be mounted to a 3/8" thick 2 1/2" by 5" birch plywood board that has two aluminum tubes epoxied to it. The arming switches will be mounted to the coupling tube but will be accessible from outside the rocket. The aluminum tubes run the width of the plywood board and are spaced at the same distance as the aluminum threaded rods so that, when assembled, the electronics board can slide onto the threaded rods and be held in place inside the coupling tube. The coupling tube will be inserted into the forward section of the rocket at the desired location top of the bay is flush with the coupler tube of the nose cone. Then four 1/4" holes will be drilled 90° apart through both the rocket body tube and coupling tube to ensure proper alignment. Four  $\frac{1}{4}$ -20 aluminum nuts will be secured into the top bulkhead of the bay and reinforced with carbon fiber plates on the top and bottom to ensure the bay connection to the rocket body is fail proof. Four nuts on either end of both threaded rods will hold the electronics bay together by "clamping" the bulk heads to the coupling tube section (with electronics board inside, sitting on the threaded rods). Once assembled, the avionics bay will be slid into the forward section and bolted into place.

The 6061-T6 threaded aluminum rods have a tensile strength of 42,000 psi. Thus, for a minor diameter of 0.188", each rod can withstand 1166 lb of force before yielding.

$$F = \sigma A = 42000 \frac{\text{lb}}{\text{in}^2} * 0.02776 \text{ in}^2 = 1165 \text{ lb}$$

With two rods, the total force that can be transferred through the avionics bay is 2332 lb. Thus for a 30 lb rocket, there is a safety factor of over 70. This will also allow for the increased load the rods will experience as the parachutes open and the rocket decelerates. The same logic also holds for the U-bolts, which are the same size and material as the threaded rods. There is one U-bolt on each end of the avionics bay. An accelerometer in the avionics bay will shed light on the impulsive loads seen during parachute deployment.

## 4.4 Mission Performance Predictions

---

### 4.4.1 Mission Performance Criteria

---

1. The rocket flight must be safe and stable.
2. The rocket must reach a predetermined maximum altitude of 5,300 ft.
3. During ascent, the payload must not shift within the rocket body.
4. At apogee, the drogue parachute will be deployed
5. During the rocket's descent, at about 700 ft., the main chute is deployed.
6. Each section of the rocket must land with a kinetic energy of less than 75 ft.-lb<sub>f</sub>.
7. The payload shall sustain no damage upon landing.
8. The rocket shall not drift more than 2500 ft. from the launch site for 25 mph winds during launch and recovery.

#### 4.4.2 Simulations and Predictions

Mission performance was predicted through the use of *Rocksim v9.0*. Rocksim was also used to model the rocket, and was run to determine the aerodynamic profile associated with the rocket. The performance predictions made use of the mass predictions in the mass statement. The pad weight was chosen to lie on the conservative side of the mass uncertainty range. As stable flight is essential, the center of gravity was set to an ideal location using a mass override. If necessary, physical weight will be added to the rocket to achieve this.

#### VANDY 16

Length: 102.0100 In., Diameter: 5.5400 In., Span diameter: 21.5423 In.  
 Mass 605.8515 Oz., Selected stage mass 605.8515 Oz. (User specified)  
 CG: 64.6174 In., CP: 75.2168 In., Margin: 1.91  
 Engines: [L1720-WT-None, ]

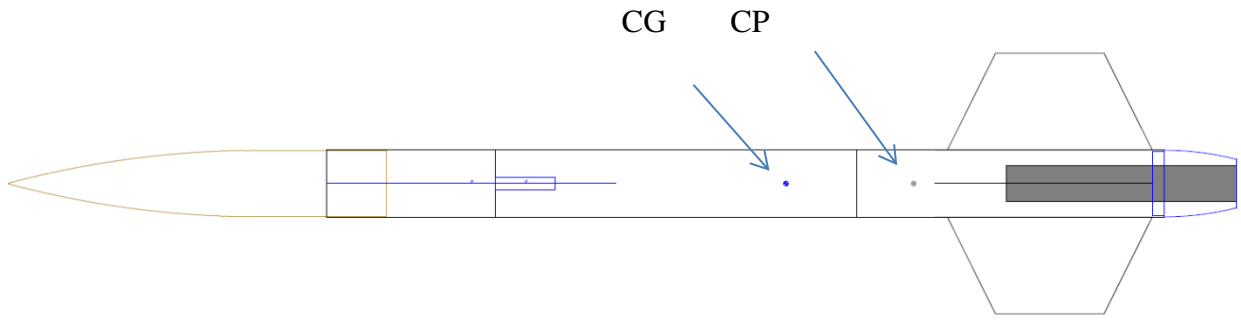


Figure 41: Location of centers of gravity and pressure of rocket

Table 10: Summary of parameters used in simulations

Vehicle & Launch Description	Recovery System
Vehicle Height: 102"	
Vehicle Diameter: 5.5"	Drogue Chute: 2.5 ft. elliptical (@ apogee)
Rocket Body Tube Material: <i>Carbon-fiber</i>	Drogue Charge: 1.1 g
Nosecone Shape: 4:1 (Ogive)	Payload Chute: 12 ft. elliptical (@apogee)
Launch Weight: 37.9lbf	Shear Pin Usage: Drogue Chamber: 3 pins (#4-40); Payload Chamber: 3 pins (#4-40)

Launch Rail: 144"	<b>Avionics</b>
Static Stability Margin: 1.91	Altimeter: Strato Logger (3 units)
T/O Thrust-weight: +12 average	Drogue Charge: 1.1 g Main Charge: 3.5 g
Ground Wind: ~ 11 mph	
Motor Specifications	Apogee: 5300 ft.
Motor: Cesaroni Pro-75 L1720	Velocity @ launch rail departure: 85 fps
Length: 48.6 cm, Diameter: 75mm	Landing speed under drogue: 69 fps
Motor Weight: 3341g , Propellant: 1755 g	Landing speed under main: 13.4 fps
Average Thrust: 1720 N , Burn Time: 2.1s	Landing energy of largest section: 67 lbf-ft
Max Thrust: 1947 N	Rocket drift at landing < 500 ft.

The simulation results are shown below

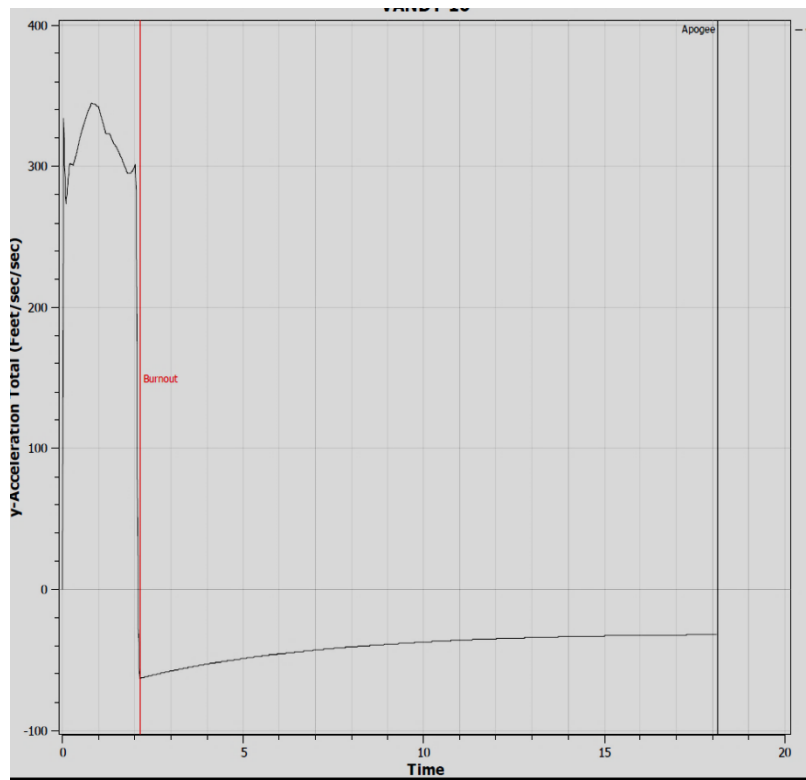


Figure 42: Acceleration vs. Time (maximum acceleration of +12g)

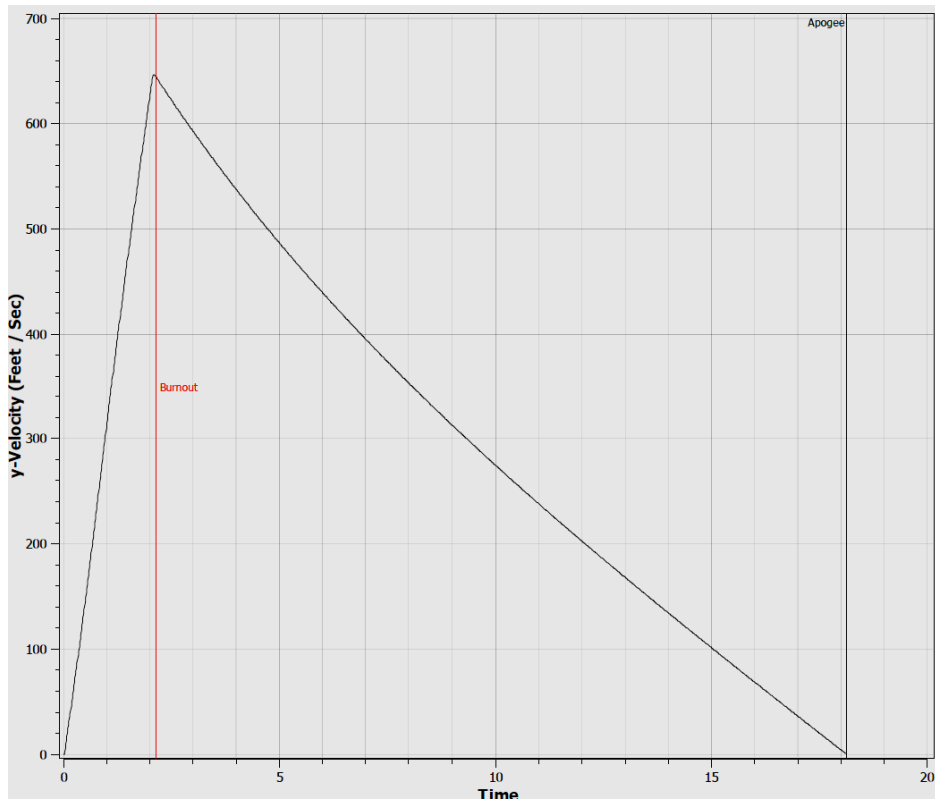


Figure 43: Velocity vs. Time (maximum velocity at motor burnout is 650 fps)

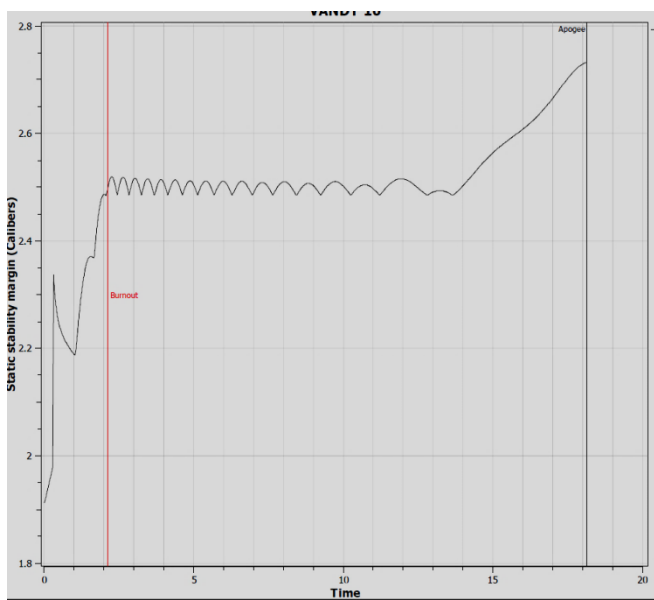


Figure 44: Static Stability Margin vs. Time (stability margin starts at 1.9 and quickly increases to 2.5)

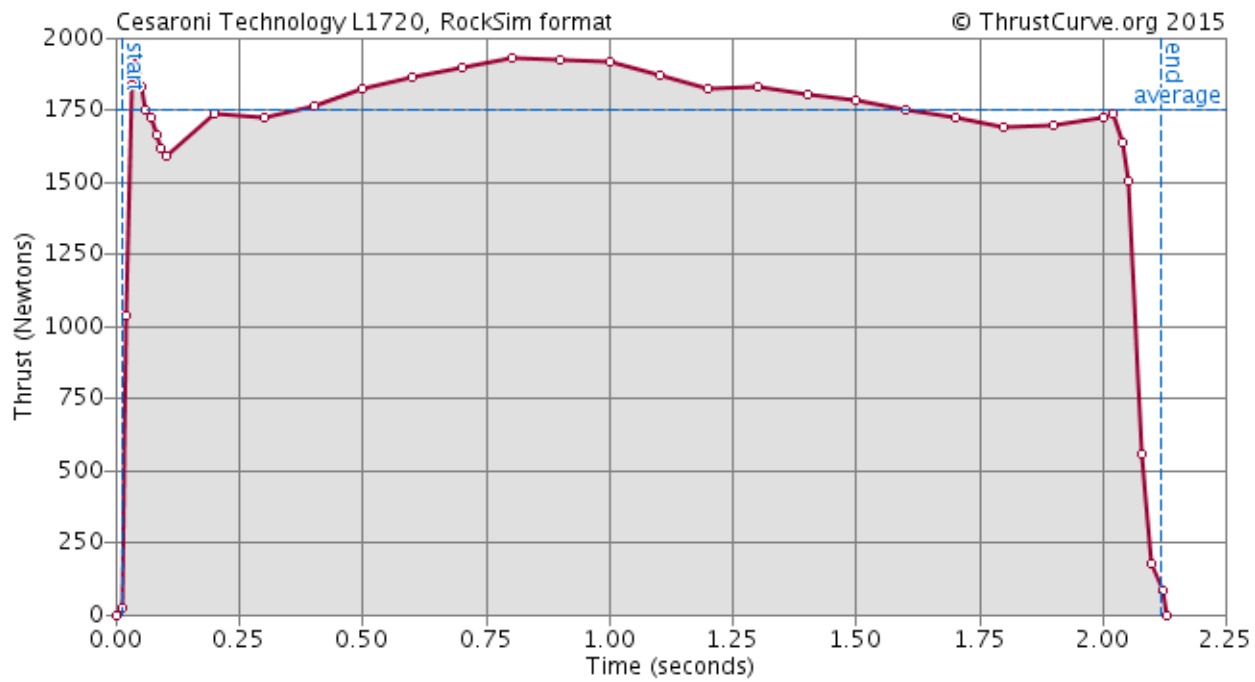


Figure 45: Cesaroni L1720 Thrust Curve

## Change in Rocket t/o Mass from 30.5lb

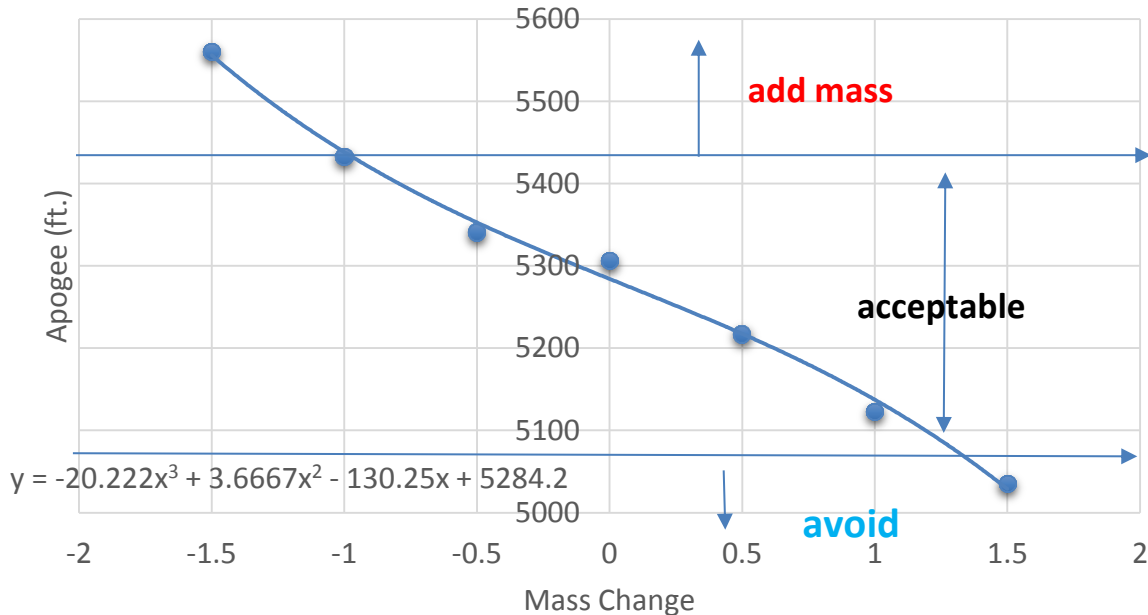


Figure 46: Rocket Apogee vs. Launch Mass changes (baseline: 30.5 lb)

## Apogee Variation

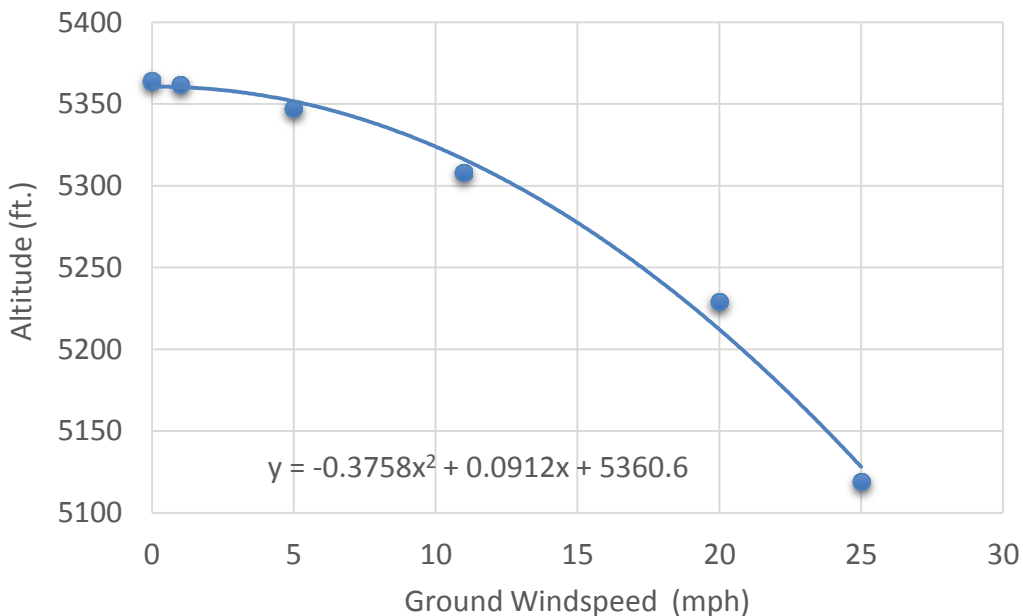


Figure 47: Rocket Apogee vs. Ground Wind Speed (11 mph ground winds are typical in April)

The salient features of the simulations are as follows:

- (i) The maximum positive acceleration during take-off is ~ 12g (5.0g avg.)
- (ii) The maximum flight speed at motor burnout is ~ 650 fps.
- (iii) The velocity at launch rail departure is a robust 85 fps.
- (iv) The stability margin of ~ 1.9 at launch pad, and quickly rises to 2.5 just at motor burnout. Rocket flight will be stable and can handle robust side winds.
- (v) Minimal apogee variation with windspeed as simulated up to 25 mph.

Landing drift is within 2500ft of the launch pad for winds up to 25 mph.

#### 4.4.3 Kinetic Energy

---

The kinetic energy of the rocket at landing is restricted to less than 75 ft-lbf. Section 4.3: *Recovery Subsystem* shows that the descent speed after the main parachute deploys is 13.4 fps. The heaviest section of the rocket, the tail + payload section, is 24 lbs. The kinetic energy of this section as it hits the ground is  $KE = \frac{1}{2}mv^2 = \frac{1}{2}(24\text{ lb})(13.4\text{ fps})^2 = 67\text{ ft-lbf}$ . This assumes no low level winds and lofting resulting from it.

#### 4.4.4 Drift Calculations

---

The *RockSim* simulations provided the following results of landing drift with ground windspeed. The simulations have been run for -5 deg (into wind) launch scenarios. The simulations basically take a constant lateral windspeed in the estimations. As winds greater than 25mph constitute a launch abort condition, drift greater than 2500ft is not anticipated.

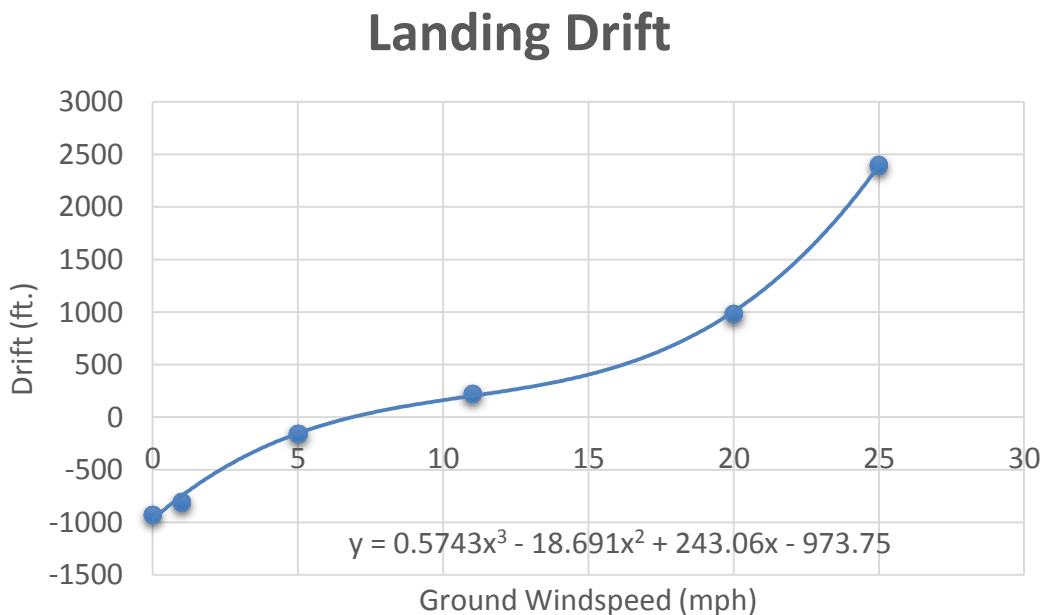


Figure 48: Drift vs. Wind Speed for Full-Scale Launch

## 4.5 Interfaces and Integration

---

### 4.5.1 Payload Integration Plan

---

#### 4.5.1.1 Fuel Delivery System Integration

---

The structural (non-electronic) elements of the Fuel Delivery System payload that are internal to the rocket body are the pressure reservoir and pressure regulator assembly, the airline supplying pressure to the fuel tank (controlled with a solenoid, which is electronic), the fuel tank with Slosh Abatement System installed, the fuel delivery line to the two H<sub>2</sub>O<sub>2</sub> thrusters, and during the first two test flights the GoPro camera and illumination assembly.

The most important aspect of the retention system is ensuring that the above components remain rigidly fixed at all times during the launch and recovery, and that any tube connections that are under pressure are sufficiently secured such that the connections are not broken by sudden increases in pressure. It is also vital to ensure that all the components are compatible with the H<sub>2</sub>O<sub>2</sub> fuel used in this design and that all plumbing is vacant of substances that would react with the fuel.

For this reason, Al 6061 has been selected as the material for air and fuel lines. Flexible hose has not yet been purchased, but 316 stainless steel interior hose will likely be selected. This hose will be used to prevent a connection to thruster from exerting a force that distorts the thrust readings obtained. These materials (Al 6061 and 316 SS) are both strong enough to withstand the internal pressures and external accelerations with a healthy factor of safety well in exceedance of 4. It has been shown that 316 stainless steel is unreactive with hydrogen peroxide. Literature also suggests that Al 6061 should be unreactive within a relevant timescale for hydrogen peroxide. Al 6061 is unsuitable for long-term (a month or more) storage of hydrogen peroxide, but the fuel lines are expected to see ~5 seconds of exposure, which should have no effect.

For the current payload section prototype construction, see section 5.1.1.2.1 *Payload Section Retention System*.

Upstream of the fuel tank, a check valve will assure that no back-flow of hydrogen peroxide can contaminate the air lines or flow backwards towards the default-closed solenoid. A fuel line will run from the fuel tank through holes in the bulkheads and centering rings, and out to the connection apparatus for delivering fuel to the H<sub>2</sub>O<sub>2</sub> thrusters. The fuel line consists of ¼" OD aluminum tubing connected with Swagelock (also known as Yor-lock) fittings to the fuel tank and the thruster.

#### 4.5.1.2 Monopropellant Thruster Integration

---

The Vanderbilt Aerospace Design Laboratory has decided to place the thrusters within the tail cone that will aerodynamically camouflage it. Originally, the thrusters were to be cantilevered onto the outside of the rocket body. Previous teams from Vanderbilt have performed experiments examining the use of externally mounted ramjets.



**Figure 49: CAD of Vanderbilt’s 2013-2014 USLI rocket with externally mounted ramjets**

Instead of continuing in the vein of externally mounted thrusters, the thrusters will be mounted on cantilevers within the rocket body. Past teams mounted the thrusters externally because of its dimensions (approximately 4.05” diameter, 13.51” height) and propellant requirements (the nature of a ramjet requires high speed flow velocity entering the intake diffuser to function). The initial design of the thruster places the dimensions at 0.75” diameter, 4.81” height. Furthermore, the monopropellant thruster’s fuel will be completely contained within the rocket body. In addition to the lack of constraints necessitating outside placement, locating the thrusters internally is preferable for improving the testing and evaluation of the hydrogen peroxide thrusters. Externally mounted thrusters will cause increased drag force or severely increase total rocket weight via aerodynamically shaping of the thruster housing. This will require a motor with a higher impulse than the selected Cesaroni L1720 solid rocket motor. Externally mounting the thrusters will also cause buffeting loads and resulting complications with thrust measurement. The random variations in fluid pressure and velocity due to the turbulent nature of airflow will cause unpredictable fluctuations in loading. Considering the total force provided by each thruster is estimated to be roughly 20N, moderate noise from inconsistent drag and structural vibrations will contaminate data collection. The aforementioned reasons were sufficient to justify thruster relocation. A proposed design showing the modified boat tail can be seen in the figure below with the thrusters placed within. Justifications for exact tail cone dimensions will be further discussed in section 5.3.2.3.4 and validated with CFD.

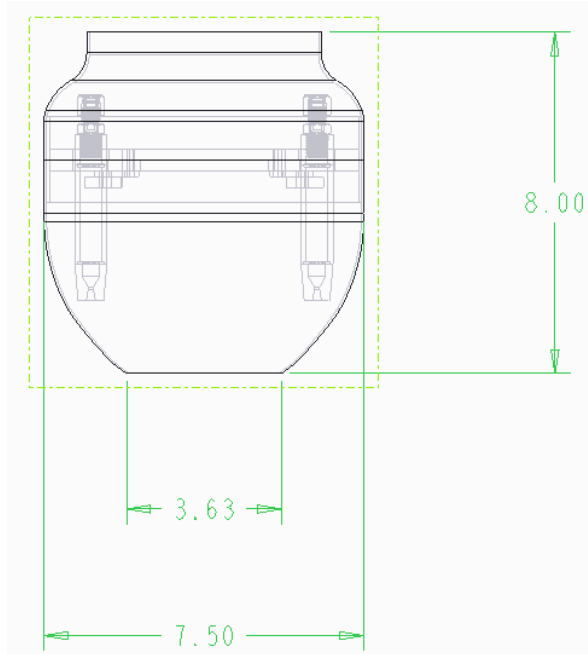


**Figure 50:** Modified tail cone with internally mounted monopropellant thrusters

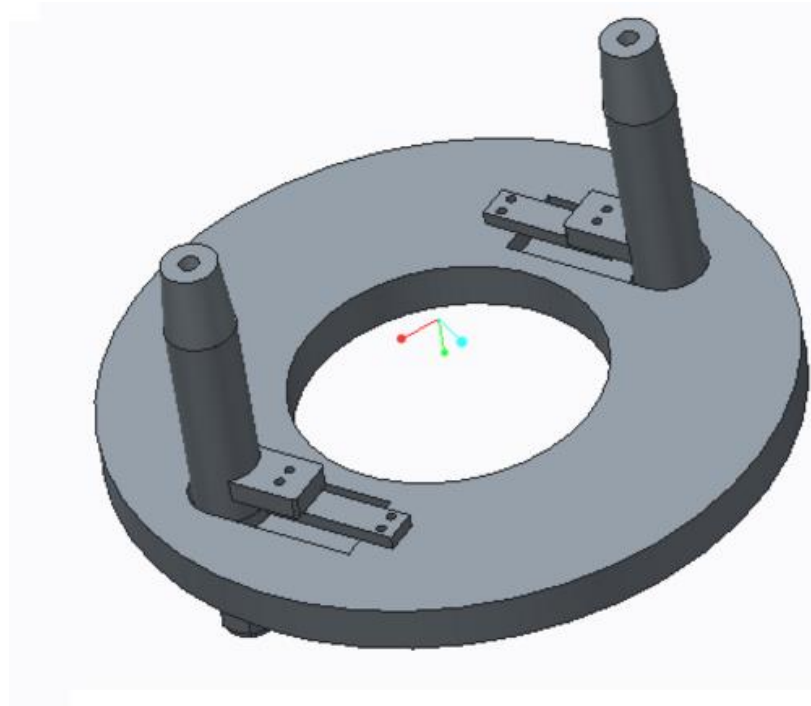


**Figure 51:** Diagram of thruster-pylon configuration attached to a bulkhead

#### 4.5.1.3 Structural Analysis Integration

Three accelerometers will be rigidly attached to the internal body of the rocket. The first accelerometer will be secured to the inside wall of the avionics bay, near the nose cone, with epoxy. The second accelerometer will be attached to a flat, rectangular, piece of aluminum with

epoxy. A hole will be drilled into each corner of the aluminum plate and a screw will run through each hole and into a bulkhead in the upper part of the payload section. This will secure the accelerometer to the payload section but still allow it to be removed and reused in the full-scale rocket. The third accelerometer will first be attached to a rectangular, curved, section of carbon fiber coupler tube. A hole will be drilled in each corner of the carbon fiber section and a matching set of holes will be drilled into the upper part of the tail section body tube. Small rivets will run through each corresponding set of holes to hold the small section of carbon fiber tube and the attached accelerometer in place. These rivets will be removed after the subscale flight to detach the accelerometer and allow it to be reused on the full-scale launch.

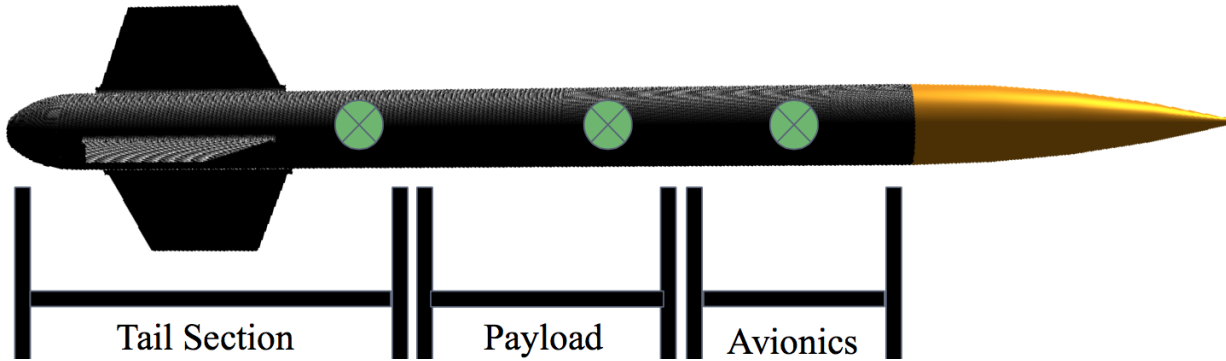


**Figure 52: Diagram of sensor placement for subscale launch**

#### **4.5.2 Interfaces within Launch Vehicle**

---

There are 4 distinct sections in the rocket joined by 1/16" thick coupler tube. 2 of these sections will be rigidly joined by bolts, leaving 2 sets of shear pins and 3 distinct bodies tethered after deployment of both parachutes. The rear tail section is bolted to the payload section immediately forward of it using 4 1/4-20 bolts and nuts through the body diameter and 3.75" of coupler tube overhanging from the payload section. This joined section comes down as one body under the drogue parachute and then under the main parachute. 3.75" of coupler overhanging the payload section (the coupler runs the full length of the payload section) is connected to the forward section using shear pins to facilitate deployment of the drogue parachute. 4.4" of coupler tube and another set of shear pins join the nose cone to the forward section. These shear pins are severed when the main parachute, stowed in the nose cone, is deployed. Kevlar shock cords connect the sections after parachute deployment. The shock cords are anchored to U-bolts on structural bulkheads of their respective sections.

#### **4.5.3 Interfaces between Launch Vehicle and Ground**

---

This is described in detail in section 4.6.1: *Launch System and Platform*.

#### **4.5.4 Interfaces between Launch Vehicle and Ground Launch System**

---

This is described in detail in section 4.6.1: *Launch System and Platform*.

## 4.6 Launch Operations Procedures

---

### 4.6.1 Launch System and Platform

---

#### 4.6.1.1 Launch Pad

---

The Vanderbilt Aerospace Design Laboratory will use a launch pad that was originally developed by the 2007-2008 Vanderbilt SLI team and modified by the 2014-2015 SL team. After an examination of all parts and structure stability, this pad continues to be satisfactory in all criteria for successful rocket launches. The original design included angled leg mounts that were replaced by the 2014-2015 with threaded rods and nuts welded to the steel pad in an effort to reduce the distance from the pad to the ground. This design is easier to adjust and level, as well as lighter weight for transportation and assembly.

Key features:

- Removable legs for easy transportation, minimal storage space, and weight reduction
- Adjustable-length legs allow for precise leveling and adjustable height to ensure a level launch surface on any terrain
- 1/4" steel base plate
- Hinged and locking rail erector; allows rocket to be loaded on rail horizontally, and then the rail and rocket are erected together
- Rail is removable
- Rail is made of two 8020 aluminum rails, joined together by 3 custom-made joints, to provide a straight guiding path for rocket
- Rail is supported by a 3-mast aluminum tower section for enhanced stability

#### 4.6.1.2 Launch Ignition System

---

The launch ignition system consists of a 12V battery connected to 500ft leads. The leads go through a safety switch system to the motor igniter. The safety switch ensures that no voltage differential is delivered to the electric match igniter until a key is inserted into the safety switch and a button is pressed.

### 4.6.2 Launch Checklist

---

The team will review system preparation requirements well in advance of the launch. Safety oversight and launch procedures are managed by the launch leader. The student safety officer, Ben, will oversee all operations where danger to people or rocket might exist. Team leaders will supervise the preparation of their respected areas. Formal integration of systems requires the

launch leader's oversight. A member of NAR with appropriate certifications will oversee the assembly of the propulsion system. This is a quality control measure to ensure that mission essential systems are properly prepared for launch. All launch procedures are divided into systems along with the personnel required.

A final assembly and launch checklist for the subscale launch is provided below. This checklist will be adapted and modified to fit the full scale vehicle.

#### 4.6.2.1 Setup and Assembly Checklists

---

##### ***Launch location Setup***

- Unload equipment and materials from vehicles.
  - Setup tent and secure with stakes.
  - Assemble portable tables.
  - Setup bag for trash collection.
  - Place stands for each rocket section on tables.
  - Place rocket sections on stands.
  - Place avionics/electronics box on own table.
  - Ensure desired launch pad location will provide a sturdy base for rocket launch.
- WARNING:** If no such ground condition exists, abort launch.
- Place launch pad components near desired launch location.

##### ***Launch Pad Setup***

- Insert the four launch pad legs into the launchpad plate.
- Minimize the height the launchpad is configured from the ground.
- Bolt on the launch rail base to the main launch pad and face it away from any spectators.
- Pivot the launch rail joint into a horizontal configuration.
- Secure the top launch rail section to the base via the joining piece and secure with bolts ensuring a flush fit.
- Reorient the launch rail to the vertical configuration and secure with bolts.
- Use a level placed on the launch pad in a vertical configuration to verify that the launch pad is oriented perpendicular to the launch area. Adjust the leg heights by twisting the launch legs using a wrench to the necessary positions in order to ensure the launch rail is in the correct vertical alignment.

**WARNING:** This step is imperative for straight flight.

- Undo the bolts that secure the launch rail in the vertical position and pivot the launch rail to be horizontal for rocket integration.
- If necessary, use ladder to support launch rail in horizontal position so that tipping does not occur.
- Inspect fully assembled launch pad to ensure it provides a sturdy base for the rocket during launch.

**WARNING:** If any damage exists, abort launch.

##### ***Tail Section Check and Assembly***

- Insert the tail cone around the exposed rocket motor tube and along the rear coupler tube, fastening it in place with expanding plastic rivets.

- Inspect the tail section for any damage from transportation and handling, specifically the structural integrity of the fins, body and motor tubes, and centering rings.

#### ***Avionics Assembly and Integration***

- Inventory all avionics equipment.
  - Inspect all avionics equipment for safety and security.
- WARNING:** If any such components or equipment that cannot be readily repaired or replaced damage exists, abort mission.
- Ensure the StratoLoggerCF altimeters are secure and set for correct parachute deployment altitudes and that the connections are secure.
  - Connect all charge ignition wires connecting altimeters to wire terminals outside the avionics bay. Seal interior holes on the bulkhead with putty.
  - Connect arming switches to each altimeter.
  - Place battery in clip. Tape and zip tie. Check the 9V battery terminals.
  - Check voltage on new 9V batteries.
  - Connect 9V batteries to each altimeter and secure to lower avionics bay bulkhead using zip ties/tape.
  - Verify correct wiring scheme for both altimeters.

**WARNING:** Failure to perform this step may result in incorrect deployment of recovery system in flight.

- Install top avionics bay bulkhead thus enclosing avionics bay.
- Place parachute charges in blast caps and secure with blue painters tape.
- Inspect all separation ignition wires.
- Seal wire passage holes into avionics bay with removable putty.
- Place putty over all wire terminals in parachute sections to ensure connections are maintained.

#### ***Payload Section***

- Install GoPros in mounts.
- Secure all bulkheads in flight location on threaded rods.
- Load payload skeleton into rear section and fasten into place
- Bolt together tail section and payload section

*Following payload steps performed with vehicle in vertical position on the pad through access window.*

#### ***Fuel Tank Assembly***

- Place Slosh Abatement systems in tanks
- Fill tanks with 67 cc water with care to avoid bubble formation

**WARNING:** Failure to load tanks without bubbles can lead to gas intake in fuel system.

- Fasten lids to tanks
- Fasten Tanks to bulkheads

#### ***Data Collection Unit***

- Turn on lights in Payload bay
- Turn Go Pros and ensure recording function

**WARNING:** Failure in these steps will cause failure in primary mission success criteria.

- Place cover over payload access window and fasten in with expanding plastic rivets.

### ***Accelerometer Installation***

- Place empty SD card into ADXL345 Board.
- Turn on and verify function with shake test and status LEDs.
- check shake test data from SD card and confirm functionality.
- Wipe SD card and reinstall into board.
- Assemble accelerometers on mounts into tail section, Payload Section, and Avionics Bay
- Turn on accelerometers and verify status LEDs in Logging State

### ***Recovery System Assembly and Integration***

- Take inventory of all recovery equipment.
- Inspect all Kevlar fiber shock cords, protective blankets, and anti-zipper devices for safety and security.
- NOTE:** Connect shock cords to bulkheads and bays before insertion when possible

### ***Forward section***

- Mount avionics bay inside forward section, align and secure.
- Confirm that altimeter switches can be reached after installation inside forward section
- Seal avionics bulkheads with removable putty.
- Inspect static pressure ports for obstructions.
- Inspect rocket parachute for hardware defects and security
- Ensure all shock cord and parachute connections are in their proper locations.
- Visually inspect the deployment charges for secure connection.
- Visually verify that deployment charges are secured in their respective blast caps.
- Fold and load main parachute into nose cone followed by shock cord, folded using a z-fold.
- Join nose cone to forward section of rocket via three 4-40 nylon shear pins.

**WARNING:** failure to use three shear pins may result in premature jettison of payload section in flight.

### ***Payload section***

- Connect shock cord to top of payload section.
- Connect opposite end of shock cord to parachute.
- Place payload parachute charges in blast caps on rear of avionics bay and secure with blue painters tape.
- Inspect all separation ignition charges.
- Connect parachute to avionics bay rear bulkhead via a shock cord.
- Inspect payload parachute for hardware defects and security.
- Ensure all shock cord and parachute connections are in their proper locations.
- Visually inspect the deployment charges for secure connection.
- Visually verify that deployment charges are secured in their respective blast caps.

- Load drogue parachute and shock cord, folded using a z-fold, into forward section of rocket below avionics bay.
- Join forward section of rocket to the aft section via three 4-40 nylon shear pins.
- Once rocket is loaded onto launch rail and ready for launch, arm each altimeter and listen for correct sequence of beeps before launching.

#### ***Rocket Motor Installation***

- Motor should be stored in own container for transport and secured to avoid drops or impacts.
- WARNING:** Failure to transport motor safely and securely may result in cracking of propellant grains and inflight motor failure.
- Inspect the motor to ensure that no damage occurred during transportation or handling that could result in such failures.
- WARNING:** If such damage has occurred, abort mission and safely dispose of faulty motor under the supervision of the safety officer.
- Insert the Cesaroni P54-6G K1440 motor into rocket motor tube and tighten the positive screw cap retention ring. Applying baby powder to the exterior of the motor can help facilitate installation.
  - Verify that the positive screw cap retention ring is securely fastened to the rocket.

#### ***Launch Vehicle Final Integration***

- carry rocket assembly to the launch pad.
  - Line up the launch lugs that are attached with the rocket to the launch rail slots. Very slowly slide the launch lugs onto the rail guides making sure not to put a bending moment the rocket.
- WARNING:** failure to slide launch lugs onto the rail guides slowly may result in detaching the launch lugs and flight failure
- Once the Launch vehicle is oriented so that the tail cone is at placed one foot off the launch pad, slowly raise the launch rail back into a vertical configuration and bolt down the pad so that it will not pivot.

#### **4.6.2.2 Launch Checklist**

---

- Altimeter-beeping sequence is all systems go.
- Check for loose fittings in the fins, rocket sections, payload, and launch lugs.
- Insert the Cesaroni Profire igniter into the rocket motor and attach the leads that connect the igniter to the ignition trigger.
- Ensure the ignition system is wired to the power source.
- Move to safe distance, at least 100yd from the launch pad.
- Loudly announce that the “range is hot” and ensure everyone is a safe distance from the launch pad.
- Insert the key and listen for high-pitch sound of continuity.
- Ensure skies are clear of aircraft and birds.
- Begin initial countdown to launch at T-minus 10 seconds.
- At T-minus 1 second, depress button on ignition system to launch.
- Immediately after launch, remove key from ignition system.
- Disconnect ignition system leads from power source.

#### 4.6.2.3 Post-Launch Checklist

---

- Visually track the rocket throughout the flight. Once the main parachute has opened, begin to predict the landing position. As soon as the launch vehicle lands during a full scale test flight begin heading towards the launch vehicle. Or on competition day, as soon as NASA gives the OK to go recover the launch vehicle begin to head towards the launch vehicle.
- Record apogee as measured by the altimeters by listening to the audible beeps produced by the StratoLogger altimeters.
- Carry the sections of the rocket back to the staging area.
- Mark and discard the 9V battery.
- Check for structural damage on the airframe.
- Check for rocket and payload parachute damage.
- Discard the spent engine casing.
- Check for fractures in the avionics section.
- Debrief the launch, including: motor used, rocket configuration, altitude achieved, avionics on-board, and rocket recovery.

#### 4.6.2.4 Launch Abort Conditions

---

Along with the pre-launch checklists, a series of questions have been put together to ascertain whether the rocket is safe to launch. These questions must be answered by the safety officers prior to giving the go ahead to launch and serve to ensure there are no conditions with the rocket, payload, or environment that would prevent a safe launch. If any of the following questions are answered with a “**YES**”, the launch **must be aborted** unless the issue can easily and safely be solved.

Did damage occur to any of the following rocket/payload components during transport?

- Motor
- Main or Drogue Parachute
- Avionics Board or *Stratologger* Altimeters
- Rocket Vehicle Sections
- Vehicle Fins, Nose Cone, or Tail Cone
- Launch Pad

Are any untested or non-certified motors or other potentially unsafe materials being used in the flight?

Are motors being used that require certifications higher than those possessed by anyone present?

Is there any risk of the launch pad being unstable due to poor ground conditions?

Did any parts/connections become loose during transport?

Is there anyone within 300 feet of the launch pad?

Is there any equipment within 100 feet of the launch pad?

Is the launch pad within 1500 feet of any inhabited buildings or roadways?

Do known wind speeds exceed 20mph?

Will weather conditions (precipitation, extreme heat, etc.) compromise the integrity of rocket materials, payload bay electronics, or otherwise damage functionality of rocket components?

Are there any questions or concerns about the safety of the launch and those involved?

Have any items from the checklists or launch operational procedures been missed?

Is the actual rocket center of gravity location different from the simulated center of gravity location?

If any of the above questions are answered with a “**YES**,” **abort launch** unless the problem can be fixed without compromising the safety of the team, bystanders, or the rocket.

After the launch, the payload system and remainder of the rocket must first be retrieved from their landing locations. Before handling any of the equipment, we first verify that there were no failures during flight that may cause injury if touched. Then, we first package up the parachute to avoid tearing the fabric and return to the launch site. Starting with the payload system, we first verify that the exterior and interior support systems are still intact. Data is gathered from GoPros and Accelerometers (on SD Cards). We then inspect the avionics bay and determine the height reached by the rocket and compare it to our simulations. After verifying that the avionics bay has been proven to have returned safely, we turn our attention to the tail section. The structural integrity of the fins is checked first, then the motor retainer is removed. The motor and motor casing are extracted from the tail section and the integrity of the motor mount tube is inspected. Last, the shock cords and parachutes are checked for any burns or tears.

## 4.7 Vehicle Safety and Environment

---

### 4.7.1 Safety Officer

---

The Vanderbilt SL rocketry and safety mentor is Robin Midgett, a member of the National Association of Rocketry who holds Level 2 certification. In conjunction with Dexter (NAR Level 1) and Ben, our student Safety Officer, Robin will oversee the rocketry team to ensure safety precautions are taken during the design, construction, testing, and storage of all rocket materials and equipment. During the course of the year, other members of the Vanderbilt SL team may pursue various NAR certifications as well.

### 4.7.2 Preliminary Failure Modes Analysis

---

See section 4.1.5 for tables explaining various risks the team may face during a launch in relation to the overall rocket vehicle, the consequences each risk has and our plan to mitigate these risks.

### 4.7.3 Personnel Hazards and Concerns

---

A thorough evaluation of the possible hazards associated with the vehicle has been made with respect to the user as well as the environment. This evaluation has led to the Vanderbilt Aerospace Design Laboratory adopting its own set of safety practices and rules that must always be followed when performing operations that could potentially be hazardous. This includes using heavy machinery or equipment, hand tools, chemicals, energetic materials, electronics, high-pressure vessels and lines, combustible or flammable materials, and any other potentially harmful substance or tool. The use of tools, machinery, and chemicals or energetic materials

must be accompanied by the wearing of safety glasses and any other relevant safety equipment as well as proper lighting and ventilation. All parts must be properly supported before machining with any tool and all loose clothing, hair, or jewelry must be tied back or removed.

At the core of the construction and launch procedures will be a Team Operating Unit (TOU). This is a subset of the team who have been assigned a specific task (either by the leadership, their peers, or via volunteering) to be accomplished. For the purpose of safety and accountability, this group will never consist of less than two individuals. All TOUs are informed by the Safety Administration and Safety Documents and are expected to pause prior to beginning any task to ask a few basic questions. First, is there a protocol? If yes, follow it and then give feedback for future improvement. If there is no protocol, does the task contain significant hazards to either person or property? Stop and write a protocol with approval required prior to execution. For tasks with no significant hazards, it is permissible for the members of the TOU to pause, write a safety plan, and then execute the task with a follow-up report on the condition that the members of the TOU have appropriate training with directly applicable skills. A flowchart of this safety structure is shown below.

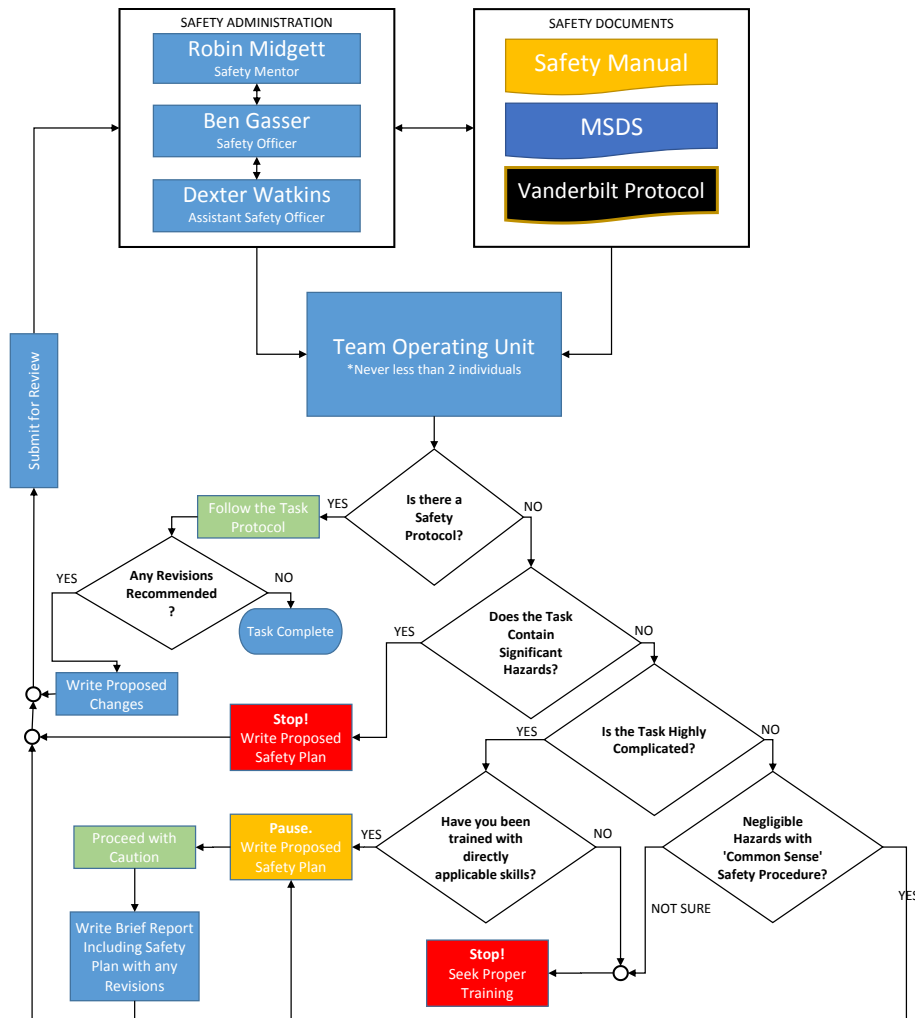


Figure 53: Safety structure flowchart

The hazards associated with the vehicle involve the storage of combustible substances such as motors and black powder as well as the igniters and adhesives. The material safety data sheets pertaining to any aspect of the vehicle and its operation have been obtained and thoroughly studied in preparation for the fabrication and future use of the materials necessary. Precautionary measures are being taken to ensure that no harmful or explosive substances can be misplaced or misused. Any explosive materials such as the black powder, motors, and motor replacements are kept locked in a type-4 MAGloc U.S. Explosives box, the key to which is held solely by the safety and rocketry mentor Robin Midgett. The adhesives are kept on low, sturdy shelves to prevent spilling; and aprons, latex gloves, and particle masks are mandatory during any fabrication process. Composite materials such as fiberglass and carbon fiber are also kept on designated shelves and are each wrapped in a layer of plastic followed by a subsequent layer of thick brown paper in order to minimize the amount of fibers released throughout the lab. With respect to the environment, no toxic substances are poured down the drain but rather are sealed in plastic containers and properly disposed.

Serving as the student safety officer, Ben Gasser oversees and signs off on all activities after carefully evaluating protocols, procedures, exposures, etc. He retains the right to assign multiples of students on a project and establishes the best operating condition for each hands-on activity. Ben is also in charge of ensuring that all members of the team, particularly those involved in the fabrication and machining of rocket/payload components, are properly trained and use safe practices when using machinery, tools, chemicals, and any other potentially hazardous fabrication methods. As stated in section 4.7.1: *Safety Officer*, Ben is well qualified to ensure these safe practices, but the rest of the team is also well-versed in safe use of equipment. All team members who use the machine shop have either taken Vanderbilt's machining course or have other education and extensive experience in the use of the equipment.

All relevant safety documents and information are posted on the VADL website. These include Federal Aviation Regulations, High Power Rocket Safety Code, Shop Safety Guidelines, Design Studio Rules and Bylaws, SDS Information, and various Standard Operating Procedures. After consulting the SDS sheets for the hazardous materials that the team could possibly come in contact with or use, the following summarizing table has been developed for quick referencing:

**Table 11: Risk and Risk Mitigation table for hazardous materials**

Material	Risk to Health	Risk Mitigations
3M Super 77 Spray Adhesive	Eye, skin, and respiratory irritation	Use in a ventilated area, wear protective gloves and eye protection, keep away from heat sources
Devcon 2 Ton Epoxy	Eye, skin, and respiratory irritation	Use in a ventilated area, with chemical resistant gloves and eye protection
Devcon 5 Minute Epoxy	Eye, skin, and respiratory irritation	Use in a ventilated area, with chemical resistant

		gloves and eye protection
Great Stuff Foam Sealant	Eye, skin, and respiratory irritation	Use in a ventilated area, with chemical resistant gloves and eye protection
Rust Oleum Painter's Touch 2x Primer	Eye, skin, and respiratory irritation	Use in a ventilated area, with chemical resistant gloves and eye protection
Rust Oleum Flat Black Spray Paint	Eye, skin, and respiratory irritation	Use in a ventilated area, with heavy-duty gloves and eye protection.
Cesaroni Pro75 Profire Igniter	Combustion, burn risk	Use outside, with face and body protection. Have fire-fighting method on hand. Keep away from heat.
Cesaroni Pro75 Rocket Motor Reload Kit	Combustion, burn and explosion risk	Use outside, with face and body protection. Have fire-fighting method on hand. Keep away from heat.
Black Powder	Combustion, burn and explosion risk. Respiratory irritation	Use in a ventilated area/outside. Use body/face protection. Have fire-fighting method on hand. Keep away from heat.
Hydrogen Peroxide	Fire and explosion risk. Eye, skin, and respiratory irritation	Store properly. Keep away from ignition sources. Have fire-fighting method on hand. Use in a ventilated area, with chemical resistant gloves and eye protection
SCIGRIP 4 Solvent Cement for Acrylic	Eye, skin, and respiratory irritation	Use in a ventilated area, with chemical resistant gloves and eye protection
MINWAX Clear Aerosol Lacquer	Eye, skin, and respiratory irritation	Use in a ventilated area, with chemical resistant gloves and eye protection
Acetone	Eye, skin, and respiratory	Use in a ventilated area, with chemical resistant

	irritation	gloves and eye protection
Gorilla Epoxy—Hardener	Eye, skin, and respiratory irritation	Use in a ventilated area, with chemical resistant gloves and eye protection
Gorilla Epoxy—Resin	Eye, skin, and respiratory irritation	Use in a ventilated area, with chemical resistant gloves and eye protection
Loctite Super Glue Liquid	Eye, skin, and respiratory irritation	Use in a ventilated area, with chemical resistant gloves and eye protection
West System 105 Epoxy Resin	Eye, skin, and respiratory irritation	Use in a ventilated area, with chemical resistant gloves and eye protection
West System 205 Fast Hardener	Eye, skin, and respiratory irritation	Use in a ventilated area, with chemical resistant gloves and eye protection
West System 206 Slow Hardener	Eye, skin, and respiratory irritation	Use in a ventilated area, with chemical resistant gloves and eye protection
West System 207 Special Clear Hardener	Eye, skin, and respiratory irritation	Use in a ventilated area, with chemical resistant gloves and eye protection
West System 209 Extra Slow Hardener	Eye, skin, and respiratory irritation	Use in a ventilated area, with chemical resistant gloves and eye protection
Mineral Spirits	Eye, skin, and respiratory irritation	Use in a ventilated area, with chemical resistant gloves and eye protection
Fibre Glast PVA Release Film	Eye, skin, and respiratory irritation	Use in a ventilated area, with chemical resistant gloves and eye protection
Fibre Glast MEKP Hardener	Eye, skin, and respiratory irritation	Use in a ventilated area, with chemical resistant gloves and eye protection
Fibre Glast Polyester	Eye, skin, and respiratory	Use in a ventilated area, with chemical resistant

Molding Resin	irritation	gloves and eye protection
Meguiar's Mold Polish Conditioner and Release Wax	Eye, skin, and respiratory irritation	Use in a ventilated area, with chemical resistant gloves and eye protection
Fibre Glast CSM Fiberglass	Eye, skin, and respiratory irritation	Use in a ventilated area, with chemical resistant gloves and eye protection
Fibre Glast Fiberglass Fabric	Eye, skin, and respiratory irritation	Use in a ventilated area, with chemical resistant gloves and eye protection
Rexco Partall Paste #2	Eye, skin, and respiratory irritation	Use in a ventilated area, with chemical resistant gloves and eye protection
Fibre Glast 3K 2x2 Twill Carbon Fiber	Eye, skin, and respiratory irritation	Use in a ventilated area, with chemical resistant gloves and eye protection
Fibre Glast System 2000 Epoxy Resin	Eye, skin, and respiratory irritation	Use in a ventilated area, with chemical resistant gloves and eye protection
Fibre Glast 2020 Epoxy Hardener	Eye, skin, and respiratory irritation	Use in a ventilated area, with chemical resistant gloves and eye protection
Fibre Glast 2060 Epoxy Hardener	Eye, skin, and respiratory irritation	Use in a ventilated area, with chemical resistant gloves and eye protection
Fibre Glast 2120 Epoxy Hardener	Eye, skin, and respiratory irritation	Use in a ventilated area, with chemical resistant gloves and eye protection
Fibre Glast Orange Tooling Gel Coat	Eye, skin, and respiratory irritation	Use in a ventilated area, with chemical resistant gloves and eye protection

All relevant SDS information can be found in the Appendix.

## **4.7.4 Standard Operating Procedures**

---

To ensure the safe handling of some of our most dangerous materials and chemicals, a set of Standard Operating Procedures has been created in conjunction with our Student Safety Officer, Ben. The Standard Operating Procedures below are

### **4.7.4.1 Hydrogen Peroxide Standard Operating Procedure**

---

Full text of the Hydrogen Peroxide Standard Operating Procedure can be found in the Appendix.

### **4.7.4.2 Carbon Fiber Standard Operating Procedure**

---

Full text of the Carbon Fiber Standard Operating Procedure can be found in the Appendix.

### **4.7.4.3 Epoxy Resin Standard Operating Procedure**

---

Full text of the Epoxy Resin Standard Operating Procedure can be found in the Appendix.

### **4.7.4.4 Polyester Resin Standard Operating Procedure**

---

Full text of the Polyester Resin Standard Operating Procedure can be found in the Appendix.

## **4.7.5 Environmental Hazards and Concerns**

---

The environmental concerns related to the construction of the rocket are primarily the proper disposal of all hazardous materials, such as epoxy resins and hardeners. The disposal of materials such as these will be conducted according to the SDS information that is available. Precautions are also taken to ensure that materials are disposed of quickly such that people are not exposed to them while working in the lab.

### **1. Battery Disposal:**

As per Duracell, Alkaline batteries can be safely disposed of with normal household waste. Never dispose of batteries in fire because they could explode.

### **2. Rocket Motor Disposal**

Misfire motors and motor shells will be neutralized by soaking them in water and leaving them in there until the casings unwrap and the propellant grains fall apart. The chemicals used are not environmentally harmful for disposal.

### **3. Trash and Used Field Material Disposal**

All trash will be properly bagged and disposed appropriately, and the field site will be left as is after the launch.

### **4. Resin Disposal**

Allow to cure and dispose of by all applicable local, state, and federal federations.

# 5 Payload Criteria

---

## 5.1 Selection, Design, and Verification of Payload Experiment

---

This payload experiment will be comprised of the following four systems that will work together to accomplish the payload objectives:

- 1) Two High Test Peroxide (HTP) Monopropellant Thrusters
- 2) Fuel Delivery System
- 3) Structural Analysis
- 4) Payload Instrumentation

A simplified schematic of the Monopropellant Thruster and Fuel Delivery System is shown below.

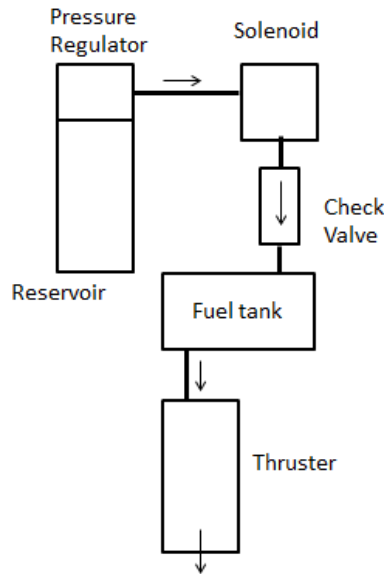


Figure 54: Schematic of thruster and fuel system payload

### 5.1.1 Fuel Delivery and Liquid Fuel Tank Slosh Abatement Systems

---

#### 5.1.1.1 Fuel Delivery and Slosh Abatement Systems

---

The purpose of the Fuel Delivery System is twofold. The entire system functions to supply high pressure H<sub>2</sub>O<sub>2</sub> fuel to the thrust generating monopropellant engine, where the fuel will undergo decomposition and its chemical potential energy will be converted to thrust. In this context, the fuel tank which must hold the H<sub>2</sub>O<sub>2</sub> fuel serves as an excellent test bed for a Liquid Fuel Tank Slosh Abatement System. This system is critical for ensuring reliable and consistent delivery of high pressure fuel to the monopropellant thruster and provides the environment necessary to examine payload requirements outlined in 4.1.1.2.2. The main goal of this payload centers on

eliminating the possibility of air entering the fuel pickup. Due to the deceleration of the flight vehicle after the initial engine burns out, the fuel will have a natural tendency to climb the tank walls in the negative ‘g’ environment. Air entering the fuel lines results in the interruption of fuel delivery and could lead irregular thrust environments. This is an unacceptable condition necessitating the creation of a Slosh Abatement System to eliminate this issue. Thus, a set of requirements for the fuel delivery system can be developed that encompasses the goals that must be met for the SL flight.

1. The system must deliver high pressure fuel at 450 psi to the thruster at the requisite time during rocket flight.
2. The system must extract a majority of the fuel in the fuel tank and deliver it in such a way that air is not present in the fuel lines (Slosh Abatement System).
3. The system must be capable of venting if excessive pressures are reached in the fuel tank ( $>600$  psi).
4. There must be some method to verify the functionality of the Slosh Abatement System.
5. The system must be accessible and secured while in the rocket and fit within the confines of the rocket geometry.
6. The system must be modular in design to enable simple troubleshooting, ease of installation, and performance upgrades.
7. Every component in the fuel delivery system must be compatible and non-reactive with hydrogen peroxide fuel.

These requirements lead to several possible options which could be utilized to accomplish the payload objectives. The first requirement necessitates some type of potential energy storage in order to compress the fuel to the 450 psi needed for high pressure fuel delivery. The most obvious methods of accomplishing this are through mechanical devices (such as a spring), hydraulic means (such as pressurizing the fuel tank with the fuel itself or having an external hydraulic pressure reservoir) or pneumatic means (pressurizing the fuel tank with a head of compressed air, or through an external pneumatic pressure reservoir). In the past, our team has had a great deal of success with using an external pneumatic pressure reservoir for fuel pressurization, namely in the form of a high pressure compressed air vessel. The compressed air tank has the benefit of being able to be mounted in any orientation without concern for venting or pressure buildup. This design is also inherently safer than an all-in-one fuel tank and pressure vessel combination. While the latter option initially appears more desirable by integrating two components into one, the problem resides with storing fuel at very high pressures. In order to provide consistent delivery at 450 psi, the fuel would have to be compressed to much higher pressures and then regulated down to provide a constant pressure head over time. This condition is not desirable because a leak or over pressurization of a highly compressed hazardous chemical is very dangerous. The compressed air tank solves this issue by storing inert compressed air at 2000 psi and has a built in regulator capping air outlet pressure at 450 psi for delivery to the fuel tank.

Fuel release will be controlled by a solenoid valve rated for high air pressure operation. It will be directly connected to the compressed air tank via an air source adapter (ASA) that screws onto the compressed air tank. This system will require power supply for the valve, as well as control logic for actuating the valve upon rocket launch. Through ground based testing, the effectiveness and feasibility of fuel delivery and proper atomization will be evaluated.

Tubing with a working pressure of 4,700 psi will carry the pressurized air to the fuel tank, which will be designed and fabricated in-house. The design of the fuel tank is similar to the design that was successfully flown in USLI 14, but with an updated Slosh Abatement System. The function of this system is to fulfill the second design requirement of extracting a maximal amount of fuel from the fuel tank without allowing air into the fuel lines. The team has developed two possible Slosh Abatement Systems—one based on dynamics and the other based on statics. The design flown in USLI 14, shown in figure 55a, utilizes dynamic properties of fluid flow to prevent air from reaching the pickup line. An air bubble must traverse a tortuous path in order to reach the bottom of the tank. The design created by this year's team, shown in figure 55b, uses statics and surface tension effects to prevent air from displacing the liquid fuel. In order to meet the third requirement, a 600 psi vent valve will be installed on the fuel tank to allow depressurization in case dangerously high pressures are reached.

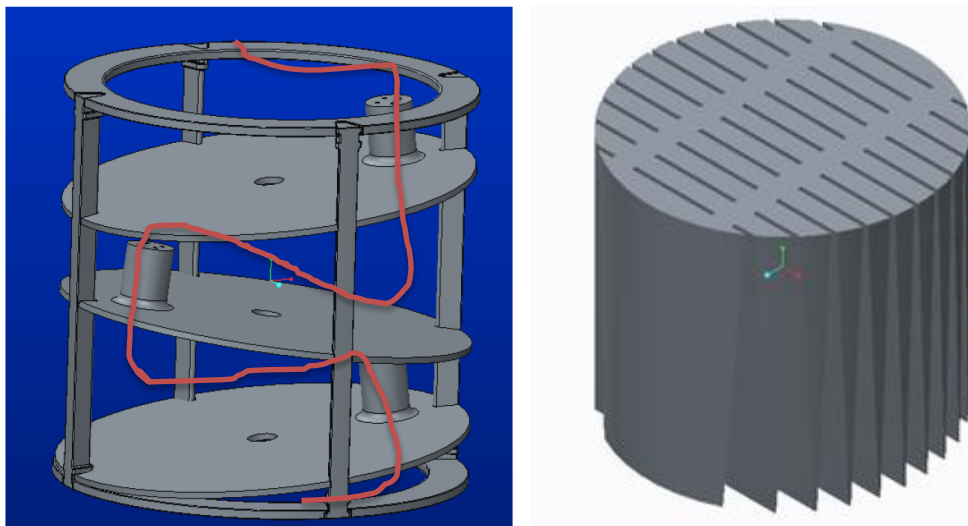


**Figure 55:** (a) USLI 13-14 Fuel Tank insert schematic with the trajectory that a bubble has to take to reach the pickup,  
(b) USLI 15-16 Fuel Tank insert design

Since fuel delivery is such a vital aspect of the payload performance during negative ‘g’ flight, extensive flow visualization studies will be conducted using polycarbonate and acrylic fuel tanks with the two proposed baffling system designs. These prototypes mimic the final fuel tank’s size and shape, but are not pressurized and are used solely for visualizing how the fluid will behave in the final opaque aluminum tank. Internally mounted cameras (GoPro) facing the fuel tank can be used to acquire video during subscale flight, which will provide an analysis of the effectiveness of the baffling systems. LED flashlights mounted below the tank provide illumination so the camera can see inside the dark body of the rocket. These preliminary flights will be crucial to developing a working design which can be utilized for the SL flight and fulfill requirement four.

Along with these in flight testing methods, the VADL Drop Test Stand (details in section 5.3.1.3.4 VADL Drop Test Stand) will be used for ground based testing and to rapidly see advantages and disadvantages of various designs and design iterations.

The compressed air tank and the fuel tank will be mounted in a vertical orientation within the payload section of the rocket. Interaction with these systems will be available through an access

door in the side of the rocket. This will allow simple removal and installation of payload components and ensures that requirement five is fulfilled.

#### 5.1.1.2 Fuel Delivery and Slosh Abatement Subsystems

---

A modular approach to the Fuel Delivery System is desirable since modular systems offer numerous benefits when compared to a completely integrated system (requirement six).

- A modular system allows independent testing and verification of each subsystem before they are integrated into the whole.
- The subsystems can be constructed in parallel since there is not dependent functionality shared between subsystems.
- If a particular subsystem does not function as required, it can be redesigned and implemented without having to modify the rest of the design.
- Improvements can be made to specific modules in order to enhance overall system performance.
- Installation and troubleshooting are simplified since components are broken into discretized parts.

One of the main objectives of the Vanderbilt Aerospace Design Lab is a developmental program that incorporates continuous improvement and refinement of our payload and rocket design. In this context, a scalable, modular design for the Fuel Delivery System makes sense. As components undergo further testing and their performance characteristics are better understood, they can be suitably modified as their performance is enhanced. Therefore, there must be several subsystems which comprise the fuel delivery system and function in concert to achieve the desired goals of our flight. A functional architecture for the Fuel Delivery System can be created. See figure 56 below:

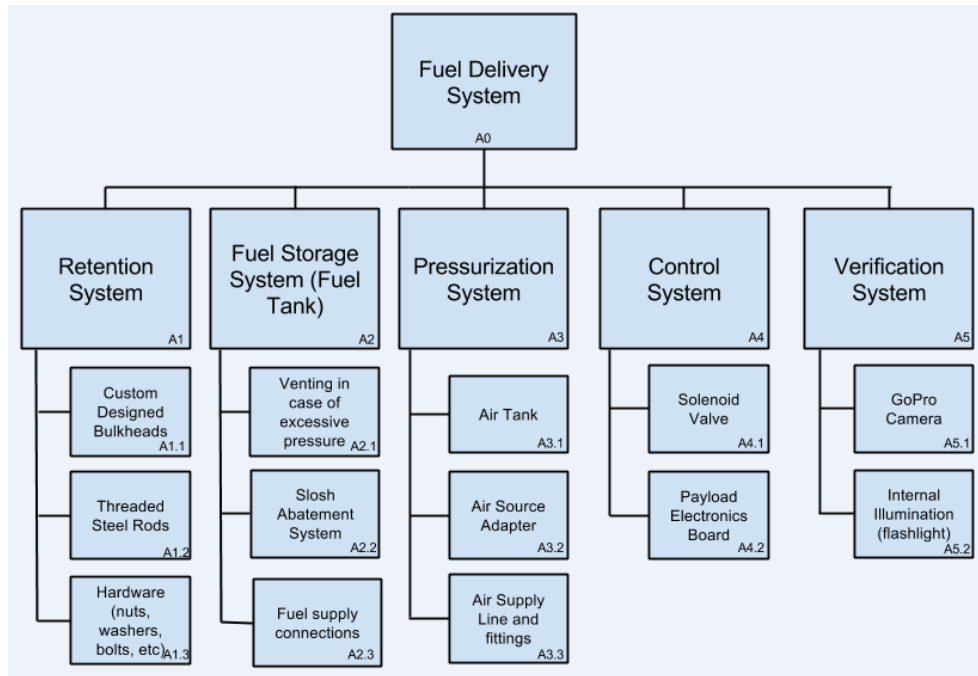


**Figure 56: Functional Architecture of Fuel Delivery System Modules**

#### 5.1.1.2.1 Payload Section Retention System

Figure 57 shows the payload section of the subscale rocket. In the subscale, there are two tanks that will be observed during launch with two GoPro cameras. Each tank will have a different slosh abatement system that will be tested during flight. Both tanks and cameras will be placed into the rocket via the window on launch day. All of the bulkheads were laser cut to size in Vanderbilt's Design Studio and are made of half inch plywood. The tanks will be attached to the bulk head with four one-inch screws with hex nuts to hold them in place. It was decided to remove the fittings from the tanks for the subscale launch in order to save space. To mount the cameras, first there are two steel tabs that are epoxied into the bulkheads inside of thin slits. Each tab has two holes for bolts. The cameras are encased in a 3D printed body. The casing is then attached to the two metal tabs with bolts with hex nuts on the end. There are two threaded rods that run along the payload section for added stability. Each bulkhead is attached to the rods with hex nuts on the top and bottom.

Looking at the top bulkhead in Figure 57 it can be seen that there are square weld nuts which have been epoxied in place. There will also be pieces of carbon fiber epoxied on the top and bottom of this bulkhead to reinforce the square weld nuts. There are holes drilled into the carbon fiber tubing that line up with the four square weld nuts. Bolts will then be inserted to hold the internal payload section in its correct orientation. Looking at Figure 57, it can be seen that the bottom bulkhead has a slightly larger diameter.

While all the other bulkheads in the payload assembly have a diameter of 5.25" to fit inside of the coupler tube, the bottom bulkhead has a diameter

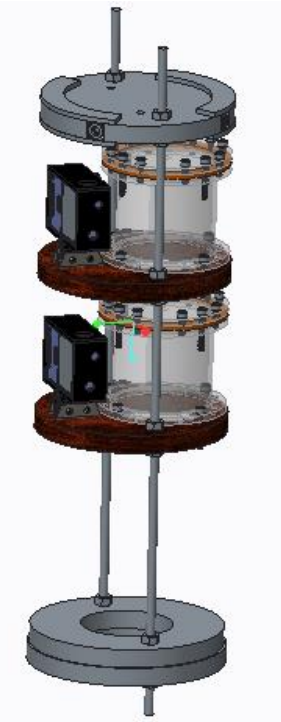


**Figure 57: CAD Model of subscale fuel delivery payload**

of 5.375” so that it can be pressed up against the bottom of the coupler tube in the payload section for added stability.

After the subscale launch is complete and data is collected from the fuel tank slosh abatement systems, the final payload assembly will have a single tank and GoPro camera. The payload section will be elongated to allow for the housing of a compressed air tank, solenoid valve and fittings for the fuel tank. There will also be additional holes cut into the bulkheads for the fuel, air and electrical lines to run through.

### 5.1.1.2.2 Fuel Tank

#### 5.1.1.2.2.1 Design of fuel tank

The current fuel tank design for the subscale launch is constructed using polycarbonate and acrylic materials that model the dimensions and shape of the fuel tank to be flown on the final test flight and SL flight and can be seen below in Figure 58. As mentioned previously, the purpose of this fuel tank is to provide flow visualization via recorded footage from the GoPro camera system during different launches to verify the functionality of different Slosh Abatement System designs. The acrylic ring on the bottom will be used to secure the tank to the bulkheads in the rocket. It will not be pressurized and is sealed using a rubber gasket to prevent leakage. Water will be used as the visualization fluid as it has similar density and viscosity to the hydrogen peroxide that will be used on the final flight.

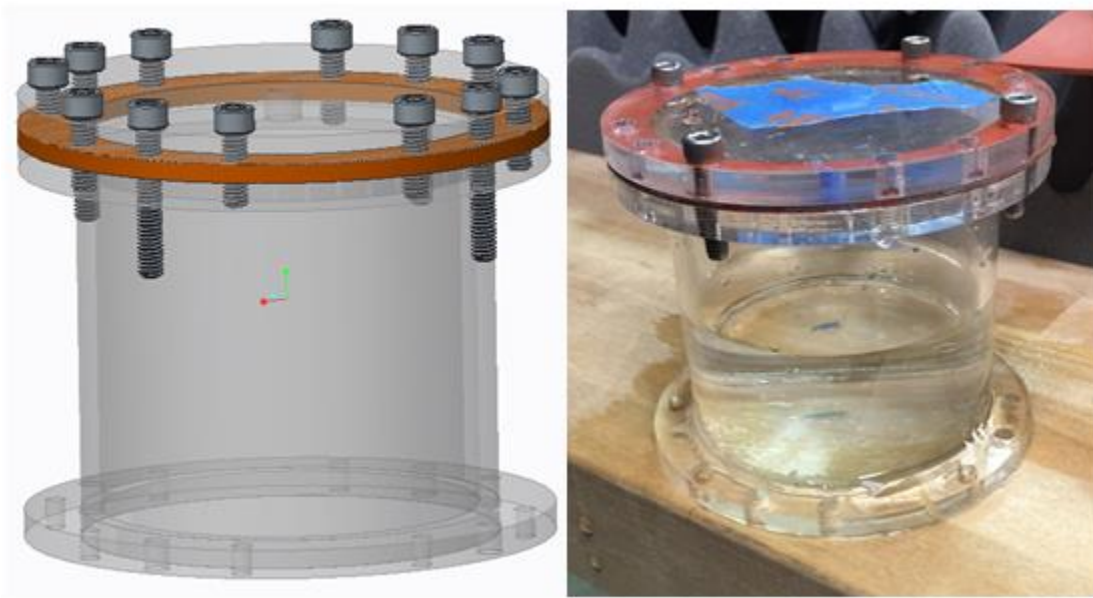


**Figure 58: Acrylic Fuel Tank CAD and Actual**

The fittings to be used in the final design for fuel extraction and air injection have been removed to save space and weight in the payload section. The removal of these simplifies the design and construction of the tank along with allowing for two tanks to be installed in the section rather than the one for the final flight. A fuel pickup tube is still located in the center of the tank,

however, as the effects of this line on the slosh abatement system are very important to the experiment.

#### *5.1.1.2.2.2 Venting In Case of Excess Pressure*

As this tank will not be pressurized there is no vent valve to release pressure because the tank will be at ambient pressure. As per SL guidelines, there will be a valve in the final pressurized tank design, in the context that a compressed air tank regulator failure or dissociation of the hydrogen peroxide could lead to a pressure rise.

#### *5.1.1.2.2.3 Design Considerations and Safety*

To safely design the fuel tank an analysis of the stresses involved must be undergone. It will be modeled as an ideal thin walled pressure vessel and as such the wall will act as a membrane and therefore will be unaffected by bending stresses.

The material used for the fuel tank is 6061 T6 Aluminum (properties from ASTM B209-10) and will be fabricated in house. Aluminum also has the added benefit of being non-reactive with hydrogen peroxide. It will be operated at 450 psi and have a volume of 200 cc. It is a thin walled cylindrical vessel with a 2.5" diameter, a height of 2.71", and a wall thickness of 0.125".

$$\frac{R}{t} = \frac{3 \text{ in}}{0.1 \text{ in}} = 30$$

Because  $R/t > 10$ , we can assume that the stresses are uniform across the wall.

Other assumptions for the analysis below are as follows:

- Homogeneous Material Properties
- Symmetry of Stresses Across Cylinder
- Uniform Internal Pressure
- End Effects are Negligible

From these numbers the hoop stress, axial stress, and radial stress can be calculated and then combined to find the Von-Mises' Failure Criterion. These calculations are shown below.

$$\text{Hoop Stress} = \sigma_h = \frac{P * d}{2t} = \frac{450 \frac{\text{lb}}{\text{in}^2} * 3 \text{ in}}{2 * 0.1 \text{ in}} = 6750 \frac{\text{lb}}{\text{in}^2}$$

$$\frac{P * \pi r^2}{2 * \pi r t} = \frac{P * d}{4t} = \frac{450 \frac{\text{lb}}{\text{in}^2} * 2.5 \text{ in}}{4 * 0.125 \text{ in}} = 2250 \text{ psi}$$

$$\text{Von - Mises' Failure Criterion} = \sigma_{eq} = \sqrt{\frac{(\sigma_h - \sigma_a)^2 + \sigma_h^2 + \sigma_a^2}{2}}$$

$$\sqrt{\frac{(4500 \frac{lb}{in^2} - 2250 \frac{lb}{in^2})^2 + (4500 \frac{lb}{in^2})^2 + (2250 \frac{lb}{in^2})^2}{2}} = 3900 \text{ psi}$$

*P = Pressure*

*d = Vessel Diameter*

*t = Vessel Wall Thickness*

#### 5.1.1.2.2.4 Axial Stress = $\sigma_a$ =Design Results

The above analysis provides an equivalent stress of 3,900 psi. The yield stress of the material used is 35,000 psi. This leads to a factor of safety of 9 and a max pressure that the vessel can withstand of 4,050 psi. The vent valve to be installed will open at 600 psi, which is far below this failure point.

#### 5.1.1.2.2.5 Design for Cyclical Stress

One has to examine pressure vessel failure due to cyclical fatigue. With repeated cyclical loading the endurance limit of the pressure vessel decreases. The number of cycles that will cause fatigue failure depends on the magnitude of strain that is incurred during each cycle of loading. Pressure vessel codes normal use a factor of safety of up to 20 based on cyclic operation. From Figure 59 below, it is apparent that even with an alternating stress in the 5ksi category, the designed fuel tank can withstand in excess of a billion cycles to failure.

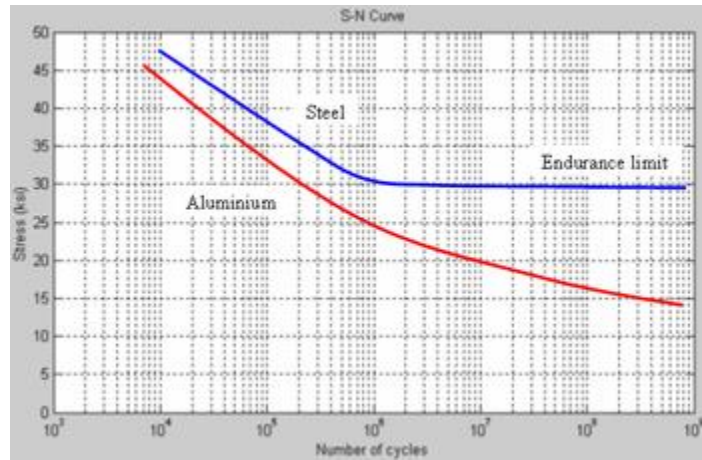


Figure 59: Cyclical Stress

During the course of SL testing and evaluation it will be operated far below this limit.

#### 5.1.1.2.3 Slosh Abatement System

### 5.1.1.2.3.1 Overall Goals

The overarching goal of the Slosh Abatement System (SAS) is to enable as much fuel to be extracted from the tank as possible while preventing any air bubbles from entering the fuel lines leading to the thruster. The SAS is designed as an insert (which is H<sub>2</sub>O<sub>2</sub>) that easily installs into the fuel tank. Because of this modular design, it can be removed and upgraded without having to modify the fuel tank in any way. It is also designed to be a passive system in order to improve reliability and performance.

### 5.1.1.2.3.2 Operation Window

The flight window in which the thruster will be operated highlights the difficulty of the problem. As can be seen below in Figure 60, during the operation window (3-10 seconds into flight) the acceleration of the rocket is estimated to range from -2g's to just over -1g of net acceleration. This causes the liquid to stack on the top of the fuel tank and away from the pickup. This necessitates the use of an SAS.

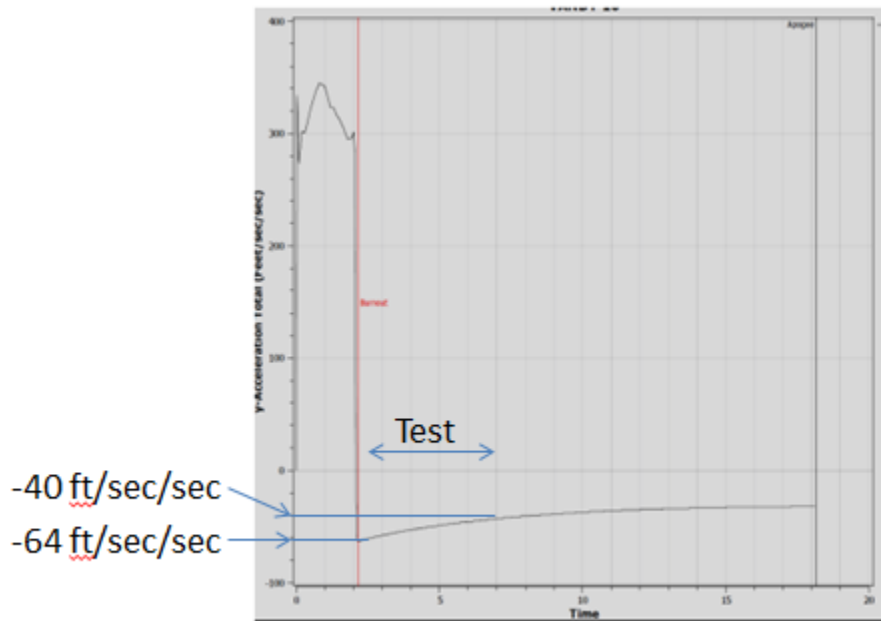
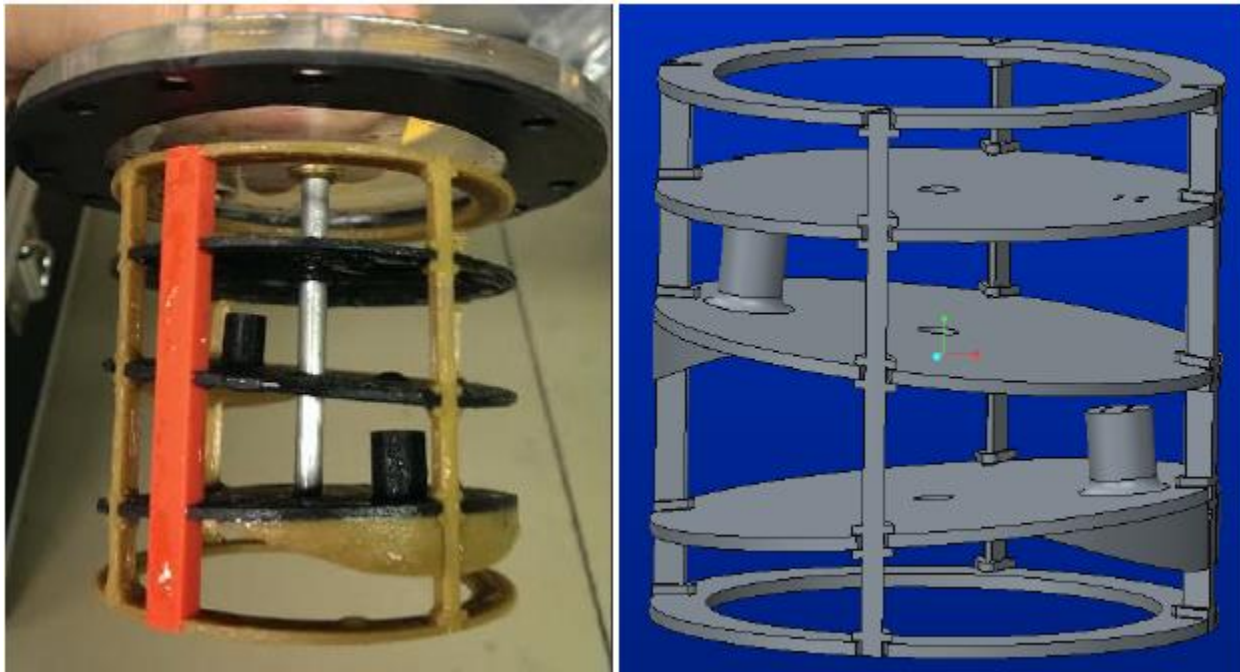


Figure 60: Operation Window

### 5.1.1.2.3.3 ULSI 14 Design

Two different SAS's will be tested using in flight flow visualization in the first launch. The first system is based on fluid dynamics and was developed and utilized in the USLI '14. It was originally based on ring type baffles which eliminate large vertical components of fluid velocity near the wall of the fuel tank. Different iterations of the design were built and tested. The design was modified to have the ring baffles to be slightly angled and raised bobbins were added. These two features created a tortuous path for any air bubble attempting to reach the fuel pickup along with limiting the liquid's ability to travel upwards during g-turnover. The design is seen below in figure 61. While this design was validated through in-flight usage testing during that

year along with ground based flip testing, it is of interest to see a flow visualization of this design in flight to better understand the advantages and disadvantages of the design. It will also provide information on how in flight flow visualizations correlate with actual in-flight performance under pressure.



**Figure 61: USLI '14 SAS Design**

This design was recently tested using the VADL Drop Test Stand to see preliminary results along for comparison with other designs. A schematic of the VADL Drop Test Stand is shown below in Figure 62 for reference. For more details about the stand see section 5.3.1.3.4 VADL Drop Test Stand.

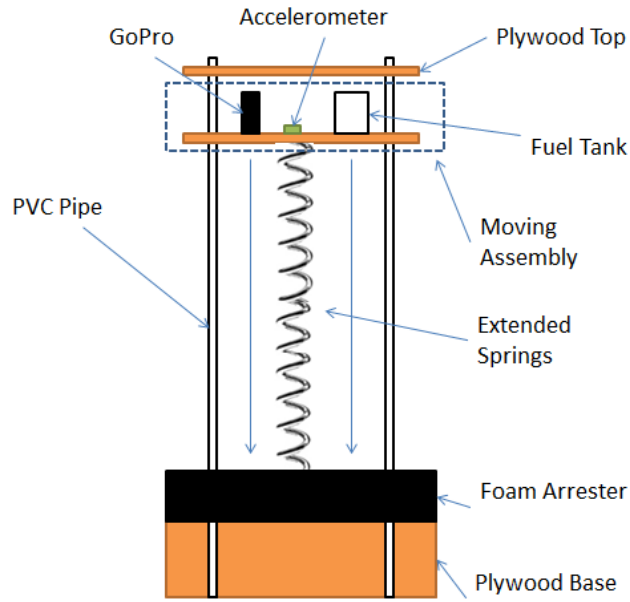


**Figure 62: VADL Drop Test Stand Schematic**

In the stand the acrylic tank was filled around two-thirds full with water while the insert was inside. It was then attached to the stand and dropped. Frame 1 is just before release at the top of the stand, Frame 9 shows the last frame before reaching the bottom of the stand, and frames 2-8 show increments between these two times as the tank and camera accelerate downwards. At the time no accelerometer data was available, but the maximum negative gravity condition is estimated by the dynamics model discussed in 5.3.1.3.4 VADL Drop Test Stand to be -2g. The platform traveled approximately 4ft in 0.5s validating this acceleration estimate. This maximum acceleration towards earth will occur in Frame 1 and the acceleration will decrease to -1g as the platform approaches the bottom of the test stand.

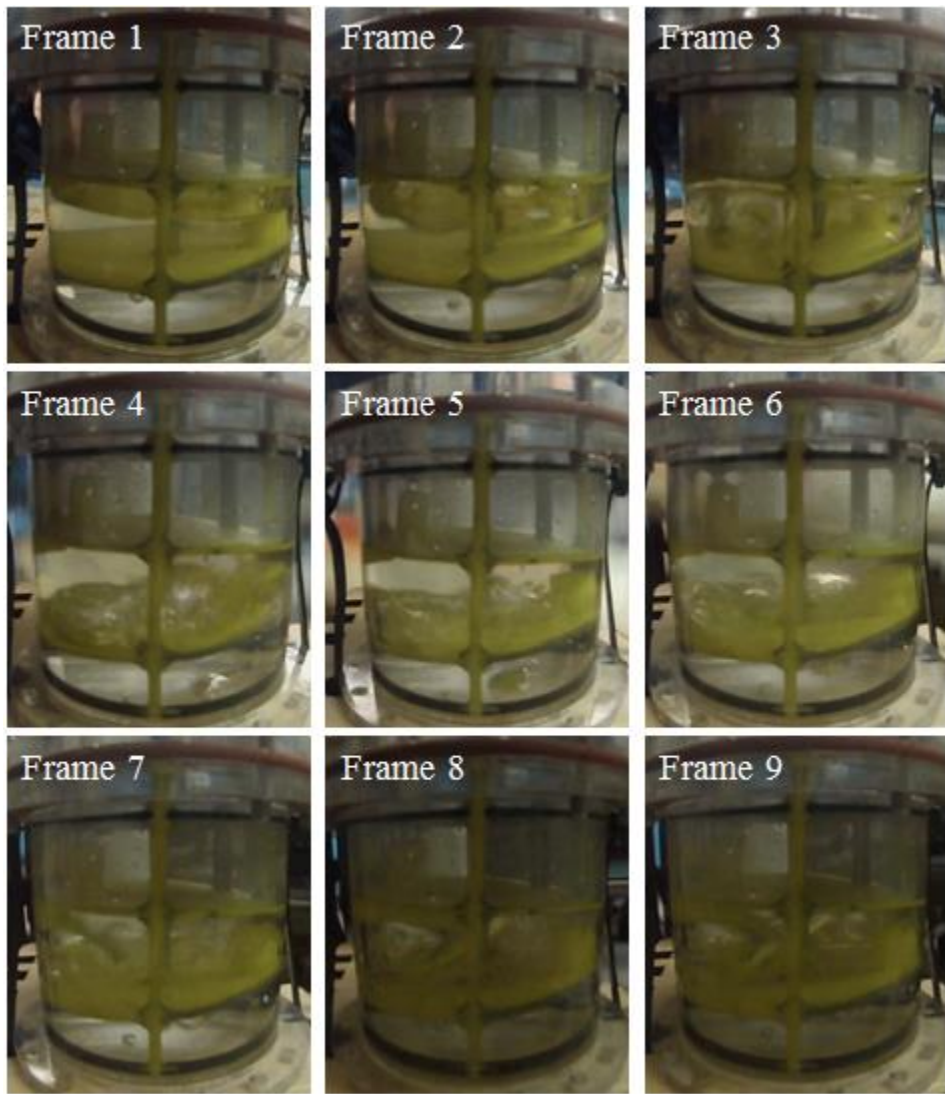


**Figure 63: USLI 14 Drop Test Stand -1g Results**

From these first test images of this design we can begin to see how the insert functions. Starting in Frame 2 and continuing until the end of the sequence, only one very small and hard to see air bubble enters the bottom compartment (where the fuel pickup would be located) from the compartment above it. This is desirable for fuel extraction as fuel picked up from this area would be free of air.

As the test begins in Frame 1, the fuel level can be seen just above center in the second compartment from the bottom. The platform has not moved at all and is still being held at the top of the test stand. In Frame 2, the platform has begun to accelerate downwards and the liquid fuel has begun to move upwards, especially on the left side as one would expect near the wall. Frame 3 then shows the turbulence that begins to form as the fuel hits the top baffle of the second compartment. The liquid in the bottom-most compartment, where the fuel pickup will be located, appears undisturbed. In Frames 4, 5, and 6, the liquid stacking on the top of the

compartment can be seen. The air and fuel have switched positions and the air has migrated to the low section of the angled baffle and is below the level of the top of the bobbin. This is depicted below in Figure 64.

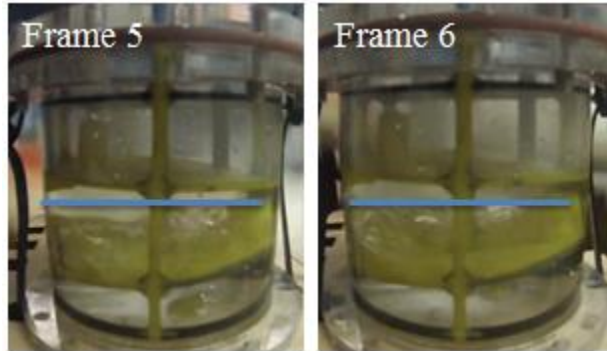


**Figure 64: Fluid Level is Below Bobbin Level**

This is exactly how this bobbin is supposed to act, keeping air from being drawn into the bobbin where they would enter the lower compartment and ultimately the fuel line.

As this fluid stacks on the top side of this compartment, one would expect fluid to flow out the hole located in the top bobbin. This can in fact be seen in Frames 5 and 6, as highlighted below in Figure 65. This is significant to validate the reversal of liquid and air.

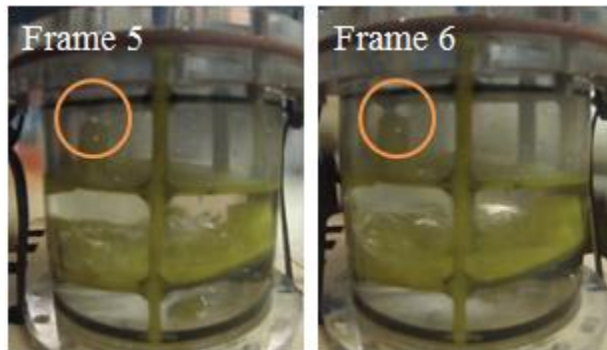


**Figure 65: Fluid Leaking Out of the Top Bobbin**

By Frame 7 the net acceleration of the moving platform is decreasing as the spring is no longer accelerating it downwards with the same magnitude as in the earlier frames. This is because its displacement from equilibrium position is decreasing as the platform moves downwards. This causes the air bubbles to mix more freely with the liquid and the area becomes more difficult to analyze.

Note that the bubble seen in the lowermost compartment in Frames 3-8 was in the compartment only due to improper filling procedures. It can be seen resting near the upper right side of the compartment in Frame 1 before any dropping occurred. This is shown below in Figure 66.

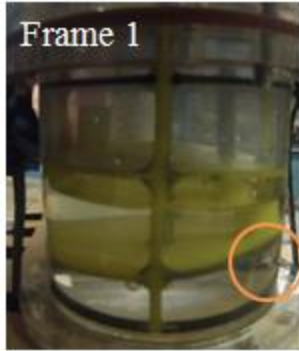


**Figure 66: Filling Error Bubble**

These positive results where air bubbles were kept from entering the fuel pickup area correlate well with the successful ramjet firing and thrust data from USLI 14. It shows that the air bubbles congregate in the lower section of each compartment away from the bobbins through which the fuel would be extracted. Further ground testing will validate this under more rapid deceleration conditions and the in-flight flow visualizations will show how this fuel tank design functions over longer time scales.

#### 5.1.1.2.3.4 *USLI 16 Sponge Design*

##### 5.1.1.2.3.4.1 *Version 1*

The second design to be flown will be the design created this year. After reviewing a series of AIAA papers, one in particular was chosen to be the basis for the conceptual design. The paper describes the conceptual design behind sponge based propellant management devices (PMD). Sponge based PMD's are created with planar panels separated by a tapered gap. A typical device can be seen below in Figure 67.

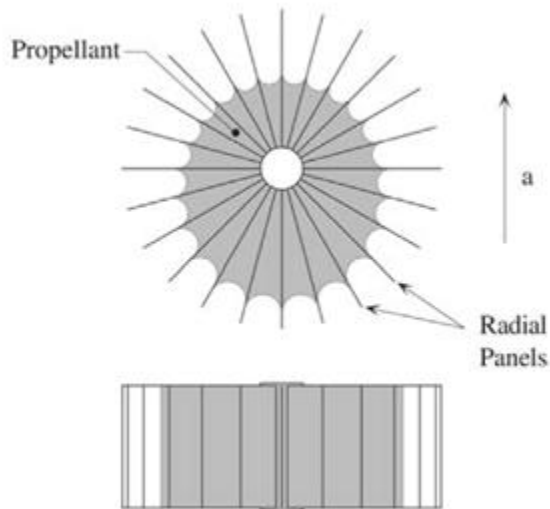


**Figure 67: A Typical Sponge**

From the paper it was found that hydrostatic forces could be countered by differences in surface tension forces due to the change in the radius of the fluid. This is summarized and quantified by the equations shown below.

$$\Delta P_{st} = \sigma \left( \frac{1}{R_{up}} - \frac{1}{R_{low}} \right)$$

$$\Delta P_{hydrostatic} = \rho a \Delta z$$

$$\sigma \left( \frac{1}{R_{up}} - \frac{1}{R_{low}} \right) = \rho a \Delta z$$

*With differentiation and rearranging:*

$$\frac{dw}{dz} = \frac{1}{2\sigma} a w^2 = \frac{1}{2\sigma} (a_z + g) w^2$$

$\rho$  = fluid density

$\sigma$  = absolute surface tension

$a$  = net acceleration

$w$  = mean gap width

One can then plug in our expected net acceleration and produce the equation shown below.

$$\frac{dw}{dz} = -\frac{\rho}{\sigma} (g) w^2$$

What is important about this equation is that it shows that for our negative acceleration conditions, the width of the sponge design should decrease as height increases. This is shown below in Figure 68.

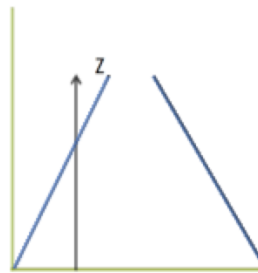
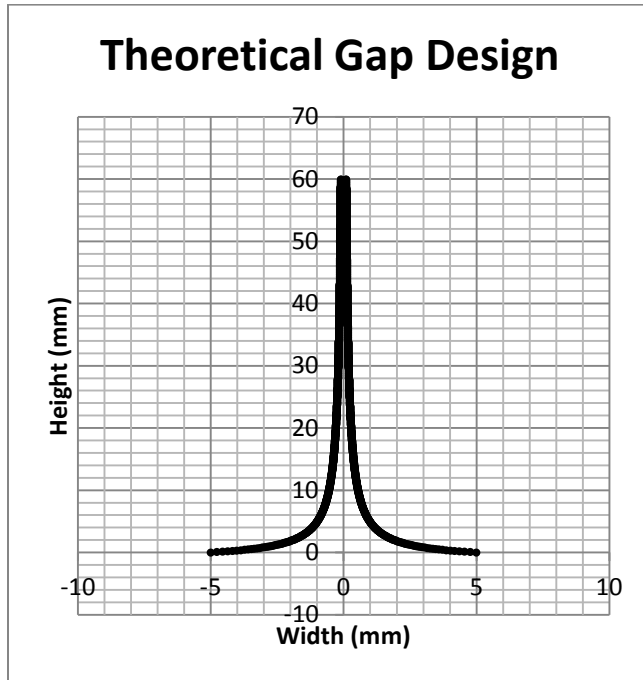


Figure 68: Sponge Width Change

The question after determining this overall design notion was to transfer this to a practical design. To accomplish this, one can plug in the fluid density and surface tension of 70% hydrogen peroxide at our expected operating temperatures along with the acceleration of gravity. It can then be integrated and solved to come up with an exact geometry. An excel program was created which would accept a height and bottom width (boundary conditions) and output a graph of the theoretical width at each height. An example of this output is shown below in Figure 69

for a height of 60mm and a bottom width of 10mm. Note the scales on the graph are not the same and the dimensions are in mm.



**Figure 69: Theoretical Gap Design**

The output of this program, however, gave a design that was extremely impractical to create. It would not only be very difficult to fabricate the required gap width accurately, but the overall design patterned throughout an insert would lead to much wasted space. It was therefore decided to simplify the design and pattern a straight angled cutout. The CAD for this design is shown below in Figures 70, 71, and 72. Note the dimensions are in mm.

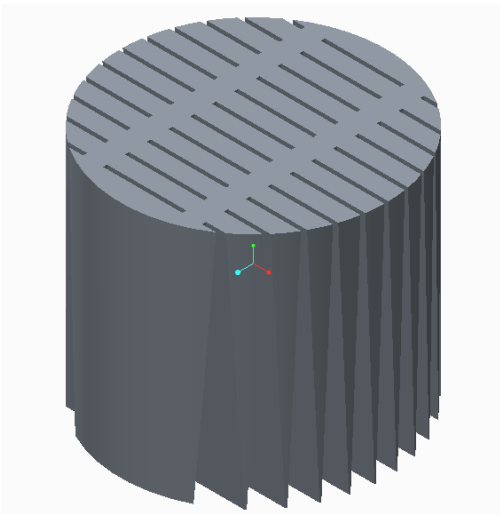


**Figure 70: USLI 16 Sponge Design Version 1 CAD View 1**

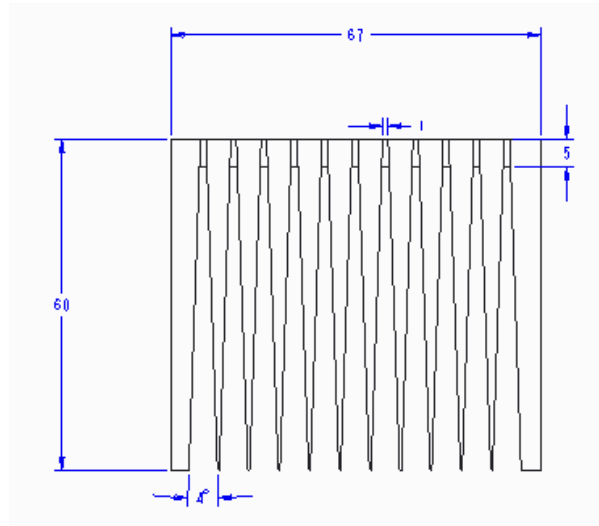


**Figure 71: USLI 16 Sponge Design Version 1 CAD View 2 (dimensions in mm)**

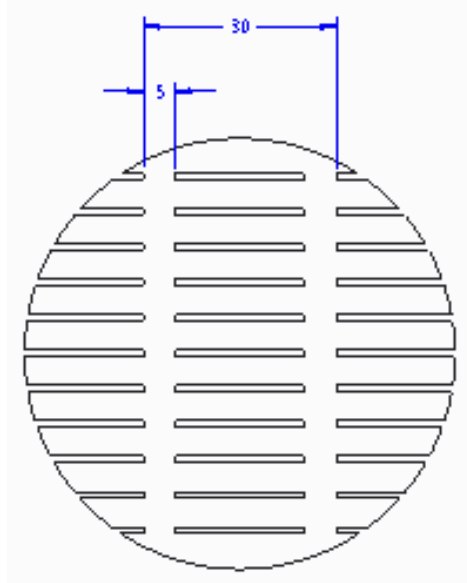


**Figure 72: USLI 16 Sponge Design Version 1 CAD View 3 (dimensions in mm)**

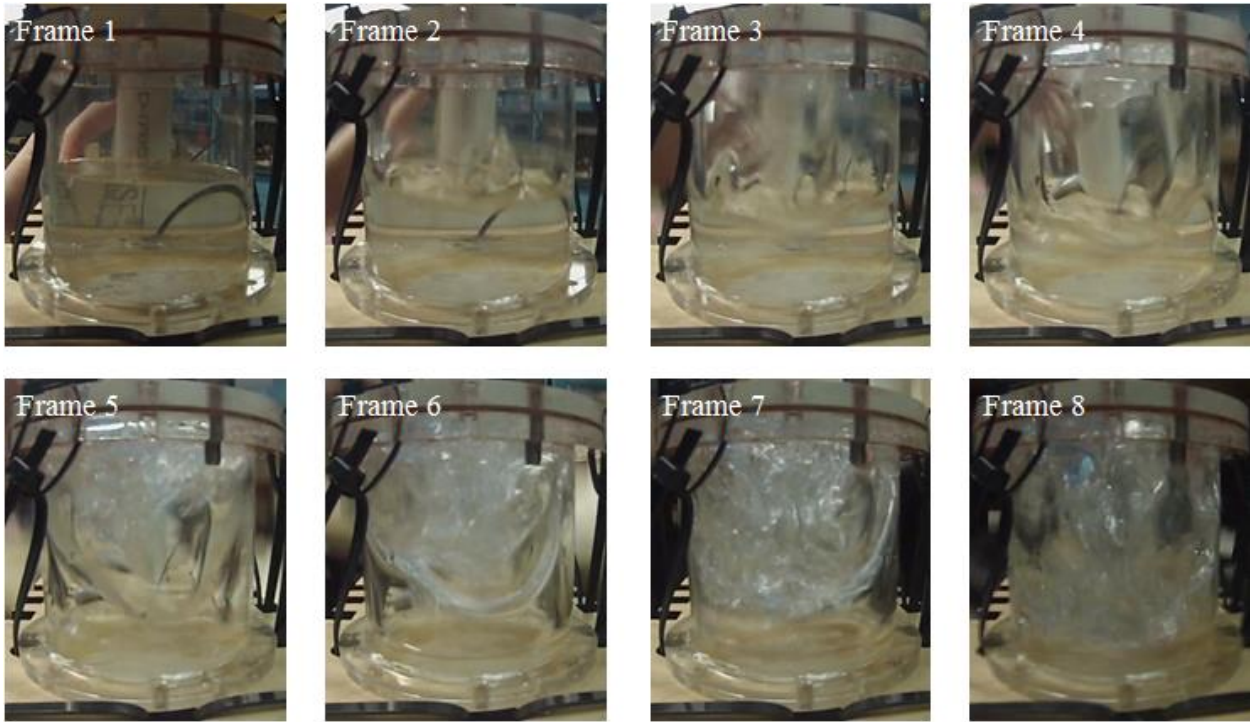
The part was fabricated using a Makerbot 2 and the actual printed part inside of the acrylic fuel tank is shown below in Figure 73.



**Figure 73: USLI 16 Sponge Design Version 1 Actual**

After this design was fabricated, it was tested using the VADL Drop Test Stand to see preliminary results.

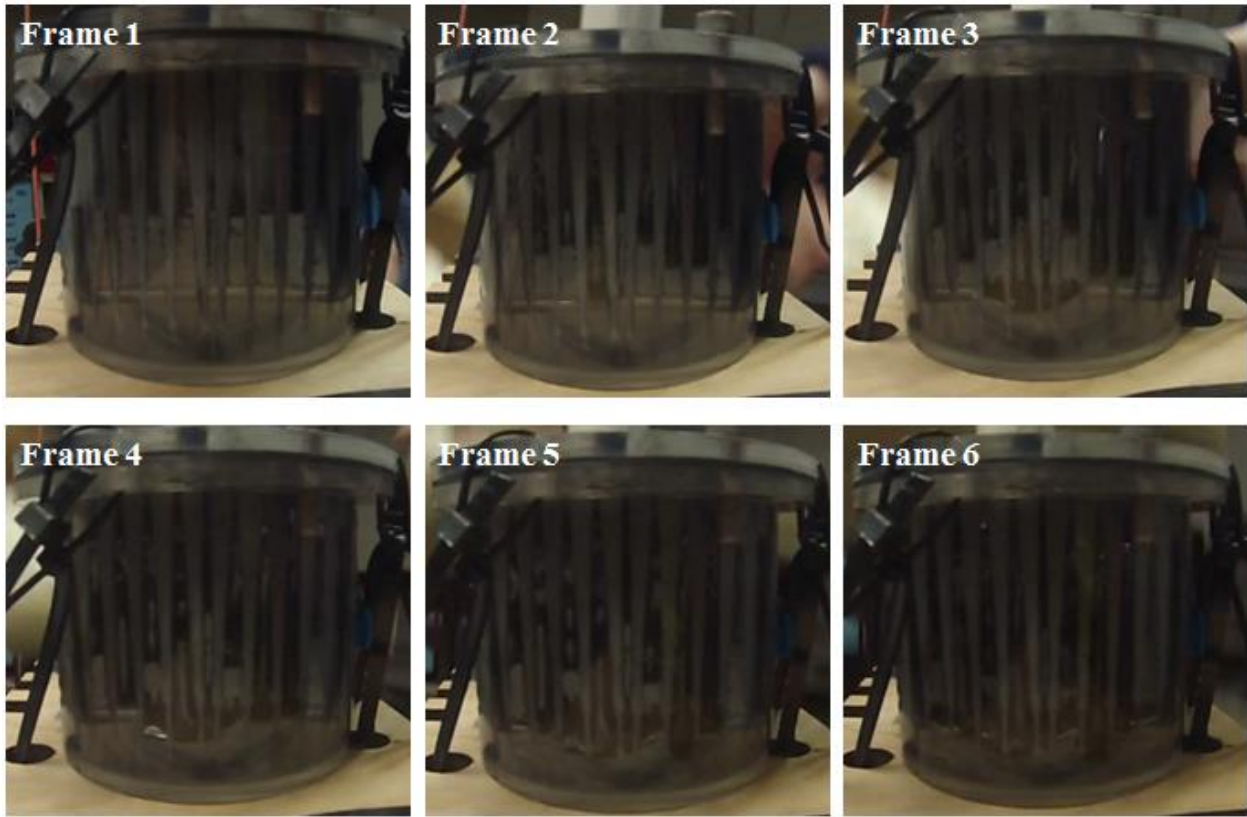
To interpret the results of dropping the Sponge design, however, one must first examine slosh in a tank without a SAS. To see this, a tank was dropped in the VADL Drop Test Stand. Figure 74 shows the results when a tank was dropped without a SAS. Frame 1 is just before release at the top of the stand, Frame 8 shows the last frame before reaching the bottom of the stand, and frames 2-7 show increments between these two times. At the time no accelerometer data was available, but the maximum negative gravity condition is estimated by the dynamics model discussed in 5.3.1.3.4 VADL Drop Test Stand to be -1g. The platform traveled approximately 4ft in 0.5s validating this acceleration estimate. This maximum acceleration will occur in the Frame 1 and the acceleration will decrease towards 0g of net acceleration as time moves along.



**Figure 74: No Baffle Fuel Tank Slosh**

There are multiple phenomena that can be observed in these frames above. The first is the small fuel jump in the middle of the tank seen in Frame 2. After this, the water starts to climb the walls of the tank in Frames 3 and 4 and a clear U shape can be seen in Frames 5 and 6 as the vertical components of the fluid velocity increase close to the wall. This is the phenomenon that the ring baffles in USLI '14 initially set out to counter. Along with this, the curl of the fluid hitting the top of the tank is visible in Frames 6 and 7 and finally the flow becomes very turbulent and convoluted in Frame 8 before hitting the bottom of the test stand.

Now that a baseline for the behavior of the fuel in the tank has been set, the next design can be compared and its effect on the fuel observed.



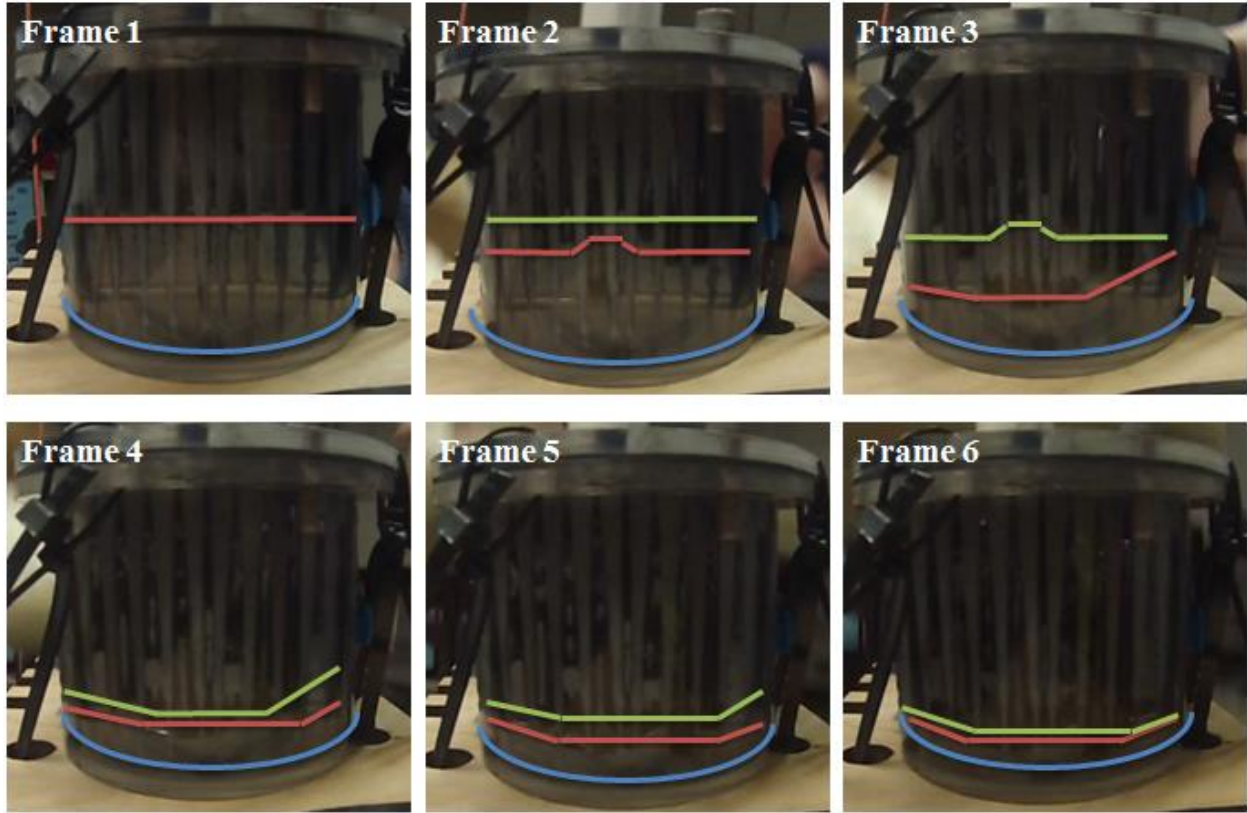
**Figure 75: USLI '16 Sponge Design Version 1 Drop Test**

Figure 75 above and Figure 76 below show the results of from the drop test of the first version sponge design described above. The same conditions as the baseline test (estimated  $-1g$ 's, 0.5s of test, 4ft of travel). Figure 76 below is the same image as Figure 75, but lines have been added to show different fluid levels and references. The red line shows the fluid level in the current frame, the green line shows the fluid level in the previous frame, and the blue line shows the bottom of the baffle in the tank. The lighting scenario in this tank is non-ideal and will be improved in future tests, but useful conclusions can still be drawn from the results as the reflection of light off bubbles and the interface between the liquid and gas can be seen in most frames.

Similar to the unabated baseline condition, an initial jump is seen in the middle of the fluid level, though in this case the baffle opposed the motion and limited its movement. The phenomenon of the fluid climbing the walls is then seen in Frame 3 and 4, but to a much lower extent than in the baseline. This is the first evidence that the baffle is successfully abating some of the slosh. This level continues to move downwards towards the bottom of the baffle as the tank travels along the stand, but interestingly enough never actually leaves the end. The surface tension holds the bubble at the bottom of the SAS. This can be seen in Frames 5 and 6.

This result, while promising, is not definitive for three reasons. First, the test did not simulate the full negative gravity conditions that are expected in the flight. In flight the baffle will face even more difficult sloshing scenarios than seen here because of the increased accelerations. Second, this test does not replicate the pressure gradient caused by the extraction of the fuel

through the pickup. This could drastically negatively affect the ability of the baffle to retain the fuel near the pickup. Third, the short time duration of this test is not representative of the actual flight. While this test lasted approximately 0.5s, the actual flight will require fuel for 5s. This longer time scale combined with the previous two points are the reasons that in flight flow visualization along with tests of fuel extraction are required before designs are implemented in the full scale rocket.



**Figure 76: USLI '16 Sponge Design Version 1 Drop Test with Fluid Level Lines (Red = Current Level, Green = Level from Previous Frame) and Bottom of Baffle Line (Blue)**

The moderate success of this design led to further evaluation of the sponge concept. Because this design was not made according to the theoretical equation, it was determined that a design that was closer to the ideal theoretical case would perform even better. To evaluate this, a metric was created that compared the width each point along the height to its theoretically determined width. The percentage difference between these two values was averaged over the entire height. This value was used to evaluate the closeness of a design to the theoretical version with same height and bottom width dimensions. It is important to note that the theoretical design is determined by only the height and width at the bottom of the baffle. Table 12 below summarizes the findings.

**Table 12: Average Percent Deviation from Ideal**

<b>Design</b>	<b>Height (mm)</b>	<b>Bottom Width (mm)</b>	<b>Top Width (mm)</b>	<b>Average Percent Deviation from Ideal</b>
USLI Sponge Design Version 1	60	2	0.5	207%
Linear Approximation	60	2	0.19	148%
Theoretical	60	2	0.19	0%

This table is supplemented below by Figure 77 which shows the three designs compared against each other. The conclusion from this was that the design was very far from the theoretical and could be altered to better represent the equation and perform better. The “Linear Approximation” is defined by a design with the same top and bottom dimensions, but instead of the inward curved design a simple line is drawn between the two points. This maximizes the amount of fuel that can be held in the tank with the insert placed inside and simplifies construction.

## Sponge Design

Theoretical USLI Sponge Design Version 1 Linear Approximation

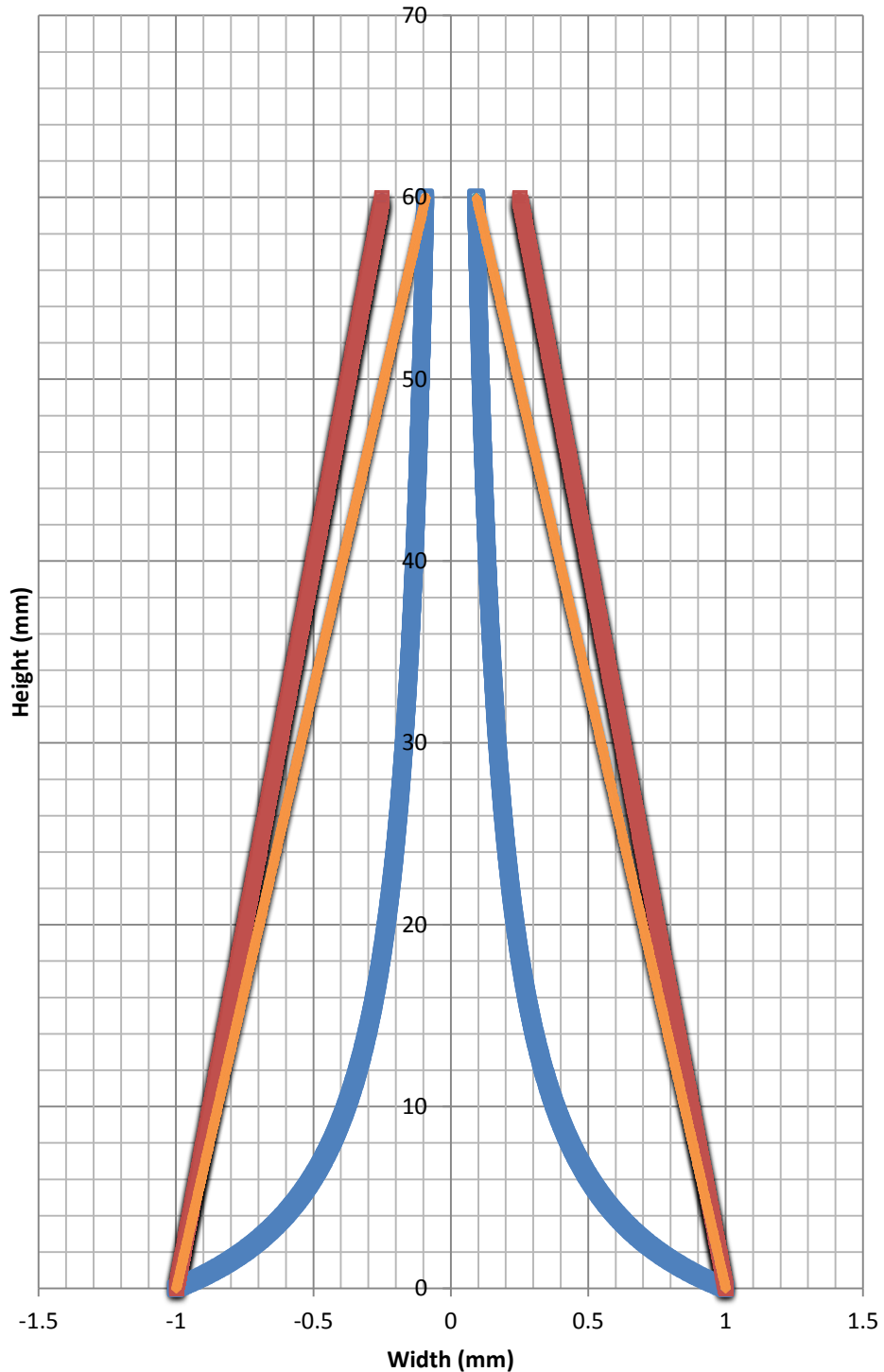


Figure 77: Sponge Design Comparisons

#### 5.1.1.2.3.4.2 Version 2

To make the design more close to ideal the height was shortened from 60mm to 20mm. With this change in height, the theoretical top width with a bottom width of 2mm was 0.47mm. Table 13 below has been updated to include the new dimensions and show the improvement in theoretical performance from Version 1 of the design. The theoretical design against which each design is compared is based on the height and bottom width of that design.

**Table 13: Updated Average Percent Deviation from Ideal**

<b>Design</b>	<b>Height (mm)</b>	<b>Bottom Width (mm)</b>	<b>Top Width (mm)</b>	<b>Average Percent Deviation from Ideal</b>
USLI Sponge Design Version 1	60	2	0.5	207%
Linear Approximation	60	2	0.19	148%
Version 1 Theoretical	60	2	0.19	0%
USLI Sponge Design Version 2	20	2	0.5	44%
Version 2 Theoretical	20	2	0.47	0%

One can see that there are multiple advantages in terms of closeness to the theoretical design from this reduction in height. Because the lowered height calls for a larger top width, the theoretical design is more practical to manufacture. This design at this time is yet to be evaluated but will be evaluated and verified as is discussed in following sections.

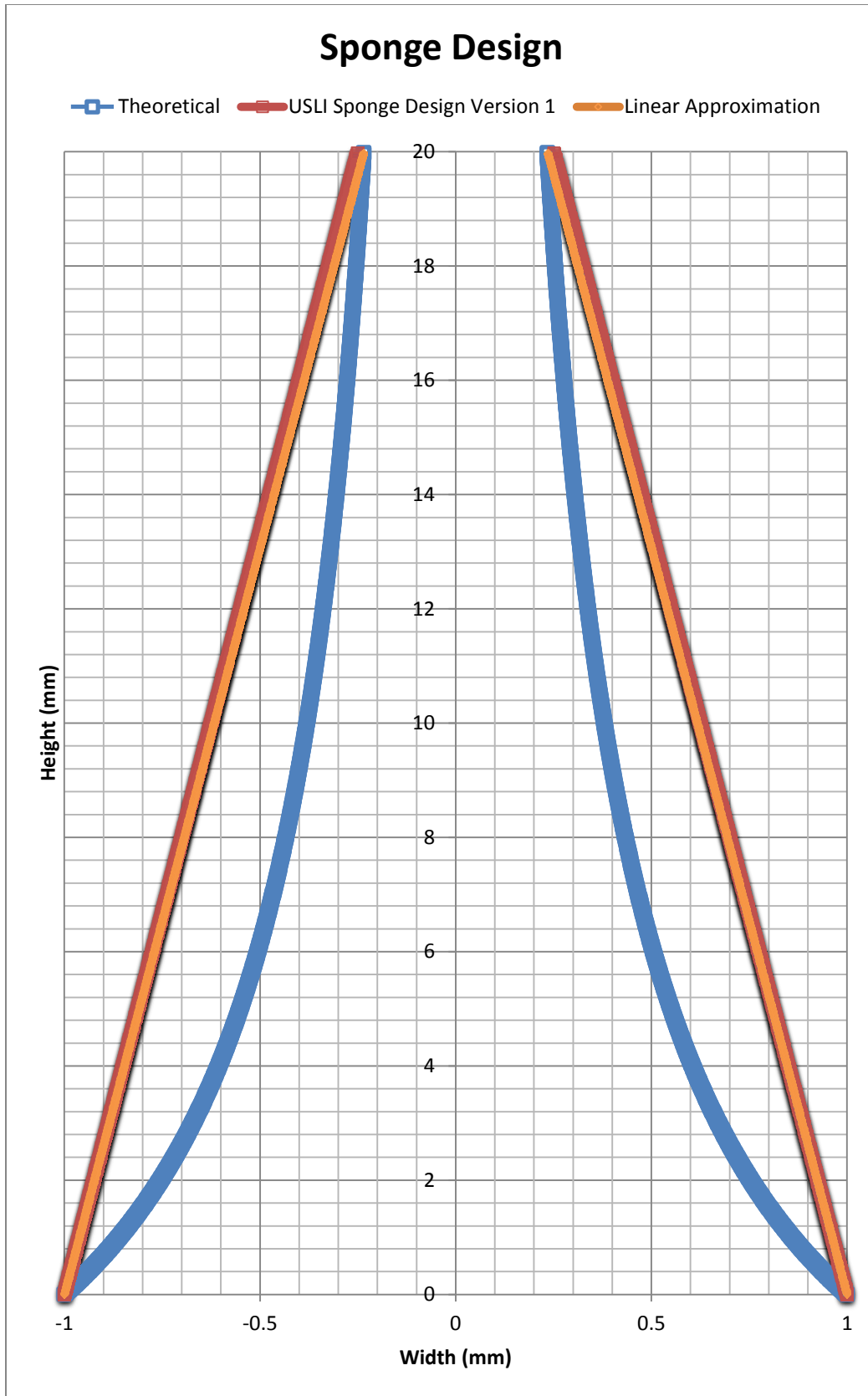
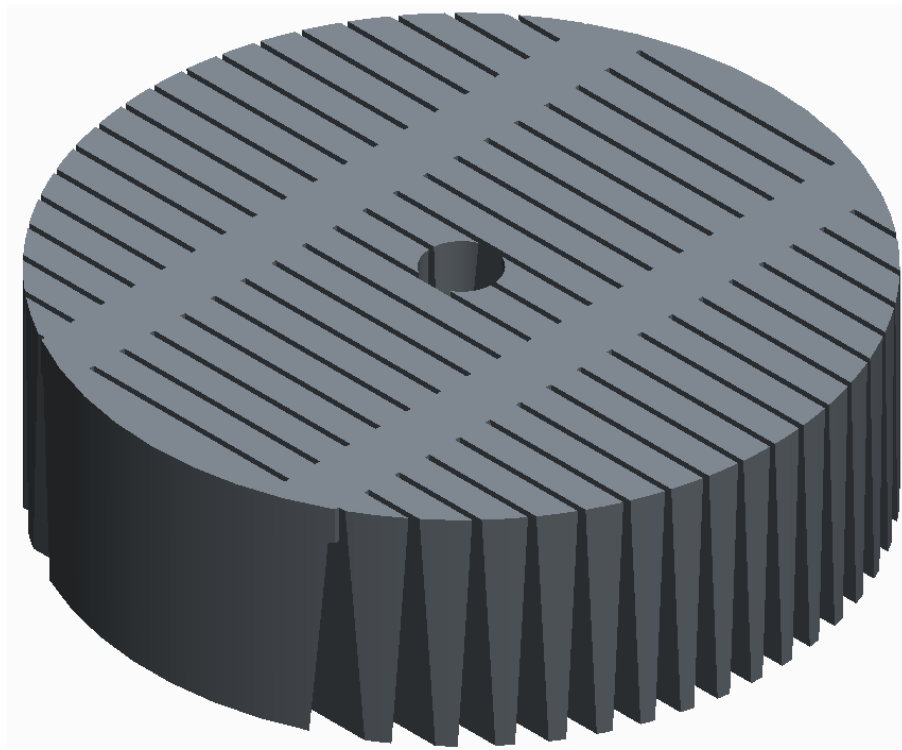
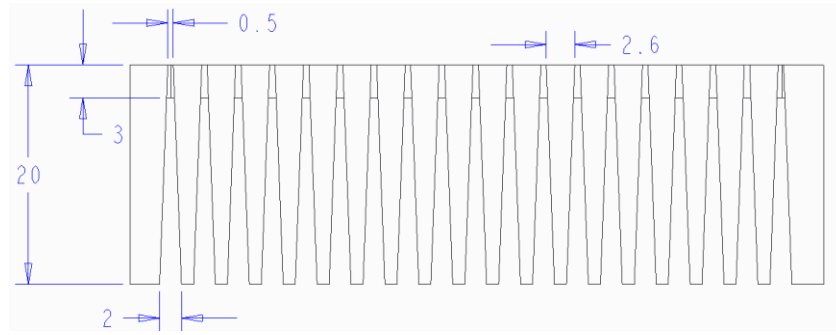


Figure 78: USLI Version 2 Sponge Design Theoretical Design

Below in Figures 79, 80, and 81 can be seen the CAD model for this new Version 2 insert. Three of these inserts will be stacked on top of each other to create the final SAS design. One conclusion from the testing of the previous design is that some room should be left between the three layers. This will allow bubbles to form at the bottom of each insert without touching the surface of the insert below it and transferring the air downwards. The hole in the center of the insert is to allow the fuel pickup line to reach the bottom of the tank.



**Figure 79: USLI 16 Sponge Design Version 2 CAD View 1**



**Figure 80: USLI 16 Sponge Design Version 2 CAD View 2 (dimensions in mm)**

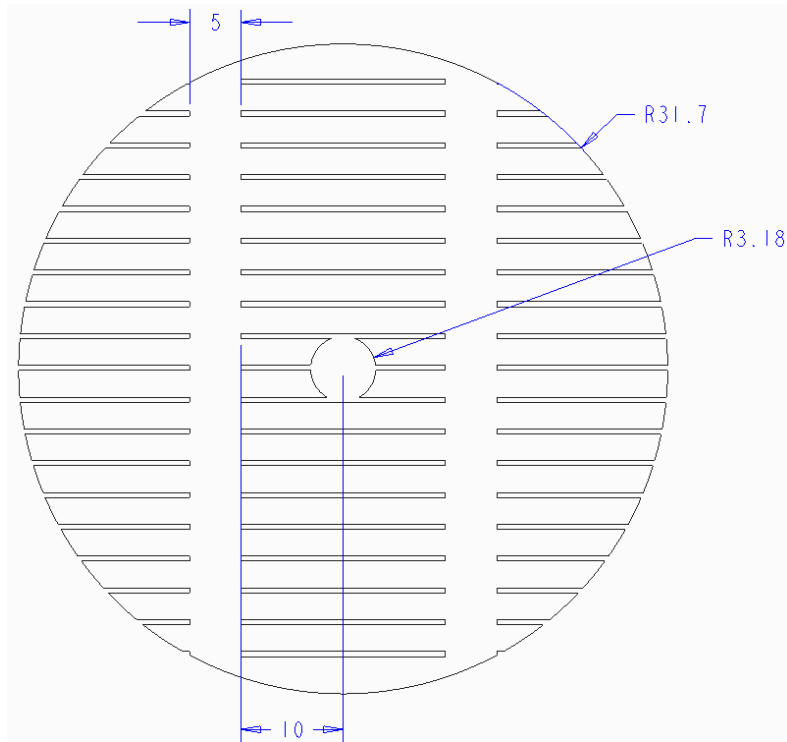


**Figure 81: USLI 16 Sponge Design Version 2 CAD View 3 (dimensions in mm)**

A final, yet important point of comparison between the various designs is the amount of space they take up in the tank. This will determine the maximum amount of fuel that can be extracted from the tank as any volume taken up by the SAS will be unavailable for fuel storage. Therefore this will be an important performance metric moving forwards. Table 14 below shows the percentage of the total tank volume (200cc) taken up by each design.

**Table 14: SAS Volumes**

<b>Design</b>	<b>Volume (cc)</b>	<b>Percentage of Fuel Tank Taken Up by SAS</b>
USLI 14	25	12.5%
USLI 16 Sponge Insert Design Version 1	97	48.5%
USLI 16 Sponge Insert Design Version 2	115	57.5%

#### 5.1.1.2.3.5 References

Jaekle, J. (1993). Propellant management device conceptual design and analysis – Sponges. *29<sup>th</sup> Joint Propulsion Conference and Exhibit*.

#### **5.1.1.2.4 Pressurization System**

The fuel system will be pressurized by a reservoir which connects directly to a regulator. The regulator and reservoir are both commercially available models designed to be routinely operated at  $\sim 4000\text{psi}$ . Since this pressure is unnecessary, the system will only be pressurized to  $\sim 2000\text{ psi}$ . The pressure regulator will be connected via high-pressure rigid tubing to the fuel tank, and similar tubing will handle the pressurized fuel.

#### **5.1.1.2.5 Control System**

The fuel delivery system is controlled by a custom, hardware-based timing control circuit. In the payload bay, an independent gravity switch is implemented to detect takeoff conditions. A simple switch debouncing circuit will be used to eliminate noise inherent in the gravity-switch, and assure proper launch detection. A generalized, example debouncing circuit is shown below.

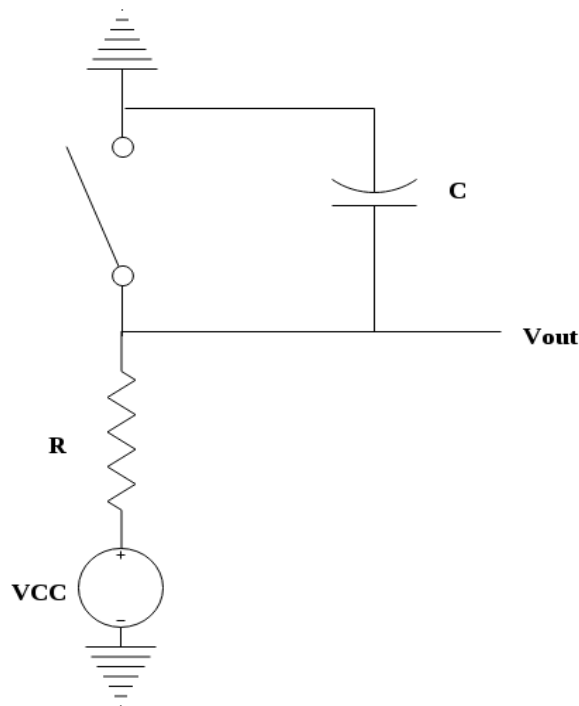


**Figure 82:** Schematic of a general debouncing circuit

After assured launch is detected, a custom timing circuit is used to measure time  $t$ , the delay for activating a normally-closed high-pressure solenoid placed between the pressure regulator and fuel tank. Upon reaching time  $t$ , the circuit will output a high-voltage to open the solenoid valve, ensuring that fuel delivery occurs at the proper time, and the thruster is able to fire, allowing sufficient time for high-frequency data collection about thruster operation prior to the apogee event.

#### **5.1.1.2.6 Verification System**



Figure 83: GoPro Hero 3 White Edition

The camera selected is a GoPro Hero 3 White Edition Camera seen in Figure 83. The camera provides video footage at 720p and 60 frames per second, which is more than sufficient for our needs. Additionally, it provides an ultra-wide field of view, which is crucial since the camera is mounted extremely close to the fuel tank due to size constraints in the rocket. The GoPro uses a rechargeable lithium ion battery and stores data on a removable SD card. One crucial feature that led to the selection of this camera is its capability to be controlled remotely through the GoPro application, which is available to most smartphone users. The camera broadcasts its own Wi-Fi signal to which the user can connect to and remotely control camera settings and recordings. With Wi-Fi enabled, the camera has a battery life of around two hours with the camera on, which is more than sufficient for our purposes. This means that once all systems have been installed and the rocket is ready to launch, the cameras can be turned on remotely and recording can be initiated.

The cameras are mounted securely to a bulkhead below the fuel tank using a special frame. The frames for the GoPros is a slim design for minimum foot print and were rapid prototyped in house. Two steel tabs are epoxied into the bulkhead and machine screws thread through these tabs and the frames to hold the cameras in place. (Figure 84)



Figure 84: GoPro Camera Mount CAD

An LED flashlight is used to illuminate the fuel tank during flight inside the darkness of the rocket. This flashlight was cut in half on a lathe and the batteries were mounted remotely to increase the compactness of the design. The switch is mounted to the right of the flashlight as shown in figure 85. The flashlight uses two CR2032 lithium ion batteries. Because the flashlight can be turned on just prior to putting the access door in place and the batteries last for more than several hours, there is little concern of the flashlight not being illuminated during recording.

As is discussed in detail in section 5.3.1.3.4 VADL Drop Test Stand, the in flight testing described above will be supplemented by extensive ground based testing. This testing is more flexible and can be performed much more easily than in flight flow visualizations. The camera used for this testing is the same GoPro as described above. This camera is sufficient for the testing purposes of this stand and supplemental lighting is unnecessary as the stand is open to the ambient light of the room. A picture of where the GoPro is attached can be seen below in Figure 85.

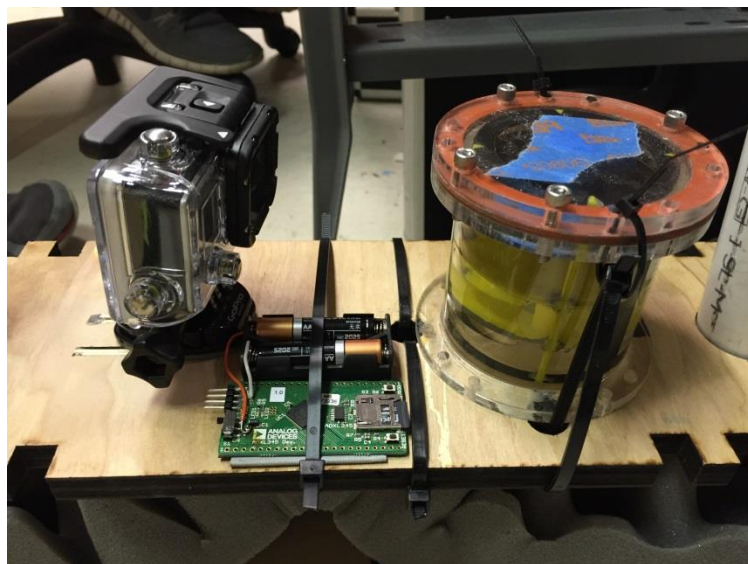


Figure 85: GoPro attached to the Drop Test Stand

## 5.1.2 Hydrogen Peroxide Monopropellant Thruster

---

### 5.1.2.1 Payload Systems Design Review

---

The objectives of the Monopropellant Thruster are fourfold:

1. To exhibit the safe and environmentally friendly use of High Test Peroxide (HTP) as a propellant.
2. To verify the thruster and collect performance data for a period of at least 5 seconds.
3. To validate the design of a simple monopropellant actuator capable of producing at least 20N of thrust.
4. To verify the success of the slosh abatement experiment by receiving and running on a continuous fuel supply.

The monopropellant thruster will function by exposing 70% HTP to an iridium catalyst. The resulting deterioration of the HTP and release of heat will produce heated steam, which will create thrust. HTP will be fed into the thruster via a high pressure fuel delivery system discussed in Section 5.1.1.2.4. The fuel will then pass through an injector into the catalyst bed. The injector design will insure consistent flow into the catalytic bed, prevent quenching (or flooding) of the catalyst, and prevent channeling (preferential flow along the chamber walls) of the HTP. After decomposing in the catalytic bed, decomposition products will pass through a retaining screen to prevent loss of catalyst, and then exit the thruster via a nozzle.

The structure of the monopropellant thruster is composed of (i) Fuel Injector: to deliver a constant flow of HTP to the thruster, (ii) Catalytic Bed: to decompose the HTP to produce thrust, and (iii) Nozzle: to accelerate flow and reduce static pressure.

The thruster will be constructed from 6061 aluminum stock. Initial prototypes will be constructed from hexagonal stock, with the three pieces listed above connected via pipe threading and sealed with gaskets (and a suitable sealant thread tape, potentially). This modular construction and easily workable outer geometry will allow the interior and exterior of the thruster to be examined between ground-based tests to verify performance and facilitate easy modification of specific sections based on the data collected. Once the complete internal geometry of the thruster has been verified, it may be deemed worthwhile to produce and test a flight version of the thruster, fabricated out of Al 6061  $\frac{3}{4}$ " round stock with a welded construction. This version would emulate the functionality of the hex-stock based thruster, while being lighter and having a smaller footprint inside the rocket. For both the prototype and flight model, the design is optimized to allow easy fabrication in-house by design team members using only standard machining operations.

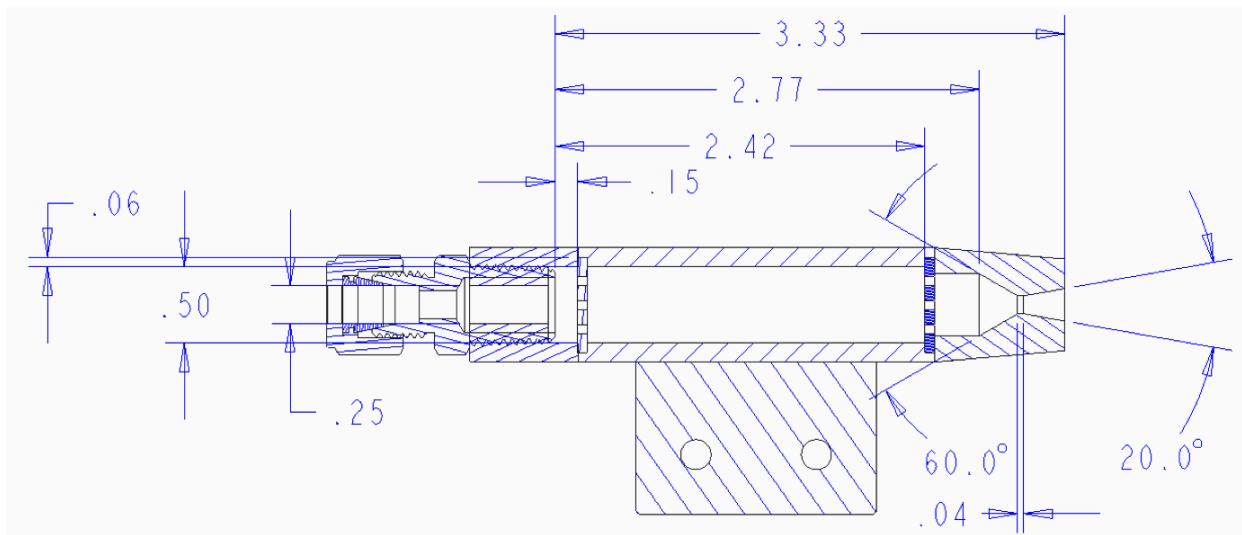


**Figure 86: Internal thruster geometry**

As mentioned previously, the thruster is expected to run for 5s while producing at least 20N of force. Preliminary design calculations have been done using higher values to account for any unforeseen inefficiencies or sub-optimal conditions affecting the system. Each firing is expected to use no more than 100 mL of fuel, with an expected propellant flow rate of 16.5 mL/s entering

the catalyst bed ~300 psi. These performance values should be small enough to not have a significant impact on the flight of the rocket, while still be readily measurable to produce useful data.

### 5.1.2.2 Monopropellant Thruster Subsystems

---

The thruster was designed following an analysis conducted using MATLAB. This generated the functional (inner) geometry of each section. Material selection (AL6061) was based on availability, specific strength, machinability, and short-term suitability for contact with HTP. The outer geometry of each section was determined by placement inside the rocket assembly fabrication compatibility.

#### 5.1.2.2.1 Fuel Injector

The furthest upstream component of the thruster, the fuel injector serves as a connection between the catalyst bed and the fuel tubing. Fuel flowing through the input hose runs through a standard tube-to-pipe connector that attaches to the fuel injector. Once inside the fuel injector, the internal diameter exposed to the fuel increases to match the internal diameter of the catalyst bed. Fuel then flows through the upper retaining plate into the catalyst bed. The fuel injector attaches to the thruster body in such a way that the upper retaining plate is locked in place between the two parts. This allows for easy removal of the retaining plate for access to the catalyst bed when the fuel injector is removed. The key design constraints of the fuel injector are based off of the geometry of the surrounding pieces, the loads sustained, and the fluid flow conditions inside.

#### 5.1.2.2.2 Catalytic Bed

The catalytic bed of the thruster sits inside the main body of the thruster and converts incoming HTP fuel to steam. Fuel passing through the retaining plates interacts with iridium pellets to produce heated steam and oxygen. The catalytic bed is designed to operate at a pressure of 300 psi (See Figures 114 and 115 in section 5.3.2.5). For our given fuel flow rate, this pressure provides a stable amount of thrust and maintains a favorable environment for the complete disassociation of the HTP fuel. Given the fuel pressure, flow rate, and the necessity of a complete reaction, the dimensions of the catalytic bed were calculated.

#### 5.1.2.2.3 Exit Nozzle

The nozzle vents the products of the catalytic reaction out the back of the thruster, producing thrust. The thruster design assumes isentropic gas flow out of the thruster and choked flow in the nozzle throat due to sonic conditions. These assumptions allowed a dynamic analysis to be conducted, which produced the key dimensions of the nozzle. The nozzle is optimized for use at 3000 feet above sea level; the exhaust plume will be over-expanded at sea-level, resulting in a negative pressure thrust during ground testing.

### 5.1.3 Structural Analysis

---

#### 5.1.3.1 Structural Analysis Systems Design Review

---

Structural design in rocketry poses the challenge of predicting the response of materials and interfaces to a dynamic launch environment that can be difficult to characterize. Many rocketry programs respond to this challenge by using heavily overdesigned vehicles or heritage designs

that have survived the launch environment in the past. The cost of this design approach is mass, and in an era where it costs \$10,000 to put a pound of mass into orbit, this cost is extremely high. Below, the VADL lays out our path forward to attempt to understand the material behavior of our vehicle, the nature of the launch environment, and the causes of failure in advanced materials.

The objectives for the structural analysis payload are three fold and outlined below:

1. Develop a finite element model of the launch vehicle that captures the dynamic behavior of the carbon fiber-reinforced polymer vehicle structure and internal vehicle interfaces.
2. Dynamic sensing of lateral and axial acceleration during flight and during ground-based modal tests will be used to validate mass and stiffness properties of the finite element model.
3. The finite element model will be used to optimize the vehicle design mass through stress analysis with low model uncertainty after model verification through data-based correlation.

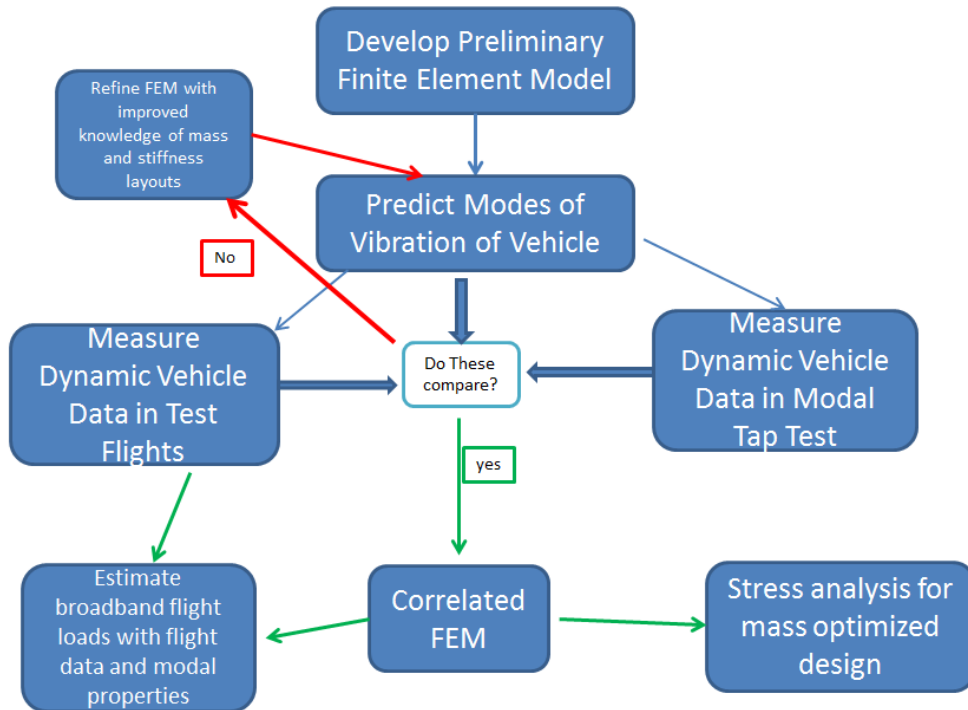


**Figure 87: Overview of structural analysis initiative**

To accomplish these goals preliminary parallel finite element models have been developed in Ansys and Abaqus. These models are developed to estimate the geometry and material properties of the rocket. These programs solve the classical dynamic eigenvalue problem shown below using the inputs of the mass and stiffness matrices of the model to output the modeshapes and modal frequencies of the structure.

$$([M] - \lambda[K]) = \lambda\mu$$

The greatest challenge in modeling of the launch vehicle is capturing the material properties of our carbon fiber composite materials. Elasticity in 3 dimensions relates material stresses to material strains through a tensor. For common isotropic materials such as 6061 Aluminum, this tensor can be assembled using the Young's Modulus and Poisson's ratio as the inputs. For our purposes we define isotropic as having the same material properties in all directions. Most Finite Element software allows for the input of these material properties and assembles the finite element model with the 3D elasticity tensor assembled behind the user interface. Carbon Fiber Reinforced Polymer matrices are considered *anisotropic* because these materials behave differently in each direction. To model anisotropic materials properly in Ansys or Abaqus, the elasticity tensor must be generated externally and programmed into the finite element model.

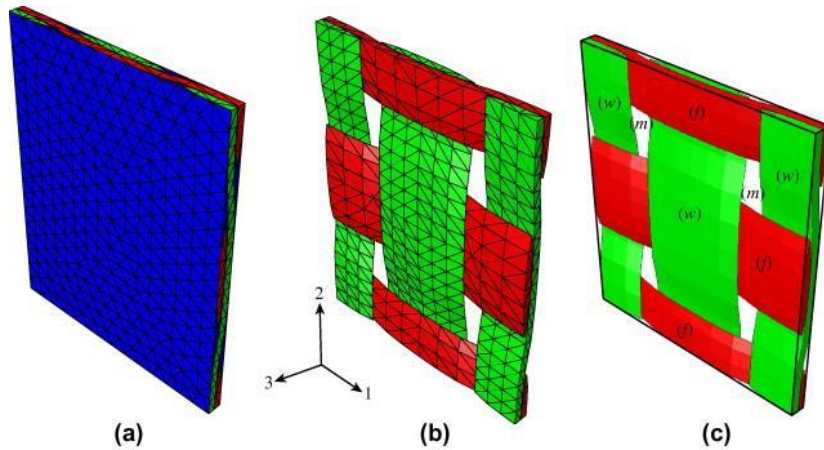


**Figure 88: Woven Fiber microstructure and computer discretizations**

To overcome this challenge in materials modeling, the team collaborated with Vanderbilt's Multiscale Modeling and Simulation (MuMS) center to understand elasticity in anisotropic materials. Dr. Calgar Oskay, whose research focus is computational modeling of composites and other heterogeneous materials, has developed a series of python programs that can assemble the necessary anisotropic elasticity tensor for heterogeneous materials through use of representative volume elements that characterize the microstructure of the composite and the material properties of its ingredients.

Through collaboration with MuMS and Dr. Oskay, we were able to develop a 3D elasticity tensor representative of our 2x2 twill woven carbon fiber structures. The tensor is shown below.

**Table 15: 3D elasticity tensor for 2x2 twill woven carbon fiber**

PSI	PSI	PSI	PSI	PSI	PSI
14740000					
3317000	15200000				

1150000	1119000	3341000			
-1600	1351	1557	715100		
-2281	-2402	-896.1	-219	811400	
-14250	-11250	137	-1460	-1610	4205000

This tensor represents not only the material properties of the resin and the individual fibers, but also the geometry of how fibers are interwoven within the microstructure.

The remainder of the materials in the rockets such as 6061-T6 Aluminum, Polystyrene, and epoxy are modeled as isotropic. Many improvements can be made in the current models- such as better modeling of mass distribution, and accommodation for lumped masses in the payload and avionics electronics sections. The models will be rigorously reviewed and physical data is produced for model validation and correlation.

Drawing on objective 2, dynamic structural data will be collected during flight on ADXL345 Accelerometers sampling data at 800 Hz. Early estimates suggest that relevant modal frequency content of interest will be in the range of 100-200 Hz. The team considers the Nyquist sampling criterion of 400 Hz as a lowpass frequency filter to be insufficient for data quality and will filter data down at Sampling Rate divided by 2.5, or 320 Hz for an 800 Hz sample. This will prevent processing of aliased data. The data acquisition system outlined in 5.1.4.2.5 *Structural Analysis Instrumentation Subsystems* samples raw data at 3200 Hz before passing it through an analog 1600 Hz low pass filter. The data is then decimated down to the programmed sample rate- which has been selected as 800 Hz for the purpose of the VADL structural experimentation protocol. This data collection scheme will provide high quality modal data in the frequency band of interest. Accelerometer data will be collected on test flights in November and February. This data will then be post-processed for frequency content using common techniques described in 5.3.3.3 *Experimental Logic, Approach, and Method of Investigation*. The results of this data collection initiative will be used to validate the finite element models, and the models will be subsequently updated to increase their accuracy and reflect the dynamic nature of the launch vehicle.

A second method of validating our models with test data will be a modal tap test. The modal tap test will arrange to rocket in its flight like configuration, simulating the “free-free” boundary conditions. The tap test is further described in 5.3.3.4 *Test, Measurement, Variables, and Control*.

Between flights and modal testing, the finite element models will be continually refined to reduce model uncertainty. With accurate models reflecting the launch vehicle, transient simulations of flight forces can be performed to study internal stresses in the vehicle. Knowledge of internal stresses will allow for reduction of mass in the vehicle in areas of low stress, and geometries optimized to produce a low mass, structurally optimal rocket for competition.

### 5.1.3.2 Structural Analysis Subsystems

---

#### 5.1.3.2.1 Onboard Sensors

The structural analysis subsystems consist of an Analog Devices ADXL345 Datalogger Development Board. This board was chosen based on its previous familiarity with team members, which will reduce the chances of encountering a major roadblock, and the fact that it houses all the necessary components to measure and record acceleration data in a self-contained package. The board houses an ADXL345 three-axis accelerometer, an on/off switch, a serial interface for reprogramming, an ADuC7024 microcontroller and a micro-SD card port. The microcontroller reads data from the accelerometer and an internal clock and writes to a text file on the micro-SD card. The board is powered by two AAA batteries, which make it very portable and easy to integrate into the rocket structure.



Figure 89: Accelerometer Board and Battery Pack

#### 5.1.3.2.2 Finite Element Models

The Finite Element Models developed for the structural analysis payload are created to accurately represent the following items of the flight vehicle.

1. Geometry
2. Materials
3. Mass
4. Stiffness
5. Interfaces

2 Models have been developed in parallel in Abaqus and Ansys. The Abaqus model is computationally smaller in size and utilizes shell elements. The Ansys model is larger and uses solid elements to represent the body of the rocket. The Ansys model contains 14556 Elements currently. The Abaqus model contains 1673 shell elements and 990 solid elements. These

models are preliminary, and will be iteratively updated over the year to better reflect the true rocket characteristics.

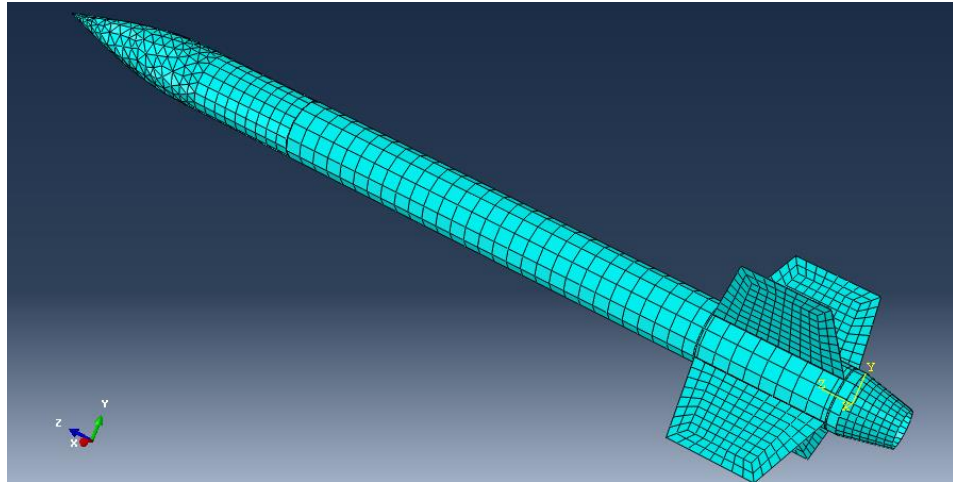


Figure 90: Abaqus Finite Element Model

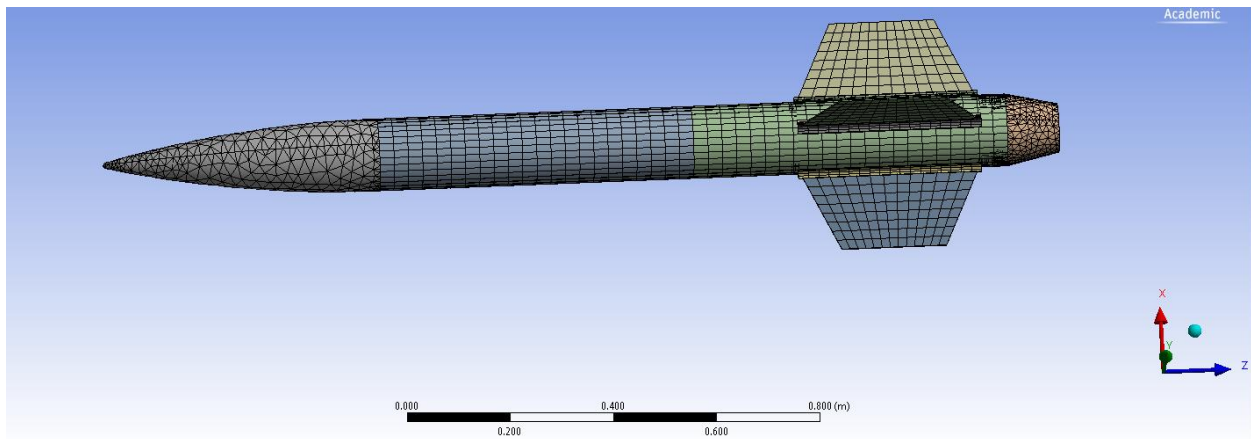


Figure 91: The Ansys Finite Element Model

## 5.1.4 Payload Instrumentation Systems

---

### 5.1.4.1 Instrumentation Systems

---

The rocket's payload electronics serve two purposes: 1) passively collect data from various meters in-flight for later retrieval and analysis and 2) actively block and release fuel to the experimental thruster at predetermined points in time. Thrust data collection, temperature data collection, and acceleration data collection function as three independent subsystems of the integrated data collection system, while the fuel delivery system is independent of the data collection circuitry.

Our payload electronics support our payload initiatives of hydrogen peroxide thruster performance analysis and in-flight vehicle structural analysis. The data that we collect via the data acquisition system will be used to assess the efficacy of the green monopropellant thruster and to complete structural health monitoring (SHM) analysis of the rocket body post-flight.

Through this combination of data acquisition and SHM, in-flight acceleration and strain data can be correlated to weaknesses in the rocket body to identify the *cause* of rocket damage for prevention rather than simple mitigation of damage for subsequent flights. The fuel delivery system will deliver fuel to the thruster at the appropriate experimentation start point following launch and cease fuel delivery at the experimentation end point.

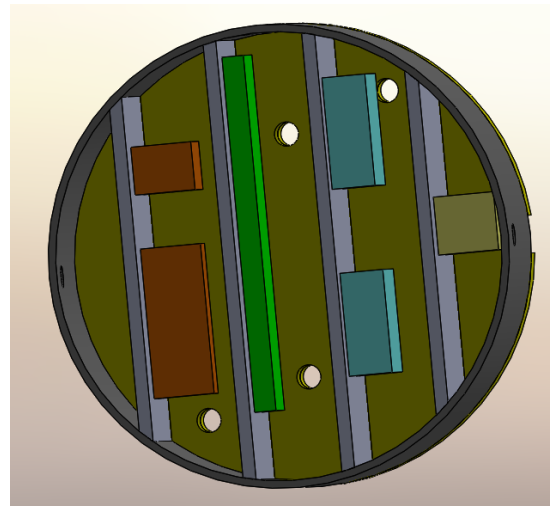
In past years, the rocket's data acquisition has consisted of an entanglement of sensors, sensor amplifier and filter boards, a central Rocket Data Acquisition System (RDAS), power supplies, and a homemade, epoxied-over fuel delivery circuit [see picture below]. The many loose wires and haphazardly connected components were sufficient for lower-g flight conditions but won't be able to withstand this year's 14g launch forces, nor is the system the safest and most transparent configuration for long-term use. The intensity of launch forces has motivated a new, optimized design for the data acquisition system, featuring full encasement and the migration of fuel delivery circuitry and some sensor board and data acquisition functionality to more secure printed circuit boards (PCBs) wherever possible.



Figure 92: Old RDAS used in previous years

Optimization of the preexisting data acquisition design is a primary focus of this year's data acquisition initiative. As mentioned, we are seeking to move away from breadboard circuitry systems and migrate this functionality to custom PCBs wherever possible. Minimizing the usage of off-the-shelf parts, which can be burdened by unnecessary functionality, is a secondary goal. While off-the-shelf parts and materials have the benefit of being verified by an external source, their excess functionality hinders our design efforts. Additionally, this year's design will optimize space within the rocket body as well. The existent system mounts on either side of a 3/8" piece of plywood with width equal to the diameter of the rocket body; this piece slides into the body and is held in place by two aluminum support rods. This design wastes a great deal of lateral space in the interior of the rocket.

To minimize this wasted space, this year's design will be housed in a compartmentalized, cylindrical encasement in an effort to utilize as much of the interior diameter of the rocket at possible. A preliminary sketch of the compartment can be seen below. All payload electronics, with the exception of the sensors that are distributed throughout the rocket and their associated wiring, will be centralized in this encasement, which is located in the payload bay.



**Figure 93:** Top view of proposed electronics layout

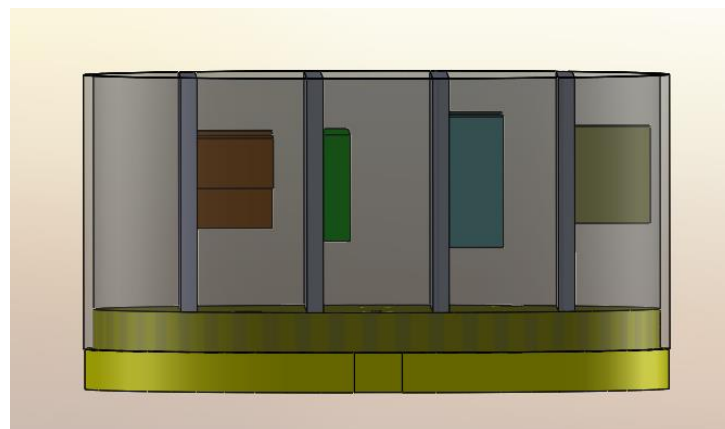


**Figure 94:** Side view of proposed electronics bay

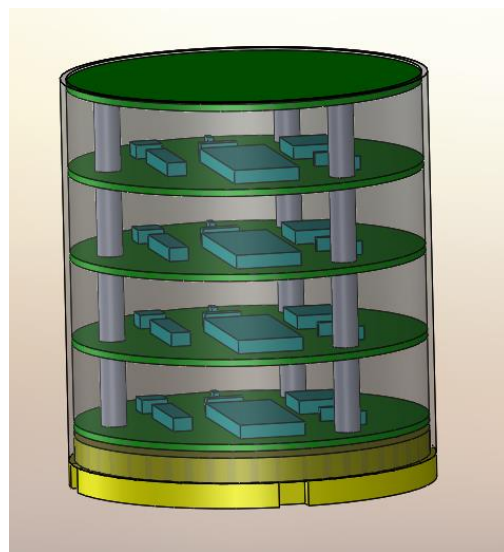


**Figure 95:** Proposed bay design if multiple vertical layers are required

### 5.1.4.2 Instrumentation Subsystems

Detailed descriptions of the three subsystems of the data acquisition system – strain measurement, temperature measurement, and structural analysis accelerometers – and the fuel delivery system can be found below.

#### 5.1.4.2.1 Fuel Delivery

The fuel delivery system relies on a solenoid in conjunction with RC timing circuits to delay entry of fuel into the thruster until some  $x$  seconds after launch. The time constant of our RC circuits and therefore the amount of time between launch and fuel release can be altered as necessary to suit the needs of our payload experiments by varying R and C. The ultimate goal of the fuel delivery circuitry is to release fuel into the thruster at some specific time after launch for initiation of thruster experiments and to cut off fuel to the thrusters after another designated interval of time has elapsed.

Operation of the fuel delivery circuitry proceeds as follows:

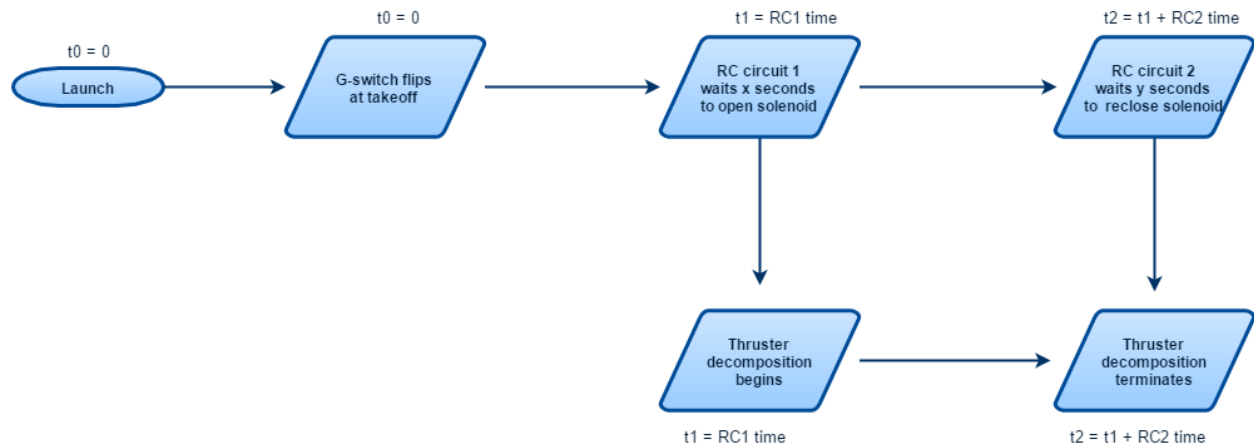


Figure 96: Flowchart of fuel delivery instrumentation

Launch represents  $t = 0$ ;  $t = 0$  is indicated to the system by the closing of a g-switch (a switch flipped by the g-forces the rocket experiences at takeoff). The closing of the g-switch releases current to RC circuit 1, which triggers RC circuit 2 and the opening of the fuel solenoid after a period of time  $t_1 = RC1$  time has elapsed. At  $t_1 = RC1$  time, the solenoid opens and fuel is passed to the thrusters to begin experimentation. At  $t_2 = t_1 + RC2$  time, RC circuit 2 triggers the closing of the solenoid, shutting off fuel flow to the thrusters and marking the end of the thruster experiment.

A preliminary electrical schematic of the fuel delivery system can be found in 5.1.9 *Drawings and Electrical Schematics, Payload*. The fuel delivery system is where we hope to implement much of the PCB optimization mentioned above; when the correct time constants for the RC circuits have been determined, the board can be designed and printed. A printed board saves space and improves reliability over the existing design by eliminating the potential for components to loosen and separate from an in-house proto or bread board.

For safety, the solenoid is normally closed, allowing no fuel passage. Only the concerted opening of the solenoid by the application of a voltage will allow fuel flow.

#### 5.1.4.2.2 Rocket Data Acquisition System

The Rocket Data Acquisition is implemented with AED Electronics R-DAS. The RDAS has the following operating characteristics:

**Table 16: Summary of R-DAS operating characteristics**

<b>Analog channels</b>	6 analog channels
<b>Digital channels</b>	4 digital channels
<b>Input voltage</b>	0 – 5.0 V
<b>Power supply</b>	9 – 10.6 V
<b>Supply current</b>	70 – 90 mA

The RDAS samples and stores incoming data via six analog channels accessed through ribbon cable; each stream of data sends information to the RDAS over a separate analog channel. Each channel has a max sample rate of 200 samples/second. Sampling is triggered by an onboard g-switch; when  $>2.5\text{g}$  have been sensed for 0.25 seconds, sampling and recording begin. Data is stored and retrieved through computer software post-flight.

The R-DAS was selected as it is a standard in rocket data acquisition and incorporates sampling, storage, g-triggering, igniters for ejection charges, pressure sensors, and accelerometers on board a physically small device with modest power usage. Additionally, data can be lifted directly to a computer from a board over a USB connection.

#### 5.1.4.2.3 Strain Measurement

Strain is measured via strain gauges, attached to the thruster pylons, together with a strain amplifier board. Each strain gauge is connected to an associated amplifier, which sends data to the RDAS through a ribbon cable connection.

#### 5.1.4.2.4 Temperature Measurement

Temperature data will be collected using two or more thermocouples placed on and around the monopropellant thruster. Each thermocouple is connected to a corresponding amplifier and filter before temperature measurements pass to the RDAS for storage and post-flight retrieval.

#### 5.1.4.2.5 Structural Analysis Accelerometers

3 ADXL345 accelerometers located throughout the interior of the rocket body will sample launch data, accelerations, and vibrations at 800 Hz. Each accelerometer is contained in an all-in-one datalogging unit with a microcontroller and SD card for data storage. Through reprogramming of the firmware of the board, the accelerometers have been purposed to sample

at 800 Hz across a +−16 g range considered sufficient for our predictions of the launch environment. With a 13-bit readout, the resolution of the system is .0039 g/least significant bit, sufficient to pickup of vibratory excitements of primary vehicle modes even with small sources of excitation. Each board is calibrated upon arrival using a vertical alignment jig and testing each axis at +1 G, 0G and -1 G orientations. The ADXL345 is a DC accelerometer that reads out data to the microcontroller digitally. Aliasing of the data is avoided by oversampling the analog data at 3200 Hz and lowpass analog filtering at 1600 Hz. The data is then digitally decimated to the programmed sample rate downstream of the Analog-Digital converter.

### **5.1.5 Performance Characteristics and Evaluation and Verification Metrics**

---

#### **5.1.5.1 Fuel Delivery Performance Characteristics and Evaluation and Verification Metrics**

---

A large majority of the Fuel Delivery System can be tested and validated on the ground prior to being utilized in flight conditions. Performing ground based shake tests of the payload section while the GoPro camera is recording has given some insight as to how the Slosh Abatement System damps fluid, but ultimately when compared to the test flight footage the two have no correlation whatsoever. For this reason, the VADL Drop Test Stand has been constructed (details in Section 5.3.1.3.4 VADL Drop Test Stand) and will be used to provide ground based verification. It also, however, will not replace in flight testing. This means that further test flights in combination with ground based testing are necessary to refine the Slosh Abatement System so it functions perfectly during the SL launch.

Table 17 lists the five subsystems from the functional architecture in figure 56 from section 5.1.1.2 and examines their performance and verification metrics.

**Table 17: System Analysis Summary Table for Fuel Delivery System**

<b>Subsystem</b>	<b>Functional Requirements and Performance Characteristics</b>	<b>Evaluation and Verification Metrics</b>
Fuel Delivery (Main System)	Supplies fuel to the firing thruster at the requisite time without allowing air into the fuel lines.	Each subsystem will be evaluated and verified through ground based testing and full-scale launches.
Retention System	Holds all components of the Fuel Delivery System securely within the rocket body. Supports components to avoid excessive forces and moments from acting on components during launch.	Ground based shake tests will ensure that components are thoroughly secured. Flight tests will verify that the retention system secures all components in place when high launch forces act upon them.
Fuel Tank	Must be a safe container for Hydrogen Peroxide, must be capable of withstanding far	The fuel tank design will be verified through ground based testing and through the full-scale rocket launch.

	<p>higher pressures than will be experienced at any point during rocket launch or assembly, and must be mounted such that lateral and vertical movement is strictly prohibited.</p> <p>Additionally, the Slosh Abatement System must ensure that no air enters the fuel pickup during fuel delivery.</p>	The ground based testing will ensure the adequate pressurization of the fuel vessel, and the full scale launch will verify that the Slosh Abatement System functions as designed.
Pressurization System	Must be capable of delivering compressed air at 450 psi to the solenoid valve to be relayed to the fuel tank. Must be able to pressurize and depressurize reliably with no leaks.	Ground based testing will ensure that the system pressurizes the fuel tank to 450 psi. Flight based testing will validate functionality prior to the SL launch.
Control System	Must actuate at the correct time to allow compressed air to pressurize the fuel tank at the correct time to enable proper decomposition.	Ground based testing will validate that the solenoid valve performs as designed several hundred times before launch. The final launch test will corroborate proper functionality with thruster ignition.
Verification System	Must be capable of acquiring high quality, properly illuminated footage of the inside of the prototype fuel tank to provide flow visualization for the Slosh Abatement System.	Ground based shake testing to ensure proper image calibration of the system and good quality flight based results to examine the effectiveness of the Slosh Abatement System.

#### 5.1.5.2 Thruster Performance Characteristics and Evaluation and Verification Metrics

Table 18: System Analysis Summary Table for Thruster System

Subsystem	Functional Requirements and Performance Characteristics	Evaluation and Verification Metrics
Thruster (Main System)	Intakes fuel and converts it into consistent thrust for the desired timescale	Each subsystem will be evaluated and verified through ground based testing
Retention System	Holds the thrusters in place within the rocket body. Must prevent oscillation of the thrusters	Ground based testing of thrust output will ensure that the components are secured

	due to forces during takeoff and MECO.	properly.
Fuel Injector	Deposits fuel from the fuel lines into the thruster catalysts bed at the desired rate	Ground based testing will be performed to confirm that fuel reaches the catalyst bed at the desired rate
Catalysts Bed	Catalyzes the decomposition of hydrogen peroxide to generate heat and thrust.	Ground based testing will confirm the full decomposition of the hydrogen peroxide fuel in the catalyst bed
Nozzle	Normalizes the output fluid from the catalyst bed to a specific exit velocity	Ground based testing will confirm that the fluid speed created by the nozzle produces the correct amount of thrust. A strain gauge on the pylon will be used in flight to confirm that the proper amount of thrust is generated and for the desired duration. A thermocouple will be placed in the nozzle to ensure that the exit gas is at the desired temperature
Strain Gauge	Measures the strain put on the cantilever pylon by the thrust generated by the thruster	Ground based testing will be used to calibrate the strain gauge and verify that it reads the correct strain
Pressure Sensor	Measures the pressure in the fuel line entering the fuel injector	Ground based testing will be used to calibrate and confirm the accuracy of the pressure sensor
Thermocouple	Measures the temperature of the fluid exiting the nozzle	Ground based testing will be used to calibrate the sensor and confirm its accuracy

### 5.1.5.3 Structural Analysis Performance Characteristics and Evaluation and Verification Metrics

---

Subsystem	Functional Requirements and Performance Characteristics	Evaluation and Verification Metrics
Finite Element Model (FEM)	Represents the appropriate length and mass of vehicle	Flight Mass and Length Measurements of rocket and comparison to FEM
Finite Element Model	Represent the modal characteristics of the vehicle	Modal Frequencies and Mode shapes identified in flight and in tap test and correlation with the FEM
Accelerometers	Collection of usable and distinct dynamic modal data	Data post-processing for modal parameters and self orthogonality check

## 5.1.6 Verification Plan and Status

---

### 5.1.6.1 Fuel Delivery System Verification Plan

---

Table 19: Summary of Verification Plan for Fuel Delivery System

Mission Success Criterion	Verification Method	Status
The system must deliver high pressure fuel at 450 psi to the ramjet at the requisite time during rocket flight	The payload electronics will activate the solenoid valve at the appropriate time such that fuel is delivered to the fuel injector. This will be verified through ground based testing and confirmed during the full scale launch.	Design in first stages. Construction and testing incomplete.
The system must be able to extract the majority of the fuel in the fuel tank and deliver it in such a way that air is not present in the fuel lines	Several flight tests of the Slosh Abatement system with verification footage from the GoPro camera must be performed so the system can be perfected for the SL Launch. These results should be used in conjunction with results from the VADL Drop Test Stand	Ground based testing has shown preliminary success in slosh abatement system designs. Further updating of system in progress. Evaluation checkpoint at subscale launch.
The system must be capable of venting if excessive pressures	Final iteration of the fuel tank will be equipped with a	Incomplete.

are reached in the fuel tank (>600 psi).	600 psi vent valve to meet SL specifications.	
There must be some method to verify the functionality of the Slosh Abatement System.	GoPro camera will acquire ground and flight based footage to verify that the system functions properly and footage can be used to develop an improved Slosh Abatement System.	Ground based testing in VADL Drop Test Stand functioning as intended. Addition of accelerometer in progress. Flight system verification incomplete.
The system must be accessible and secured while in the rocket and fit within the confines of the rocket geometry.	The system should be able to be accessed through the access door to install the fuel tank and GoPros and turn on the flashlight to provide illumination for recording. Additionally, all components need to stay secure within the rocket body to prevent damage.	CAD models along with preliminary construction mock ups show promise. Final verification in subscale launch and continued verification on subsequent launches.
The system must be modular in design to enable simple troubleshooting, ease of installation, and performance upgrades.	This is an inherent design characteristic of the system that was implemented so upgrades and changes could easily be made to the system as research progresses.	Initial design and build complete. Further design revisions will be forthcoming.
Every component in the fuel delivery system must be compatible and non-reactive with Hydrogen Peroxide fuel.	Background research and attention to detail will lead to information and verification that each component and material used throughout the system follows this requirement.	All components that will react with the fuel are non-reactive over the relevant time scale. This does not include the Slosh Abatement System yet but once conceptual designs have been finalized after testing, the requirement will be stringently applied.

#### 5.1.6.2 Thruster Verification Plan

Table 20: Summary of Verification Plan for Monopropellant Thruster

Mission Success Criteria	Verification Method	Status
Thruster generates correct	Strain gauge in thruster	Ground based testing

amount of thrust for correct duration	support pylon will measure thrust generated and the length of thrusting action	facility is under construction. Thruster design is being finalized so that construction can begin. Testing of strain gauges pending completion of both
Hydrogen Peroxide fully decomposes in catalyst bed	Generated thrust is consistent at target force and output gas is at target temperature	Catalyst bed is designed and construction methods are being finalized. Ground based testing facility is under construction. Testing is pending completion of both
Full data collection on thruster for entirety of firing duration	Strain gauge and thermocouple report data similar to predictions from ground based test facility for the desired time period	Ground based test facility is under construction. Thruster design is being finalized. Testing of strain gauge and thermocouple are pending completion

#### 5.1.6.3 Structural Analysis Verification Plan

---

Table 21: Summary of Structural Analysis payload Verification Plan

Mission Success Criterion	Verification Method	Status
No structural vehicle failures across all launches.	Rocket reaches apogee and is recovered after sustaining minimal structural damage such that it can be reflown again to target apogee altitude with no refurbishment.	Test launches planned for November and February
Accelerometers collect usable data for the entirety of flight time.	Download and post-processing of accelerometer data after launch for quality and frequency content.	Test launches planned for November and February
Modal frequencies within 15% between test and finite element models.	Comparison of quantitative modal frequencies of primary modes identified in both the models and the test data	Modal Frequencies predicted for the models. Test data is pending flight and tap test.

Modal Assurance Criterion above 80% on diagonal and below 20% on off-diagonal terms in Cross-Orthogonality check between modal test data and Finite Element Model simulations.	Mode Shape Cross Orthogonality check outlined in 5.3.3	Mode shapes predicted in 2 finite element models. Test data pending flight and tap test.
--	--	--

### 5.1.7 Preliminary Integration Plan

The integration plan has been discussed in detail in Section 4.5.1 *Payload Integration Plan* of this document.

### 5.1.8 Precision, Repeatability, and Recovery

More detail on the precision of instrumentation can be found in section “Relevancy of Data and Analysis” of this report. For the fuel delivery system, refer to section 5.3.1.5 and for the monopropellant thruster system, see section 5.3.2.5.

Furthermore, this experiment will be able to be recovered and repeated after a successful landing of the vehicle.

### 5.1.9 Drawings and Electrical Schematics, Payload

Drawings and pictures of essential payload elements have been provided in the system review section about the payload. See section 5.1.1 for fuel delivery, 5.1.2 for the monopropellant thruster systems, and 5.1.4 for the instrumentation.

Below is a schematic of dataflow from the data acquisition subsystems to the RDAS centralization system.

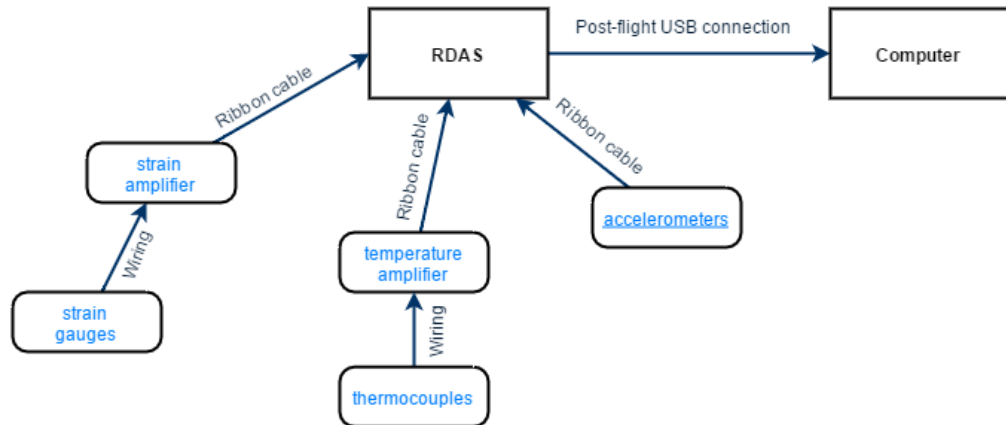


Figure 97: Schematic of data flow from the instrumentation subsystems

Below is a schematic of data flow in the Accelerometer Datalogging boards. This system is highly optimized to mitigate the dropping of critical data during SD card write commands. 3

Data buffers are used to channel the flow of data, and an analog lowpass filter is used to prevent signal aliasing. Data is written from an ADXL345 accelerometer in “batch-logging” design, to allow for data to be collected in one 400 sample buffer, while data is being written from the other buffer to the SD card data storage device. These 2 buffers max out the available static random access memory on the aduc7024 microcontroller, which is 4 times the size of an arduino. 800 Hz logging would not be possible on an Arduino.

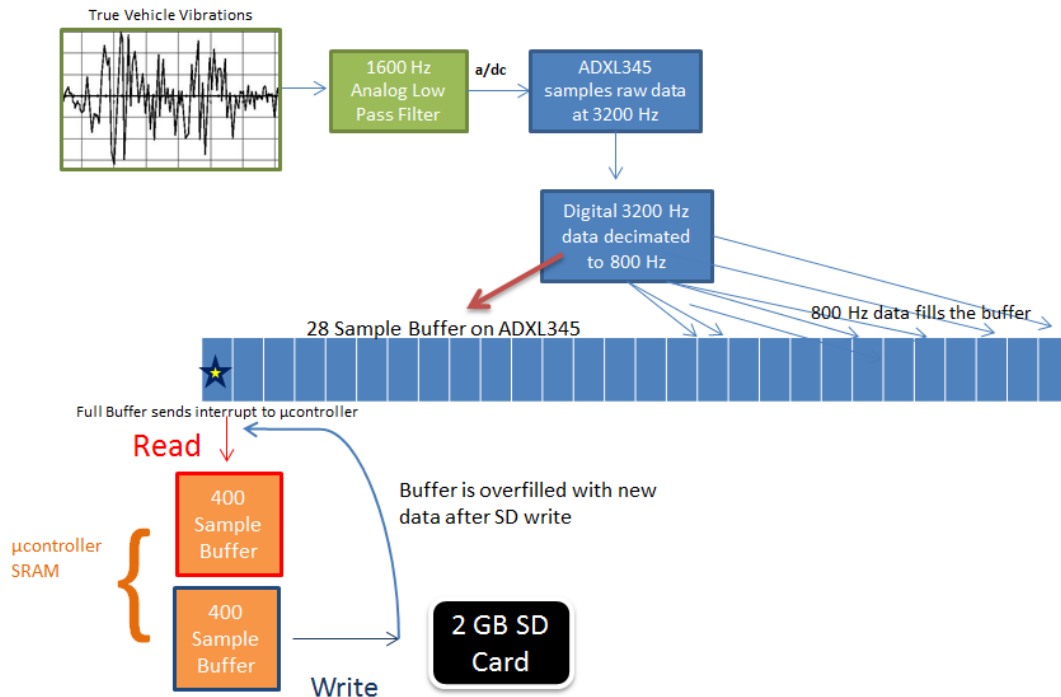


Figure 98: Data flow in Accelerometer Dataloggers

Below is an electrical schematic of the fuel delivery system. Boxes have been used to indicate RC timing circuits; these circuits will be optimized variants of a generic timer circuit (including a resistor, capacitor, transistor, and power source).

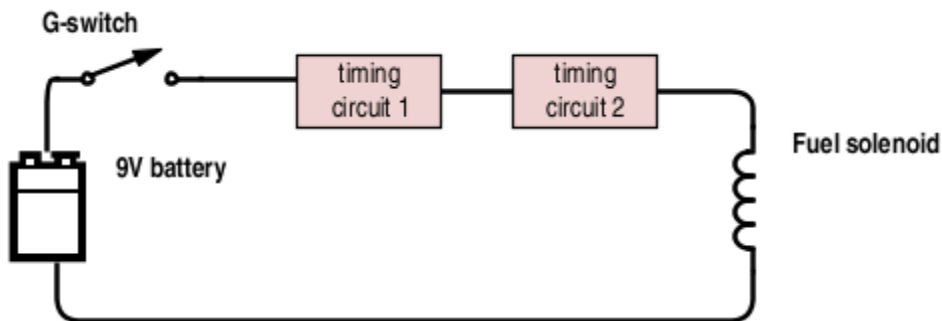


Figure 99: Schematic of the fuel delivery system

The payload electronics will be configured in the payload bay so as to maximize vertical space usage; this will be accomplished by compartmentalizing a cylinder with the same diameter as the

rocket body (5.5"). The height of said cylinder will be the minimum height required to encompass all payload electronics. Sensors are located outside of the payload bay at different points in the rocket; shielded wires will run from any given sensor to its associated processing board within the payload bay.

### **5.1.10 Key Components and Desired Results**

---

There are several principle components to the payload. There are three major subsystems that compose the payload in total. The fuel injection system and the monopropellant thruster assembly are two subsystems that work in conjuncture with each other towards a single goal. The fuel injection system, which will be internal to the rocket, consists of a pressurized compressed air tank to provide the driving force for the fuel injection. It is connected to the hydrogen peroxide tank, which in turn has fuel lines leading down the body of the rocket to the fuel injector assembly within the thruster itself, which is also internal to the rocket body. The fuel injector leads into the catalysts bed inside the thruster. This is where the hydrogen peroxide is decomposed and forced out through the next thruster section, the nozzle, generating thrust. The thruster is held in place by a cantilever beam attached to the lower centering ring in the tail section of the rocket body. The physical structural analysis systems consist of accelerometers rigidly attached throughout the internal rocket body. One is attached within the avionics bay near the top of the rocket. A second one is screwed onto a bulkhead within the payload section, near the middle of the rocket. The third is riveted onto the rocket body wall in the tail section. There is a digital component of the structural health monitoring system that is not present in the rocket at launch. A finite element model of the rocket has been constructed to predict the performance of the carbon fiber and how it will hold up under flight conditions.

There is a cascade of actions that will characterize good performance of the entire payload system. First of all, the injection system should function to provide a consistent predetermined flow-rate into the decomposition chamber for the desired range of time during flight. Then, of course, the decomposition must successfully be sustained for the entire thrust phase of the monopropellant thruster. The temperature measurements should validate that the decomposition is sustained, and that a positive thrust is produced from the flow passing through the monopropellant thruster. The strain signal from the connecting pylon should validate the net load on the engine. The thrust measurement will be reconfirmed by comparison with the measurement of total load and the theoretical drag. The readings from each accelerometer should have similar peaks and valleys when the rocket first lifts off, at MECO and when the blast caps are detonated. The presence of these major events occurring at the same time and at similar magnitudes in all three accelerometer data sets will confirm the accuracy of the data being collected. This data should then confirm the accuracy of the finite element model that has been constructed of the rocket. The lift acceleration and drag acceleration recorded by the accelerometers should confirm the values predicted before takeoff.

### **5.1.11 Mass Statement**

---

The following table details the mass of the subscale payload section.

**Table 22: Mass Statement for subsection payload**

Part	Mass (lbs)
Bottom Bulkhead	0.35
First Bulkhead	0.3
Fuel Tank 1	0.5
GoPro1	0.2
Water 1	0.25
Second Bulkhead	0.3
Fuel Tank 2	0.5
GoPro 2	0.2
Water 2	0.25
Top Bulkhead	0.35
Threaded Rod	0.26
Tubes and Window	1.87
<b>Total</b>	<b>5.33</b>

Preliminary estimates for the full scale payload add an additional 2 lbs for the pressurization system and another 2 lbs for payload electronics. The full scale will contain only one fuel tank and will not include GoPros or an illumination system.

## 5.2 Payload Concept Features and Definition

---

### 5.2.1 Creativity and Originality

---

2015-2016 will be a landmark year in payload originality for the Vanderbilt Aerospace Design Laboratory. Payload design and scientific innovation is the cornerstone of this program and is the center that the entire rocketry program is built around. The basis set by this team's payloads will set the tone for up to 5 years more of projects evolving on this experiment's concepts. Creativity and originality of the 2015-2016 VADL rocket is split into 3 primary science investigations and is outlined below:

1. “Green” Monopropellant H<sub>2</sub>O<sub>2</sub> Thruster

- a. Utilizes novel fuel to replace toxic and dangerous hypergols prevalent in spacecraft attitude control thrusts
  - b. Hand machined and welded by design team to tight tolerances
  - c. Designed to optimal geometry for optimal performance
  - d. Control system design for pulsed or continuous operation
  - e. Data Acquisition System design for performance evaluation
  - f. Design of complex aerodynamic shrouding to serve functions of:
    - i. Thruster accommodation
    - ii. Drag reduction
    - iii. Specific structural strength
    - iv. Resilience in high temperature environment
  - g. Validated through ground test facility designed from ground up by students
2. Anti-Sloshing Fuel Tank
- a. Builds on slosh abatement lessons of 2013-2014 teams
  - b. Research into surface tension “sponge” designs for passive slosh abatement
  - c. Ground based performance evaluation in new drop test stand with high speed camera and accelerometer instrumentation
  - d. Modular tank design allows for iterative advancement of baffling design
3. Advanced Structural Dynamics
- a. Distributed flight accelerometers for measurement of:
    - i. rigid body vehicle motions
    - ii. modal vibrations
  - b. Development of a full vehicle finite element model
    - i. Prediction of primary modes of full vehicle
    - ii. Prediction of vehicle response to in flight forces
      - 1. Motor burn
      - 2. Section separation from pyrotechnic shock
      - 3. Landing
      - 4. Aerodynamic gust and buffeting
  - c. Correlation of dynamic instrumentation data to modeling predictions
  - d. Ground based modal tap testing
  - e. Fabrication of “smart structures” with embedded structural health monitoring
  - f. Mass optimization through utilization of advanced carbon fiber materials and fabrication and modeling techniques

### **5.2.2 Uniqueness and Significance**

---

The creation of a passive slosh abatement system, as opposed to a dynamic system, greatly simplifies the design while simultaneously achieving robust and uninterrupted fuel delivery throughout flight.

The development of a full scale HTP thruster highlights a simple, relevant, and environmentally friendly aerospace actuation system. The success of this system will lay the groundwork for a series of further experiments researching environmentally friendly monopropellant propulsion, and represents a large step forward for the team in the development of fabrication of a complicated system, specifically in terms of the stringent design and safety requirements.

Due to increasing societal concerns regarding the clean energy, Vanderbilt's payloads have placed an emphasis on green fuels, fuel efficiency, and energy availability. Green propellants used for satellite-level propulsion system have become attractive in recent years because of non-toxicity and lower requirements of safety protection. High-concentration hydrogen peroxide is easy to manufacture and the operating temperature is lower than traditional monopropellant propulsion. With the expected proliferation of small near-earth experimental payloads on low-cost scientific missions, the need for orbit transfer and maintenance requirements will require an on-board propulsive technology in the 1N – 10N category. In such scenarios, a monopropellant thruster would be a welcome addition, especially in scenarios where long fuel shelf life will not be required.

This system has medium performance where the specific impulse range is between 130 and 225 seconds. Hydrazine ( $N_2H_4$ ) liquid is the most used monopropellant system because it gives a good performance and has a very long shelf life. However, hydrazine is a very toxic and inflammable substance. An alternative solution is to use hydrogen peroxide, a known green propellant, which can be stored as a liquid, and has high density level.

The creation of a passive slosh abatement system, as opposed to a dynamic system, greatly simplifies the design while simultaneously achieving robust and uninterrupted fuel delivery throughout flight. This system facilities the other experiment flown on the rocket while demonstrating a cost effective solution to a persistent design constraint.

The conventional approach to fuel and liquids handling in space would be the use of bladder-type fuel tanks, where the fuel will not suffer any disorientation during rocket launch and deceleration or during the microgravity flight. However, bladder type devices can have size, space and actuation requirements making them expensive and difficult to incorporate without complicated testing protocols. Also, such devices cannot be useful in short duration rocket flights, where the actuating mechanism inertia-based delays could jeopardize a mission. In such contexts, a passive slosh-abatement fuel tank would be the best way forward.

This project evaluates slosh abatement during rapid deceleration (touching -4g) following a 14 g launch, realize maximum fuel extraction from a passive tank both in the pulsed and the continuous mode, and in-flight performance evaluation of a 10N  $H_2O_2$  thruster with a total target impulse of 50 Ns against a 5000 Ns impulse of the rocket propulsive motor.

### **5.2.3 Challenge Level**

---

This payload experiment takes on a high challenge level. Over the course of this competition, team members will use topics from a wide variety of mechanical engineering courses to create, optimize, and test a hand-crafted green monopropellant thruster with high pressure hydrogen peroxide fuel delivery. Fluid Mechanics, Heat Transfer, Thermodynamics, Controls, Mechatronics, Instrumentation, and Material Science are a few of the advanced courses team

members will need to have a solid understanding in for the payload to be a success. The multiple payloads further widen the horizon of required knowledge and engineering.

## 5.3 Payload Science

---

### 5.3.1 Fuel Delivery System Science

---

#### 5.3.1.1 Payload Objectives

---

The objectives of the Fuel Delivery System payload are as follows:

- 1) Deliver hydrogen peroxide fuel at the correct time to ensure proper decomposition within the monopropellant thruster payload
- 2) Serve as a test bed that investigates liquid sloshing in microgravity conditions and mitigates sloshing effects to enable reliable fuel delivery under a variety of launch conditions.
- 3) Continuously improve the fuel delivery system to the point where a scalable developmental program exists that can be applied to a diverse number of scenarios.

In order to fulfill these objectives, rigorous ground based testing in the new VADL Drop Test Stand along with two test launches will be carried out to ensure the effectiveness of the Fuel Delivery System. The subscale test flight will be used for flow visualization within the fuel tank. These test flights will take place in November 2015. The footage collected from these launches will be used to incrementally improve the Slosh Abatement System to a point where it is suitable for the final competition. This test investigates worst case scenarios to assure that the system is failure proof under ideal launch conditions.

The full scale test flight involves testing the final design of the fuel tank and baffling system by validating proper fuel delivery through sustained thrust production in the monopropellant thruster. In this case, flow visualization with the GoPro camera will not be possible due to fuel tank being made out of aluminum. Therefore, results from ground based thruster testing will be corroborated with the data collected from the thruster thermocouples and strain gages used in this final flight to ascertain that the pressurized fuel tank provides adequate fuel delivery through all stages of flight. More on the methodology behind these launches will be discussed under section 5.3.1.3 Experimental Logic, Approach, and Method of Investigation.

#### 5.3.1.2 Payload Success Criteria

---

As stated before, the success of the Fuel Delivery System is contingent on providing reliable, air free fuel delivery to the firing ramjet. Fuel injection to the monopropellant thruster will occur about four seconds after launch (.5 seconds after MECO). The delivery window ranges from four seconds to fourteen seconds after launch. Because the majority of the sudden acceleration turnover caused by main engine cutoff occurs during the fuel delivery window, the Fuel Delivery System must be capable of functioning under these conditions.

But additionally, the success of this payload hinges upon the incremental improvements that are made to the system which enable it to be used in a variety of situations, as opposed to being

tailored to a singular goal. For example, it is desirable to extract a maximum amount of fuel from the fuel tank reliably under a variety of launch conditions as opposed to only being able to extract a fraction of the fuel reliably under certain situations. The fuel tank design of 2013 was adept at delivering fuel to the ramjets because ignition occurred prior to MECO. The fuel tank ensured that the requisite amount of fuel for ramjet combustion was already in the fuel lines prior to g turnover and also incorporated an air bubble separation mechanism as an additional safeguard. See figures 100 and 101 below.

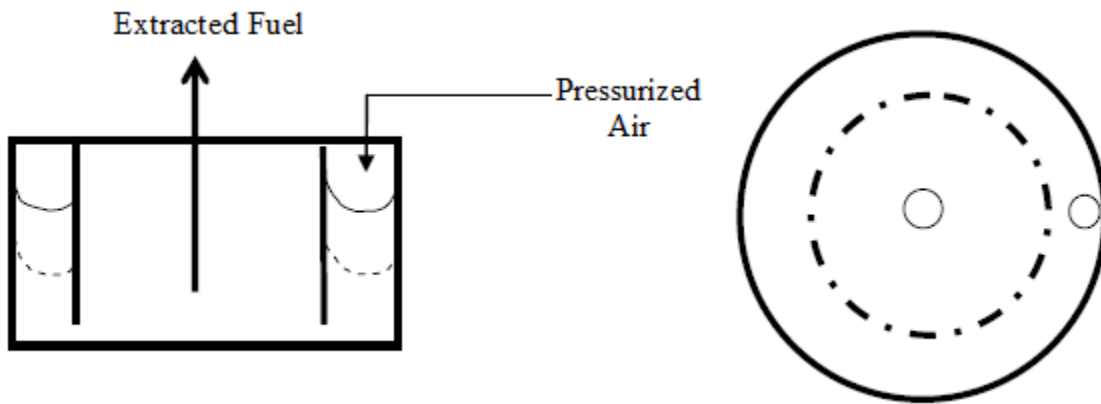


**Figure 100:** Air Bubble Separation mechanism from USLI '13



**Figure 101:** USLI '13 Fuel Container Design

The problem with implementing this system in a launch scenario after g turnover is that an air bubble could still feasibly make its way to the fuel pickup by going under the separation ring. Additionally, once the volume of fuel occupying the outer boundary has been consumed, air certainly will make its way into the internal chamber where the pickup is housed, which means that reliable combustion can no longer be assured. Depending on the size of the separation ring, this means that only roughly half of the fuel can be extracted from the fuel tank and even then only under certain launch conditions. Because hydrogen peroxide decomposition will occur over a longer period than in previous years' combusted fuel in a ramjet, being able to extract additional fuel is even more crucial. The objective of this year's Slosh Abatement System is to ensure that fuel delivery is possible under a greater variety of launch conditions and with

different fuel levels. The increased flexibility of this modular design means it will be scalable to future launches based on the requirements necessitated by those endeavors.

### 5.3.1.3 Experimental Logic, Approach, and Method of Investigation

---

#### 5.3.1.3.1 Summary

The success of the Fuel Delivery System hinges upon the effectiveness of the Slosh Abatement System. Verification is accomplished through means of testing in the VADL Drop Test Stand, flow visualization in the first two test flights and through successful sustained decomposition in the monopropellant thruster in the third and final test flight. Ground based shake testing does not correlate with flow visualization results that have been obtained in flight. For this reason, designs are tested in the VADL Drop Test Stand that uses both gravity and a system of springs to replicate microgravity and negative gravity conditions. Along with this, extensive flight based testing is necessary. As mentioned before, a worst case approach is undertaken for the flow visualization tests to validate that the system will function perfectly during the final test flight and the SL flight. This means the following:

- The amount of liquid in the prototype tank is set at 65 cc (maximum capacity is 200 cc of liquid)
- The test liquid is water, which has a slightly lower viscosity than the fuel that will be used for the actual launch
- Main engine cut off occurs with this low level of fluid to verify that air bubbles will not reach the pickup in this scenario

#### 5.3.1.3.2 Test Fluid Selection

Through repeated ground based footage tests, water was determined to be an excellent fluid for flow visualization because of its clarity and ability to allow light to diffuse through the tank. Additionally, because it has a slightly lower viscosity than the fuel that will be used for the final flight, it is more prone to movement when acted upon by external forces and exhibits slightly lower surface tension qualities. This means that if the Slosh Abatement System is capable of adequately damping water during flight, it most certainly will be able to do so with the hydrogen peroxide fuel.

#### 5.3.1.3.3 Tank Filling

Filling the tank to less than a third of its rated capacity and subjecting it to g turnover conditions is one method of verifying that the baffling design can perform in extreme conditions. During the final flight, the tank will be completely filled and purged of air. However, the worst case situation is implemented during the flow visualization phases to diversify the conditions under which the Slosh Abatement system is functional. If there is a large amount of air within the fuel tank when g turnover occurs, the possibility of air reaching the fuel pickup is greatly increased. This means that if GoPro footage shows that no air reaches the pickup during launch under these conditions, then the Slosh Abatement System is functional not only in these worst case scenarios but under the more ideal operational parameters that will be encountered in the SL launch.

#### 5.3.1.3.4 VADL Drop Test Stand

#### 5.3.1.3.4.1 Motivation

The most novel experimental approach is the new VADL Drop Test Stand. It was discovered that the flip or shake tests used previously did not provide flow visualization results that correlated to later in flight data.

The most commonly used flip test, in which the tank was quickly inverted, has three issues. The first is the unrealistic accelerations experienced during the inversion. While the resulting upside down tank is providing some information, to get there the tank and fuel inside undergoes lateral and centripetal accelerations that it would never see in flight. Second, the test is inherently short and difficult to film. One of the most important parts of this test is the moment of turnover and this moment is almost impossible to see because of the movement of the tank and change. Third, the test is limited to simulating only a constant -1g once the tank is fully inverted. This does not accurately represent the non-constant deceleration from -3g that is expected in flight.

#### 5.3.1.3.4.2 Design Summary and Advantages

At its core, the VADL Drop Test Stand is a spring and gravity accelerated platform that has mounted to it both a fuel tank with an insert to be tested along with a camera and an accelerometer. This allows visual data to be taken and correlated with acceleration values to give insight to slosh abatement studies. A schematic of the design can be seen below in Figure 102.

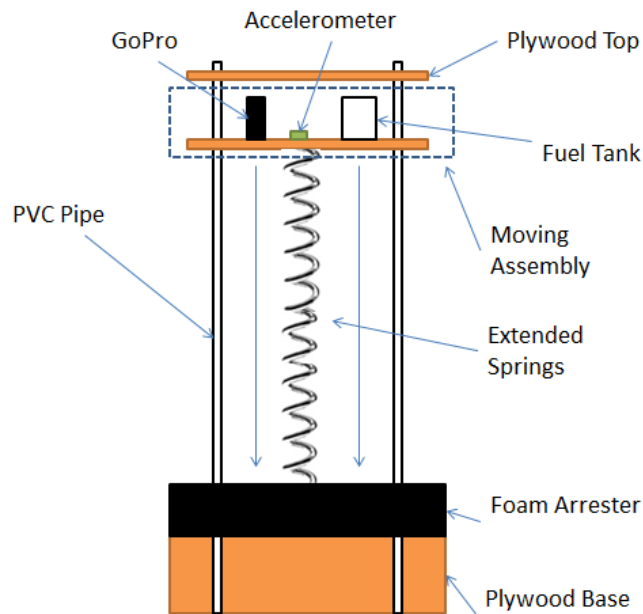


Figure 102: Schematic of the Drop Test Stand

The overall design of the drop test stand is a laser cut plywood box that supports two 5ft sections of PVC pipe. Along these two guide rails slides a laser cut plywood piece to which a GoPro and fuel tank are mounted. The two pieces of pipe are connected again at the top by a plywood piece which fits snugly on the rails and keeps the spacing between them constant. On top of the

plywood base, a piece of foam sits to arrest the moving assembly once it reaches the bottom. It was intentionally cut long so that it acts as a foam spring that more slowly arrests the moving assembly. The springs which accelerate the moving assembly downwards are attached to the top of the plywood base, travel through a hole cut in the foam, and attach to the moving assembly. An image of the Drop Test Stand is shown below.



**Figure 103: Drop Test Stand lifted to its maximum height**

This design is superior to previous testing methods in two ways. First, it much more accurately recreates the accelerations expected in the actual launch. The vertical travel direction eliminates the lateral and centripetal accelerations. Along with this improvement in direction, the combination of springs and gravity allow a model of negative g's to be simulated in the lab. This is a massive leap in VADL's ground based testing abilities. Second, the actual visualization abilities of the test were improved. Because the camera and tank move in sync, there is a constant frame of reference that allows improved insights and analysis.

#### *5.3.1.3.4.3 Detailed Design Analysis*

To design the spring system, a simple dynamics model was created. Figure 104 below shows the model, assumptions, calculations, and the estimated spring constant required. The mass estimation came from a mass audit of the platform and its components. The acceleration value was derived from flight simulations.

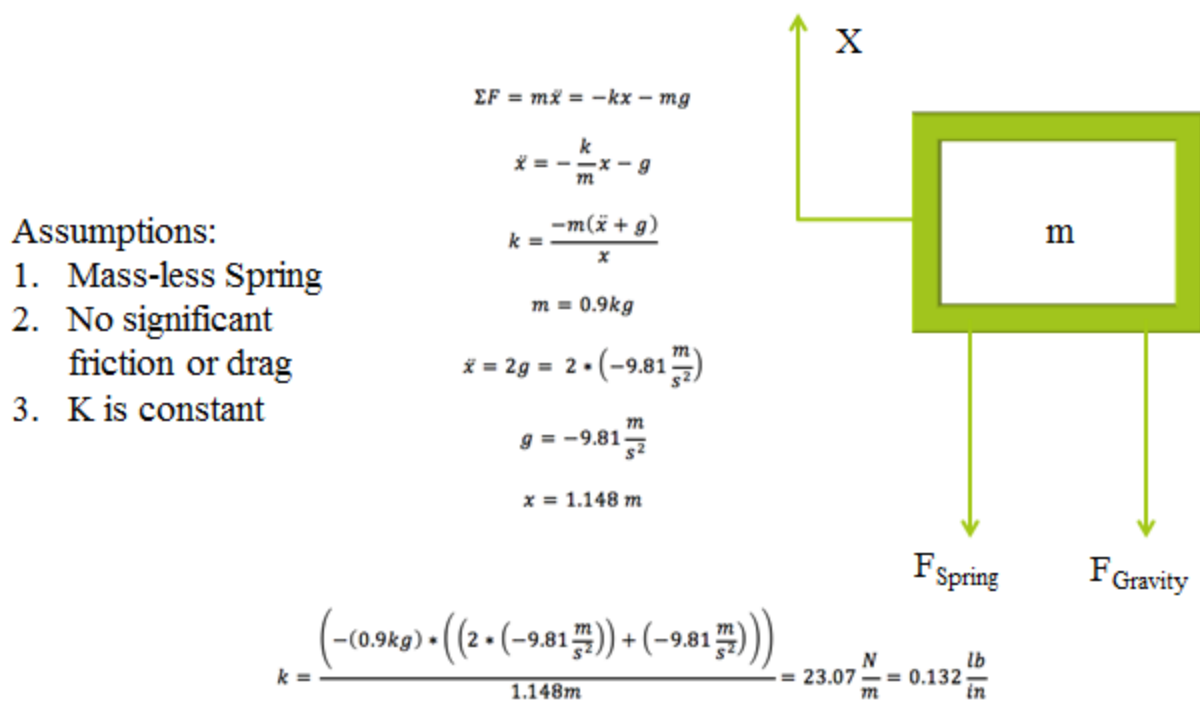


**Figure 104: Drop Test Stand Dynamics Model**

Multiple questions also accompany this result that involve both safety and usability of the design. Using the model shown above, it was calculated that at max acceleration the stand could reach a speed of around 18.2 miles per hour at the bottom. Along with this, it would require about 7.5lb of force to hold the moving assembly at the top of the rig. This shows that the design was practical to use and also safe. By incrementally increasing the number of springs attached to the assembly, it was shown that it could be safely arrested at the bottom with the foam shown above.

A key issue of the design of any drop test stand is the duration of the test. This increases with height, and due to space and practicality constraints the height of the stand was limited to 5ft. This provided between 0.3 and 0.5 seconds of experiment time. By using a slow motion film enabled GoPro, however, the test can be visualized and anywhere between 8 and 30 frames of film can be taken.

An addition to the design discussed above is the attachment of an accelerometer to the moving assembly. This allows for calibration and measurement of the actual acceleration of the moving assembly and a better interpretation of the results and their applicability to the final slosh abatement design. The accelerometer used is an Analog Devices XL345 and is pictured below in Figure 105.

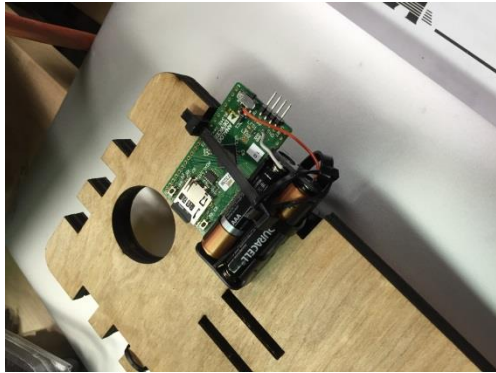


**Figure 105: Drop Test Stand Accelerometer**

#### *5.3.1.3.4.4 Drop Test Stand Experimental Methods*

The experimental method for this stand is twofold as far as slosh abatement testing is concerned. Three springs are used to simulate the maximum deceleration experienced during flight. This allows for four different scenarios to be tested. An SAS can be tested in microgravity conditions along with 3 incremental deceleration conditions up to the maximum. This can be used to show how increasing deceleration affects the design in question. Along with this, the position of the tank can be varied over multiple tests to see the effects of different accelerations on different areas of the tank.

#### *5.3.1.3.4.5 Drop Test Stand Benefits*

The Drop Test Stand is a large step forward in the testing abilities of the VADL. First, it allows for the simulation of not only microgravity, but also negative gravity conditions in the lab. Second, several tests can be run on multiple design iterations much more quickly and effectively than with in flight or flip testing. This combined with rapid prototyping will allow for a greatly quickened design process where experimental Third, it provides consistent acceleration conditions by which different designs can be compared. Finally, because we are not limited in the number of tests run, as we are with in flight testing, slosh phenomena without baffles can be examined and used as a baseline for comparison as well as inspiration and basis for future designs.

### **5.3.1.4 Test, Measurement, Variables, and Controls**

---

Test procedures for the Slosh Abatement System will occur under the conditions described in sections 5.3.1.3 Experimental Logic, Approach, and Method of Investigation. Actual measured data that was collected from the VADL Drop Test Stand can be found in 5.3.1.5 Relevancy of Data and Analysis. Ground based testing for the rest of the Fuel Delivery System can be found in section 0 Ground Based Testing of Fuel Delivery System.

Variables that must be considered during system testing include:

- Fluid level for flow visualization
- Fluid type used for flow visualization
- Type of Slosh Abatement System

- Location of fuel pickup

The control in this experiment is the footage obtained from the preliminary test flight which will occur in November of 2015 along with footage and accelerometer results from the VADL Drop Test Stand.

#### 5.3.1.5 Relevancy of Data and Analysis

---

For the Fuel Delivery System, the relevant data that will be acquired by the payload will concern the Slosh Abatement subsystem.

The data that has been and will be acquired first will be visual and accelerometer data from the VADL Drop Test Stand. This system will test and provide information about the performance of the slosh abatement system and its performance under different negative g scenarios. This data is quite relevant to its performance in the actual SL flight as it relatively accurately simulates the deceleration that will affect the fuel tank after MECO. It is also prone to error, however, as sometimes the visual data can be misinterpreted. Depending on lighting conditions and the angle from which the video is taken, results could vary and the entire picture may not be seen by the user. For this reason fuel tanks that are difficult to visualize may be viewed from multiple angles to better understand their performance. Along with this the color and amount of the liquid inside the tank may be varied to see different results. Finally, this test fails to replicate two important aspects of the final flight. The first is the duration of the test. The drop test lasts only 0.25-0.5 seconds while the actual tank will provide fuel for 5s. Second, fuel is not being extracted from the tank while it is dropping and therefore the pressure gradient between the pressurized air and lower pressure fuel pickup is not observed.

The second set of data about the fuel delivery system will come with the subscale launch. Two acrylic fuel tanks will be flown in the launch and GoPros combined with illumination systems mounted internally will capture video of fluid placed in the tanks. This second set of data will be used in conjunction with ground based testing to determine the success of the slosh abatement subsystem in the fuel delivery system. This method of testing is more accurate than the ground based testing for two reasons. The first is that it replicates almost exactly the acceleration conditions that will be seen in the final launch because the video will be taken during an actual flight. This may provide different results than have been seen on the ground. The second advantage is the longer duration of the test. Video will be available from the entire flight, and because of this the performance of the SAS's over longer time scales will be examined. Despite these advantages, this test is still not a perfect analysis on which to base success or failure of a slosh abatement system. This method still does not include the pressure gradient caused by the pressurization of the air and removal of the fuel. The liquid and gas will remain at ambient pressure during the test.

The final test of the slosh abatement system performance will be the data acquired from the thruster during firing both in flight and in ground based tests. The thrust data will be used to see that fuel was provided at a consistent rate and without the air bubbles. This data when combined with the ground based testing as well as previous in-flight flow visualization tests will provide a substantial amount of data relevant to the success or failure of the slosh abatement system. There is, however, a possible source of error in this data as well. This data represents

the estimated thrust produced by the hydrogen peroxide thruster. If the data shows inconsistent thrust, there could be multiple reasons. It could be an issue with the fuel provided to the system, but it could also be problems in the catalyst bed, the nozzle, or a multitude of other components. Repeated tests will provide one source of possible insight. If the thruster provides consistent thrust when the fuel tank is under normal acceleration conditions, then it may be determined that more research should be done into the slosh abatement system.

### 5.3.1.6 Preliminary Experiment Procedures

---

#### 5.3.1.6.1 Fabrication of Fuel Delivery System

The fuel delivery system will consist of commercially available pressurization equipment, a purpose-ordered solenoid valve, and an already tested fuel tank. Components will be connected with  $\frac{1}{4}$ " aluminum tubing. This tubing can operate at 4,700 psi and will not significantly react with hydrogen peroxide on a similar time scale to the exposure. Structurally, a system of bulkheads and supports will assure that no structural stress is placed on the fuel system.

#### 5.3.1.6.2 Ground Based Testing of Fuel Delivery System

A ground based testing system will verify the key components and design choices of the fuel delivery system. This ground based system will be the same system used to test the thruster, so the entire system will be validated before launch. The system currently under construction uses a modular arrangement of aluminum rails to support the key components. The system also includes a Lexan shield between the operator and the thruster and integrates with the facility to safely vent the thrust produced.

#### 5.3.1.6.3 Test Launch

A subscale launch will be accomplished in mid-November 2015 to evaluate the functionality of the two proposed Slosh Abatement Systems. From the results of the subscale launch, a design will be chosen as the final design. This will undergo a full scale launch test in January 2016 to validate the final design in terms of slosh abatement abilities. After using the results from the first full scale launch, the design will be finalized. A final full scale test launch in March 2016 will validate the performance of the Fuel Delivery System through proper monopropellant decomposition and thrust generation.

#### 5.3.1.6.4 Integration on Launch Day

A detailed check list of the processes and procedures involved with payload integration can be found in section 4.6 *Launch Operations Procedures* of this report.

### 5.3.2 Monopropellant Thruster Science

---

#### 5.3.2.1 Monopropellant Thruster Objectives

---

The objectives of the hydrogen peroxide thruster are as follows:

- 1) To generate 20N of thrust for a duration of 5 seconds
- 2) To collect data on thruster performance at altitude for the full firing duration
- 3) To have full decomposition of the hydrogen peroxide in the catalyst bed

### 5.3.2.2 Monopropellant Thruster Success Criteria

---

The primary objective of the Monopropellant Thruster is to fully verify the design of the thruster and assure that the behavior of the system matches the expected behavior. Specifically, each thruster should produce 20N of thrust for 5s while consuming less than 100 mL of fuel.

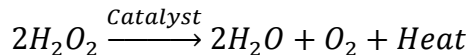
While this is not a small project on its own, the true success of this project will come in future years, as the experience collected from this project will allow the team to push forward on to more advanced research in the future. This will allow the same incremental progress that has led to our current slosh abatement project to produce a much enhanced thruster in the future.

### 5.3.2.3 Monopropellant Thruster Experimental Logic, Approach, and Method of Investigation

---

#### 5.3.2.3.1 Decomposition and Fuel

The fuel being used to power the thrusters is a solution of 70% hydrogen peroxide. In the presence of an iridium catalyst hydrogen peroxide decomposes into steam and oxygen through the following relationship:



#### 5.3.2.3.2 Decomposition Chamber Science

The decomposition chamber, or catalyst bed, is filled with small iridium coated pellets. These pellets act as a catalyst that stimulates the hydrogen peroxide decomposition to occur at an increased rate. Iridium has the advantage over other catalysts in that it does not need to warm up first and can therefore catalyze decomposition at room temperature.

#### 5.3.2.3.3 Monopropellant Thruster Drag

The thrusters will be positioned within the body of the rocket and therefore create no additional drag with its presence. There will be holes cut into the boat tail of the rocket to allow thrust to escape but the effect of these as an aerodynamic protuberance is expected to be negligible. This will be confirmed through CFD analysis later in the design process.

The boat tail will require dimensional adjustments to the tail cone in order to accommodate thruster relocation. Aerodynamic analysis of structural protuberances will focus on the modification of the boat tail geometries and its effect on the coefficient of drag as a function of maximum tail cone diameter normalized by rocket body diameter ( $C_D = f(D_2/D_1)$ ) as well as the effect of changing maximum tail cone diameter on the center of pressure location and its resulting influence on the static stability margin. Initial simulations with Rocksim suggest that the drag coefficient will remain relatively unchanged until a  $D_2/D_1$  ratio of 1.4 (maximum tail cone diameter 7.7") at which point the drag coefficient will begin to see a sharp increase. An expected trend plot displaying this behavior can be seen below. The second expected trend graph shows the ratios of modified tail cone static stability margin to a reference static stability margin (where the maximum diameter is 5.5"). A small and constant increase is expected in the static stability margin ratios. Five points, ranging from ratios of 1 to 1.4, will be used to form geometries that will subsequently be used in aerodynamic analysis simulations.

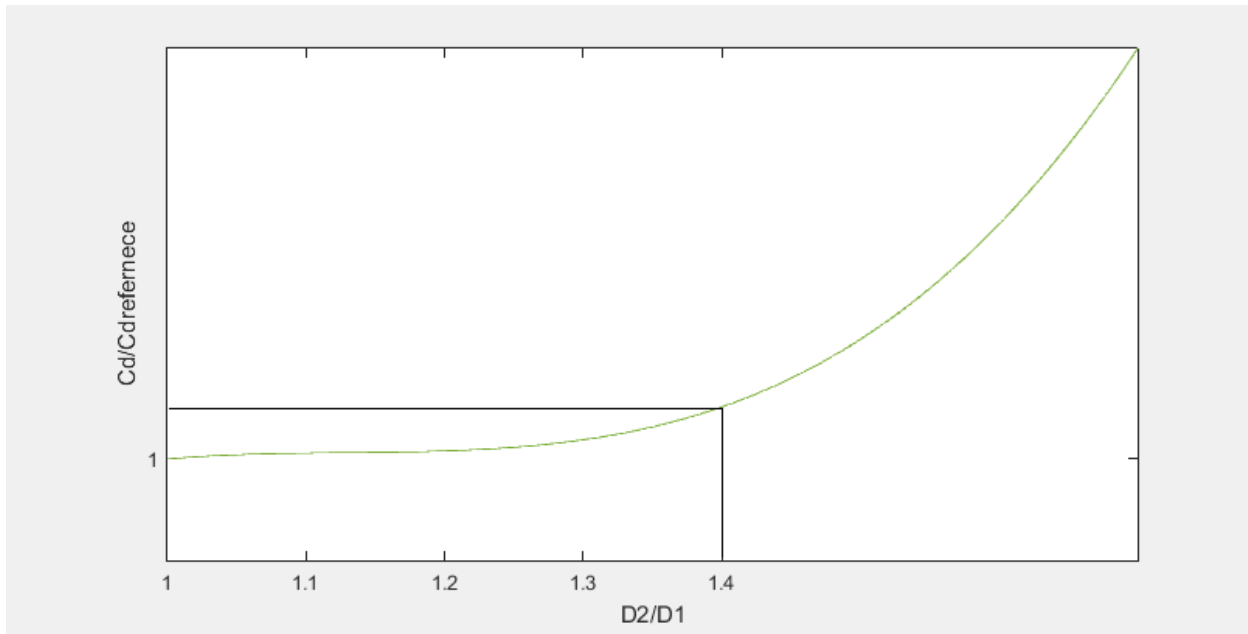


**Figure 106:** expected trends plotting new coefficient of drag to reference coefficient of drag ratio for multiple values of  $D_2/D_1$

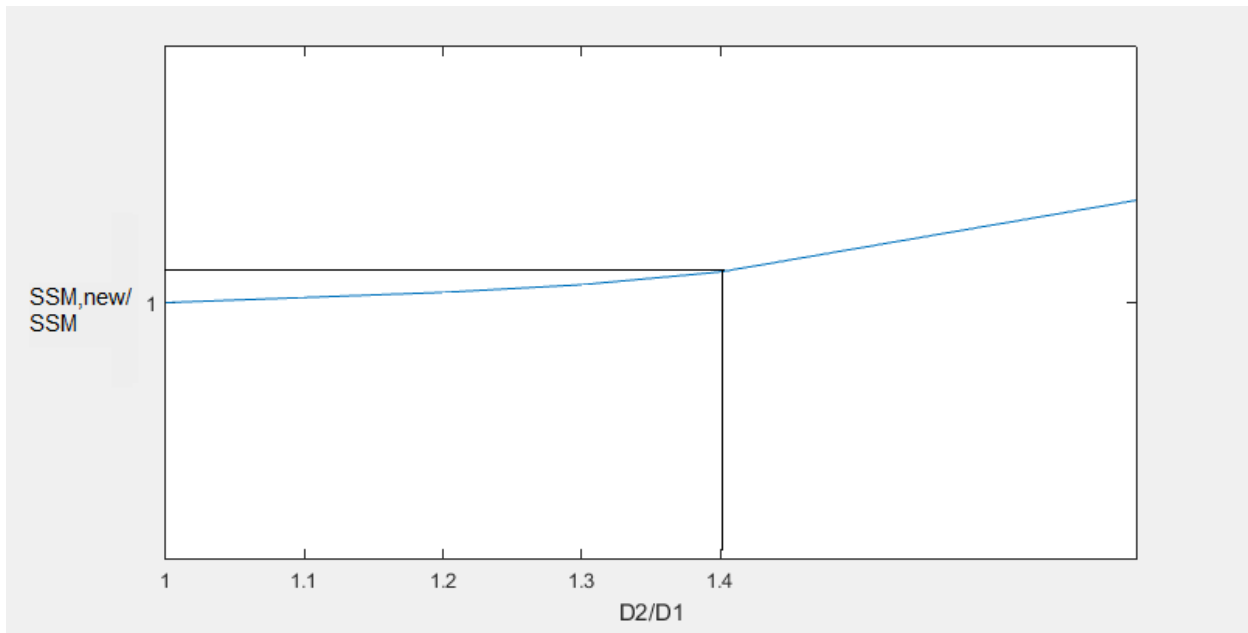


**Figure 107:** expected trends plotting new static stability margin to reference static stability margin for multiple values of  $D_2/D_1$

The preliminary analysis was done using ANSYS Fluent. The initial study was to establish a baseline drag coefficient for the unmodified subscale rocket. The geometry of the rocket and fluid domain used in the first simulation can be seen in figure 108.

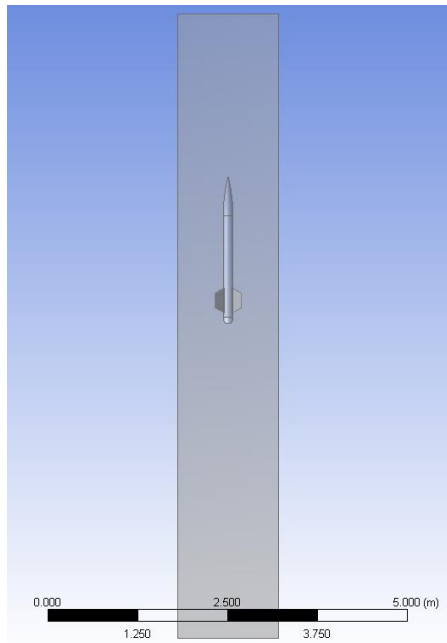


**Figure 108: Geometry for subscale rocket's initial drag simulations**

Symmetry conditions were applied across the rocket in order to decrease computational time. The dimensions of the fluid domain are approximately four times the rocket length in height and ten times the rocket diameter in width. The size and shape of the fluid domain took into account wake formation being located near the tail of the rocket and the selected fluid domain length allowed the simulation to converge. The top of the fluid domain was constrained as a velocity inlet normal to the plane with a fluid flow speed of 100m/s. A speed of 100m/s (Mach 0.29) as opposed to 200m/s (Mach 0.58) was used in order to maintain the validity of incompressible flow assumptions. The mesh (figure 109a) was set to a medium fineness and had an inflation mesh of a maximum of ten layers incorporated along the rocket surfaces to better model the boundary layer (figure 109b), raising the number of elements from 96,099 to 117,852. The slight increase in computational time was justified by the increase in accuracy, especially as boundary layer effects largely determine the resulting drag and pressure. The coefficient of drag was calculated at approximately 0.29. Velocity and pressure plots are in Figure 110.

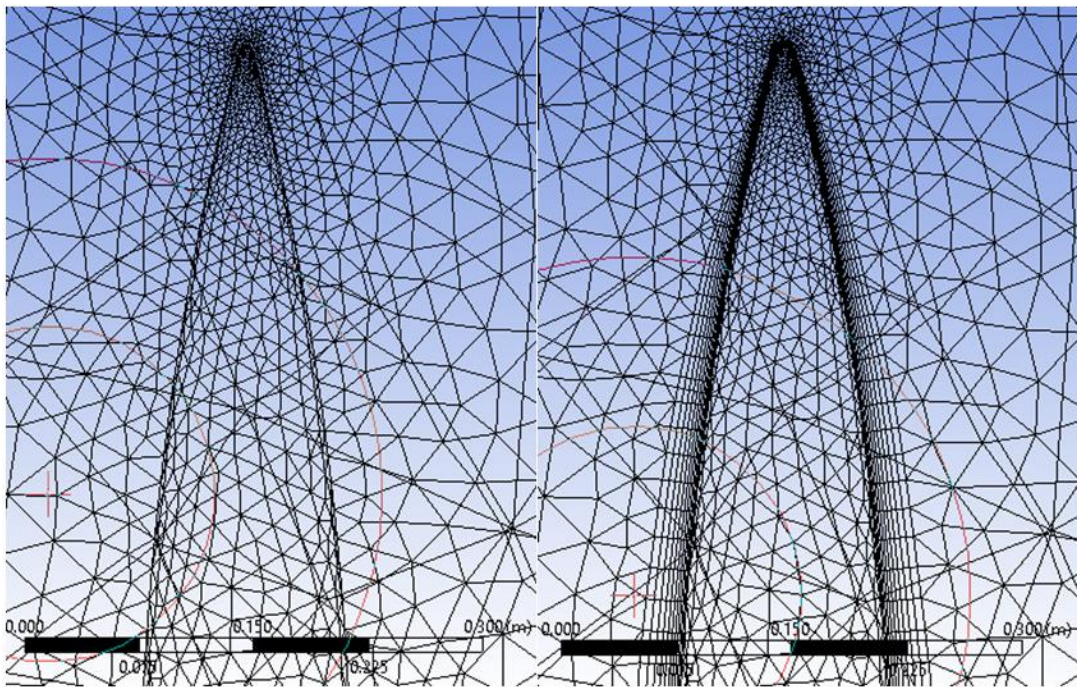


**Figure 109: Magnified view of the nosecone mesh with a) a mesh of medium fineness and b) a mesh of medium fineness with added inflation's effect on the original mesh**

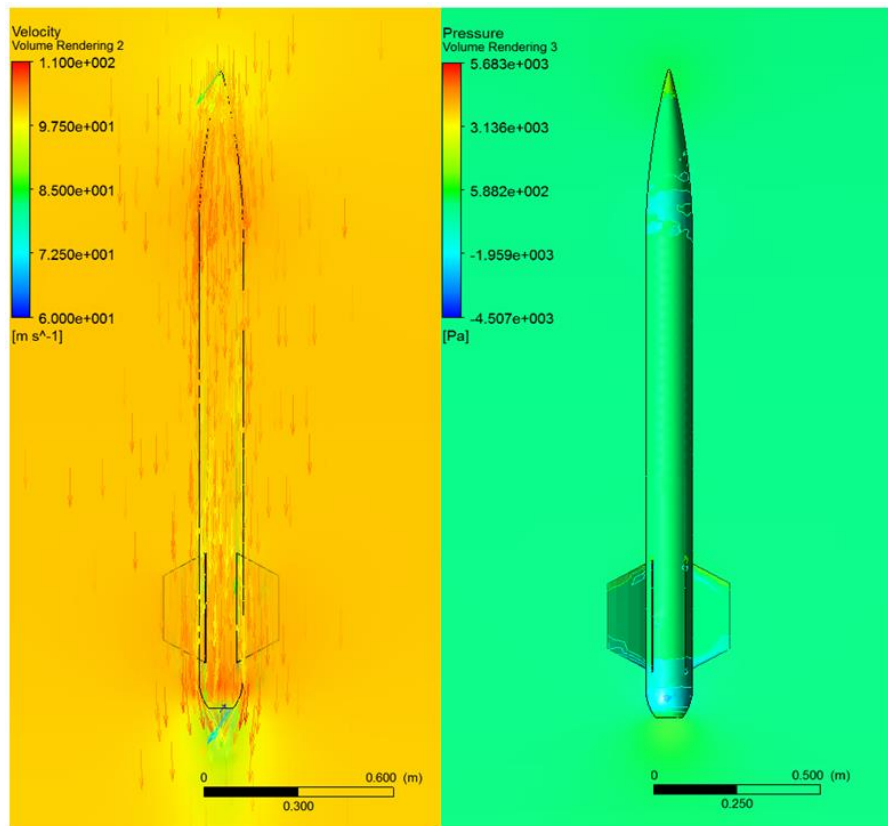


**Figure 110: Axial flow of 100m/s a) velocity volume plot with velocity vectors b) pressure volume plot with pressure surface on the rocket**

The geometry for the initial center of pressure simulation for the subscale rocket (figure 111) had the height of the domain decreased and the distance between the rocket surface and the right side (pressure outlet constraint) increased. The change in fluid domain width was necessary for convergence due to wake formation occurring right of the rocket. A similar mesh (medium fineness with identical inflation settings at the rocket surface) was used. The resulting velocity and pressure plots are in Figure 112. Using the drag force perpendicular to the rocket and the moment about the origin, the location of the center of pressure was found to be 57.7 inches from the nosecone (close to the RockSim data of 56.8 inches). Figure 113 shows the location through which the center of pressure will act.

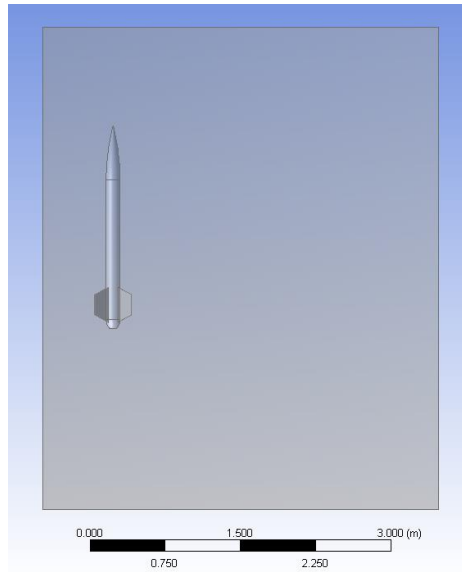


**Figure 111:** Geometry for initial simulation to establish center of pressure for subscale rocket

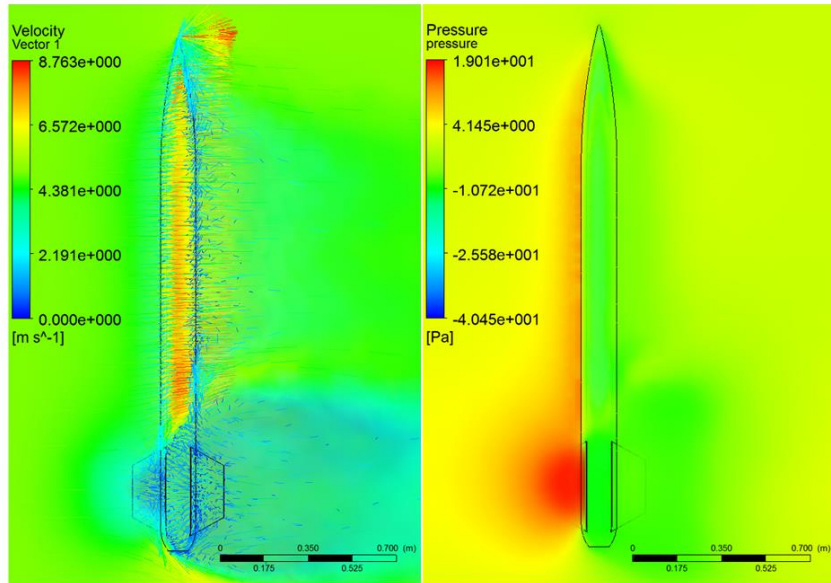


**Figure 112:** Flow visualization for the center of pressure a) velocity volume plot with velocity vectors b) pressure volume plot

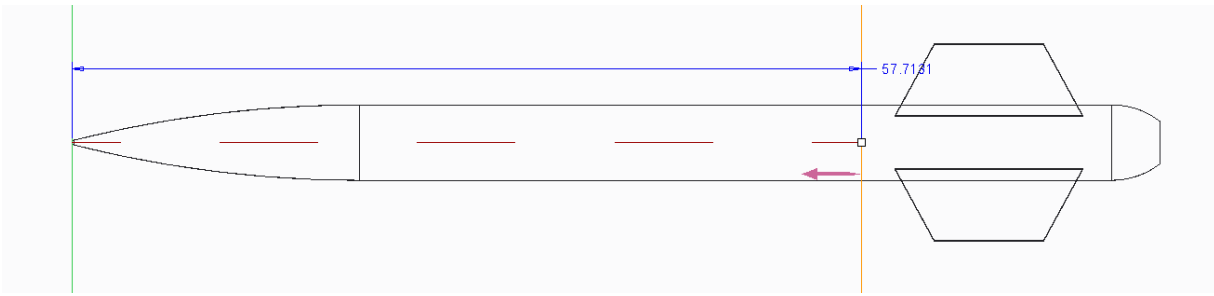


Figure 113: Center of pressure relative to the tip of the nosecone

#### 5.3.2.3.4 Monopropellant Thrust Generation

The hydrogen peroxide decomposition outlined above shows an increase in the number of molecules present after decomposition. It also shows a release of heat which increases the temperature of the decomposed fluid. Both the increase in the number of molecules and the temperature of those molecules lead to a rise in pressure which flows out the nozzle into the ambient air. This flow of fluid through the nozzle is what generates thrust.

#### 5.3.2.4 Test, Measurement, Variables, and Controls

---

The monopropellant thrusters will be tested on the ground before flight using a custom designed and constructed test stand. It will consist of a fuel system similar to the actual system to be flown, including a solenoid, pressure reservoir, fuel tank and prototype thruster.

Three key pieces of data will be recorded: thrust force generated temperature of the thrust products, and upstream pressure of the fuel. These pieces of data will be used to analyze the operating conditions of the thruster and to potentially optimize the design.

Thrust force will be measured with a strain gauge mounted to the connecting pylon between the thruster and the test stand. A calibration curve will be developed for this strain gauge using known forces; this curve will be used to process sensor outputs. Fuel pressure will be monitored with a commercially purchased pressure sensor attached to the fuel supply line. Temperature will be monitored with a thermocouple attached to the nozzle surface.

Once the testing system is verified and preliminary data is collected, it is possible that a small change to fuel pressure or thruster geometry will need to be effected to optimize thruster performance. Thruster testing will also verify the safety and reliability of the thruster through repeated firings from a stable position. Since launch forces on the thruster are expected to be of a similar order of magnitude to the thrust produced, repeated testing should also verify the reliability of the thruster mount. Since the originally tested prototype will not be flown, fatigue stress is not a significant concern, and a failure in ground-based testing would be safely contained. However, no failure is expected.

#### 5.3.2.5 Relevancy of Data and Analysis

---

In order to evaluate the results of our design calculations, a response surface was created to illustrate how fuel flow rate and chamber operating pressure affect the total output thrust. The surface reflects the theoretical thrust delivered by the thruster assuming complete, adiabatic

decomposition of the monopropellant. These assumptions establish a theoretical maximum by which to evaluate the performance of our thruster. It is important to recognize that this surface reflects the maximum theoretical performance of our thruster, and that the thruster will deliver a lower output thrust as our assumptions of adiabatic, isentropic flow become less valid.

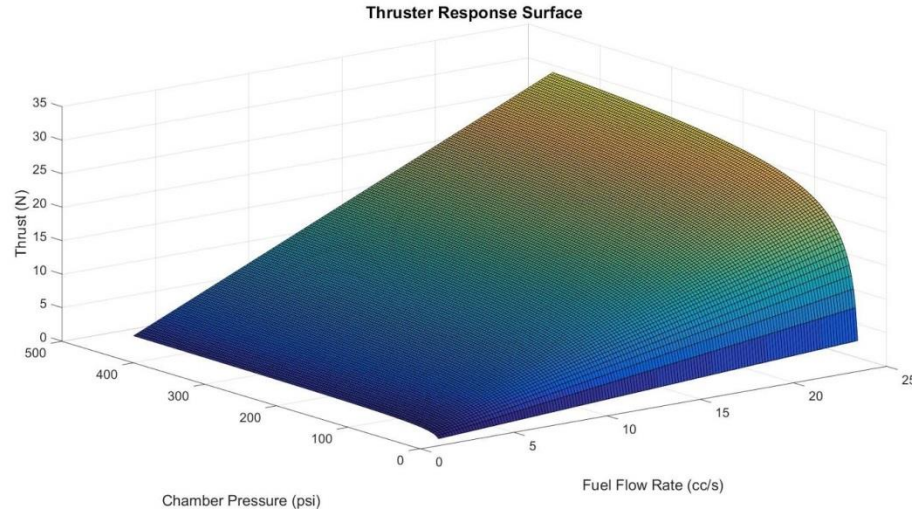


**Figure 114: Thruster response surface plot**

For a desired thrust of 20 N, multiple combinations of chamber pressure and fuel flow rate can be used, as indicated by the 20N contour which is labeled in the bottom right. The following plot shows contours of constant thrust. These results were generated from the above response surface, with grid lines hidden and contours applied. This view allows for visualization of the output thrust by means of the color code applied to the surface.

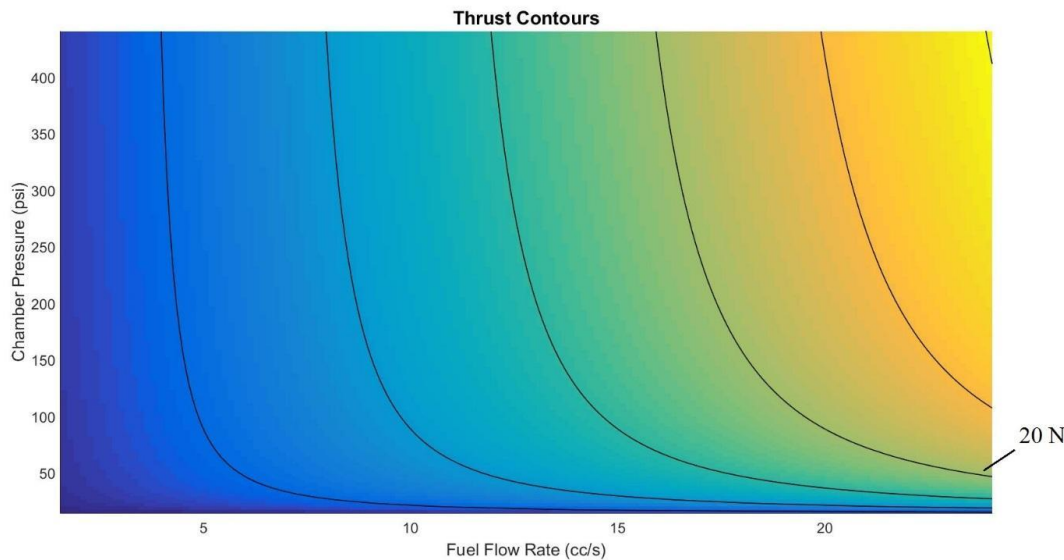


**Figure 115: Thrust contours plot**

From our simulation results it can be concluded that a range of operating pressures and fuel flow rates may be used to realize a given thrust. It is notable that fuel flow rate essentially behaves as a linear scaling factor for thrust. Varying chamber pressure, on the other hand, results in a very non-linear variation in thrust. Furthermore, chamber pressure influences the chemical decomposition of the monopropellant fuel, which will further effect the output thrust in a complex and unpredictable manner. For this reason, fuel flow rate will be the design parameter that is varied to produce a given output thrust. Chamber pressure will be determined based on both propulsive efficiency, and the completeness of monopropellant decomposition in the catalyst bed.

#### **5.3.2.5.1    Ground Based Testing**

A ground based testing system for the thruster is currently under construction. This system emulates the fuel delivery system expected to be built into the rocket, supports the thruster in a safe firing position, and connects key instrumentation with the thruster. A modular design built around extruded aluminum rods allows for easy reconfiguration in case of a design change, and dimensions are specifically set to interface with building facilities for thrust system testing while shielding the operator from the thruster with a Lexan plate.

#### **5.3.2.5.2    Test Launches**

There will be two test launches of the rocket before the actual competition launch, a subscale launch and a full scale launch. The full scale launch will feature the thrusters and allow them to be tested at altitude in an active rocket environment.

### **5.3.3    Structural Analysis Science**

---

#### **5.3.3.1    Payload Objectives**

---

The objectives for the structural analysis payload are threefold and sequential:

- 1.) Develop a finite element model that captures the material behavior of the custom built carbon fiber-reinforced polymer vehicle structure.
- 2.) Dynamic sensing of lateral and axial acceleration during flight and during ground-based tap tests will be used to validate mass and stiffness properties of a finite element model.
- 3.) A validated finite element model will be used to analyze stresses that occur during launch.

The first objective will be primarily achieved with the two initial test launches. Flight and tap-test data processing, to determine experimental modal properties, and model correlation will be carried out after both the subscale launch and the first full-scale launch since the modal properties of the two vehicles will be substantially different. The test launches will be in November 2015 and February 2016. Thus the second objective of calculating stresses during launch will be carried out for the final vehicle and can be achieved prior to the final launch in April 2016.

Finite element modeling is a method potentially fraught with error. The purpose of the first objective is to minimize the error in a model that can be used for the second objective. Error will be minimized not only through this experimental corroboration, but also through the use of two

different finite element software packages and two different modeling schema. Models will be constructed in both Ansys and Abaqus. Both models will include the anisotropic nature of the laid-up carbon fiber vehicle structure. The model in Ansys will utilize solid continuum elements, while the model in Abaqus will simulate the exterior of the vehicle with shell elements and some interior structure with solid elements coupled to the exterior shell.

### 5.3.3.2 Payload Success Criteria

---

The success of this payload is based on the ability to effectively and convincingly validate a finite element model. Several success criteria can be established to guide the quality of correlation of modal properties between a finite element model and experimental data.

Before tuning the finite element model to match dominant values and characteristics in the experimental data, the experimental modal properties need to be checked for quality. A long established industry method for this is one of several orthogonality check schemes. The general principle is that mode shapes represent linearly independent eigenvectors to the problem  $([M] - \lambda[K]) = \lambda\hat{u}$ . As linearly independent vectors, they are orthogonal, so that a matrix  $[U]$  whose columns are the mode shapes should satisfy  $U^T U = I$ . This process, referred to as a Modal Assurance Criteria (MAC), is deemed successful if the off-diagonal terms of the product of  $U$  and its transpose are less than ten percent of the diagonal values.

Once the quality of the experimental modal properties is assessed, the finite element model can be refined through iterative geometry or material changes to capture the natural frequencies and mode shapes determined experimentally. The percent error between the modal frequencies can be checked against an acceptable threshold. This threshold must be large enough to account for both experimental error and the difference between the free-vibration natural frequencies determined in a finite element formulation and the damped natural frequencies measured in tap tests or in flight. Similarly, the experimentally determined mode shapes can be compared qualitatively to the finite element solution to ensure that general shape and in-phase, out-of-phase points are consistent.

### 5.3.3.3 Experimental Logic, Approach, and Method of Investigation

---

The process and method behind the structural analysis payload is grounded in minimizing error through parallel paths. Two finite element models will be used to reduce error and provide two competing solutions. Two experimental surveys will be conducted, one being a traditional tap-test and one being the flight environment.

The tap test can be carefully controlled and repeated to ensure quality data is collected. The tap test will be conducted by hanging the vehicle from two points, to simulate the free-free boundary conditions of flight. An impact hammer, instrumented with a load cell, will be used to transversely excite the vehicle. Accelerometers will capture the transient, impulse response of the vehicle. Modal frequencies can be determined through one of many frequency decomposition techniques. A power spectral density approach based on time window averaging and multiple trial averaging is likely to prove the most effective, though Shock Response Spectrum (SRS) analytical techniques will also be explored. Similarly, mode shapes will be determined through averaging the phase component over repeated trials of experimental relative Frequency Response Functions (FRFs) between accelerometers.

Transverse vibrations will occur during flight due to two effects. The first is simply the coupled three dimensional behavior of the vehicle. As the thrust axially excites the vehicle, structural members that connect the skin of the rocket to the motor will induce lateral accelerations. The second is aerodynamic forces that will transversely excite the rocket body. External pressure fluctuations will buffet the vehicle over a broad range of frequencies, causing the rocket to vibrate at modal frequencies. These natural frequencies can be determined from the on-board accelerometer time histories and compared with tap-test and finite element predictions.

#### 5.3.3.4 Test, Measurement, Variables, and Controls

---

The structural analysis payload consists of three unique methods of measuring or calculating variables of interest – modal frequencies and mode shapes. Despite the difficulties that occur in experimental modal analysis, the tap test results will likely represent the control of the data set, as finite element solutions will be tuned to these results and flight data may have additional effects that obfuscate determining modal parameters. The measurements for the experimental work will be taken with the system described in 5.1.3.2. This sensor package will provide high bandwidth, forced response and impulse response acceleration time histories, from which frequencies of vibration can be determined as was described in Section 5.3.3.3.

#### 5.3.3.5 Relevancy of Data and Analysis

---

Reaching the third objective listed in Section 5.3.3.1, makes the data collected and analysis conducted immediately relevant to the structural integrity of the vehicle. The region of particular interest, the custom mold formed tail section, will be a focus point for stress analyses.

This analysis is also relevant to the inverse problem that is present in flight: modeling forcing functions. When the system is characterized through tap test experiments, the system parameters can be employed to inversely calculate the nature of the forcing functions, such as the broadband pressure fluctuations that originate from aerodynamic buffet.

#### 5.3.3.6 Preliminary Experiment Procedures

---

##### 5.3.3.6.1 Finite Element Modeling Simulation

Thus far, work has been done to achieve the first of the three objectives. Two initial finite element models have been developed, with the two unique software and schemes of formulation as described in Section 5.3.3.1. Work is undergoing to bring these two methods into agreement as the subscale vehicle itself is nearing completion. Once the subscale rocket is constructed and flown the secondary objective can be started.

These finite element models both consider the anisotropic nature of the carbon-fiber reinforced polymer. The geometry differs between the two, as concessions are made to simulate interior structure based on the difference of solid versus shell simulation of the rocket skin. Current results for the first transverse bending mode are shown for the Abaqus and Ansys model below in Figures 116 and 117. The respective frequencies of vibration of 257.4 Hz and 153.4 Hz constitute a 60% discrepancy. Both models have potential improvement, especially in the area of refining the mass distribution in the rocket.

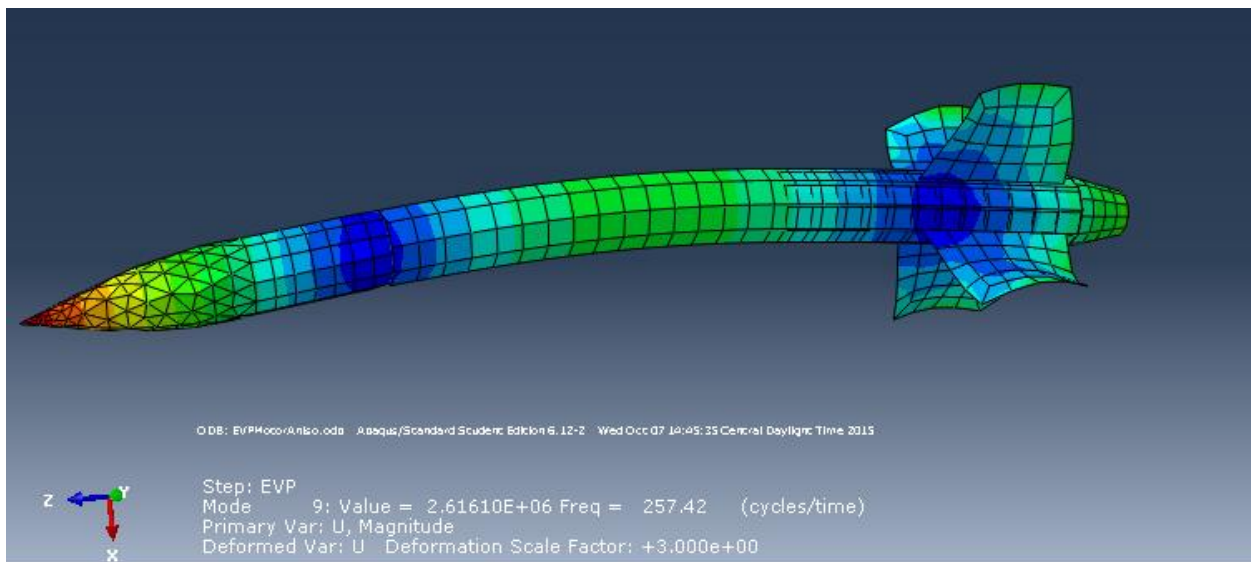


**Figure 116: Abaqus 257.42 Hz Bending Mode**

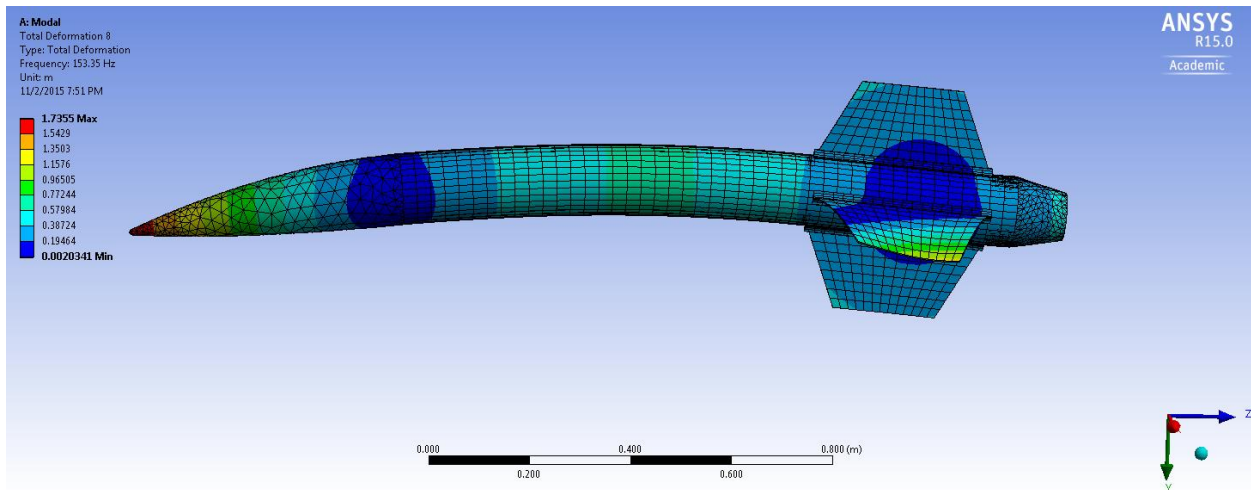


**Figure 117: Ansys 153.35 Hz Bending Mode**

Transient analyses have also been set up, though results are expected to change as eigen-properties are tuned to match. These transient analyses involve applying the motor thrust curve in tabular form to the base of the simulated motor tube and reporting the acceleration time history at a node on the rocket body. This is an excellent check, before experimental data is collected, in ensuring that the acceleration of the vehicle is close to the initial acceleration anticipated at launch.

#### 5.3.3.6.2 Test Launches

Launches in November and February will be instrumented with dynamic accelerometer sensing suites for collection of critical flight data to the experiment. The November launch will carry 3 3-axis accelerometers. The February launch will boast an upgraded suite with the lessons learned from the subscale sensing experience.

## 5.4 Payload Safety and Environment

---

### 5.4.1 Safety Officer

---

The Student Safety Officer is Ben Gasser, and the team Safety Mentor for the Vanderbilt Aerospace Design Lab is Robin Midgett. As a team they will guide the team toward good practices and procedures that ensure all appropriate measures are taken to mitigate risks associated with the payload and maintain a safe working environment.

In relation to payload safety, one of the single most important considerations is the safe handling of the hydrogen peroxide fuel. The team has a Standard Operating Procedure for the safe use of hydrogen peroxide that it will consult and follow any time the fuel will be handled. In summary, the number of people exposed at any time to the HTP will be minimized, proper personal protective equipment (PPE) will be used at all times, safe handling techniques will be engaged by all individuals involved, and site cleanliness and order will be a priority to avoid accidental spilling or container contamination that could result in unintended catalyzation. Additionally, generous amounts of water will be on hand to dilute and/or wash away any accidental spills.

### 5.4.2 Preliminary Analysis of Failure Modes and Mitigations

---

The analyses of the payload sections are broken up into three sections for the monopropellant thruster, fuel delivery, and structural analysis subsystems.

#### 5.4.2.1 Risk Assessment Matrix

---

In order to fully assess the risks associated with the launch, we have developed a risk assessment matrix that categorizes and ranks all risks according to their likelihood of occurrence and severity of consequence. Likelihood of occurrence is given a rating from 1 – 5 with 1 being the least likely and 5 the most. The corresponding designations for each in order from 1 – 5 are **rare**, **unlikely**, **moderate**, **probable**, and **very likely**. The consequence is given a rating from A – E with A being the least consequence and E being the greatest. The designations for each in order from A – E are trivial, minor, moderate, high, and critical. When each scale is set up in a matrix, a combination of the two values can be very enlightening as to the relevance of the risk.

Interpreting the risk designation is also quite intuitive since low alphanumeric combinations correspond to the least worrisome risks while high alphanumeric combinations represent larger risks.

Color-coding has also been added to the matrix to designate which risks require mitigation of some sort. Risks highlighted in green are considered low risk and either require no mitigation or have no reasonable means of additional mitigation. These have either a very low risk of occurrence or the consequence of occurrence is so small that serious consideration to mitigate the risk is not necessary. Risks highlighted in yellow are considered moderate risks and should be mitigated in some way however possible, but the overall risk posed to the mission and safety of those involved has been deemed acceptable. Risks highlighted in red are more serious than those in green and can have serious consequences on the success of the mission or the safety of those involved, but the combination of their occurrence and consequence ratings places them in the middle of the matrix. This means that the risk to mission success or injury is either fairly low/unlikely or that the risk has been mitigated in some way to bring it down from the most

serious category. The most critical category is highlighted in red, signifying that these are the most hazardous risks to either mission success/personal safety or have the greatest likelihood of occurrence. These risks are deemed unacceptable and must be mitigated in some way for the rocket/payload to be safe to launch. In the tables outlining risks for the various sections/payloads of the rocket, no risk can be classified with a red rating post-mitigation.

	Consequence					
Likelihood		Trivial	Minor	Moderate	High	Critical
	Rare	A1	B1	C1	D1	E1
	Unlikely	A2	B2	C2	D2	E2
	Moderate	A3	B3	C3	D3	E3
	Probable	A4	B4	C4	D4	E4
	Very Likely	A5	B5	C5	D5	E5

Figure 118: Risk assessment matrix

The explicit meanings of each likelihood and consequence rating are outlined as follows:

### Likelihood

- Rare (1) – Chances of occurrence are almost non-existent. Mitigation need only exist for the most critical risks.
- Unlikely (2) – Chances of occurrence are very low but do exist. Mitigation should exist for high-risk consequences.
- Moderate (3) – Chances of occurrence are moderate. Mitigation should exist for all risks resulting in greater than minor consequence.
- Probable (4) – Occurrence is more likely than not. Mitigation should occur for all but the most trivial risks.
- Very Likely (5) – Occurrence is to be expected. Mitigation is required for all but the most trivial risks.

### Consequence

- Trivial (A) – Occurrence of risk results in no effect on rocket/payload performance or safety of all persons involved. No mitigation is needed.
- Minor (B) – Occurrence of risk results in minor damage that is either easily repairable or has no effect on rocket/payload performance. No risk for injury to persons involved. Mitigation should exist for the most likely risks.
- Moderate (C) – Occurrence of risks results in some damage to rocket/payload that could negatively affect performance and/or result in minor injury to persons involved. Mitigation should exist for most risks.
- High (D) – Occurrence of risk results in major damage to rocket/payload that will negatively affect performance and/or result in serious injury to persons involved. Mitigation should exist for all but the rarest risks.

- Critical (E) – Occurrence of risk results in catastrophic damage to rocket/payload that will eliminate performance capability and/or result in serious injury/death to persons involved or bystanders. Mitigation must exist where possible.

### Combined Rating

- Low (Green) – Risk falls within an acceptable range of probability and consequence. Mitigation strategies should be implemented if possible but are not mission critical.
- Moderate (Yellow) – Risk should be evaluated for potential mitigation strategies.
- Critical (Red) – Risk has an unacceptable level of likelihood and consequence. Mission should not proceed until viable mitigation strategies are created and implemented.

#### 5.4.2.2 Monopropellant Thruster Safety and Failure Analysis

---

All use of hydrogen peroxide will follow the established protocols. See 5.4.2.3 directly below for elaboration. The thruster system is specifically designed to completely convert all HTP to steam and oxygen, resulting in no toxic emissions. The very nature of the thruster requires that it emit hot vapors and operates at pressure, but this is mitigated by the design and implementation of the thruster.

**Table 23: Monopropellant Thruster Risk and Mitigation Table**

Monopropellant Thruster Risk and Mitigation				
Risk	Consequence	Risk Rating	Mitigation	Post-Mitigation Risk Rating
Thruster disconnect from rocket	Catastrophic failure of thruster	E2	Ground-based testing	E1
Thruster rupture	Catastrophic failure of thruster	E1	Built with factor of safety of 4; ground-based testing	E1
Thruster leaking during flight	Catastrophic failure of thruster	D2	Ground-based testing	D1
Screen Breaks	Iridium pellets released from rockets	B3	Ground-based testing with frequent inspection of screen to assess wear	B1

Overheats	Damages other rocket components and thruster instrumentation	C3	Ground-based testing	C1
Incomplete disassociation of Hydrogen Peroxide inside thruster	Emissions of dangerous unreacted fuel	D3	Ground based testing, rigorous design and analysis	C1
Clogging of catalytic bed or other component	Catastrophic failure of thruster	E1	Ground-based testing with frequent inspection of catalyst, flow testing with water	E1
Unforeseen internal gas dynamics	Mild inconvenience to catastrophic failure of thruster	A4	Analysis of ground-based testing data	A2

#### 5.4.2.3 Fuel Delivery System Safety and Failure Analysis

Any and all use of hydrogen peroxide fuel will be conducted under the strict supervision of the safety officer and all of the guidelines from the material safety and data sheet will be met. These guidelines are posted on the Vanderbilt Aerospace Design Lab website. The main points of safety that should be met when dealing with the fuels are as follows: wear safety goggles and protective clothing, have fire-fighting material on hand, keep away from heat sources, and avoid inhalation, ingestion, and skin contact.

Table 24: Fuel Delivery System Risk and Mitigation Table

Fuel Delivery System Risk and Mitigation				
Risk	Overall Effect	Risk Rating	Mitigation Strategy	Post-Mitigation Risk Rating

Fuel Leaking During Flight	Catastrophic failure of fuel delivery system and rocket	E3	Ground based of all components	E2
Fuel Tank Rupture	Catastrophic failure of fuel delivery system and rocket	E2	Built with factor of safety of 6; ground-based testing	E1
Reaction of H <sub>2</sub> O <sub>2</sub> with a fuel delivery system component causes failure	Catastrophic failure of fuel delivery system and rocket	E1	Ground based testing of all components, extreme caution taken in handling of H <sub>2</sub> O <sub>2</sub>	E1
Reaction of H <sub>2</sub> O <sub>2</sub> with a foreign contaminant fuel delivery system component causes failure	Catastrophic failure of fuel delivery system and rocket	E3	Ground based testing, cleaning with deionized water to create standard operating procedures	E1
Fuel Line Rupture	Catastrophic failure of fuel delivery system and rocket	E2	Ground based testing	E1
Air in fuel pickup	Non-continuous thrust generation from the thruster	A3	Anti-slosh techniques employed	A1

Compressed air tank leak	Decreased fuel flow to thruster; possible loss of thrust generation; damage	D2	Ground based testing	D1
Mounting System Failure	Possible catastrophic failure of fuel delivery system and rocket	D2	High strength epoxy, fasteners, and materials used	D1
GoPro verification system malfunction	Inability to verify anti slosh system in flight	B2	Distance testing and verification of system	B1

#### 5.4.2.4 Structural Analysis Safety and Failure Analysis

The main safety hazard in the structural initiative of the VADL would be a structural failure in flight causing the rocket to deviate from planned navigation. This risk is mitigated by the very nature of the protocol to reduce risk to the vehicle and mission with modeling of the rocket and stresses. Other failure modes may lead to loss of payload mission success and our outlined in the table below.

Table 25: Structural Analysis Risk and Mitigation Table

Risk	Overall Effect	Risk Rating	Mitigation Strategy	Post-Mitigation Risk Rating
Accelerometer loss of power	Loss of flight data and risk to primary payload success criteria	C3	Ground testing of redundant soldered power supply to shock and vibration	C2

Accelerometer/DAQ data collection failure	Loss of flight data and risk to primary payload success criteria	C3	Failsafe programming and extensive hardware and software testing	C2
Finite Element Model vastly differs from vehicle test/flight data	Failure of primary payload mission success criteria	B5	Continuous refinement of finite element model with iterative design process to converge on accurate model	B2
FEM predicted stresses exceed ultimate material strengths	Potential in flight structural failure	D1	Custom addition of material in areas of high stress and vehicle redesign to conservative safety factors	B1
Accelerometers measure local “mounting” mode as opposed to vehicle mode	Failure to detect usable structural data from test launch	B4	Mount accelerometers with epoxy directly to vehicle structure	B1

### **5.4.3 Personal Hazards and Concerns**

---

General rocket personal hazards and concerns are addressed in section 4.7.3 *Personal Hazards and Concerns* relating to the general flight of the rocket.

#### **5.4.3.1 Ground-based Payload Testing and Safety**

---

The payload testing process will be initiated after a safety review by faculty advisor Dr. Anilkumar. The following are the safety recommendations that have been incorporated into the test facility:

- Default-closed solenoid valve.
- Required factor of safety of at least 4, generally over 6
- Check valve to prevent backflow
- Relief valve to prevent over pressure
- Manual vent valve to allow depressurization of fuel tank in a safe manner
- Lexan shield placed between user and thruster

#### **5.4.3.2 Ground-based Testing Protocol**

---

Ground based testing will only occur with director mentor oversight following a rigorous review of the system and all applicable safety protocols. The system will initially be tested using water (preferably deionized water) to ensure it functions properly. Only after the system has been fully validated will actual fuel be used to test the thruster. This will be done in accordance with the already established procedures and protocols for fuel handling, and will only be done by properly qualified persons. Any venting or thrust produced from the system will be directed into the facility's system for safely venting out of the laboratory.

#### **5.4.4 Environmental Concerns**

---

All environmental concerns are addressed in section 4.7.5 *Environmental Concerns* relating to the general flight of the rocket.

# 6 Activity Plan

---

## 6.1 Budget Plan

---

The funding this year is \$16,000. This revenue comes from the NASA SL 2014-2015 Award of \$5,000, the Boeing sponsorship of \$2,500, and the Vanderbilt University School of Engineering sponsorship for the remaining requirement. Throughout the course of the year, the team will attempt to gain sponsorship from Space-X, Denso, Blue Origin, and Northrop Grumman. If sponsorship from any of these sources is acquired, the VUSE sponsorship will decrease appropriately. Below are tables and pie charts detailing this year's purchases, prior years' purchases that will be reused, and anticipated expenditures. A detailed list of this year's purchases is maintained by the team. Purchases go through Robin Midgett. A flow chart displaying material acquisition plan is shown below. Taxes and shipping fees are accounted for by inflating the expected costs while still leaving a large contingency fund. Projected costs were estimated using prior years or online catalogs when available.

For material acquisitions, there is a three step process. Orders are written in an Excel spreadsheet and sent to Robin Midgett with the appropriate details (part numbers, names, and vendor). Robin processes the order and locates the requested parts through online vendors. If the vendor is a preferred supplier to the university, Robin will order using his university card. If the vendor is not a preferred supplier, then Robin will place the order through the Department of Mechanical Engineering's Procurement Office.

A color coding system is used in the table to designate the intended purpose of each item. Orange is shop equipment, green is rocket hardware, light blue is slosh abatement, red is monopropellant thruster, purple is structural analysis, white is taxes and/or shipping, dark blue is outreach, and pink is launches and competition.

**Table 26: Itemized list of expenditures**

Company	Item	Part cost	Quantity	Total cost	Order cost	
Grainger	Nozzle, Mixing, Pk10	\$14.85	2	\$29.70		
	Applicator,Dual Cartridge	\$49.28	1	\$49.28		
	Adhesive,Epoxy,Hysol	\$20.89	6	\$125.34	\$204.32	
AllRed	DragonPlate Solid CF Laminate	\$587.00	1	\$587.00		
	Shipping	\$29.95	1	\$29.95	\$616.95	
ANS Gear	Ninja Pro V2 SLP Series Tank Regulator - 4500 PSI	\$69.95	1	\$69.95		

	Shipping	\$4.04	1	\$4.04	\$73.99	
PerfectFliteDirect	StratoLoggerCF Altimeter (SLCFA)	\$51.46	2	\$102.92		
	Shipping	\$7.15	1	\$7.15	\$110.07	
Amazon	SE 9NRC10 Set of 10	\$15.30	1	\$15.30		
	Tax	\$1.41	1	\$1.41	\$16.71	
	DeWALT DCD760KLR 18V 1/2" (13mm) Cordless Compact Lithium-Ion Drill/Driver Kit (Reconditioned)	\$157.39	2	\$314.78	\$314.78	
Fibre Glast	3K, 2 x 2 Twill Weave Carbon Fiber Fabric - 5 yd Roll	\$249.95	1	\$249.95	\$887.35	
	Breather and Bleeder - 4 oz - 5 yd Roll	\$24.95	1	\$24.95		
	Chavant Le Beau Touché Clay - 2 lb. Block	\$11.95	3	\$35.85		
	Gray Sealant Tape - Single Roll	\$7.95	3	\$23.85		
	Low Temperature Release Film - 5 yd Package	\$29.95	1	\$29.95		
	Orange Tooling Gel Coat - Gallon w/ hardener	\$131.95	1	\$131.95		
	Perma-Grit Rotary Attachments - 1-1/4" Cutting Wheel	\$15.95	1	\$15.95		
	Perma-Grit Rotary Attachments - 3/4" Cutting Wheel	\$14.95	1	\$14.95		
	Polyester Molding Resin - Gallon w/ hardener	\$51.15	1	\$51.15		
	Stretchlon® 200 Bagging Film - 5 yd Roll	\$19.95	1	\$19.95		
	System 2000 Epoxy Resin - 120 Minute Pot Life - Quart	\$44.95	1	\$44.95		
	System 2000 Epoxy Resin - Gallon (8lbs)	\$104.95	1	\$104.95		

	Vacuum Connector - Each	\$4.75	4	\$19.00		
	Shipping	\$119.95	1	\$119.95		
Featherweight Altimeters	Screw switch	\$5.00	5	\$25.00	\$60.00	
	Featherweight Magnetic Switch (Small)	\$25.00	1	\$25.00		
		\$10.00	1	\$10.00		
	Shipping and handling					
Lowes	1-in x 10-ft 450-PSI Schedule 40 PVC Pipe	\$4.43	1	\$4.43	\$107.71	
	3M 10-Pack Sanding and Fiberglass Respirators	\$19.89	2	\$39.78		
	Jasco Green Muriatic Acid	\$7.68	1	\$7.68		
	3M Sanding and Fiberglass Respirator	\$3.97	2	\$7.94		
	M Large Neoprene Cleaning Gloves	\$7.98	2	\$15.96		
	GORILLA TAPE 1.88-in x 105-ft Black Duct Tape	\$8.98	2	\$17.96		
	3M 1.88-in x 165-ft Black Duct Tape	\$6.98	2	\$13.96		
GoPro	SanDisk Extreme® 32GB microSDHC™	\$34.99	1	\$34.99	\$256.72	
	GoPro Hero+	\$199.99	1	\$199.99		
	Tax	\$21.74	1	\$21.74		
PerfectFliteDirect	Mounting hardware	\$1.49	10	\$14.90	\$22.05	
	Shipping	\$7.15	1	\$7.15		
Chris' Rocket Supplies	Solid rocket motors	\$157.95	3	\$473.85	\$518.07	
	Shipping	\$44.22	1	\$44.22		
Carolina Composite Rocketry	5.5" x 48" Carbon Fiber Airframe	\$350.00	1	\$350.00	\$1,087.00	
	5.5" x 45" Carbon Fiber Coupler	\$337.50	1	\$337.50		
	54mm x 26" Carbon Fiber Motor Tube	\$337.50	1	\$337.50		
	Slot airframe per dwg	\$7.00	1	\$7.00		

	Shipping	\$55.00	1	\$55.00		
Fruity Chutes	24" elliptical parachute	\$60.00	1	\$60.00		
	18" nomex blanket	\$48.00	1	\$48.00		
	Shipping insurance	\$1.50	1	\$1.50		
	Shipping	\$20.28	1	\$20.28		
McMaster-Carr	Stainless Steel Pipe Fitting (1/8 to 1/4)	\$12.43	4	\$49.72	\$1,023.96	
	Stainless Steel Pipe Fitting (1/8 to 1/2)	\$25.21	1	\$25.21		
	Aluminum Tubing 1/4" OD, .12" ID	\$16.60	1	\$16.60		
	Spring-Loaded Ball Fastener for Aluminum T-Slotted Extrusion M5 Thread Size	\$1.33	8	\$10.64		
	Compact End-Feed Fastener for Aluminum T-Slotted Extrusion M5 Thread Size	\$1.99	2	\$3.98		
	Bracket, Single Profile Aluminum T-Slotted Framing Extrusion 3/4" Long for 20mm	\$5.82	4	\$23.28		
	Plate, Single Profile Aluminum T-Slotted Framing Extrusion 1-1/2" Long for 20mm	\$6.87	2	\$13.74		
	Angle Mount Caster 2" x 7/8" Rubber, 75 lb	\$14.12	4	\$56.48		
	Tubing 6' of 1/4" OD 1/8"ID Al 6061	\$16.60	1	\$16.60		
	Connector (1/4" Yor Lok to 1/4" Yor Lok)	\$13.02	1	\$13.02		
	Connector (1/4" Yor Lok to 1/4" Male NPT)	\$8.36	6	\$50.16		
	Check Valve (Inline, 1 psi cracking pressure, 3 kips max)	\$57.65	1	\$57.65		
	Ball valve (stainless Yor lok 1,000 psi max)	\$60.92	1	\$60.92		

	Stainless steel relief valve	\$159.38	1	\$159.38	
	Relief valve Adjustable 316 SS	\$291.58	1	\$291.58	
	Pressure Transducer	\$175.00	1	\$175.00	
	High-Speed Steel Metric Size Chucking Reamer 3mm/.1181" Dia, 7/8" Flute Lg, .1120" Shank Dia	\$13.44	2	\$26.88	\$453.47
	Tapered High-Speed Steel End Mill 10 Deg Taper, 3/32" Tip Dia, 1/2" Length of Cut	\$20.58	2	\$41.16	
	High Speed Steel Six-Flute Countersink 60 Degree Angle, 5/8" Body Dia, 3/8" Shank Dia	\$19.61	1	\$19.61	
	High Speed Steel Six-Flute Countersink 60 Degree Angle, 1/2" Body Dia, 3/8" Shank Dia	\$13.44	1	\$13.44	
	Countersink 3 Flute, 60 Deg Angle, 1/2" Body Dia, 1/4" Shank Dia	\$12.72	1	\$12.72	
	Type 316 SS Socket Head Cap Screw 4-40 Thread, 3/8" Length, Packs of 50	\$6.74	1	\$6.74	
	Type 316 SS Socket Head Cap Screw 4-40 Thread, 3/4" Length, Packs of 25	\$8.05	1	\$8.05	
	Type 316 SS Socket Head Cap Screw 8-32 Thread, 3/4" Length, Packs of 25	\$5.60	2	\$11.20	
	Type 316 SS Socket Head Cap Screw 8-32 Thread, 1" Length, Packs of 25	\$4.00	2	\$8.00	
	Type 316 SS Socket Head Cap Screw 8-32 Thread, 1-1/2" Long, Fully Threaded, Packs of	\$4.73	2	\$9.46	

	10				
Type 316 SS Socket Head Cap Screw 1/4"-20 Thread, 1/2" Length, Packs of 10	\$8.02	3	\$24.06		
Type 316 SS Socket Head Cap Screw 1/4"-20 Thread, 3/4" Length, Packs of 10	\$2.97	3	\$8.91		
Type 316 SS Socket Head Cap Screw 1/4"-20 Thread, 1" Length, Packs of 10	\$3.41	3	\$10.23		
Type 316 SS Socket Head Cap Screw 1/4"-20 Thread, 3/8" Length, Packs of 10	\$3.99	2	\$7.98		
Type 316 Stainless Steel Flat Washer Number 4 Screw Size, 0.125" ID, 0.312" OD, Packs of 100	\$3.37	2	\$6.74		
Type 316 Stainless Steel Flat Washer Number 8 Screw Size, 0.174" ID, 0.375" OD, Packs of 100	\$3.40	1	\$3.40		
Type 316 Stainless Steel Flat Washer 5/16" Screw Size, 0.344" ID, 0.750" OD, Packs of 100	\$11.18	1	\$11.18		
Low-Strength Steel Hex Nut Zinc Plated, 4-40 Thread Size, 1/4" Wide, 3/32" Ht, Packs of 100	\$0.87	1	\$0.87		
Low-Strength Steel Hex Nut Zinc Plated, 8-32 Thread Size, 11/32" Wd, 1/8" Ht, Packs of 100	\$1.60	1	\$1.60		
Low-Strength Steel Hex Nut Zinc Plated, 1/4"-20 Thread Sz, 7/16" Wd, 7/32" Ht, Packs of 100	\$2.68	1	\$2.68		

Steel Round Base Weld Nut 4-40 Thrd Sz, w/9/64" Dia X 1/8" Ht. Barrel, Packs of 100	\$6.33	1	\$6.33	
18-8 SS Tab Base Weld Nut 1/4"-20 Thrd Sz, w/5/16" Dia X 5/16" Ht. Barrel, Packs of 10	\$8.47	2	\$16.94	
Steel Easy-Align Weld Nut W/Steel Retainer, 1/4"-20 Thread Size, Packs of 20	\$15.81	1	\$15.81	
Easy-to-Machine Polypropylene Sheet 1/8" Thick, 24" X 48" Opaque White	\$19.89	1	\$19.89	
Nylon Split Shank Rivet .115" Hole Diameter, .135" Material Thk, Black, Packs of 100	\$5.99	1	\$5.99	
Nylon Split Shank Rivet .165" Hole Diameter, .125" Material Thk, Black, Packs of 100	\$5.70	1	\$5.70	
Low-Strength Steel Threaded Rod Zinc Plated, 1/2"-13 Thread, 3 ft Lg, Fully Thrded, Packs of 1	\$4.85	4	\$19.40	
Low-Strength Steel Extra-Wide Hex Nut Zinc Plated, 1/2"-13 Thread Sz, 7/8" Wd, 31/64" Ht, Packs of 50	\$9.43	1	\$9.43	
Multipurpose 6061 Aluminum 3/8" Thick, 3" Width, 1' Length	\$10.07	1	\$10.07	
Multipurpose 6061 Aluminum Short Tube, .500" Wall Thickness, 5- 1/2" OD, 3" Lg	\$16.56	1	\$16.56	
Plastic Cup Polypropylene, 8 oz Cap, 3-1/8" Top OD X 3-1/4" H, Packs of 25	\$13.04	1	\$13.04	

	Compartmented Plastic Box with Handle 21 Compartments, 18-1/2" Overall Length	\$30.07	1	\$30.07	
	Optically Clear Cast Acrylic Tube 2-3/4" OD X 2-1/2" ID, 1' Length	\$33.73	1	\$33.73	
	Corrosion-Resistant 304 SS Woven Wire Cloth 40 X 40 Mesh, .01" Wire Diameter, 12" X 12" Sheet	\$7.46	1	\$7.46	
	Corrosion-Resistant 304 SS Woven Wire Cloth 80 X 80 Mesh, .007" Wire Diameter, 12" X 12" Sheet	\$8.14	1	\$8.14	
Jason's Deli	Refreshments for Les Johnson Seminar	\$250.00	1	\$250.00	
Loftis Steel and Aluminum	Raw Aluminum, 6"x12"x0.5"	\$20.00	1	\$20.00	
Analog Devices	ADXL 345 Evaluation Board	\$60.00	5	\$300.00	

The table below outlines all items that the team plans to reuse. These do not factor into expenditures, but do contribute to cost as flown.

Table 27: Relevant previous year purchases

Company	Item	Cost estimate	
Lowes	4x8x1/2" Plywood	\$33.00	
ApogeeRockets	Rail guides and recovery systems	\$1,100.00	
ApogeeRockets	Nose cone	\$39.90	
Giant Leap	Antizippering devices (Fireballs)	\$90.00	
ApogeeRockets	Shock cords	\$40.00	
ApogeeRockets	Blue tube	\$12.00	
McMaster-Carr	U-bolts	\$4.00	
McMaster-Carr	Acrylic	\$10.00	
GoPro	GoPro Camera and memory card	\$234.98	
McMaster-Carr	Pressure vessel	\$30.00	
Unknown	Fan Carts	\$40.00	

The budget is divided into shop equipment, rocket hardware, fuel delivery system, monopropellant thruster, structural health monitoring, outreach, and launches and competitions. The amounts allocated for each section are shown below.

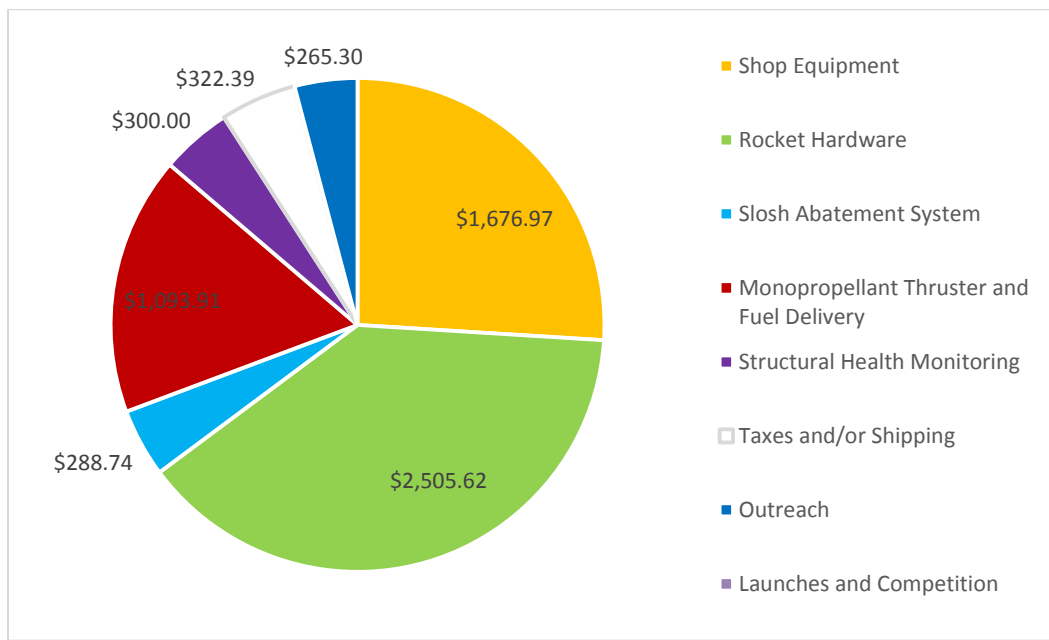


**Figure 119: Overall budget distribution**

## 6.2 Preliminary Timeline

In the preliminary timeline shown below, NASA-designated dates are shown in grey and Team-designated dates pertaining to rocket construction are shown in blue

**Table 28: Timeline**

9/11/2015	Proposal Due
9/16/2015	Parts and sensors ordered for subscale
9/17/2015	Finalized vehicle and test rig design
9/24/2015	Design presentation of subscale fuel flow visualization system
10/2/2015	Schools notified of selection
10/7/2015	Kickoff and PDR Q&A
10/8/2015	Full thruster design and fabrication plan laid out
10/15/2015	Design sections made for full scale vehicle fabrication
10/23/2015	Web presence established for each team
11/6/2015	Preliminary Design Review (PDR) and PDR presentation slides posted on the team Web site
11/11/2015	Subscale Launch Readiness Review
11/14/2015	Subscale Launch
12/8/2015	Modal Tap Test

12/15/2015	Ground firing of thrusters
1/15/2016	CDR presentation slides, report, and flysheet posted on team website
1/19/2016- 1/29/2016	Critical Design Review video teleconferences
2/3/2016	Flight Readiness Review Q&A
2/14/2016	Flight systems completion
2/27/2016	Full scale test launch with thruster and fuel delivery system
3/14/2016	FRR presentation slides, report, and flysheet posted on team website
3/17/2016- 3/30/2016	FRR video teleconferences
4/13/2016	Travel to Huntsville, AL
4/13/2016	Launch Readiness Reviews
4/16/2016	SL Launch Day
4/29/2016	Post-Launch Assessment Review (PLAR) posted on team website
5/11/2016	Announcement of winning SL team

## 6.3 Educational Engagement Plan & Status

---

The Vanderbilt Aerospace Design Laboratory, in conjunction with Vanderbilt's Department of Teaching and Learning, has reached out to several Nashville proper, and rural Tennessee elementary and middle schools to spend a day working with students to understand the importance of STEM fields, the role of engineers, and the future of space exploration. The team has already visited Percy Priest Elementary School to work with the Encore (gifted) students in the 2<sup>nd</sup>, 3<sup>rd</sup>, and 4<sup>th</sup> grades. The team has completely overhauled the former outreach curriculum to create brand new presentations, class activities, and a fun bottle-rocket demonstration to end the day. The lesson plans are easily tailored to different age ranges, and are specifically meant for student ages 10-13 (5<sup>th</sup> – 8<sup>th</sup> grade). The team is currently planning at least two additional outreach events for the remainder of 2015. In the coming weeks, the team plans to travel to John Early Museum Magnet Middle School to serve mixed-socioeconomic class students with our lessons and activities. Additionally, the team plans to visit the Whitecreek Academy for Renewable Energy to discuss the topics of “Space-based Solar Energy” before Christmas. At the start of 2016, the team hopes to visit the Nashville Adventure Science Center to present our work to visiting community members.

### 6.3.1 Educational Plan

---

#### 6.3.1.1 Perceived Benefits to Teachers

---

We aim to give teachers an avenue to introduce engineering as a meaningful part of their curriculum by serving as a real-life example of how engineering can be applied to the physical sciences. The opportunity to apply their science, math, and technological knowledge to real world applications has the potential to bolster students' interests in engineering. Additionally, the VADL aims to further elaborate on the collaborative nature of engineering to students, a point which enhances their interest in the field and is often not conveyed by teachers.

In middle Tennessee, the counties with the lowest science scores for 3rd-8th grade are Davidson, Clay, and Perry. Both Clay and Perry County are in a rural part of Middle Tennessee, which is dominated by manufacturing and factory work. Most of the students grow up and stay in the area working in the local factory-based industries. While we understand the vital role these industries play, it is also important to ensure that the students are aware of the other opportunities they may have. Less than 11% of residents in both Clay and Perry County possess a Bachelor's degree or higher. Many of these students may have never met an engineer before. Through outreach events in these areas, we will help teachers serving in these oftentimes understaffed and underfunded areas impart to students the many prospects available for education and careers by acting as living proof of what is possible for them.

Through outreach, we will provide teachers with a new set of experiments and lessons they can continue to modify and use in their classrooms. Additionally, they can build upon this basis for future lessons involving Newton's Laws of Motion and other physics and engineering based topics. Since we are not a regular part of the curriculum in these classrooms, we will be able to generate extra excitement by breaking up the routine. We hope and anticipate that this will lead to the students readily engaging in the lesson and retaining the information.

#### **6.3.1.2 Perceived Benefits to Students**

---

A shift in the national science standards put forth by the National Research Council in 2012 suggests that science education should be more strongly connected to the real world. Instead of being taught science concepts such as Newton's third law and forces involved in flight purely theoretically, the students will have the opportunity to apply these ideas in hands-on experimentation with fan carts, as well as a bottle-rocket demo. This allows them to see the connections between scientific ideas and their real world applications and to realize how this relates to space flight.

Since we are new faces to the students, we will be seen as experts in engineering, and direct contact with us gives the lesson more authenticity and relevance. This interaction increases the students' awareness about engineering as a career choice and gives them an opportunity to ask questions about what engineers do, how they deal with science, concepts in design and fabrication, and what kinds of jobs are available.

The lesson is designed to include several hands-on experiments that pull together relevant science concepts and provide them with exposure to the engineering design process. Additionally, students will work with others in a group and be able to consult with experts, effectively opening up the classroom community by bringing in other voices and talents and breaking up the usual classroom order.

Our goal is to introduce and explore engineering and Newton's Laws of Motion in the context of rocketry in a manner that will be engaging and exciting. Through this we hope to generate enough interest in engineering and rockets for some of the students to pursue them as hobbies or careers in their futures.

#### **6.3.2 Educational Lesson Plan Summary**

---

Our goals for outreach are:

- 1) First and foremost, bring an excitement to learning about math and science. This is achieved through bringing an energetic attitude to the table while engaging with the students, flashing fun props like previous years' rockets, employing aesthetically pleasing teaching materials, and appealing to our "street cred" as fun college students to keep students interested.
- 2) Imbue students with a fundamental understanding of the concept of a force, the relationship between force and acceleration or motion, the relationship between weight and thrust in rocket flight, and the major considerations for ensuring successful rocket flight. This understanding is accomplished through a combination of educational presentations and interactive discussions and activities.
- 3) Engage students and reinforce presented theoretical information through hands-on and discussion based activities; these activities include a fan cart activity, discussions about why it's important to keep supporting space exploration (see goals 4 and 5).
- 4) Leave students who may not have known anything about engineering prior to our visit with a knowledge of what engineering is, what engineers do, why engineering is important (and cool!), and what the engineering design cycle is in a very broad sense.
- 5) Prompt students to formulate opinions about why continuing space exploration should or should not be a priority for the future by presenting arguments for why space exploration continues to be important and relevant.

These goals are realized through our lesson plan for our outreach events, which is presented in detail in the sections below.

### **6.3.3 Educational Lesson Plan Details**

---

A typical classroom visit will flow as follows. We usually have around an hour in a classroom, so we try to structure our time as presented below.

- 1) **Before visit:** Pre- and post-assessments are administered to students by teachers before and after an outreach event and then returned to us so that we may assess the efficacy of our lesson and activities. This year's assessments are novel in that they incorporate a variety of non-standard assessment techniques. We developed the assessments in this way in the hopes that it would decrease our likelihood of being seen as teachers and thus losing our credibility and "coolness" with students. Some questions present on the pre-assessment but not on the post-assessment are included to get students thinking about what qualities render an object better able to fly (that is, more aerodynamic) before the lesson even begins.
- 2) **VADL introduction (5 mins):** Introduce presenters and give an overview of the VADL, the team's background, NASA SL, and the nature of engineering through a VADL overview presentation. The overview contains general information about the VADL, NASA SL, how we as a team prepare for competition, and the nature and practice of engineering.
- 3) **Lesson on rocket physics (17 mins):** Deliver a rocket physics presentation. The presentation is a high-level, conceptual lesson on the physics and forces behind rocket flight and the challenges that these forces present when it comes to getting a rocket off the ground. The elementary school version does not cover drag or lift and includes no math, only concepts of force balancing or lack thereof and an unbalanced force's relationship to

acceleration, while the high school version covers all four aerodynamic forces (thrust, weight, lift, and drag) and gives an overview of force calculations using Newton's Second Law. The high school version also touches on Newton's Law of Universal Gravitation.

- 4) **Fan cart activity (10 mins):** Transition to a hands-on application of the physics principles just presented in the lesson. A worksheet provides a step-by-step guide to our fan cart activity, a engaging way for students to visual and physically equate the concepts of weight and thrust. The fan cart activity uses variable-speed fan carts with “frictionless” wheels in conjunction with a pulley system and container with contents of variable weight to demonstrate the concepts of thrust and weight and the result of their balance or imbalance. Students are first directed to quantify a relationship between the force of the fan (thrust) and the weight of the container and its contents (rocket) – “How much weight does it take to keep the container from moving when the fan is at a low speed?”, “What happens when you increase the speed of the fan?”, “What can we say about the force of the fan and the weight of the container when the container is not moving?”, etc. After the students have established the relationship between acceleration, weight, and thrust, we ask them to think about how those same concepts would apply to rocket flight – “What do we have to do to ensure that a rocket we try to launch can get off the ground?” This activity provides the hands-on validation of our presentation on theoretical physics in accordance with our goal of active student engagement in the learning process.

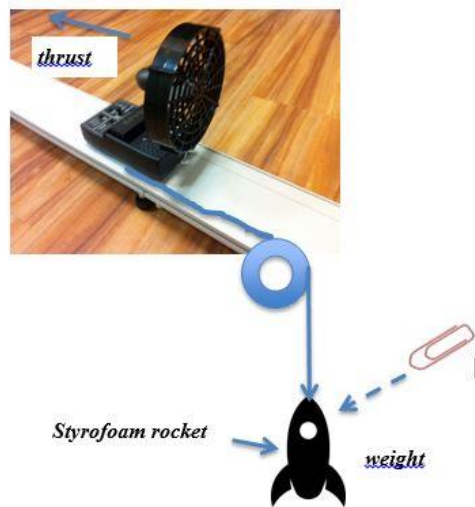
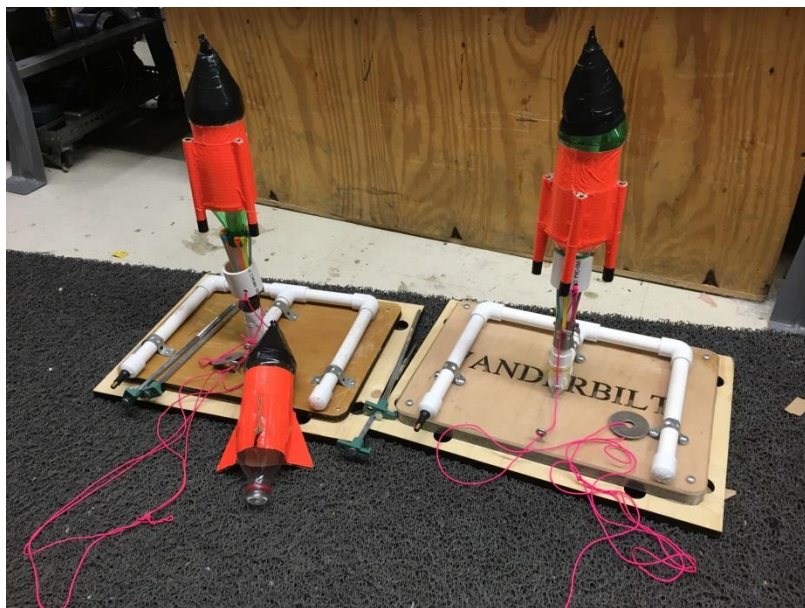


Figure 120: Simplified schematic of the fan cart demo

- 5) **Kerbal Space Program videos (6 mins):** Present and illustrate the concept of the design – simulate – test – improve engineering design cycle, identifying the virtual rocket launch in Kerbal Space Program as the simulation phase of the design cycle. Kerbal Space Program is an online software module that allows one to virtually build and launch rockets and is unique in that it produces highly accurate simulation results for launches of rockets built within the program. The outreach team has “designed” three different rocket concepts, each with different numbers of thrusters, on Kerbal to illustrate the impact of varying thrust on a real

rocket. At outreach events, we “launch” each rocket in KSP and probe students to compare the results of the simulations of the three rockets (“What’s the result of adding more thrusters to the rocket?”). We tie our KSP simulations back to our discussions about what it means to be an engineer today by emphasizing the modern engineering process – engineers will often design a few concepts and then simulate the designs with computer software to get an idea about how the design will behave under real test conditions – before going outside to test our simulation results through a bottle rocket launch.

- 6) **Bottle rockets (10 mins):** Take students outside to illustrate the test phase of the engineering design cycle through the launch of bottle rockets producing various amounts of “thrust.” At outreach events, we have three rockets – one with one thruster, one with three thrusters, and one with four thrusters – and we ask students to predict which rocket will go the highest based on their observations from our Kerbal simulations. For launch, we pressurize the rocket with four thrusters the most, with three pressurized less and one the least, with the resulting apogee difference in the rocket flights verifying the computer simulations.



**Figure 121: Bottle Rocket launch stand**

The bottle rockets are slid over the open-ended, upright piece of PVC in the middle of our launch stands as pictured above. Zip ties and a ring of PVC fit over the mouth of a bottle, securing it while the bottle is pressurized. A bike pump is attached to the valve on the front of the stand and is used to pressurize the bottle to a pressure of no greater than 60 psi. Once a bottle rocket has been pressurized, it is launched by pulling the fitted PVC ring away from the mouth of the bottle, causing the zip ties to pop away from the mouth and the bottle to be released upwards along the remainder of the pipe rail.

The outreach team has taken every precaution to ensure the safest possible operation of the bottle rocket stand. During outreach events, the launch stand is staked into the ground to

prevent displacement of the stand itself or the accidental launching of a rocket toward students. The soda bottles used as rockets are rated up to 150 psi and have been tested by the team up to 100 psi to ensure safe operation at all pressures below 60 psi. At events, students are required to observe the launch from no less than 50 feet away from the launch stands.

- 7) **Importance of continued space exploration (7 mins):** Engage students in a thoughtful conversation about why space exploration is important and what discoveries and byproducts of space exploration improve our daily life right here on Earth.
- 8) **Wrap up and closing questions (5 mins):** Briefly recap the key points of forces, the engineering design cycle, and the importance of supporting science and space exploration. Answer questions with the remaining time.

## *7 Conclusion*

---

The task of designing and constructing a high powered rocket which serves as a test bed for liquid sloshing research, onboard structural analysis, and green monopropellant thruster technology is a unique challenge that lends itself well as a topic that can be explored far beyond this year's competition. The modular design of the above payloads enables the pursuit of a developmental program that incorporates continuous improvement and refinement of the overall rocket design. Ultimately, we hope that the progress made on this year's vehicle yields a strong vantage point that future Vanderbilt teams can utilize to make increasingly substantive contributions to NASA's SLS program.

## *8 Appendix*

---

For ease of use, the appendix with SDS sheets, high powered rocket code, etc. is posted on the Vanderbilt SLI Team website in a separate section.

See [www.vanderbilt.edu/usli](http://www.vanderbilt.edu/usli)

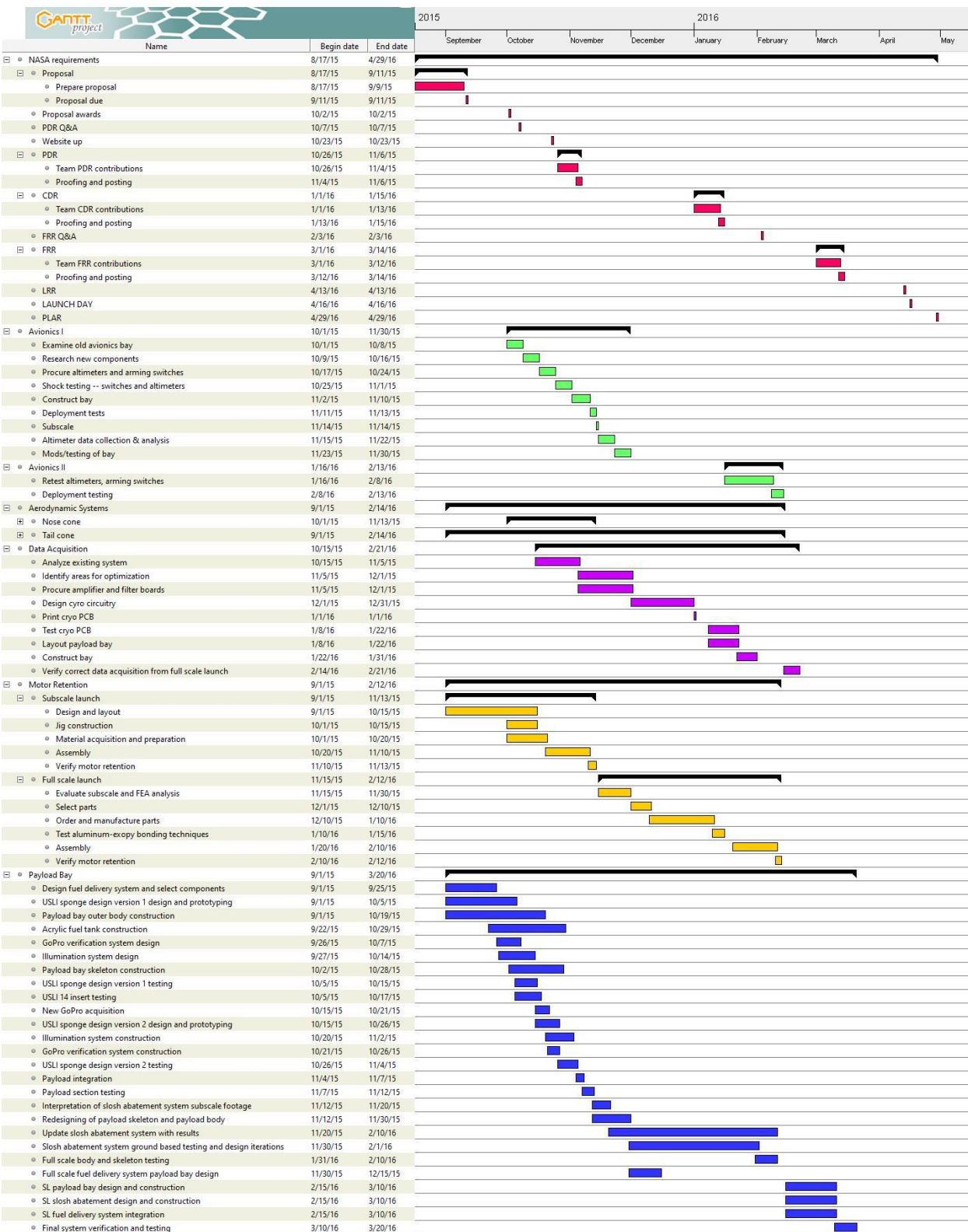


Figure 122: Gantt Chart for project plan

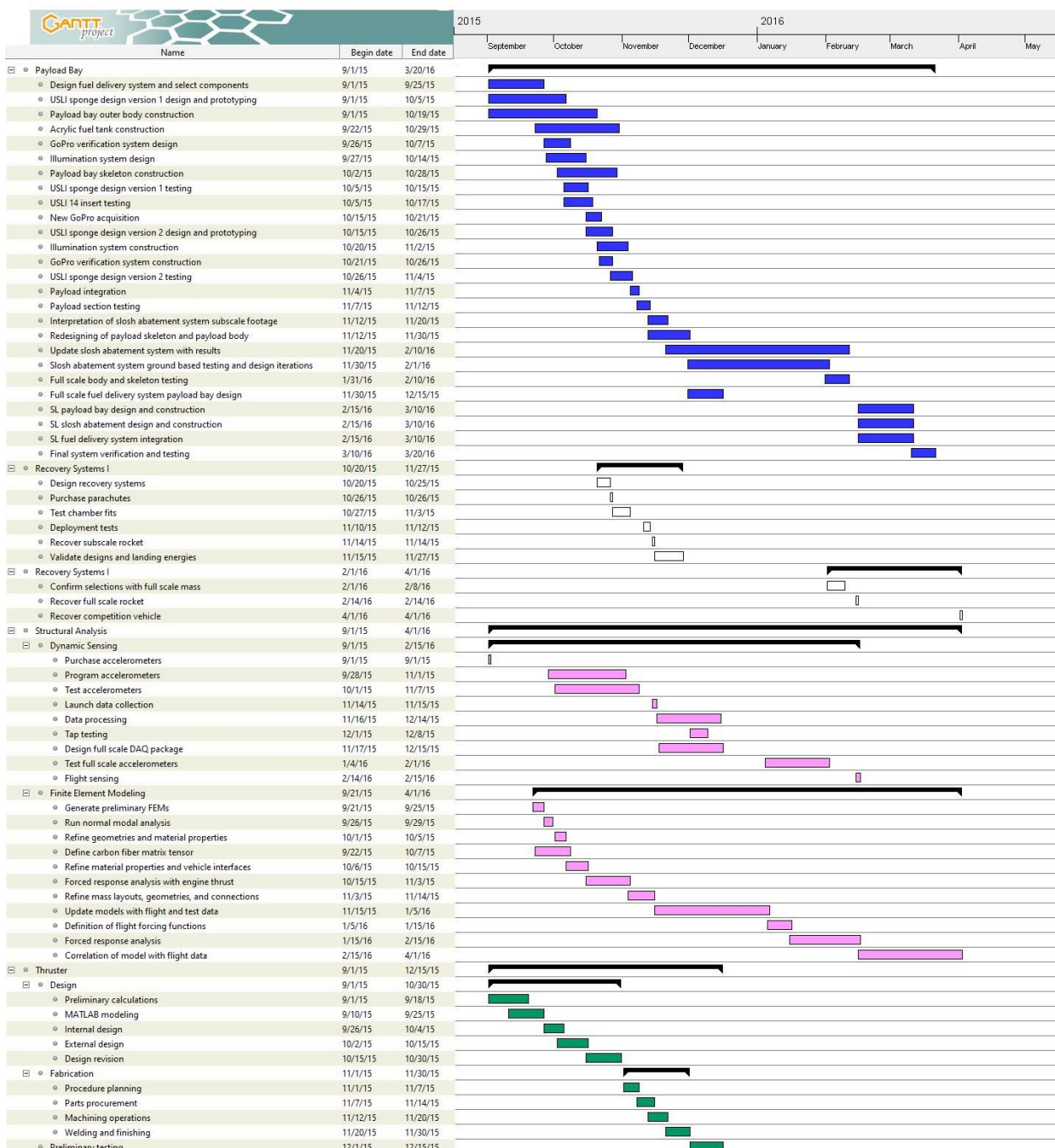


Figure 123: Gantt Chart for project plan